Modulation of T-cell function using Pharmacological Agents and Retroviruses

Elaine Mary Breslin

Section of Infection and Immunity
Wales College of Medicine
Cardiff University

Supervisor: Dr. Paul Brennan

A dissertation submitted to Wales College of Medicine, Cardiff University in candidature for the degree of Doctor of Philosophy

February 2005

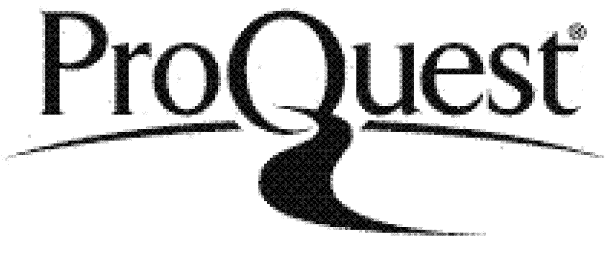

ProQuest LLC
789 East Eisenhower Parkway
P.O. Box 1346
Ann Arbor, MI 48106-1346

SUMMARY

Cellular immunotherapy aimed at reconstituting T-cell responses to Epstein-Barr Virus (EBV) has proved extremely effective in the treatment of Post Transplant Lymphoproliferative Disorders. The application of gene therapy to improve the efficacy and survival of T-cells remains a major goal in the development of an optimal immunotherapeutic strategy and current research indicates that the use of genetically modified T-cells in adoptive transfer is a feasible therapy for the clinic. Immunosuppresive drugs such as rapamycin and CsA inhibit T-cell proliferation and may impair the function and efficacy of adoptively transferred T-cells *in vivo*. Our objective of this project was to enhance the efficacy and survival of Primary Human T-cells *in vitro* by modification with a retroviral vector containing an immunosuppressive resistant gene.

Cell proliferation experiments using a CFSE cell protein dye elucidated the optimal cell stimulation requirements and the optimal day to target Primary T-cells for retroviral infection. Two distinct retroviral infection systems were established in the laboratory and applied to transduce Kit225 T-cells, Primary Human T-cells and EBV-Cytotoxic T-cells. These T-cells were modified with a retrovirus to confer rapamycin resistance (pBabe mTOR S2035T) or a retrovirus to confer CsA resistance (pBabe CNA V314R). The data showed that both the pBabe mTOR S2035T virus and the pBabe CNA V314R virus could confer immunosuppression resistance in the modified T-cell but that this was not demonstrated for every infection. The data also showed that the modification of Primary Human T-cells with these viruses generated cells with a growth advantage and increased cytokine production compared to Primary T-cells modified with control pBabe puro virus. This suggests that the modification of PBLs with the immunosuppressive resistance genes mTOR S2035T or CNA V314R may be a useful strategy to improve the efficacy and function of T-cells.

During the course of this project, experiments also showed that the PI3-Kinase inhibitor LY294002 and rapamycin co-operate to inhibit T-cell proliferation. Taken together, the results demonstrated in this project highlight the importance of the TOR and calcineurin pathways in regulating T-cell proliferation, and suggest strategies to improve both immunosuppression and cellular immunotherapeutic regimes.

ACKNOWLEDGEMENTS

I would like to sincerely thank my supervisor Dr. Paul Brennan for his guidance, support and excellent supervision throughout this project. I would also like to thank Professor Martin Rowe for advice and encouragement throughout my PhD. I thank all the members of my group, both past and present, Pat and every other member of Infection and Immunity, for support and friendship and for ensuring Infection and Immunity is both an excellent and enjoyable place to work.

I also wish to acknowledge Dr. Richard Darley's group in the Department of Haematology and Dr. Chris Jones' group in the Department of Pathology for their retroviral expertise and for providing advice on the technology.

I acknowledge funding from the Welsh Assembly Government provided through the Welsh Office of Research and Development for Health and Social Care.

Finally, many thanks to my parents, my brothers and my friends and I extend a special thanks to Padraic for much appreciated support and encouragement during this PhD.

ABBREVIATIONS USED

ADA	Adenosine deaminase
BMT	Bone Marrow Transplant
CaM	Calmodulin
CMV	Cytomegalovirus
CNA	Calcineurin A catalytic subunit
CNB	Calcineurin B regulatory subunit
CsA	Cyclosporin A
CTL	$CD8^+$ Cytotoxic T-lymphocyte
DAG	Diacylglycerol
DNTP	Deoxynucleotide triphosphate
EBER	EBV-encoded RNA
EBV	Epstein-Barr virus
EDTA	Ethylenediaminetetra acetic acid
FDA	Food and Drug Administration (US Regulatory Administration)
FITC	Fluorescein isothiocyanate
GFP	Green fluorescent protein
GvHD	Graft-versus-Host Disease
HD	Hodgkin's Disease
HIV	Human Immunodeficiency virus
HLA	Human Leukocyte Antigen
HSV-TK	Herpes simplex virus thymidine kinase
IFN	Interferon
Ig	Immunoglobulin
IL	Interleukin
IL-2R	IL-2 receptor
ITAM	Immunoreceptor tyrosine-based activation motif
JAK	Janus kinase
LAT	Linker for activation of T-cells
LCL	Lymphoblastoid cell line
LFA	Lymphocyte function associated antigen
LMP	Latent membrane protein
LTR	Long-terminal repeat
MAb	Monoclonal antibody
MDR-1	multidrug resistant or p-glycoprotein
MHC	Major histocompatibility complex molecule
MoMLV	Moloney Murine Leukemia virus
mRNA	Messenger ribonucleic acid
mTOR	mammalian Target of Rapamycin protein
MuLV	Murine Leukemia virus
NeoR	Neomycin resistance gene
NFAT	Nuclear Factor of activated T-cells
PAGE	Polyacrylamide gel electrophoresis

PBL	Peripheral blood lymphocyte
PBMC	Peripheral blood mononuclear cell
PBS	Phosphate-buffered saline
PCR	Polymerase chain reaction
PE	Phycoerythrin
PFA	Paraformaldehyde
PHA	Phytohaemagglutinin
PI	Propidium Iodide
PI3K	Phosphatidlyinositol 3-kinase
PIC	Pre-integration complex
PIT-2	type II sodium phosphate co-transporter/receptor for MoMLV
PLC	Phospholipase C
PTLD	Post-transplant Lymphoproliferative Disorder
SCID	Severe Combined immunodeficiency Disease
TCR	T-cell receptor
Th	$CD4^+$ Helper T-cells
TNF	Tumour necrosis factor
TOR	Target of Rapamycin protein
Tregs	$CD4^+$ Regulatory T-cell
VLA	Very late antigen

TABLE OF CONTENTS

CONTENTS PAGE NO.

Chapter 2 Materials and Methods

2.1 Molecular Biology

2.2 Tissue culture

CHAPTER 1

INTRODUCTION

1.1 T-cells and the immune system

1.1.1 *General features of T-cells in the immune system*

The immune system consists of an intricate communication network between the innate immune response and the adaptive immune response. The innate immune response is the body's first line of defense and is hallmarked by a rapidly induced response to antigen. However, the innate response cannot eliminate all sources of infection (Laver, 1984) and the communication with the adaptive immune response is crucial (reviewed in Hoebe *et al.*, 2004). The adaptive immune response is a much more versatile and diverse response and is hallmarked by the fact that each lymphocyte has a single receptor type specific for only one antigen (Nossal, 1994). The adaptive immune response is divided into two categories; the antibody mediated response, which involves the activation of B-cells to produce antibody, and the cell-mediate response, which is mediated by T-cells. T-cells are the key focus of this project.

Naïve T-cells are activated into effector cells upon recognition of a specific ligand in the form of processed antigenic peptide sequences of approximately ten amino acids displayed at the surface of an antigen-presenting cell (APC) (Del Val *et al.*, 1991). The specialised molecules that display the peptides are the major histocompatability complex molecule (MHC) of which there are of two classes; MHC class I and MHC class II (Wake and Flavell, 1985). The key event during a T-cell response to antigen is the activation of the T-cell receptor (TCR)/CD3 complex. This complex is comprised of a clonally variable TCR, consisting of two different polypeptide chains α and β, each with a constant and variable domain (Davis and Bjorkman, 1988) in a non-covalent association with the invariant TCR ζ chains and the γ, δ, and ε chains of the CD3 antigen complex (Weiss, 1993). The T-cells of the

cellular immune response are divided into three categories; the $CD8^+$ cytotoxic T-lymphocytes (CTLs), which are most relevant to this project, the $CD4^+$ T-helper cells (Th) and the regulatory T-cells (Tregs). The CD8 molecule on CTLs and the CD4 molecule on Th-cells and Tregs, act as co-receptors in the TCR complex-antigen/MHC interaction (Gao *et al.*, 2002). A T-cell response also requires presentation of the co-stimulatory molecules B7-1 (CD80) and B7-2 (CD86) on the APC surface which act as a ligand for the immunoglobulin superfamily member CD28, on the T-cell surface (June *et al.*, 1994). The dendritic cells (DCs) are the most potent APC because they display all of the co-stimulatory molecules necessary to aid in T-cell activation, but macrophage and phagocytic B-cells can also act as APC.

1.1.1.1 *$CD8^+$ T-lymphocytes*

The CTLs recognise antigen presented on MHC class I (Davis and Bjorkman, 1988) and eliminate cells infected with virus or bacteria. The main mechanism through which CTLs kill infected cells is by the release of the cytotoxic granules perforin and granzyme. The pore-forming molecule perforin is a crucial effector molecule of cytolysis. A reduced ability to clear viral pathogens and a high susceptibility to spontaneous B-cell lymphoma are a typical phenotype of perforin deficient mice (Kagi *et al.*, 1994; van den Broek *et al.*, 1996). Perforin is stored in cytotoxic granules, and upon recognition of a target cell, the granules are released and perforin monomers insert themselves into the target cell membrane to form pores (Liu *et al.*, 1995). These pores cause osmotic lysis of the target cells and allow the granzyme molcules, which act as serine proteases, to enter the target cell and induce apoptosis through various downstream effector pathways including effector caspases and the mitochondrial death pathway. CTLs can also initiate apoptosis through activation of the Fas signal transduction pathway (Puppo *et al.*, 2002). Fas, is a tumour necrosis factor (TNF)-receptor family member, and is expressed on many cells including activated B and T-cells. The Fas ligand belongs to the TNF family and is expressed mainly on activated T-cells, macrophages and neutrophils. Fas mediated apoptosis is a complex series of signalling events, the first of which involves the binding of a FasL trimer on the effector CTL to a Fas trimer on the

target cell membrane. This initiates a caspase signalling pathway which leads to apoptosis in the target cell (Barry and Bleackley, 2002).

1.1.1.2 *$CD4^+$ helper T-cells*

$CD4^+$ helper T-cells 'help' both humoral and cell mediated responses. These helper $CD4^+$ T-cells recognise antigen presented on MHC class II (Davis and Bjorkman, 1988). These cells can be divided into two subsets, Th1 and Th2, characterised on the basis of functional response and cytokine production (Del Prete *et al.*, 1991). IL2, IFN-γ and TNF are cytokines produced by Th1 $CD4^+$ T- cells. IL-5, IL-4, IL-10 and TNF are typically produced by Th2 $CD4^+$ T-cells (Romagnani, 1991). The functions of Th1 and Th2 cells correlate with their distinctive cytokines (Romagnani, 1991). Th1 cells are involved in cell-mediated inflammatory reactions and Th1 cytokines activate cytotoxic and inflammatory functions (Romagnani, 1991). Helper-dependent primary CTL response to antigen depends on the activation of the APC by the Th1 cells (Bevan, 2004). There is also evidence that these Th1 $CD4^+$ T-cells are important in the maintenance of CTL-mediated antiviral or antitumour immunity (Matloubian *et al.*, 1994). The Th2 cells are are mainly involved in the humoral immune response and the Th2 cytokines encourage antibody production (Romagnani, 1991).

1.1.1.3 *Regulatory T-cells*

While $CD4^+$ T-cells are best known as helper cells, there is another subset, the T-regulatory cells (Tregs), which can regulate and hinder the effects of autoreactive T and B-cells. The most well characterised example of Tregs is the $CD4^+CD25^+$ T-cell population, which appear to play a role in the down-regulation of pathogenic autoimmune responses (Sakaguchi *et al.*, 1996). However, despite a mounting body of evidence to support the existence of these cells, whether such cells are responding to self or foreign antigens is lacking. It has been argued that there are two sub-populations of Tregs; natural Tregs which function against self-antigens; and adaptive or inducible Tregs which function to maintain homeostatic control over various adaptive responses (Jonuleit and Schmitt, 2003). Naturally occurring Tregs develop in the thymus and are thought to suppress effector T-cell proliferation *in*

vitro through a cell contact-dependent mechanism that is largely cytokine independent (Piccirillo *et al.*, 2002). Inducible Tregs depend on peripheral factors such as the type of stimulating APC (Steinman *et al.*, 2003) and appear to exert their immunosuppressive effect through the secretion of immunosuppressive cytokines such as IL-10 and TGF-β (Stassen *et al.*, 2004).

1.1.2 T-cell signalling

Efficient T-cell signalling is a key step in the induction of T-cell proliferation to mount an effective immune response (Figure 1.1 (a), (b), (c)). Defects in T-cell proliferation can lead to an array of diseases such as immunodeficiency diseases (Gaspar *et al.*, 2001), autoimmune diseases (Thomas-Vaslin *et al.*, 1997) and cancer (reviewed in Sherr, 1996). T-cell proliferation is regulated by three types of cell surface signalling molecules (Yusuf and Fruman, 2003). The main step is the recognition of peptide by the TCR. Co-stimulatory receptor activation and cytokine receptor activation are also required for maximal proliferation.

1.1.2.1 *Signalling through the T-cell receptor*

Antigen recognition by the T-Cell Receptor (TCR) complex initiates a cascade of intracellular signalling events. A key initiating event in T-cell activation is the increased phosphorylation of immunoreceptor tyrosine-based activation motif (ITAM) tyrosines in TCR associated CD3 molecules, by the Src family of PTKs Lck and Fyn (LoGrasso *et al.*, 1996). ITAM phosphorylation generates SH2 domain docking sites for the recruitment of the ζ-chain associated protein kinase of 70kD (ZAP-70) and once recruited to this complex, ZAP-70 is activated by phosphorylation of a tyrosine residue in its activation loop (Weissenhorn et al., 1996). This creates docking sites for SH2 domain containing signalling proteins (Bu *et al.*, 1995). Lack of ZAP-70 in humans leads to a severe immunodeficiency characterised by the absence of $CD8^+$ T-cells and TCR unresponsive mature $CD4^+$ T-cells (Barata *et al.*, 2001). One well established substrate of ZAP-70 is the adaptor protein linker for activation of T-cells (LAT) (Zhang et al., 1998). Tyrosine phosphorylated LAT recruits and activates several SH2 domain-containing proteins,

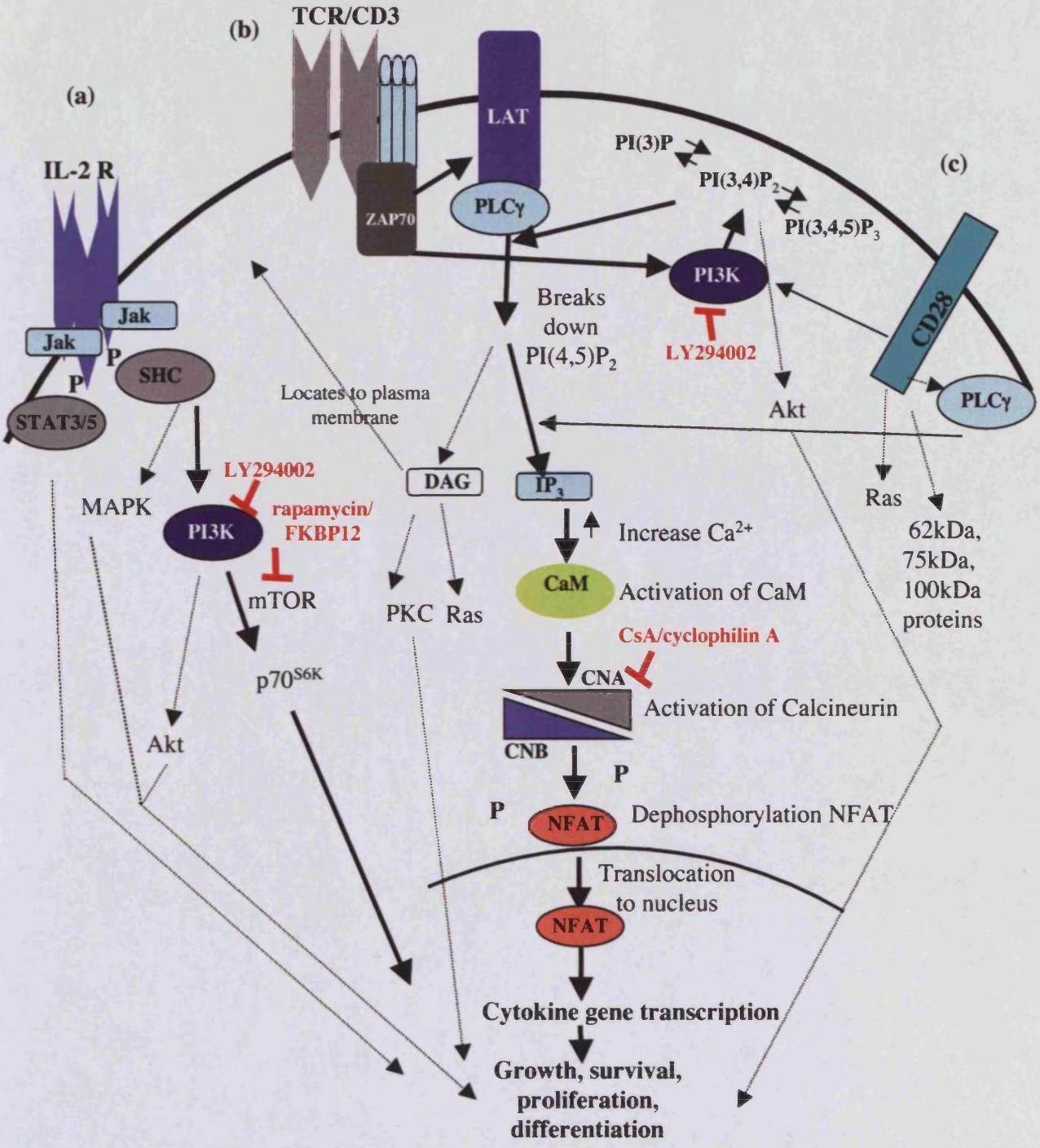

Figure 1.1 T-cell signalling A simplified schematic illustrating T-cell signalling pathways. The pathways in bold arrows are most relevant to this project. (a) Following IL-2 binding, Janus activated kinase (JAK) molecules associated with the IL-2 R phosphorylate key tyrosine residues in the cytoplasmic tail of IL-2R, inducing the association of the adaptor SHC and STATs. SHC allows the activation of the MAPK and PI3K pathways. (b) Following TCR ligation, Src PTKs are activated and lead to activation of ZAP-70 which activates LAT. LAT recruits several SH2 domain containing proteins, including PLCγ1. Activation of PLCγ1 leads to the hydrolysis of $PI(3,4)P_2$ to IP_3 and DAG. The IP_3 second messenger leads to an increase in intracellular Ca^{2+} stores. This initiates downstream signalling events which lead to translocation of the NFAT transcription factor to the nucleus. PI3K is also targeted to the membrane following TCR activation and PI3K downstream signalling pathways ensue. (b) The ligation of CD28 to its ligand amplifies components of the TCR signalling pathways, such as the PI3K pathway. CD28 activation activates PLCγ1 and Ras pathways. Data has indicated that CD28 activation also results in phophorylation of unique 62kDa, 75kDa, and 100kDa proteins. The TCR, IL-2 R and CD28 signalling pathways combine to yield optimal cytokine gene transcription, growth, survival and cell proliferation.

including PLC-γ (Williams *et al.*, 1999). This activates a cascade of events, leading to the elevation of intracellular Ca^{2+} (Figure 1.1 (b)).

PLC-γ1 mediates this elevation of intracellular Ca^{2+} through the regulation of the hydrolysis of inositol phospholipids. The recruitment of PLC-γ to the membrane is important because the inositol phospholipid substrates for PLC-γ are in the plasma membrane. PLC-γ1 cleaves phosphotidylinositol 4,5-bisphosphate ($PI(4,5)P_2$) to generate diacylglycerol (DAG) and inositol (1,4,5)-triphosphate (IP_3) (Muallem, 1989). IP_3 binds to receptors in the ER membrane, opening Ca^{2+} channels that release Ca^{2+} to the cytosol (Berridge, 2004). This increase in intracellular Ca^{2+} leads to the formation of Ca^{2+}-calmodulin complexes, which bind to the C-terminal of Calcineurin (Crabtree, 1999). Calcineurin is a protein phosphatase that is conserved in all eukaryotes and will be discussed in greater detail in Section 1.2. Binding of calmodulin to calcineurin results in the activation of the phosphatase (Fox *et al.*, 2001). The target of calcineurin is the Nuclear Factor of Activated T-cells (NFAT) transcription factor, which is required for IL-2 gene transcription and T-cell activation (Rao *et al.*, 1997). Following activation of the calcineurin complex, conserved serine residues in the amino terminus of NFAT proteins are dephosphorylated facilitating their translocation to the nucleus to serve as subunits of transcription factor complexes. NFAT proteins contain a Rel homology domain (Bassuk *et al.*, 1997) sufficient for DNA recognition and co-operative binding interactions with other transcription factors such as activator protein-1 (AP-1) and the dephosphorylation of NFAT unmasks nuclear location signals on NFAT. There are 5 NFAT transcription factors known; NFATc1 through to NFATc4 are all regulated by calcineurin while NFATc5 is not (Rao *et al.*, 1997). This PLC-γ1 mediated Ca^{2+} signalling pathway is depicted in Figure 1.1(b).

1.1.2.2 *Co-stimulation and CD28*

In addition to signals through the TCR/CD3 complex, activation of T-cells is enhanced by a second subset of stimuli, generally referred to as co-stimuli. The

membrane receptor, CD28, was found to enhance TCR signalling in naïve T-cells (June *et al.*, 1994). Data indicated that it may be the molecule responsible for the co-stimulatory signals, and investigations revealed the importance of the CD28 molecule as a regulator of gene-expression programmes activated at the onset of an immune response (Green *et al.*, 1994; Radvanyi *et al.*, 1996). The CD28 molecule is an independent signalling unit to the TCR. It is a 44 kDa homodimeric glycoprotein and is the primary co-stimulatory signal required for maximal T-cell proliferation and the enhancement of IL-2 synthesis (June *et al.*, 1994). Upon interaction with its ligands, B7-1 (CD80) and B7-2 (CD86), the co-stimulation signal from CD28 synergises with the TCR signals to promote cell cycle progression, increase the production of IL-2 and the expression of the IL-2 receptor (Ward, 1996). Studies have shown that this enhancement of IL-2 production is through an increase in IL-2 promoter transcription and stabilisation of IL-2 mRNA (Fraser *et al.*, 1991). Data has indicated that CD28 activation also results in phophorylation of unique 62kDa, 75kDa, and 100kDa proteins indicating that CD28 activation may also lead to unique signaling pathways (Lu *et al.*, 1992; Vandenberghe *et al.*, 1992). CD28 deficient mice have reduced responses to immune challenges (Beck *et al.*, 2003) and lack of CD28 co-stimulation *in vivo* and *in vitro* results in reduced T-cell proliferation (Green *et al.*, 1994), reduced Th differentiation (Schweitzer *et al.*, 1997) and compromised $CD8^+$ T-cell responses (Prilliman *et al.*, 2002).

CD28 signals are mediated through phosphorylated tyrosines and proline-rich motifs in its cytoplasmic tail (Ward, 1996). CD28 signalling acts as an amplifier of TCR signalling and one protein component identified as common to both the CD28 signalling pathway and the TCR signalling pathway is the PI3K signalling pathway (Ward and Cantrell, 2001). A simplified schematic of this is illustrated in Figure 1.1 (c). The role of the PI3K pathway in T-cell proliferation will be discussed in further detail in Section 1.1.2.4. The stimulatory effect of the TCR alone on PI3K activity is small and the combined triggering of the TCR and the co-stimulatory receptor CD28 result in optimal activation of the enzyme (Ward and Cantrell, 2001).

1.1.2.3 *Interleukin-2 and the Interleukin-2 Receptor*

IL-2 is a four bundle helical cytokine mainly produced by activated $CD4^+$ T-cells and its function in mounting an effective immune response by signalling through the IL-2 receptor is well established (Minami *et al.*, 1993). Interleukin-2 (IL-2) synthesis in T-cells is tightly regulated by signals from the TCR and CD28 (Kalli *et al.*, 1998). The IL-2 receptor itself is a multisubunit complex made up of an α, β and γ chain. The βγ chains are generally expressed on resting T-cells and have a low affinity for IL-2, while the α chain is upregulated upon activation of the T-cell through its TCR and co-stimulatory molecules (Minami *et al.*, 1993). The αβγ receptor is the highest affinity IL-2 receptor. Upon binding to the IL-2 receptor, IL-2 signals through at least three cellular pathways (Nelson and Willerford, 1998) to induce cell cycle progression through G1 to S phase of the cell cycle. These include signals to signal transducer and activator of transcription-5 (STAT5) and STAT3, the Ras-MAP kinase pathway and the phosphatidylinositol 3-kinase (PI3K) pathway (Figure 1.1 (a)). Mice homozygous for a targeted disruption of the IL-2 locus display irregularities in their immune response to antigens (Cousens *et al.*, 1995; Sadlack *et al.*, 1993). In humans, impaired IL-2 secretion is associated with immunodeficiencies (Chatila *et al.*, 1990).

1.1.2.4 *Phosphatidylinositol 3-kinase (PI3K)*

The Phosphatidylinositol 3-kinase (PI3K) family of enzymes phosphorylate phosphoinositides (PIs) on the 3-OH position of the inositol ring. PI3K enzymes are divided into four classes according to their substrate specificity and structure; class I_A, I_B, II and III (Vanhaesebroeck *et al.*, 2001). Studies have shown that PI3K is important for IL-2 induced cell proliferation (Brennan *et al.*, 1997; Brennan *et al.*, 1999). As mentioned earlier, PI3K also lies downstream of the T-cell receptor and the co-stimulatory molecule CD28 (Ward and Cantrell, 2001). Thus, links between PI3K and the cell cycle are likely to be critical for T-cell proliferation.

1.1.2.4.1 *The class I_A family of PI3K enzymes*

The class I_A family of PI3K enzymes are the most extensively studied of the PI3K enzymes. The biological significance of these enzymes in relation to the

immune system is well documented but not completely clarified. Their structure is a heterodimer of a regulatory subunit, and a 110 kDa catalytic subunit. There are five isoforms of the regulatory subunit; p85α, p55α, p50α, p85β and p55γ, which all contain two Src homology 2 (SH2) domains that bind to conserved phosphorylated Tyr-Xaa-Xaa-Met (YXXM) motifs on protein tyrosine kinase receptors or their adaptor proteins (Inukai *et al.*, 2001). The two SH2 domains are connected by an inter-SH2 domain of coil structure, and this interacts with the p110 subunit to maintain the stability of p110 in the cell (Fu *et al.*, 2003). There are three isoforms of the catalytic subunit; p110α, p110β and p110δ. The isoforms p110α and p110β are ubiquitously expressed in many tissues and organs, whereas p110δ is expressed primarily in lymphocytes (Koyasu, 2003).

In cells of the immune system, PI3K is activated by the binding of ligand to antigen receptors, cytokine receptors, antibody receptors and co-stimulatory molecules (Fruman and Cantley, 2002). In the case of T-cells and B-cells, activation through the TCR or BCR and co-stimulatory receptors such as CD28 on T-cells and CD19 on B-cells is important in the activation of class I_A PI3K (Brennan *et al.*, 1997; Okkenhaug *et al.*, 2001; Wang *et al.*, 2002). The phosphorylation of tyrosine motifs, including the YXXM sequence, in the intracellular cytoplasmic tails of these receptors recruit the regulatory subunit of PI3K to the membrane through binding of an SH2 domain present in the protein. Upon recruitment to the membrane, the catalytic subunit p110 can then phosphorylate lipid targets leading to a plethora of cell signalling events (Okkenhaug and Vanhaesebroeck, 2003a).

Gene knockout studies have shown that PI3K plays a role in the mediation of TCR dependent phosphorylation of PLCγ1 and sustained Ca^{2+} flux (Clayton *et al.*, 2002; Okkenhaug *et al.*, 2002). Other downstream PI3K dependent targets include S6Kinase (S6K), which phosphorylates the S6 ribosomal protein and regulates translation (Powers and Walter, 1999) and PKB (Akt), which regulates cell growth and survival (Scheid and Woodgett, 2001). The enzyme's lipid products are phosphatidylinositol (3) monophosphate (PI(3)P), phosphatidylinositol (3, 4) bisphosphate ($PI(3,4)P_2$), and phosphatidylinositol (3, 4, 5) triphosphate ($PI(3,4,5)P_3$)

(Auger *et al.*, 1989; Balla, 2001). These products, often termed 'second messengers' are important in intracellular signalling. They can serve as docking sites for proteins with pleckstrein homology (PH) domains of about 100 amino acids, and are central to the recruitment of cell signalling proteins to the membrane (Kavran *et al.*, 1998; Nagel *et al.*, 1998).

There are two major lipid phosphatases that regulate PI3K signalling by dephosphorylating PI3K products. PTEN is a tumour suppressor protein that converts phosphatidylinositol (3, 4, 5) P_3 to phosphatidylinositol (4, 5) P_2, and PTEN mutation is evident in a variety of human cancers (Black *et al.*, 2005). Lack of the enzyme leads to elevated levels of PIP_3 and inappropriate Akt kinase activity in the cell (Stocker *et al.*, 2002). SHIP (SH-2 containing inositol phosphatase) converts phosphatidylinositol (3, 4, 5) P_3 to phosphatidylinositol (3, 4) P_2 (Aman *et al.*, 1998).

1.1.2.4.2 *Gene knockout studies of PI3K*

Gene knockout experiments in mice have elucidated which isoforms of the enzyme are crucial in the maintenance of a normal immune response. The work of Suzuki *et al.* and Fruman *et al.*, investigated the loss of various isoforms of the PI3K class I_A regulatory subunit in mice. Their results indicated that mice lacking p85α but expressing p50α and p55α were viable but had some functional defects rendering the mice susceptible to infection, whereas mice deficient in all three regulatory subunits die after birth, suggesting that p50α and p55α have a critical role *in vivo* (Fruman *et al.*, 1999; Suzuki *et al.*, 1999). In the class I_A family, the loss of the p110 catalytic subunit isoforms, p110α and p110β is lethal to the mice (Bi *et al.*, 2002; Bi *et al.*, 1999). The p110α and p110β subunits are expressed in number of cell types and this may explain why loss of their expression affects survival. The expression of p110δ is restricted to leukocytes and may play a key role in PI3K signalling in the immune system (Chantry *et al.*, 1997). Clayton *et al.* generated p110δ $^{-/-}$ mice and demonstrated that in the absence of p110 these mice exhibited defective Akt/PKB phosphorylation, attenuated calcium flux, reduced B-cell numbers and reduced antibody responses (Clayton *et al.*, 2002).

Okkenhaug *et al.* introduced a point mutation of Asp910Ala in p110δ by gene targeting, resulting in a loss-of-function while retaining expression of the subunit (Okkenhaug and Vanhaesebroeck, 2003a; Okkenhaug and Vanhaesebroeck, 2003b). This study adopted a loss-of-function strategy rather than create deletion mutants because the loss of p110δ expression could lead to compensation by p110α and p110β. *In vitro* experiments showed that the T-cells in the p110δ D910A mutant mice had reduced proliferation in response to anti-CD3 stimulation but proliferated normally in response to anti-CD3 and anti-CD28 stimulation. However, the phosphorylation of PKB and $Ca2^+$ flux were reduced in response to TCR activation in both the anti-CD3 and anti-CD28 stimulated T-cells, indicating that CD28 stimulation may circumvent the requirement for PI3K stimulation. The T-cells in p110δ D910A mutant mice appeared normal in the thymus but were of reduced number and a naïve phenotype in the spleen, indicating that the T-cells in the p110δ D910A mutant mice failed to mature or survive in the peripherary (Okkenhaug *et al.*, 2002; Okkenhaug and Vanhaesebroeck, 2003a; Okkenhaug and Vanhaesebroeck, 2003b). The p110δ D910A mutant mice developed a mild form of inflammatory bowel disease that may be due to the failure of $CD4^+$ T-cells (which can suppress inflammation) to survive in the periphery (Okkenhaug *et al.*, 2002). The B-cells mutant mice also demonstrated reduced PKB phosphorylation and reduced $Ca2^+$ flux in response to BCR activation. These B-cells also demonstrated impaired T-cell dependent antibody production (Okkenhaug *et al.*, 2002). The demonstration of impaired antigen receptor signalling in both T and B-cells in the p110δ D910A mutant mice, coupled with the *in vivo* experiments demonstrating a failure of T-cells to mature or surive in the periphery indicates that the p110δ catalytic subunit has a key role in the immune system.

1.1.2.4.3 *Inhibitors of PI3K*

Wortmannin is a hydrophobic steroid-related product of the fungus *Taloromyces* that potently inhibits PI3 kinase signal transduction pathways in mammalian cells (Nakanishi *et al.*, 1995; Ui *et al.*, 1995). Wortmannin has proved useful in investigating PI3K signal-transduction pathways, but its many potential targets (Ferby *et al.*, 1996) make it an unsuitable therapeutic tool. A structurally

distinct PI3 kinase inhibitor, LY294002, has been developed, which is a competitive ATP binding site inhibitor and completely and reversibly inhibits PI3K (Vlahos *et al.*, 1994). In order to characterise specificity of LY294002, the compound was also tested against PI4K and data indicated that it was a selective inhibitor of PI3 kinase (Vlahos *et al.*, 1994). However subsequent analysis has shown that while LY294002 completely and reversibly inhibits PI3K it can also inhibit the structurally related PI4K at higher concentrations (Downing *et al.*, 1996). Along with gene knockout studies, both wortmannin and LY294002 have proved invaluable in elucidating the role of PI3K in the immune system and have suggested that links between PI3K and the cell cycle are likely to be critical for T-cell proliferation. This central role of PI3K signalling in cell regulation makes it a potentially valuable candidate for cancer therapy and the therapy of PI3K related immune diseases such as inflammatory disorders.

1.2 Immunosuppressive regimes

1.2.1 Immunosuppression: past, present and future

The overall aim of immunosuppression is to protect a transplanted organ from T-cell mediated rejection while maintaining adequate resistance to opportunistic infections and the development of lymphomas. It should be noted that another important application of immunosuppressive regimes is in the treatment of autoimmune disease (Bitsch and Bruck, 2002). Immunosuppression can be categorised depending on the mechanism of action of the regime. These categories include depletion of lymphocytes; inhibition of cell adhesion; inhibition of lymphocyte proliferation; and inhibition of cytokine production and signalling.

1.2.1.1 *Depletion of lymphocytes*

This immunosuppressive strategy involves the depletion of T-cells and is based upon the work of Woodruff *et al.* who showed that the administration of anti-lymphocyte serum in rats promoted the survival of skin grafts (Woodruff, 1967). This administration of polyclonal lymphocyte-specific sera quickly became a successful therapy in transplants (Kahan, 2003). One disadvantage of this therapy is

the reactivity of the sera with both lymphoid and non-lymhphoid cells. This prompted the development of monoclonal antibodies (MAbs) specifically targeting T-cells, with an antibody to the CD3 component of the T-cell receptor, OKT3, being the most successful early development (Cosimi *et al.*, 1981). New MAbs approved by the Food and Drug Administration (FDA) are designed to target the α-chain of the IL-2 receptor and are thus more specific for activated T-cells (Vincenti *et al.*, 1998). However, studies have indicated that the IL-15 receptor might be a more appropriate target than the IL-2 receptor, as it has been implicated in the inhibition of T-cell apoptosis and the maintenance of memory T-cells (Waldmann *et al.*, 2001).

1.2.1.2 *Inhibition of cell adhesion*

The selectin and integrin families of cell surface molecules allow for the efficient, coordinated recruitment of inflammatory cells to the site of graft rejection and also contribute co-stimulatory signals to lymphocytes. Given the importance of these molecules in graft rejection, the pharmacologic blockade of the interaction of adhesion molecules with their respective ligands is being explored (Schmouder, 2000). Blockade of Leukocyte function associated antigen (LFA-1) and very late antigen-4 (VLA-4) interaction with their ligands is a potential immunosuppressive strategy currently being examined in preliminary clinical trials (Yusuf-Makagiansar *et al.*, 2002).

1.2.1.3 *Inhibition of lymphocyte proliferation*

The inhibition of lymphocyte proliferation was one of the earliest immunosuppressive strategies developed and began with the use of total body irradiation that non-selectively destroyed rapidly dividing cells (Kahan, 2003). It was a successful but highly problematic procedure in that it resulted in severe bone marrow depletion and the development of serious infections. The experiments of Schwartz *et al.* heralded the beginning of the chemotherapeutic era of inhibition of lymphocyte proliferation (Schwartz *et al.*, 1959). They observed that treatment with 6-mercaptopurine, an inhibitor of purine synthesis, prolonged skin graft suvival in rabbits. However, the use of 6-mercaptopurine and azathiopurine, its imidazole derivative is associated with toxicity. Since then newer anti-proliferative chemicals

such as mycophenolate mofetil, a synthetic analogue of mycophenolic acid, have achieved FDA approval and exhibit significantly more selectivity and potency (van Mourik and Kelly, 2001).

1.2.1.4 *Inhibition of cytokine production and signalling*

A more selective approach to inhibit lymphocyte proliferation was soon developed that targeted cytokine production and signalling pathways. Agents that target these pathways have been discovered by screening the natural products of micro-organisms. Targeting cytokine signalling pathways with these agents has heralded much success in organ transplant. The discovery of cyclosporine A (CsA) revolutionised transplant medicine (Borel *et al.*, 1976; Calne *et al.*, 1978). Following its discovery, subsequent studies revealed that CsA inhibits key steps in the cytokine signal-transduction pathways required for the activation of T-cells (Borel *et al.*, 1976). The application of CsA in post-transplant treatment, to prevent and treat graft rejection following transplantation, dramatically improved the survival rates of both solid and bone-marrow transplants. The discovery of CsA dramatically highlighted the potential of targeting signalling cascades in immunosuppression, cancer and infectious disease treatment. CsA will be discussed in further detail in Section 1.2.2.

In an effort to reduce the toxicity associated with the inhibition of cytokine signalling, a newer more specific approach has recently been developed to block the activity of the CD28 co-stimulation molecule. This has been achieved using monoclonal antibodies (MAbs) against the B7.1 and B7.2 ligands for CD28 (Vincenti, 2003). Another approach to interrupt co-stimulation has been developed which involves the MAb-mediated activation of an inhibitory co-stimulatory receptor CTLA-4 (Hwang *et al.*, 2002). However, one drawback of targeting the cytokine signalling network is the diverse effects of such regimes on different T-cell subsets, in particular the Tregs which depend on IL-2 for their development (Bayer *et al.*, 2005). In addition, many of these therapies have a broad spectrum of molecular targets found in both lymphoid and non-lymphoid cells and activated versus quiescent cells. Looking to the future, molecules that are only upregulated on activated lymphocytes are being identified as potential targets. These include the

lymphocyte specific tyrosine kinase LCK and Jak3 (Saemann *et al.*, 2004; Waegell *et al.*, 2002).

1.2.2 Cyclosporin A and Calcineurin

1.2.2.1 *Cyclosporin A as an immunosuppressive agent*

Cyclosporin A (CsA) is a cyclic polypeptide consisting of 11 amino acids and a metabolite of the fungus *Beauveria nivea* (Borel *et al.*, 1976). The drug suppresses the immune system and prevents graft rejection by blocking intermediate steps in signal transduction pathways required for T cell activation. The primary event leading to the activation and differentiation of mature T-cells into effector cells is the activation of the TCR by its specific antigenic ligand. This triggers downstream signalling pathways that lead to the induction of cytokine gene transcription and cytokine receptor upregulation and activation, the end result being T-cell differentiation and proliferation of the T-cells. CsA acts to inhibit TCR signalling, the primary signal in T-cell activation and a pre-requisite to T-cell differentiation into effector cells and proliferation, and therefore its discovery and application to the treatment of graft rejection has revolutionised the word of organ transplant (Calne *et al.*, 1978). It is a lipophilic agent capable of crossing most biological membranes and the metabolism of CsA starts in the gastrointestinal tract and continues in the liver (Vickers, 1994). CsA suppression of T-cell occurs through a number of discrete steps leading to an association with the intracellular binding protein, cyclophilin A, which is a member of the immunophilin family of proteins (High *et al.*, 1994). This forms the protein/drug complexes that are the active *in vivo* agents (Cardenas *et al.*, 1995). X-ray crystallography analysis have elucidated that in the cyclophilin/CsA complex, one side of the CsA ring fits into a cleft on cyclophilin while the opposite side of the CsA ring is free to associate with the target of CsA, calcineurin (Pflugl *et al.*, 1993).

1.2.2.2 *Calcineurin*

Calcineurin is a Ca^{2+}-calmodulin activated serine and threonine specific protein phosphatase that is conserved in all eukaryotes. Calcineurin is unique among phosphatases for its ability to sense Ca^{2+} through its activation by calmodulin and has

been shown to be a major player in Ca^{2+} dependent eukaryotic signal transduction pathways (Clipstone and Crabtree, 1992; Liu *et al.*, 1991). Antigen recognition by the TCR leads to an increase in intracellular calcium and leads to the formation of Ca^{2+}-calmodulin complexes, which bind to calcineurin and lead to its activation (Crabtree, 1999). Calcineurin has a wide tissue distribution in mammals and is composed of a catalytic subunit, calcineurin A (CNA), and a regulatory subunit, calcineurin B (CNB) which binds Ca^{2+}(Rusnak and Mertz, 2000). Studies have shown the existence of 3 distinct genes encoding the α, β and γ isoforms of calcineurin A in mammalian tissues (Sugiura *et al.*, 2001). The α and β isoforms are ubiquitously distributed, while the γ isoform is restricted to testis tissue. In addition there are two isoforms of the regulatory subunit, calcineurin B, α and β (Chang *et al.*, 1994).

CNA itself is comprised of four regions, a catalytic domain (residues 70-333), a CNB binding segment (residues 348-368), a calmodulin-binding segment (residues 391-414), and a C-terminal autoinhibitory helix (residues 468-490) (Martinez-Martinez and Redondo, 2004). Figure 1.2 (a) illustrates the conserved domains of CNA and CNB. In an unstimulated cell, calcineurin forms a CNA/CNB heterodimer. Stimulation causes an increase in intracellular Ca^{2+}, which activates Calmodulin (CaM) and CNB to bind to Ca^{2+}. This leads to a conformational change and the displacement of the C-terminal autoinhibitory domain within the CNA catalytic subunit, facilitating access for a substrate to bind and become dephosphorylated (Jin and Harrison, 2002). (Figure 2.1 (b)). Activation of calcineurin leads to transcription of the IL-2 gene. The mechanism of this regulation is attributed to the NFAT family of transcription factors (Jain *et al.*, 1995) and has already been addressed in Section 1.1. In the presence of CsA, IL-2 production is inhibited; the CsA-cyclophilin complex binds to the interface between the A and B subunits, lying over the active site so access to the catalytic residues by a protein substrate is blocked (see Figure 2.1 (b)), (Cardenas *et al.*, 1995). It has been demonstrated that while CsA can inhibit the production of IL-2 induced in T-cells activated through the TCR alone or through TCR/CD28 activation, that CD28 signal transduction is resistant to the inhibitory effects of CsA. Studies have demonstrated

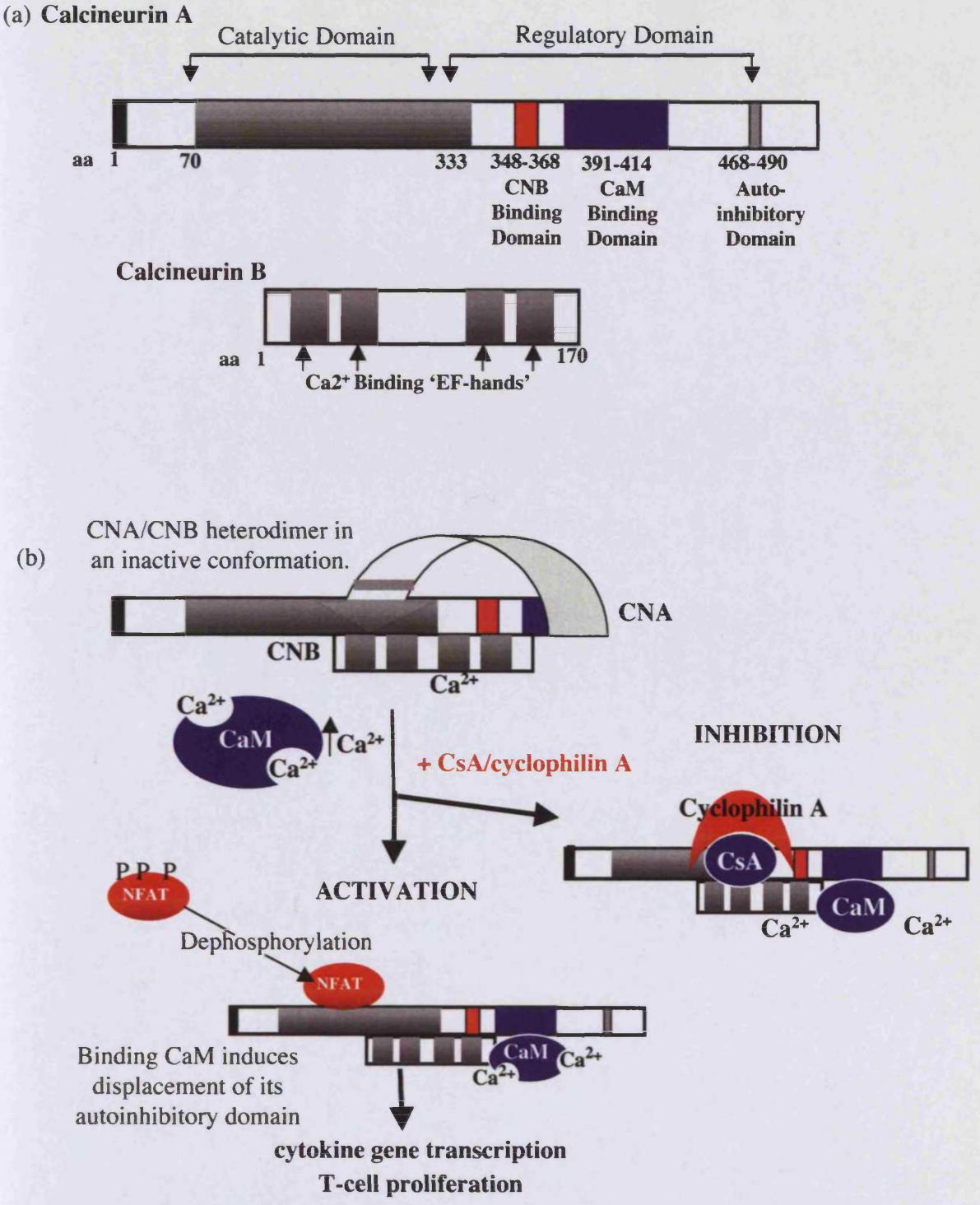

Figure 1.2 The Calcineurin complex structure and function

(a) Functional domain organisation of CNA and CNB subunits. (b) In an unstimulated cell, calcineurin forms a CAN/CNB inactive heterodimer, A stimulation such as antigen recognition by the TCR, causes an increase in intracellular Ca^{2+}, which activates calmodulin (CaM) and CNB to bind to Ca^{2+}. Activated CaM binding to calcineurin leads to a conformational change and the autoinhibitory domain of CNA moves away from the catalytic active site, opening access for NFAT to bind and become dephosphorylated. NFAT then translocates to the nucleus and initiates cytokine gene transcription and cell proliferation. In the presence of CsA/cyclophilin, access to the catalytic site is blocked, inhibiting the dephosphorylation of NFAT (adapted from Martinez-Martinez *et al.*, 2004).

that proliferation of TCR/CD28 activated T-cells in the absence of IL-2R activation was insensitive to the inhibitory effects of CsA upon initial activation, but sensitive to CsA inhibition at later timepoints (Boonen *et al.*, 1999). This indicates that CD28 is involved in initial proliferation of T-cells and that IL-2 is required for sustained proliferation.

1.2.2.3 *Alternatives to CsA treatment*

Despite the central importance of CsA in organ transplant, its toxic effects may render it unsuitable in some post-transplant situations (Lucan *et al.*, 2004). CsA only inhibits calcineurin completely at doses that are extremely toxic to the patient. The major toxic effects are nephrotoxicity, hypertension, neurotoxicity, diabetes and gastrointestinal disorders (Martinez-Martinez and Redondo, 2004). The wide distribution of calcineurin about the body is one explanation for the widespread toxic effects of CsA. Some of the side-effects may be independent of calcineurin inhibition and instead due to the impairment of the physiological function of the immunophilins to which CsA binds (Clarke *et al.*, 2002). In an attempt to address this problem, Wenger *et al.* generated structurally distinct analogues of CsA but none had reduced toxicity (Wenger, 1986). Lowering CsA dose results in partial inhibition of calcineurin which can lead to abnormal and potentially destructive cytokine production that can initiate the rejection of the allograft (Moien-Afshari *et al.*, 2003). Treatment with CsA may also prevent possible tolerance of an allograft because the inhibition of IL-2 production may prevent the IL-2 dependent development of Tregs (Malek and Bayer, 2004).

FK506 (tacrolimus) was a second drug discovered in screens for agents that would block lymphocyte proliferation, and it too improved transplant medicine. Its use in the clinic led to a dramatic improvement in post-transplant survival rates. FK506 is a macrocyclic lactone antibiotic and a natural fungal product. Like CsA, FK506 inhibits the protein phosphatase calcineurin (Schreiber and Crabtree, 1992). Both CsA and FK506 are hydrophobic drugs that are thought to diffuse across the plasma membrane and form complex with immunophilin proteins. However they are

chemically different immunosuppressant drugs that bind to discrete immunophilin proteins. In contrast to CsA, which binds to the immunophilin cyclophin A, FK506 forms a complex with the immunophilin FKBP12, which then binds to and inhibits calcineurin (Brazelton and Morris, 1996). The drug-immunophilin complexes formed have a large surface area of interaction with their calcineurin target, and bind with a specificity equivalent to growth factor interactions. Neither drug alone blocks the activity of the calcineurin enzyme and it is the drug-immunophilin complex that is the active in vivo agent. Although both drugs bind to the same target, FK506 is unrelated in structure to CsA. Unlike the CsA/Cyclophilin A comples, neither FK506 nor FKBP12 interacts directly with the active site of calcineurin, rather the immunophilin is positioned so that substrates are unable to gain access to it (Jin and Harrison, 2002). FK506 causes a similar degree of nephrotoxicity to CsA, and like CsA, can render the patient susceptible to infections and malignancies, especially lymphomas (Starzl *et al.*, 1990). Following on the discovery of CsA and FK506, more recent studies have focused on the generation of peptides containing NFAT sequences involved in interaction with calcineurin, to prevent the activation of NFAT, which would achieve a more selective and less toxic outcome (Kiani *et al.*, 2000). Additionally, endogenous cellular inhibitors such as the 79kDa protein kinase A anchoring protein AKAP79 (Coghlan *et al.*, 1995), Calcineurin Homologous Protein (CHP) (Lin and Barber, 1996) and Down's Syndrome critical region 1 (DSCR1) (Fuentes *et al.*, 2000) protein bind to calcineurin and inhibit its phosphatase activity. Further developments into the mechanisms by which these endogenous proteins inhibit calcineurin will be important to elucidate the role of calcineurin and NFAT in the development of disease. Ultimately, the development of more selective inhibitors of calcineurin and NFAT may generate a less toxic immunosuppressive regime.

1.2.3 Rapamycin and Mammalian Target of Rapamycin

1.2.3.1 *Rapamycin as an immunosuppressive agent*

Rapamycin, discovered through analysis of soil samples isolated from Easter Island, is a lyphophilic macrolide produced by a strain of *Streptomyces*

Hygroscopicus (Sehgal *et al.*, 1975; Vezina *et al.*, 1975). The work of Calne *et al.*, established rapamycin's role in the clinic and this natural microbial product has potent immunsuppressive activity (Watson *et al.*, 1999) at doses lower than CsA. The drug has gained approval for the prophylaxis treatment of renal transplant rejection as an adjunctive to CsA and, unlike CsA, rapamycin is not associated with nephrotoxicity but administration to transplant patients is associated with other side-effects (van Mourik and Kelly, 2001).

Rapamycin exerts its immunosuppressive effect in a mechanism that is distinct from CsA. Where CsA results in the prevention of IL-2 production through the interruption of TCR signalling, rapamycin results in impaired IL-2 signalling through interruption of the IL-2 receptor signalling pathway (Figure 1.1). Rapamycin blocks the downregulation of the cell cycle protein inhibitor $p27^{kip1}$ induced by IL-2. With regard to CD28 signalling it has been demonstrated that in contrast to CsA, rapamycin partially inhibits IL-2 production initiated through CD28 signalling pathways, CD28 induced downregulation of $p27^{kip1}$ and proliferation (Boonen *et al.*, 1999). Early studies of the effects of rapamycin in *Saccharomyces cerevisiae* identified the 12 kDa immunophilin FKBP-12 as its intracellular receptor (Stan *et al.*, 1994). It is this FKBP-12/drug complex that is the functional immunosuppressant *in vivo* and numerous studies over the years have identified homologous targets for the FKBP-12/rapamycin complex in yeast and mammals (Abraham and Wiederrecht, 1996; Jacinto and Hall, 2003).

1.2.3.2 *Mammalian Target of Rapamycin*

Such targets have been named target of rapamycin (TOR) proteins (Abraham and Wiederrecht, 1996). TOR, a 289 kDa serine/threonine kinase and a member of the phosphoinositide-kinase related kinase (PIKK) family, is accepted as a central mediator of nutrient and growth factor signalling (Bjornsti and Houghton, 2004). TOR is involved in the activation of p70 S6Kinase ($p70^{S6K}$) which is required for the phosphorylation of the 40s ribosomal subunit of S6, necessary to permit translation and cell cycle progression (See Figure 1.3 (b)) (Powers and Walter, 1999). The S6K signalling pathway, in many cells, is triggered by the recruitment of PI3K to the

activated receptor and the production of PIP_3. A key event in the activation of S6K is the phosphorylation of the T389 residue in its linker domain and while a number of kinases have been implicated, TOR is one of the most potent kinases to phosphorylate T389 (Powers and Walter, 1999). In the presence of rapamycin the phosphorylation of the T389 residue by TOR is prevented and this results in a prolonging of G1 transit times in the cell cycle and an inhibition of T-cell proliferation.

Mammalian TOR (mTOR) was first identified and cloned shortly after the discovery of the two yeast genes, TOR1 and TOR2, in the budding yeast *Saccharomyces cerevisiae* (Abraham and Wiederrecht, 1996). In addition to phosphorylation $p70^{S6K}$, mTOR also phosphorylates and inactivates 4E-BP1 (Figure 1.3 (b)), a repressor of mRNA translation and a key factor in cell cycle regulation (Hay and Sonenberg, 2004). Mammalian genomes encode a single TOR protein with approximately 42% amino acid sequence homology to the yeast TOR proteins. The mTOR proteins contain several distinct and conserved structural domains, illustrated in Figure 1.3 and are 2549 amino acids in length. The C-terminal contains the kinase domain and mTOR is phosphorylated at serine 2481 via the PI3K pathway and is autophosphorylated via intrinsic serine/threonine kinase activity (Peterson *et al.*, 2000). The regulation of mTOR by growth factors is through the PI3K pathway. PIP_3 recruits Akt to the membrane where it is phosphorylated by PDK1. Activataed Akt phosphorylates TSC2 resulting in the inhibition of the TSC1/2 complex. Rheb is a small GTPase that is inactivated by TSC1/2 and is a positive regulator of mTOR (Li *et al.*, 2004a; Li *et al.*, 2004b). In mammals, mTOR forms a complex with regulatory associated protein of TOR, raptor (jaHara *et al.*, 2002) and mLST8 and this complex is the mammalian equivalent of yeast TOR complex 1 (Jacinto and Hall, 2003). Evidence suggests that raptor functions as an adaptor or scaffolding protein leading to the recruitment of the mTOR substrates $p70^{S6K}$ and 4E-BP1 (Beugnet *et al.*, 2003). The binding domain of mTOR has been mapped to amino acids 2025-2114 a 90 amino acid region just upstream of the lipid kinase domain, containing a critical serine residue S2035 (McMahon *et al.*, 2002) which is homologous to serine 1972 and serine 1975 of yeast TOR1 and TOR2 respectively.

These residues are required for the FKBP12-rapamycin inhibition of TOR (Stan *et al.*, 1994). The binding of rapamycin/FKBP12 to the FRB domain causes dissociation of scaffolding proteins from mTOR and prevents the recruitment and activation of mTOR substrates to the protein, and prolongs G1 cell cycle progression (Figure 1.3 (b)).

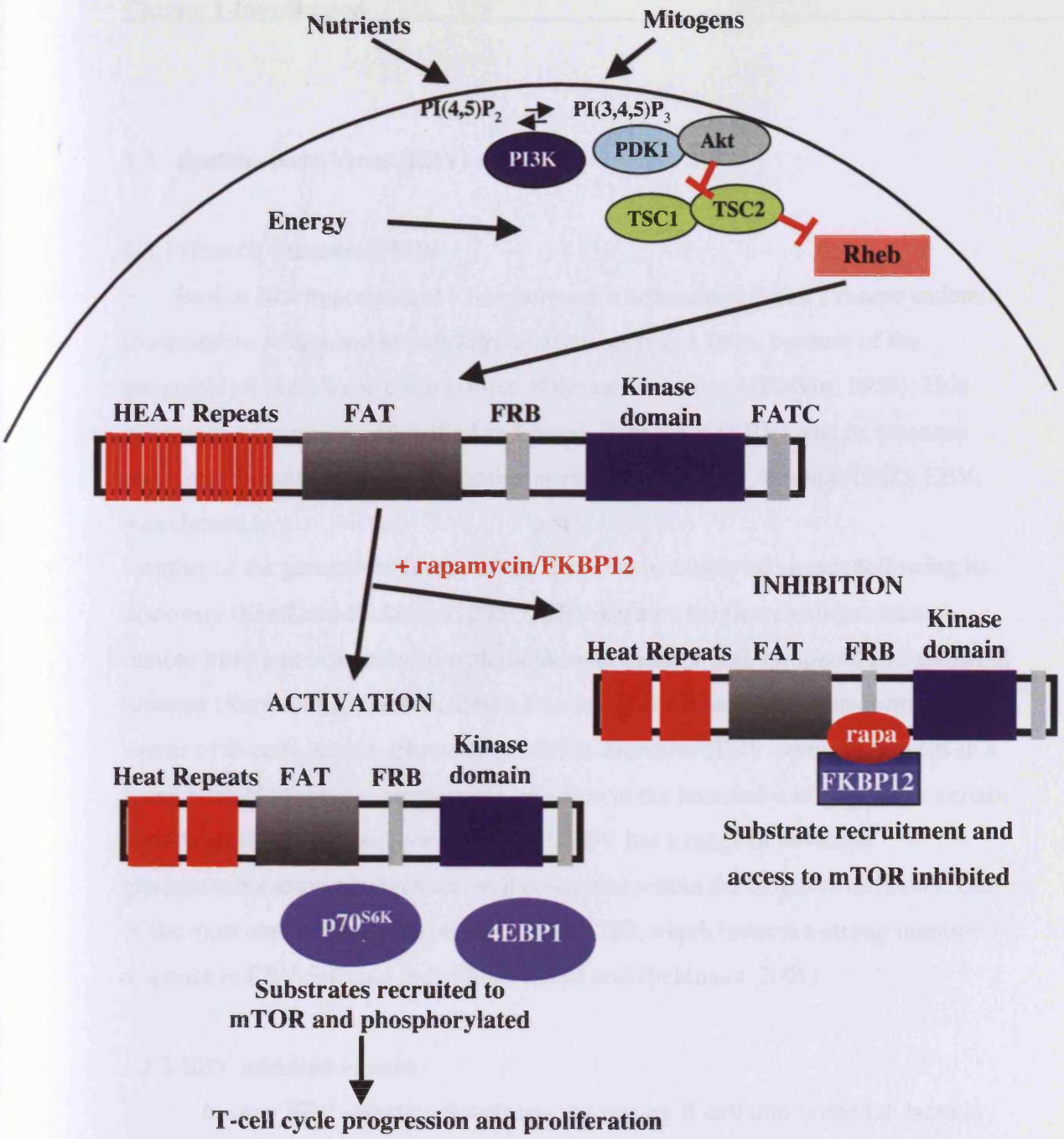

Figure 1.3 mTOR structure and function

The functional domains conserved in TOR proteins are depicted, including the N-terminal 20 tandem HEAT repeats, the central FAT domain, FKBP12-rapamycin binding domain (FRB), the kinase domain and the FATC domain. mTOR activity is regulated by mitogens, nutrient levels and energy levels in the cell. The regulation of mTOR by growth factors is through the PI3K pathway. PIP_3 recruits Akt to the membrane where it is phosphorylated by PDK1. Activataed Akt phosphorylates TSC2 resulting in the inhibition of the TSC1/2 complex. Rheb is a small GTPase that is inactivated by TSC1/2 and is a positive regulator of mTOR (Li *et al.*, 2004). Substrates such as $p70^{S6K}$ and 4EBP1 are recruited to mTOR by scaffolding proteins such as raptor and mLST8. The substrates gain access to the kinase domain of mTOR and become phosphorylated leading to a host of downstream signalling events and cell cycle proliferation. The binding of rapamycin/FKBP12 to the FRB domain causes dissociation of scaffolding proteins from mTOR, prevents the recruitment and activation of mTOR substrates to the protein, and prolongs G1 cell cycle progression

1.3 Epstein-Barr Virus (EBV)

1.3.1 General features of EBV

Burkitt first hypothesised a link between a common children's cancer endemic to equatorial Africa and an aetiological agent such as a virus, because of the geographical and climatic similarities of the cases involved (Burkitt, 1958). This agent was subsequently identified as Epstein-Barr Virus (EBV), and its presence confirmed in cultured tumour biopsies *in vitro* (Epstein and Achong, 1968). EBV was classed as a
member of the gamma subfamily of the herpesvirus family of viruses following its discovery (Kieff and Rickinson, 2001). EBV became the first candidate human tumour virus and is associated with the development of both lymphoid and epithelial tumours (Kieff and Rickinson, 2001). It is one of the most potent transforming agents of B-cells *in vitro* (Rowe *et al.*, 1992). However, EBV normally persists in a latent state of lifelong asymptomatic infection in the host and it is only under certain conditions that it has oncogenic potential. EBV has a range of envelope glycoproteins some of which are well conserved within the herpesvirus family. One of the most abundant glycoproteins is gp350/220, which induces a strong immune response in EBV-infected individuals (Kieff and Rickinson, 2001).

1.3.2 EBV infection *in vitro*

In vitro EBV infection transforms the resting B-cell into immortal, latently infected, lymphoblastoid cell lines (LCL) (Kieff and Rickinson, 2001). Human complement receptor type 2 (CD21) is the cellular receptor for EBV (Prota *et al.*, 2002). The N-terminal two short consensus repeats (SCR1-SCR-2) of the receptor interact with gp350/220. Infection is initiated by adsorption of the envelope glycoprotein gp350/220 to the CD21 receptor on the B-cell plasma membrane and aggregation of CD21 in the membrane. EBV-induced aggregation of CD21 triggers downstream signalling events that are proposed to prepare the cell for EBV infection (Thompson and Kurzrock, 2004). Internalisation of the virus into the cytoplasmic vesicles follows (Nemerow and Cooper, 1984). Upon entry into the nucleus the EBV

genome circularizes and exists as an episome. EBV genome circularization precedes or coincides with earliest viral gene expression (Alfieri *et al.*, 1991).

The *in vitro* generated LCL lines display a latency III pattern of gene expression, characterised by the expression of a panel of 11 EBV gene products that contribute to the generation of the immortal LCL (Rickinson and Kieff, 2001). These gene products include 2 EBV-encoded RNAs; EBER-1 and EBER-2, 6 EBV nuclear antigens; EBNA 1, 2, 3A, 3B, 3C, and 3 latent membrane proteins; LMP-1, 2A and 2B (Rickinson and Kieff, 2001). Transcripts from the BamHI A region of the EBV genome (BART transcripts) have also been detected in LCLs but their products have yet to be identified (Young and Rickinson, 2004). The generation of latency III LCLs following infection of primary B-cells with EBV has become a powerful *in vitro* model of EBV latent infection. LCLs also contain a small fraction of cells that have spontaneously switched into lytic cycle but virus replication in LCLs is usually minimal or undetectable (Rowe *et al.*, 1992). As a result, deciphering the biology of the infection is difficult *in vitro*.

1.3.3 EBV infection *in vivo*: lifelong persistence

EBV is an extremely successful herpesvirus in that it infects greater than 95% of the world population and establishes lifelong persistent infection in memory B-lymphocytes (Rickinson and Kieff, 2001). Primary infection, transmitted via saliva (Gerber *et al.*, 1972), is usually contracted early in childhood and is generally asymptomatic (Rickinson and Kieff, 2001). EBV infection of B-cells *in vivo* results in at least three different latency states; III, II and I (See Figure 1.4) and a lytic state (Thorley-Lawson, 2001). The lifelong persistence of the virus *in vivo* is attributed both to this latency programme and to the lytic state, which steadily produces infectious virus to be shed into saliva (Thorley-Lawson, 2001).

EBV uses its latent proteins to provide signals to the infected B-cell that cause it to become activated and then differentiate into a resting memory B-cell (Hochberg *et al.*, 2004). Initial EBV infection of a B-cell causes transformation to a proliferating B-cell blast due to the expression of the latency III growth programme (Rowe *et al.*, 1992). These latency III cells are susceptible to attack by the immune

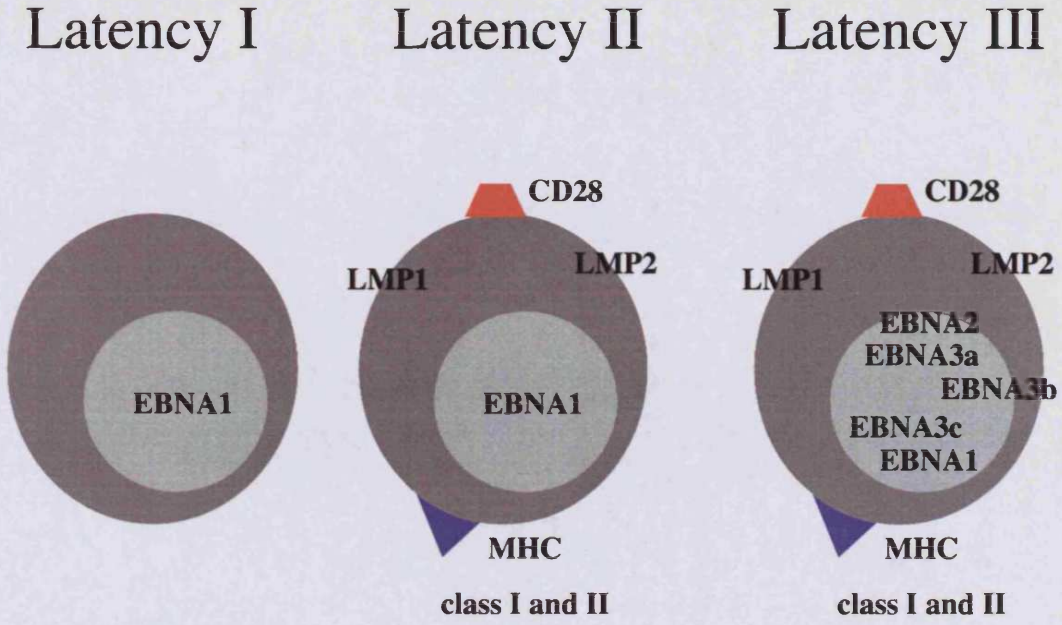

Figure 1.4 EBV antigen expression in different latency type

Latency I type cells express EBNA1 without the expression of other latent antigens, which makes the cell 'invisible' for EBV-specific T-cells. This pattern of expression is seen in Burkitt;s lymphoma. Latency II type cells have a restricted expression pattern of EBNA1 and LMP1/LMP2. The upregulation of MHC class I and II and CD28 increases the immunogenicity of the cells. This pattern of expression is seen in Hodgkin's lymphoma and Nasopharyngeal carcinoma. *In vitro* generated LCLs and lymphoproliferative tumours of immunocompromised patients display the full array of EBV antigens and are highly immunogenic (figure adapted from Straathorf *et al.*, 2003).

system. The B-cell blast enters the follicles and expands to form a germinal centre where the pattern of gene expression is restricted to EBNA-1, LMP1 and LMP2 (Thorley-Lawson, 2001). The infected B-cells then differentiate to a memory phenotype but the precise mechanism is controversial. It has been suggested that these cells are directed to differentiate into memory cells due to the expression of a more limited set of genes, in the latency II gene programme (Thorley-Lawson, 2001). These latency II cells then leave the follicle to circulate in the periphery and the expression of genes becomes even more restricted (Thorley-Lawson, 2001). Viral persistence arises because the main EBV antigens are no longer expressed and the cells are hidden from the immune system (Tierney *et al.*, 1994). Occasionally, a small proportion of latent memory cells are re-activated to enter the lytic state and initiate replication of the virus (Keating *et al.*, 2002). This results in the production of virus, which is shed in saliva and can then infect more cells.

1.3.3.1 EBV-specific CTLs

The proliferation of the latency III cells infected B-cells, coupled with the occasional reactivation of the B-cells to produce infectious virus can increase the numbers of virus-infected cells. However, latency III B-cells and lytic virus producing B-cells are susceptible to attack by EBV-specific CTLs. The equilibrium between the various infection states and clearance by host CTLs is central to EBV persistence in the immunocompetent host. The EBV specificity of the $CD8^+$ CTLs was long debated until the existence of CTLs specific for the immunodominant EBV latent epitopes such as EBNA 3A, 3B and 3C was confirmed (Steven *et al.*, 1996). Further studies demonstrated immunogenicity of immediate early and early lytic cycle protein (Bogedain *et al.*, 1995; Steven *et al.*, 1996). Analysis of LCL-stimulated bulk CTL lines indicated a hierarchy of immunodominance, with EBNA 3A, 3B and 3C being the most immunodominant, followed by LMP-2 and finally EBNA-2, EBNA-LP and LMP1 (Rickinson and Moss, 1997). Responses to EBNA-1 in these CTL lines were very weak and what determines this immunodominant hierarchy is unclear (Khanna *et al.*, 1992).

1.3.4 EBV-associated disease in immunocompetent hosts

Primary EBV infection is generally asymptomatic when contracted in childhood. However, contraction of EBV in adolescence or adulthood can result in Infectious Mononucleosis. This is a self-limiting lymphoproliferative disease, brought under control by a massive T-cell response, which leads to resolution of symptoms and the development of viral persistence after a few weeks (Rickinson and Kieff, 2001). EBV infection does not always lead to lifelong benign persistence. The ability of EBV to initially transform a naïve B-cell to a blast phenotype indicates that this virus has the potential to promote the development of tumours in certain circumstances and since its discovery as the first human tumour virus, EBV has been implicated in the developments of a wide range of cancers. The risk is particularly high when the normal surveillance of EBV-infected cells by CTLs is dysregulated and this can lead to the development of B-cell lymphomas (Ambinder, 1990). The best studied of these B-cell lymphomas are Burkitt's lymphoma and Hodgkin's disease. Evidence points towards a role for EBV in both malignancies (Faumont *et al.*, 2004; Kennedy *et al.*, 2003). EBV has also been associated with the development of T-cell and NK cell lymphomas (Kanegane *et al.*, 2002; Kwong *et al.*, 1997).

1.4 Post-Transplant Lymphoproliferative Disorders and Treatment Options

1.4.1 Post-Transplant Lymphoproliferative Disorders

1.4.1.1 EBV and Post-Transplant Lymphoproliferative Disorders

EBV is also associated with the development of lymphomas in the immunocompromised host. One such example is the heterogenous group of lymphoproliferative disorders collectively known as Post-Transplant Lymphoproliferative Disorders (PTLD) (Paya *et al.*, 1999). The abnormal lymphoid proliferations are of B-cell origin and range in diversity from benign mononucleosis like disease to potentially more aggressive lymphomas (Young and Murray, 2003). Nearly all PTLDs are associated with EBV and can be of clonal or polyclonal morphology (Loren *et al.*, 2003). The majority of the EBV positive PTLD show the latency III pattern of gene expression and appear to represent the *in vivo* version of

immortalized LCLs *in vitro* (Young and Murray, 2003). Heterogeneity of the disorder is evident even at the genomic level. There is often heterogeneity of viral expression within single lesions of PTLD and the proportion of latency III antigens presented can vary (Rowe *et al.*, 1998).

Successful maintenance of an allograft post-transplant requires prolonged administration of immunosuppressive agents to impair normal lymphocyte function. These immunosuppressive regimes impair the function of EBV-CTLs and loss of normal control over EBV-infected B-cells leads to B-cell proliferation and the onset of PTLD (Haque *et al.*, 2002). The immunosuppressive drugs CsA and FK506 have been implicated in the formation of these EBV-associated lymphomas (Nalesnik *et al.*, 1988). CsA has also been implicated in the promotion of EBV-lytic B-cells and the expression of IL-6, an EBV paracrine growth factor, which may contribute to the onset of PTLD (Tanner and Alfieri, 1996).

1.4.1.2 Risk factors involved and general outcome of PTLD

Both solid organ and bone marrow transplant (BMT) recipients are at risk of developing the disorder. BMT recipients' risk of developing PTLD can be as high as 25% particularly if the patient is receiving mismatched bone marrow that has been depleted of T-cells (Gross and Loechelt, 2003) and this risk is highest in the first six to twelve months post-transplant (Heslop *et al.*, 2004). PCR based assays that measure viral load in peripheral blood or serum are powerful aids to monitor the EBV levels in the patient. The EBV in the case of a BMT recipient is usually of donor origin because the patient often undergoes total body irradiation before transplant. The risk factors for the development of PTLD following BMT recipients generally include; T-cell depletion, HLA mismatch and BMT for a primary immunodeficiency disorder (Gross and Loechelt, 2003; Gross *et al.*, 1999).

The incidence of PTLD can vary in solid organ recipients from 1-15% (Durandy, 2001) and the EBV is usually of recipient origin indicating a reactivation of latent virus (Loren *et al.*, 2003). PTLD is more common following lung and small bowel transplants than renal, heart or liver transplants because the

immunosuppressive dose is higher in lung and bowel transplants. The risk in solid organ transplant is also highest in the first six to twelve months post-transplant. However, PTLD in solid organ transplant can develop years after transplant because the patient usually undergoes lifelong immunosuppression (Heslop *et al.*, 2004). The risk factors for the onset of PTLD in solid organ recipients include; an EBV negative recipient of an organ from an EBV-positive donor, development of primary EBV infection post-transplant or reactivation of a latent infection, high immunosuppressive doses and the presence of other viral disease such as CMV (Loren *et al.*, 2003). The risk factors for the onset of PTLD in both BMT and solid organ recipients both highlight the importance of functional EBV-CTL in maintaining control of EBV infected B-cells. Mortality rates for transplant patients who develop PTLD have been reported as high as 40-70% for solid-organ transplants and 90% for recipients of BMT (Loren *et al.*, 2003).

1.4.2 Options for the treatment of PTLD

The rapid increase in the options available to treat PTLD has improved survival rates significantly, however despite recent advances optimal treatment is still quite controversial. Early diagnosis, careful monitoring of the progression of the disorder and a treatment tailored for the patient are crucial in the regression of the disorder. When a single solid legion is evident, the intervention with surgical (Gonthier *et al.*, 1992) or radiation treatment (Koffman *et al.*, 2000) can have positive effects. However, these treatments are limited as PTLD is generally a systemic disorder.

1.4.2.1 *Reduction of immunosuppression*

The reduction of immunosuppression is widely accepted as the primary option to treat PTLD and has heralded successful but variable responses (Starzl *et al.*, 1984; Tsai *et al.*, 2001). Regression of EBV-associated PTLD lesions has been reported in 23-86% of patients (Green *et al.*, 2001). The ultimate goal of this treatment is to re-establish the EBV-CTL population in the host and regain control over EBV infection. However, the withdrawal of immunosuppression is associated with graft rejection in solid organ recipients and graft-versus-host-disease (GVHD) in BMT recipients (Tsai *et al.*, 2001). It has been shown that RAD, a derivative of

rapamycin, has an inhibitory effect on EBV-transformed B-cells (Majewski *et al.*, 2000). Majewski *et al.* suggest that because of its similarities to rapamycin, this drug may play a double-role in transplant as an immunosuppressant and anti-PTLD drug and that increasing the dose rather than reducing the dose could be more beneficial in the treatment of PTLD (Majewski *et al.*, 2000).

1.4.2.2 *Pharmacological Agents, Monoclonal Antibodies and Vaccines*

Early attempts to control PTLD progression used thymidine kinase antiviral drugs such as acyclovir (Davis *et al.*, 1995). Initial reports indicated some success but this evidence was not clarified. It later became apparent that these drugs inhibit replication of herpesviruses such as CMV, however EBV exists as an episome in the nucleus of a latently infected cell rendering these drugs relatively ineffective in the treatment of EBV-associated PTLD (Loren *et al.*, 2003). Antiviral drugs may have a role in preventing lytic B-cells within PTLD lesions from spreading EBV to naïve cells (Green *et al.*, 2001) but generally anti-viral therapy using thymidine kinase inhibitors has limited potential in the treatment of EBV-associated PTLD. Early reports of cytokine therapy using interferon-α have been encouraging and success is attributed to the fact that this cytokine inhibits the growth of EBV-transformed B-cells (Davis *et al.*, 1998).

The use of monoclonal antibodies to inhibit IL-6, which has a role in B-cell growth and proliferation is also being assessed as a potential cytokine therapeutic strategy (Haddad *et al.*, 2001). Another monoclonal antibody, Rituximab, which is an anti-CD20 monoclonal antibody for the inhibition of B-cell growth has been approved for treatment of certain B-cell lymphomas and has potential as a therapy for PTLD (Maloney, 2001). It has been used with a 69% success rate for the treatment of PTLD after BMT or solid-organ transplant (Kuehnle *et al.*, 2000).

EBV vaccine strategies being explored include the induction of gp340 antibodies which will target the viral envelope could prevent primary infection of naïve cells (Cox *et al.*, 1998). One such a vaccine is in Phase I trials but its success has yet to be verified. In addition, Duraiswamy *et al.* recently described the

development of an LMP-based polyepitope vaccine as a tool for the treatment of other EBV associated malignancies such as HD and NPC (Duraiswamy *et al.*, 2003). Such vaccines could prove useful in the induction of a prophylactic humoral or cellular immune response in a transplant patient at risk of developing EBV-associated malignancies.

1.4.3 Cellular immunotherapy to treat PTLD

1.4.3.1 Cellular Immunotherapy in Bone Marrow Recipients

Alternatives to targeting EBV-infected B-cells to treat PTLD are the immunotherapeutic strategies aimed at reconstituting T-cell responses to EBV. The transfer of EBV-specific T-cells to a PTLD patient has proved extremely effective as a therapeutic option (Heslop *et al.*, 2004). This therapy is usually limited to BMT. As the tumours in these BMT cases generally arise in donor cells, the donor is healthy and available to provide matching CTLs. The first reported trial attempted to treat established EBV-associated PTLD in BMT recipients and involved the infusion of unselected populations of donor lymphocytes (Papadopoulos *et al.*, 1994). The response rate of this initial trial was high and five BMT patients with PTLD had disease remission (Papadopoulos *et al.*, 1994). However, the presence of alloreactive T-cells in these donor lymphocyte infusions increased the risk of GVHD development (Porter *et al.*, 1994).

More refined treatments were subsequently developed generating EBV-specific T-cell lines *in vitro* before infusing them into the BMT patient. The generation of these EBV-CTLs involves a number of discrete steps illustrated in the schematic of Figure 1.5, (Straathof *et al.*, 2003). PBMCs are isolated from the donor's blood. Most are frozen but a few are infected with a laboratory strain of EBV. After four to six weeks, an EBV-transformed LCL line, which strongly express latency III EBV antigens, is established (Figure 1.4 (a)). The remaining PBMCs are then thawed and mixed with irradiated LCLs (Figure 1.5 (b)). The small percentage of EBV-CTLs in the PBMCs become activated and begin to proliferate. The culture is stimulated weekly with more irradiated LCLs and IL-2. After a number of weekly

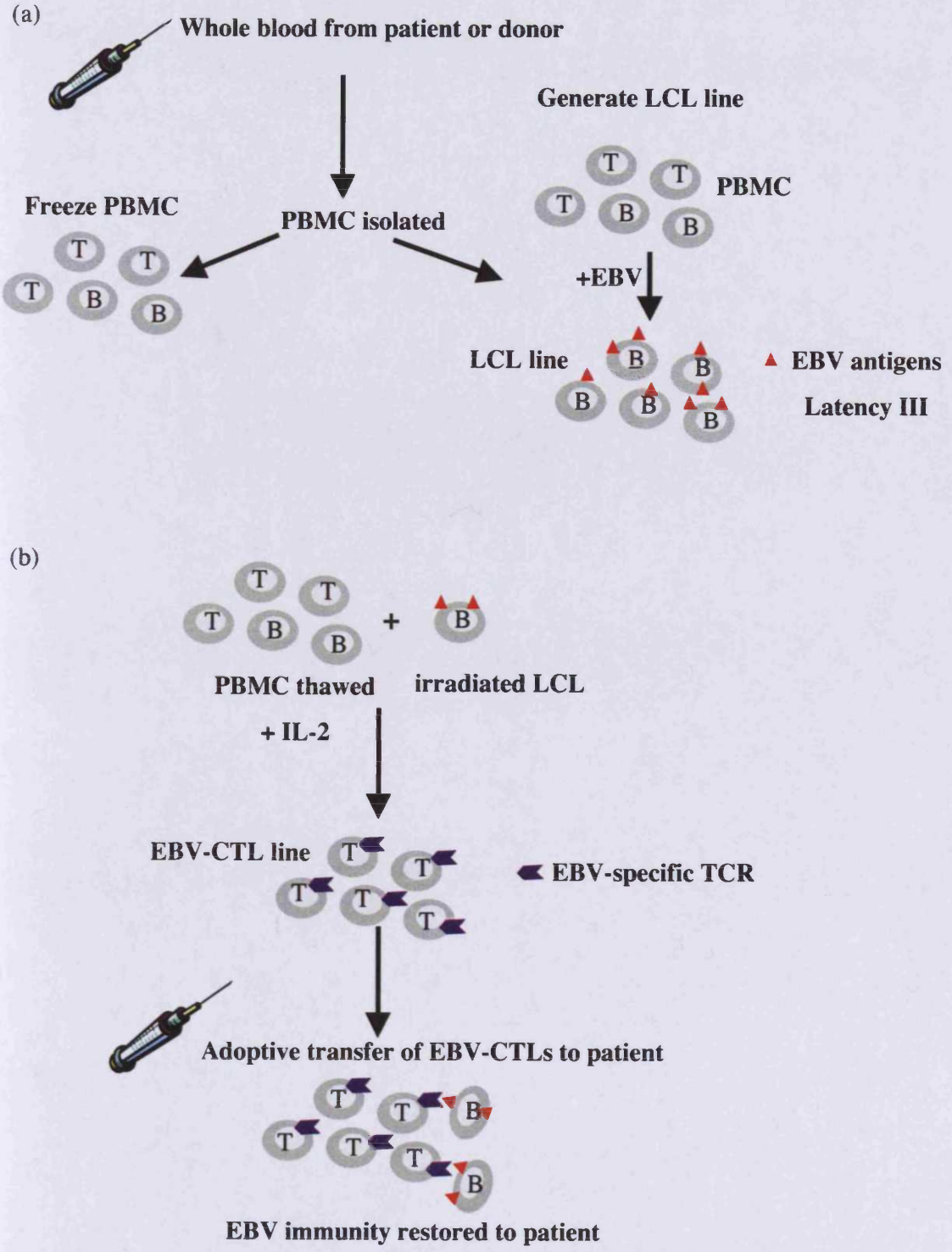

Figure 1.5 The generation of EBV-CTLs for adoptive transfer to transplant patients to treat EBV-associated post-transplant lymphoproliferative disorder

(a) PBMCs are isolated from patient's blood. Most are frozen but some are infected with a laboratory strain of EBV. After 4-6 weeks, an EBV-transformed LCL line is established, expressing a latency III pattern of EBV antigens. (b) The frozen PBMCs are then thawed and mixed with irradiated LCLs. The small percentage of EBV-CTLs in the PBMC mix recognise the EBV antigens and begin to expand. After a number of weekly stimulations, and the addition of IL-2 on discrete timepoints, a large population of polyclonal EBV-CTLs are available and after extensive testing, can be administered back to the patient.

stimulations the culture becomes a large population of polyclonal EBV-CTLs (Straathof *et al.*, 2003).

The success of this treatment in BMT has been dramatically demonstrated (Heslop *et al.*, 1996a; Rooney *et al.*, 1995a). Because the LCLs display a latency III phenotype there are an ideal *in vitro* model of an EBV-infected B-cell *in vivo* (Kieff and Rickinson, 2001). Infusion of these cells into the patient restored cellular immune response against EBV and established populations of CTLs, which persisted for extended periods, retaining their ability to react to antigenic stimulation (Heslop *et al.*, 1996a). Evidence of immune reconstitution has been demonstrated by comparisons of the precursor frequency of EBV-specific T-cells before CTL infusion and one to four weeks after. In one trial, there was a 35-fold median increase in precursor frequency in fifteen patients (Rooney *et al.*, 1998c).

Clinical trials have suggested that this treatment achieves optimal success when used prophylactically to prevent the progression of PTLD in patients with early symptoms (Wagner *et al.*, 2004). Rooney *et al.* have demonstrated the prophylactic potential of this therapy in 58 BMT patients since 1993 (Heslop *et al.*, 2004). None of

the patients developed PTLD in the follow-up period whereas the control patients, who did not receive the prophylactic CTLs had a tumour incidence of 11% (Rooney *et al.*, 1998c). EBV-DNA levels in peripheral blood were quantified prior to infusion and these levels decreased rapidly to undetectable levels post-infusion (Heslop *et al.*, 1996a). (Rooney *et al.*, 1998c). The EBV-specific CTL infusions these patients received were actually polyclonal lines containing both $CD4^+$ and $CD8^+$ cells. Rooney *et al.* suggest that the presence of the $CD4^+$cells is necessary to help establish or maintain the $CD8^+$ T-cell mediated antiviral immunity (Rooney *et al.*, 1998a). It has also been recently demonstrated that these $CD4^+$ T-cells exert specific cytotoxicity via exocytosis possibly with granulysin, the newly discovered cytolytic molecule usually co-expressed with perforin (Sun *et al.*, 2002). These studies may

have an impact on the clinical approaches to optimise adoptive T-cell therapy in BMT recipients.

1.4.3.2 Cellular Immunotherapy in Solid Organ Recipients

The generation of EBV-CTLs for solid organ recipients is complicated by the fact that the donor is usually not available. In addition, PTLD in solid organ recipients are generally of recipient origin, rendering CTLs outgrown from donors PBMCs of limited use. In order to grow autologous CTLs it is necessary to outgrow the lines from the transplant recipient themselves. A complication with this process is the massive immunosuppressive doses the patient is receiving which may impede the generation of the CTLs *in vitro* and their subsequent activity *in vivo*.

However, successful generation of autologous CTLs in patients receiving immunosuppression has been demonstrated (Savoldo *et al.*, 2001). Prophylaxis studies using infusions of these autologous CTLs to solid organ transplant patients have demonstrated an increase in EBV-precursor cells that persisted for about 4 weeks (Savoldo *et al.*, 2001). The effectiveness of this approach has also been verified in established PTLD. Khanna *et al.* demonstrated the efficacy of these CTL in resolving PTLD lymphomas in kidney transplant recipients (Khanna *et al.*, 1999). They treated one patient who had established PTLD, with multiple infusions of *ex vivo* expanded autologous EBV-specific CTLs. PTLD regressed and the frequency of EBV-specific precursors increased, without signs of graft rejection (Khanna *et al.*, 1999). However, the patient developed a secondary PTLD after ten weeks and died despite further CTL infusions. Research into treatment of solid organ patient PTLD is ongoing, and one recently concluded clinical trial in the UK used allogeneic T-cells to treat PTLD in solid organ transplant patients (Haque *et al.*, 2002). This trial involved patients with progressive PTLD that was unresponsive to conventional treatment. The patients were given infusions of partially HLA-matched allogeneic EBV-specific CTLs from a frozen bank of CTLs derived from healthy donors. Of the five patients who completed treatment, three had complete remission of the disorder and two had no clinical response (Haque *et al.*, 2002).

1.4.3.3 *Treatment of other diseases with cellular immunotherapy*

The strategies developed to optimise cellular adoptive therapy of PTLD have been applied in the treatment of other malignancies. Attempts have been made to treat other EBV-related malignancies such as Hodgkin's Disease (HD) with EBV-specific CTLs. The use of EBV-CTLs as a cellular immunotherapy strategy to treat HD is limited by the fact that the EBV antigens have a hierarchy of immunodominancy. A limited number of EBV antigens are expressed in the malignant Reed-Sternberg cells (H-RS cells) of HD with LMP1 and LMP2 being the only potential CTL targets (Herbst *et al.*, 1991). The newly generated EBV-CTLs may be predominantly specific for the more immunogenic EBV antigens such as EBNA-3A. However EBV-specific T-cells have been successfully generated from patients with advanced HD and reinfused to treat the tumour (Roskrow *et al.*, 1998). CTL persistence and efficacy was observed for up to thirteen weeks postinfusion with LMP2 specific activity detected in one of the patients (Roskrow *et al.*, 1998).

Cellular immunotherapy can also be used to treat diseases not generally associated with EBV. The studies of adoptive T-cell therapy to prophylactically treat CMV disease have heralded much success. This therapy is important because the reactivation of CMV infection in BMT patients increases the immuncompromised patients' risk of developing interstitial pneumonia or enteritis (Meyers *et al.*, 1986). The first approved study in humans, to evaluate the efficacy of adoptively transferred T-cells, was performed in BMT patients at risk of developing human cytomegalovirus (HCMV) infection or disease (Riddell *et al.*, 1992b). In addition, the adoptive transfer of autologous HIV-specific T-cells expanded *in vitro* is being developed as a potential adjunct to current drug HIV-therapies (Riddell *et al.*, 2000).

1.4.3.4 *Challenges associated with adoptive T-cell therapy*

As mentioned earlier, the EBV latency III antigens displayed on an infected B-cell have a hierarchy of immunodominance. Most *in vitro* generated EBV-specific CTLs lines display specificity for only two or three epitopes from one or two viral proteins (Gottschalk *et al.*, 2001). Thus, if a tumour mutates an immunodominant viral target antigen it can escape recognition by the infused CTLs and becomes

known as an 'escape mutant'. A deletion in the EBNA-3B antigen has been described which rendered the tumour unresponsive to donor CTL infusion and resulted in the death of a patient with progressive PTLD (Gottschalk *et al.*, 2001). Subsequent analysis revealed that the patient's tumour cells had a mutation in the EBNA3B epitope, rendering the tumour resistant to the donor CTL and this indicates a possible limitation of adoptive T-cell therapy.

There are practical considerations in the generation of the specific T-cell lines *in vitro,* with one of the biggest obstacles being the expense of the strategy. CTL lines need to be grown in specialised facilities adhering to good tissue practice guidelines, making their generation expensive. Strict criteria must be met before the cells can be verified as safe for infusion. The line must possess the donor HLA type; should contain less than 1% B-cells; should be free of contaminating bacteria, fungi and mycoplasma; should have low endotoxin; and should have minimal cytotoxic activity against recipient-derived phytohaemagglutinin-induced lymphoblasts (PHA blasts), a measure of potential graft-versus-host disease (GvHD) activity (Rooney *et al.*, 1998c).

The time required to generate the specific T-cell lines is another practical consideration. The generation of the EBV-CTLs requires two to three months, which is a major drawback if the transplant patient has an aggressive PTLD associated tumour (Bollard *et al.*, 2004). However, antigen loaded DCs which express optimal co-stimulatory signals are now being used in an effort to decrease the time required to generate a CTL line (Rooney *et al.*, 1998b). It has been suggested that the development of a bank of allogeneic EBV-specific CTLs would be potentially useful for a partially matched allogeneic transfer (Heslop *et al.*, 2004) and the remission of PTLD in patients treated with partly matched allogeneic EBV-CTLs from a frozen bank has been reported (Haque *et al.*, 2002).

The fact that the infused CTLs must function in an immunosuppressive environment can also limit the therapy. Immunosuppressive drugs such as CsA and rapamycin may impair the function and longevity of the infused CTLs. Thus large numbers of cells may need to be administered to obtain effective results, adding to

the expense of the therapy. The infusion of supplemental cytokines such as IL-7 (Lynch and Miller, 1994) which promotes naïve T-cell survival, and IL-15 (Lu *et al.*, 2002) which promotes expansion and survival of CTLs, are being studied in an attempt to increase effectiveness and survival of adoptively transferred T-cells. Co-transfer of $CD4^+$ helper T-cells and the *in vivo* administration of IL-2 are also being studied to help prolong the survival of CTLs (Blattman *et al.*, 2003). Optimisation of EBV-CTL adoptive transfer therapy could greatly advance the treatment of tumours in post-transplant and cancer patients.

1.5 The genetic modification of Human T-cells for use in adoptive transfer

1.5.1 Gene Therapy

The strategies mentioned above, involving the modification of co-stimulatory signals and cytokines both *in vitro* and *in vivo*, have resulted in greater numbers of CTLs that survive longer following adoptive transfer. However, the genetic modification of T-cells to improve efficacy and function *in vivo* may be a more attractive option to optimise adoptive transfer therapy. T-cells were the first targets for genetic modification in human gene transfer experiments and the first clinical trial using gene modified T-cells was in 1990 (Blaese *et al.*, 1995). Today there are over three hundred clinical protocols for gene therapy approved (Mountain, 2000).

The key to a successful genetic therapy is the efficient delivery of the gene of either *ex vivo* or *in vivo*. The *ex-vivo* approach involves the genetic modification of the target cells in the laboratory before transplant to the patient. The *in vivo* approach involves the direct administration of a gene transfer vector to the patient. The types of transfer systems in use can be categorised as non-viral or viral (Mountain, 2000). The non-viral approach involved the administration of naked DNA or DNA complexed with cationic lipids or polymers (Alton *et al.*, 1993; Wolff *et al.*, 1992). The viral approach involves the use of viruses which have been adapted to serve as gene delivery vehicles or vectors (Robbins and Ghivizzani, 1998). All T-cell gene transfer studies to date have used an *ex vivo* viral approach to genetically modify the T-cell before adoptive transfer. The most commonly used viral vectors are the

retroviral vectors and more clinical experience has been documented with these vectors than any other. The main vector employed in this approach is a Moloney murine leukemia virus (MoMLV) based retroviral vector (Miller *et al.*, 1990a; Miller *et al.*, 1990b). In order to explain why retroviruses are the preferential vector of choice to genetically modify T-cells, it is first necessary to discuss the retroviruses themselves.

1.5.2 Retroviruses

1.5.2.1 *Discovery of Retroviruses*

Temin and Baltimore first discovered that a group of viruses, capable of permanently alterting the heredity of cells, contained an RNA dependent DNA-polymerase (Baltimore, 1970; Temin and Mizutani, 1970). This became known as retroviral reverse transcriptase. Its discovery suggested a retrograde flow of genetic information from RNA to DNA to protein and gave the retroviruses their name. The retroviruses have a unique lifecycle. The reverse flow of genetic information and the stable integration into the host genome are hallmarks of the retroviruses (Goff, 2001).

1.5.2.2 *Classification of Retroviruses*

This *Retroviridae* family of viruses are a large and diverse group classified on the basis of sequence relatedness of the reverse transcriptases (Gerard *et al.*, 1997). Other criteria such as morphology and presence of accessory genes are also used in classifying the viruses (Goff, 2001). The family is divided into simple and complex retroviruses. The simple viruses are the alpharetroviruses, betaretroviruses and gammaretroviruses (Pringle, 1999). The MLV virus mentioned earlier is a member of the gammaretrovirus genera (Goff, 2001). The complex viruses are the deltaretroviruses, epsilonretroviruses, lentiretroviruses and spumaretroviruses (Pringle, 1999). The simple retroviruses contain the genes *gag, pro, pol* and *env*. The complex retroviruses also contain these genes, but additionally contain genes, which encode a number of small regulatory protein products (Goff, 2001).

1.5.2.3 *Structure of a retrovirus*

The virus is initially assembled as an immature virion containing unprocessed proteins. As retrovirions are budded from the cell surface, the proteins are proteolytically cleaved to release smaller proteins present in the infectious virions (Goff, 2001). After maturation, the virion changes to a spherical and more condensed structure, of about 100 nm in diameter (Goff, 2001). The virion contains the RNA genome of the retrovirus, which is highly condensed in the virion and is coated along its length with viral nucleocapsid (NC) protein (Goff, 2001). This complex is contained within a capsid (CA) protein core, which is a *gag* gene product and the shape of this core varies and determines the genus of the virus (Goff, 2001).

1.5.2.4 *The Retrovirus lifecycle*

1.5.2.4.1 *Virus entry*

A schematic illustrating the retrovirus life cycle, from virus entry into the cell through to viral budding is shown in Figure 1.6. The first step in a retroviral infection is the interaction between a receptor on the cell surface and the envelope protein on the retrovirus surface (Goff, 2001). This is an extremely complex process and the details are not fully understood. The envelope protein is the primary determinant of the type of cell that a retrovirus can infect because it recognises a specific cell surface protein as its viral receptor (Miller and Wolgamot, 1997). Four receptors have been identified for the gammaretroviruses with the ecotropic receptor and the amphotropic receptor being the most studied (Miller and Wolgamot, 1997). The ecotropic receptor is found in all strains of laboratory and wild mice of the *Mus musculus* species (Goff, 2001). The amphotropic receptor, PIT-2, is a 652 amino acid type III sodium phosphate cotransporter and is found in a wide range of mammals including humans (Salaun *et al.*, 2001). The protein is believed to have ten to twelve membrane spanning domains and residues in the extracellular loops two and four have been shown to be important for viral entry (Lundorf *et al.*, 1999). Efficient activation of cell surface PIT-2 molecules is required for efficient amphotropic retroviral infection. Previously it was believed that binding to receptors directly triggers a series of conformational changes in the viral envelope glycoproteins that

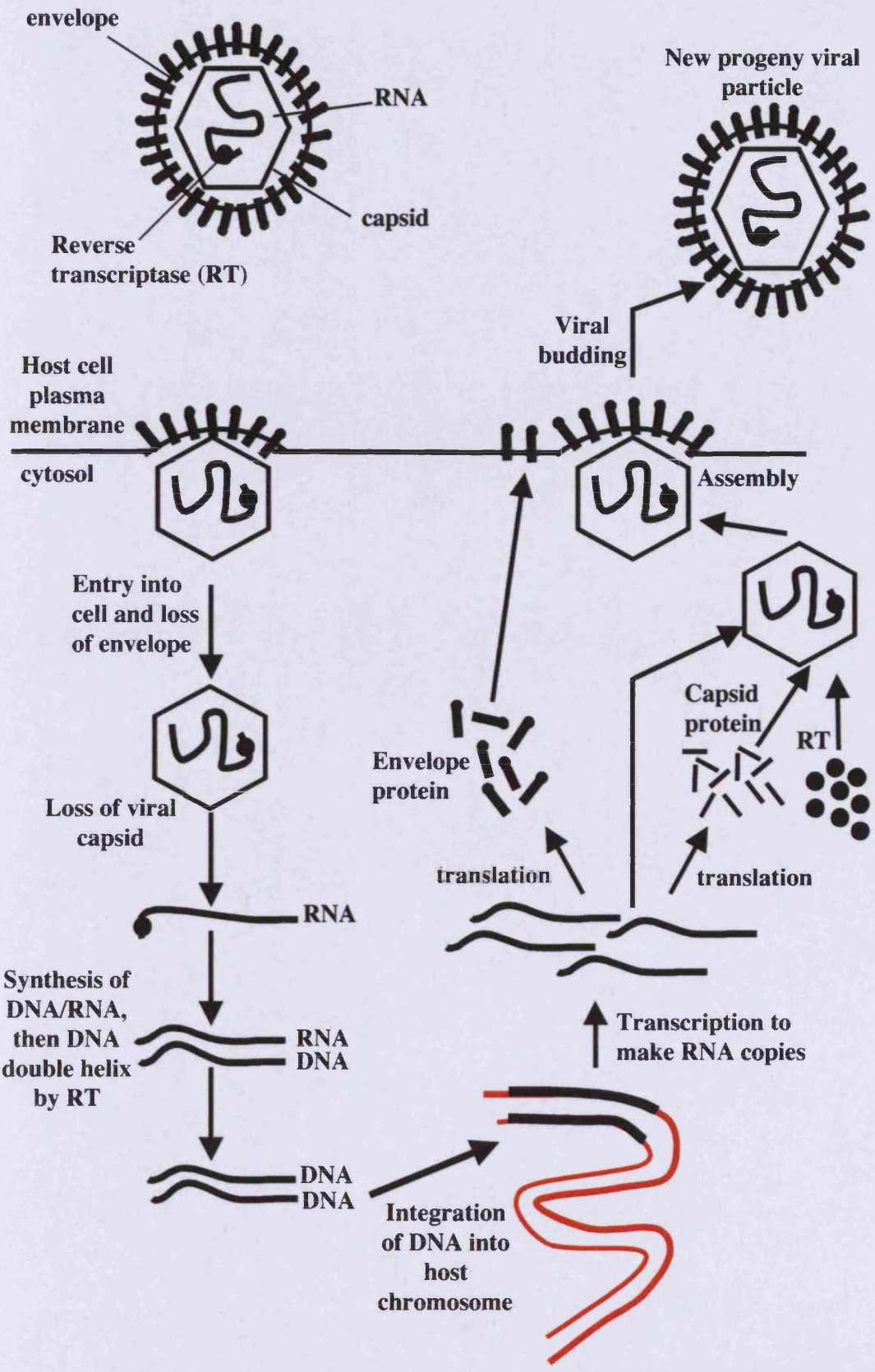

Figure 1.6 The life-cycle of a retrovirus

A simplified schematic, illustrating the retroviral life-cycle. The envelope contains proteins that enable the virus to bind to specific cellular receptors and aid its entry into a cell. Reverse transcription of RNA to DNA and permanent integration of newly transcribed DNA into the host chromosome are the hallmarks of the retrovirus life-cycle.

lead to the fusion of the viral and cellular membranes (Goff, 2001). However, recent studies have suggested that gamma retroviral association with receptors triggers an obligatory interaction or cross-talk between envelope glycoproteins on the viral surface. If this intermediate step is prevented, infection fails (Taylor and Sanders, 2003). Once bound, the viral envelope undergoes a conformational change and fuses with the cellular membrane. Internalisation of the viral nucleocapsid core into the cytoplasm of the target cell ensues (Ohno *et al.*, 1997; Rowell *et al.*, 1995).

1.5.2.4.2 *Reverse transcription*

Reverse transcription involves the transcription of a duplex DNA product from a viral RNA genome and begins shortly after viral entry into the cytoplasm (Gilboa *et al.*, 1979). The reaction takes place in a large complex, roughly resembling the virion core and containing Gag proteins and the viral RNA. This complex process is the defining hallmark of the retroviruses and precedes the integration of viral DNA in the nucleus. The catalytic processes of reverse transcription involved discrete highly ordered steps of DNA synthesis including: RNA and DNA directed DNA polymerase activity, DNA unwinding and RNAse H activity all initiated by this one enzyme (Goff, 2001).

1.5.2.4.3 *Integration, Transcription and Translation*

Entry of the viral DNA into the nucleus is an important step required before integration can take place. The newly transcribed double-stranded DNA binds to nucleoprotein preintegration complex (PIC), which facilitates its migration to the nucleus (Wei *et al.*, 1998). To complete the retroviral life cycle, the PIC must be translocated to the nucleus. For most retroviruses, including MLV, the breakdown of the nuclear membrane during mitosis is necessary to allow access of the PIC to host DNA (Roe *et al.*, 1993). This means that most retroviruses cannot infect non-dividing cells, an important point to highlight with respect to the therapeutic potential of retroviruses. Once inside the nucleus, integration, a critical step in the lifecycle of the virus, ensues. The enzyme involved, integrase, ensures permanent integration of the viral DNA in the host chromosome (Goff, 2001). Integration is a

highly ordered process involving processing of the 3' viral DNA ends, joining of the two new 3' viral DNA ends to form a gapped intermediate product and finally, repair of any gaps to complete the integration process (Goff, 2001). Integration is not site specific but retroviruses preferentially integrate into regions where genes are being actively transcribed, as detected by open chromatin structures (Cereseto and Giacca, 2004). Transcription is initiated at the 5'end of the viral DNA and involves a potent promoter located in the Long Terminal Repeat region (LTR) (Goff, 2001). Extensive processing of the newly transcribed RNA takes place before translation of the viral proteins (Goff, 2001). The *gag, pro, pol and env* genes are transcribed into precursor proteins which are cleaved into separate proteins when the virus matures (Goff, 2001).

1.5.2.4.4 *Assembly of the virion, budding and maturation*

Assembly, budding and maturation of the retroviral particles is a process that is required for the formation of an infectious virus. Assembly of the retrovirus involves the gag precursor protein and the gammaretrovirus particles are usually assembled in the plasma membrane (Goff, 2001). The viral RNA is identified as RNA to be packaged by the presence of the ψ-packaging signal in the 5' leader region (Berkowitz *et al.*, 1996). The ψ-regions on the viral genome that are recognised for incorporation are quite distinct in nucleic acid sequence among the various viruses. During and after budding from the cell, the precursor proteins are cleaved by activated proteases into a series of products (Goff, 2001). The gag precursor protein gives rise to the membrane associated (MA) protein, the large major capsid protein (CA) and the nucleocapsid protein (NC) (Goff, 2001). The gag-pro and the gag-pro-pol precursor proteins are cleaved to give rise to protease (PR), reverse transcriptase (RV) and integrase (IN) enzyme products (Goff, 2001). The morphology of the retrovirus changes to a more condensed structure after budding from the cell surface and the newly packaged virion becomes mature. Thus, processing, cleavage and restructuring of the viral proteins are crucial to generate the infectious viral particle.

1.5.3 The retroviral vector system as a tool in gene therapy

The ability of the retroviruses to stably integrate into the host genome, along with their simple genome structure, have made these viruses popular tools in gene therapy strategies (Lundstrom, 2003). Recombinant retroviral vectors use the same integration machinery of naturally occurring retroviruses to produce a single copy of the viral genome integrated into the host chromosome. This allows long-term stable expression of introduced genetic elements because all progeny cells will also express the gene of interest (Riviere *et al.*, 2000). The majority of T-cell gene transfer studies to date have used the MoMLV based vector system (Bunnell *et al.*, 1995; Mavilio *et al.*, 1994). These vectors are deleted of the *gag*, *pol* and *env* genes necessary for efficient viral replication and are called replication-defective transforming viruses. The elements retained include the LTRs required for reverse and forward transcription of the transgene cDNA (Mann *et al.*, 1983).

The loss of the structural *gag*, *pol* and *env* genes, necessary to encode key proteins of the viral particle means that these products must be supplied by 'packaging' cell lines (Markowitz *et al.*, 1988). These are cell lines engineered to express the Moloney *gag*, *pol* and *env* genes but not the ψ-signal sequences necessary for packaging, which, in contrast, are intact in the transfected recombinant vector. By complementation, the full-length recombinant vector RNA genome is therefore packaged with the products of the helper genome. The result is a functional retroviral vector capable of a single round of infection (Goff, 2001). The absence of the genetic information required to produce the structural proteins prevents subsequent spread of the vector post-infection. It is known as a 'helper-free' vector because the genes that 'helped' to construct the functional virus are not delivered. While MoMLVs normally infect mouse cells only, these vector viruses can also infect human cells because they have been engineered to harbour the *env* gene of a unique murine leukaemia virus with amphotropic range (Jolly, 1994). Many helper free retroviral vectors are designed to express the gene of interest and also a selectable marker. One example of a selectable marker is green fluorescent protein (GFP) (Introna *et al.*, 1998), which is useful to identify transduced cells by flow cytometry.

1.5.4 Application of retrovirally modified cells to the study and treatment of disease

While there are challenges associated with the application of retroviruses to gene therapy, the advantages associated with the retroviruses as vectors overcome these, and twenty eight percent of all clinical trials today involve the use of retroviral vectors. Two thirds of these trials are aimed at cancer patients and most of the remaining trials are aimed at treating patients with inherited immunodeficiency disorders and HIV patients (Mountain, 2000). As mentioned earlier, T-cells were the first targets for genetic modification in human gene transfer approaches. One of the first studies, carried out by Blaese and Anderson led to the infusion of T-cells genetically modified with the adenosine deaminase (ADA) gene to treat an immunodeficiency disease associated with a deficiency in the ADA enzyme (Blaese *et al.*, 1995). While a cure for ADA deficiency was not demonstrated, the feasibility of the adoptive transfer of T-cells genetically modified using retroviruses was demonstrated for the first time. The first true success of retroviral gene therapy was reported in 2000 with the successful treatment of an inherited immunodeficiency disorder known as severe combined immunodeficiency disorder (SCID) (Cavazzana-Calvo *et al.*, 2000). In 2002 another clinical trial to treat ADA deficiency also reported successful results (Aiuti *et al.*, 2002).

The increased interest in the use of EBV-CTLs to treat PTLD has led to an increase in studies using genetic modification to enhance the efficacy and survival of these T-cells *in vivo*. Various strategies have been employed to genetically enhance specific aspects of the T-cells in this therapy. Genetic modification may be used to enhance any component of T-cell function after adoptive transfer e.g. to mark T-cells so that they can be tracked *in vivo* to determine their fate and performance *in vivo*; to provide a regulatory mechanism whereby unwanted proliferation or activity of modified T-cells can be controlled; and to favour survival of the T-cells in a hostile tumour environment.

1.5.4.1 *Gene marking*

A gene marking strategy does not transduce the cell with a gene of any therapeutic intent, but instead allows researchers to monitor the migration of the

infused T-cells and their persistence *in vivo*. More than twenty genemarking clinical trials have been performed to date using the neomycin resistant (*neoR*) gene, which induces resistance to G418, an analogue of neomycin (Kohn *et al.*, 2003). Modification of the cell with the *neoR* gene enables a pure population of transduced cells to be selected *in vitro* and also enables the monitoring of the *neoR* cells post transfer, through PCR based analysis of PBMC samples using primers specific for the *neoR* gene (Heslop *et al.*, 1996a; Heslop *et al.*, 1996b; Riddell *et al.*, 1996a; Rooney *et al.*, 1995a; Rooney *et al.*, 1998c). The first human gene therapy experiment mentioned earlier, to treat ADA deficiency, used a retroviral vector containing a *neoR* gene in addition to the ADA gene, to tranduce two patients PBMCs (Blaese *et al.*, 1995). Real-time PCR analysis for the *neoR* gene and ADA enzyme assays, were used to assess the presence of the ADA transgene and the *neoR* gene marker (Muul *et al.*, 2003). Ten years after the last cell infusion, approximately twenty percent of the first patient's lymphocytes still carried and expressed the retroviral gene marker and the ADA gene (Muul *et al.*, 2003). The long term monitoring of the patients for more than twelve years demonstrated that genetically modified autologous T-cells, cultured *in vitro*, can be safely infused into patients (Muul *et al.*, 2003). These data demonstrate that it is possible for transgenes driven by Moloney retroviral promoter LTRs to continue to be expressed in T-cells for more than a decade.

The clinical trials conducted by Rooney *et al.* which demonstrated that adoptively transferred EBV-CTLs can be used in the prophylactic treatment of PTLD, also used T-cells genetically modified with a *neoR* gene (Heslop *et al.*, 1995; Rooney *et al.*, 1995a; Rooney *et al.*, 1998c; Smith *et al.*, 1995). The *in vitro* generated CTL lines were infected with a *neoR*-containing retroviral vector. The immunologic effects of the CTLs were monitored during and after infusion by the detection of the neomycin resistance gene marker, *neoR* and long-term tracking of these cells has showed persistence of the infused CTLs for up to seven years (Bollard *et al.*, 2004). Silencing of the transgene over time can be a problem with genetic modification. However, these results demonstrated that the genetic manipulation of

T-cells with a gene marker is useful in the assessment of the long-term effects of adoptive transfer.

The role of CTLs in HIV infection is a matter of much debate (Riddell *et al.*, 1992a). Greenberg and Riddell have applied a gene marker strategy in immunotherapy trials in order to elucidate the role of HIV $CD8^+$ T-cells in HIV infection. In one reported trial involving three HIV positive patients, they administered three infusions of unmodified autologous HIV Gag specific $CD8^+$ CTL clones in escalating doses, followed by two infusions of $CD8^+$ CTL clones genetically modified to express the *neoR* gene, to assess transfer of immunity, persistence in the peripheral blood and migration to the lymph nodes (Brodie *et al.*, 1999). PCR-based monitoring of the *neoR* gene marker in patient PBMCs and tissue sections, in addition to lymphoproliferative analysis, immunohistochemistry and quantitation of *neoR* marked cells in blood and lymph nodes, were used to monitor the infused T-cells. The results demonstrated that adoptively transferred HIV Gag-specific $CD8^+$ CTLs augment the endogenous CTL response, migrate to the sites of viral replication in lymph nodes and result in a decline in HIV-infected $CD4^+$ T-cells in the peripheral blood.

In addition to a drug resistance gene it is also possible to select transduced cells *in vitro* based on expression of a transgenic cell surface molecule that binds to specific antibodies. This would permit the enrichment of transduced cells to high purity using magnetic or FACS based cell-sorting techniques and more importantly, permit the monitoring of the persistence of transduced cells *in vivo*. Bordignon *et al.* developed a clinical protocol which involved the modification of donor lymphocytes with a retroviral vector containing the low affinity nerve growth factor receptor (Mavilio *et al.*, 1994) for the *in vitro* selection of the transduced cells and the *in vivo* follow up (nmVerzeletti *et al.*, 1998). Long-term *in vivo* survival of transduced cells was demonstrated.

1.5.4.2 *Suicide genes*

Modification of human cells for adoptive transfer with a suicide gene has enhanced the safety of gene therapy. One complication of adoptive T-cell therapy is the development of graft-versus-host disease (GvHD) (Mackinnon *et al.*, 1995). To enhance the safety of the adoptively transferred T-cells and to aid in the control of GvHD, strategies have been developed that enable the specific elimination of the transferred T-cells should a problem arise. The most common example is the modification of a T-cell with a suicide gene, which will confer drug sensitivity on the cell. The most extensively studied system is the Herpes simplex virus thymidine kinase (HSV-TK) suicide gene system. Bonini *et al.* demonstrated that this HSV-TK suicide gene renders the cell sensitive to ganciclovir and that the administration of ganciclovir to the patient could potentially eliminate the adoptively transferred T-cells, should any complications arise. Herve *et al.* also reported a study to evaluate the safety and efficacy of the administration of HSV-TK modified T-cells in BMT (Tiberghien *et al.*, 2001). Escalating doses of donor HSV-TK expressing T-cells were infused with a T-cell depleted BMT in twelve patients. An early increase in gene-modified T-cells followed by a progressive decrease and long-lasting circulation with no associated toxicity was demonstrated. Ganciclovir treatment resulted in a significant rapid decrease of circulating HSV-TK modified T-cells.

However, the gene products of suicide genes or drug resistant genes are potentially immunogenic and the immune response to these products can limit survival of the modified cell *in vivo*. Retroviral vectors are less immunogenic than other vectors employed in gene therapy but the immune response is still a potential hazard (Mountain, 2000). Bonini *et al.* demonstrated that $CD8^+$ CTL responses to the epitopes derived from the TK proteins were induced in five of the six patients in the trial. Riddel *et al.* also reported the T-cell mediated rejection of HIV specific CTL modified with the HSV-TK gene (Riddell *et al.*, 1996b). To address this, recent studies have involved the use of endogenous proapoptotic molecules as non-immunogenic suicide genes. Thomis *et al.* modified T-cells to express a chimeric molecule derived from human proteins that contains an extracellular binding domain for a non-toxic drug and an intracellular signalling domain of the Fas receptor.

Administration of the drug caused dimerization of the chimeric receptor and initiates the Fas-mediated apoptotic cascade in the cell (Thomis *et al.*, 2001).

1.5.4.3 *Improved efficacy and survival*

The efficacy of adoptively transferred T-cells can also be enhanced by genetic modification. To enhance the efficacy of T-cells *in vivo*, a number of approaches have been studied. One such example is the engineering of T-cells to increase their reactivity to poorly presented antigens on tumour cells by modifiying the T-cell receptor. Chimeric receptors, based on the observation that signalling through the ζ-chain of the TCR can mediate signals that suffice to induce immune effector functions (Geiger *et al.*, 1999; Muniappan *et al.*, 2000), have been developed against a wide range of tumour antigens. Ligation of an extracellular domain fused to the ζ-chain results in tyrosine phosphorylation of ITAMs in the cytoplasmic domain of the ζ-chain, initiating T-cell signalling to the nucleus. One example of such chimeric receptors is the ligand, which binds to erb-B onocoreceptor family members overexpressed on human adenocarcinoma cells (Muniappan *et al.*, 2000).

The survival of adoptively transferred T-cells can be a limiting factor of cellular therapy. T-cells can be modified to express cytokines such as IL-2 and IL-15 to sustain survival post-infusion. Liu *et al.* transduced PBMC with a retrovirus containing an IL-2 gene and demonstrated that the transduced cells were able to secrete IL-2 and maintain their viability in the absence of exogenous IL-2 upon restimulation (Liu and Rosenberg, 2001). Another approach involves the modification of T-cells to express a growth factor receptor or a cytokine receptor. In a recent study, the extracellular domain of the GM-CSF receptor was fused to the intracellular domain of the IL-2 receptor (Cheng *et al.*, 2002). Antigen recognition by murine CTLs resulted in the normal production of GM-CSF and this led to the development of an autocrine growth factor loop delivering IL-2 survival signals to T-cells. A further strategy to improve the survival of T-cells *in vivo* involves the introduction of genes that will confer protection from inhibitory cytokines released by many tumours. TGF-β is a cytokine renowned for its immunosuppressive effects on CTLs (Johnson and Newfeld, 2002). Modifying T-cells with a dominant negative

receptor for TGF-β resulted in resistance to the inhibitory effects of the cytokine and enhanced survival (Bollard *et al.*, 2002).

Following on from these strategies to enhance the survival of transferred cells *in vivo*, are the studies designed to confer a drug resistance to transplanted cells, in order to enhance survival in an *in vivo* drug environment. One approach, involves the transfer of genes encoding resistance to chemotherapeutic agents into haematopoietic stem cells. This strategy is based on the hypothesis that the ability to deliver higher dosages of chemotherapy without severe suppression of bone marrow function could lead to a higher rate of cure of the underlying malignancy. The drug resistant haematopoietic stem cells would be transplanted to cancer or leukemia patients who have developed severe myelosuppression as a result of the high dose chemotherapy. Initial clinical trials have examined transfer of the multidrug resistant (MDR-1 or p-glycoprotein) cDNA into haematopoietic stem cells of murine models (Carpinteiro *et al.*, 2002; D'Hondt *et al.*, 2001). MDR-1 acts as a drug pump eliminating a variety of clinically relevant chemotherapeutic compounds. These studies demonstrated low but detectable numbers of MDR-1 expressing cells and have demonstrated that a better chemoprotection was evident in the mice transplanted with the modified cells (D'Hondt *et al.*, 2001). The longterm benefits have yet to be demonstrated and clinical trials in humans have yet to demonstrate the effectiveness of MDR-1 to confer chemoprotection (Abonour *et al.*, 2000; Devereux *et al.*, 1998). However, the transgenic mouse experiments prove the principle that the modification of cells for transplant with a drug resistance gene could potentially mediate chemoprotection of human clinically relevant stem cell populations with marrow engraftment potential.

1.6 Objectives of this project

The application of gene therapy to improve the efficacy and survival of T-cells remains a major goal in the development of an optimal immunotherapeutic strategy to treat cancers and infections. The *neoR* gene marker trials have demonstated that the modification of transplant cells with a drug resistant virus is advantageous to the application of transferred cells in the treatment of disease. In

addition, the preliminary MDR-1 trial results have indicated that the modification of T-cells with a drug resistant gene in order to increase survival in a hostile drug environment is a feasible approach to enhance cellular therapy. Bordignon *et al.* and others have demonstrated that genetically-engineered donor T-cells maintain a normal TCR immune repertoire and retain antigen specific lytic activity against an allogeneic target or an autologous EBV cell line at CTL precursor frequencies comparable to unmodified lymphocytes (nmVerzeletti *et al.*, 1998). Taken together the current research discussed in Section 1.5 indicates that the use of genetically modified CTLs in adoptive transfer is a feasible therapy for the clinic. Immunosuppressive drugs such as CsA and rapamycin can impair the function and longevity of T-cells *in vitro* and may impair function and efficacy of adoptively transferred T-cells *in vivo*. Our objective in this project was to enhance the longevity and survival of primary human T-cells *in vitro* by modification with a retroviral vector containing an immunosuppressive resistant gene.

(1) The first objective was to elucidate the conditions required for efficient primary human T-cell proliferation (Chapter 3).

(2) Following on from these experiments, our next objective was to successfully transfer and establish retroviral technology in our laboratory. The successful establishment of the retroviral technology would enable the generation of rapamycin resistant and CsA resistant retroviruses (Chapter 4).

(3) Once the technology was established, the next objective was to modify a human leukemic T-cell line Kit225 used routinely in our laboratory, primary human T-cells isolated from buffy coats and EBV-CTLs generated from healthy donors with a rapamycin resistant retrovirus and assess the phenotype of these modified cells *in vitro* (Chapter 5).

(4) The final objective was to extend this study to another immunosuppressive resistant gene. We aimed to modify primary human T-cells with a CsA

resistant retrovirus and assess the phenotype of these modified cells *in vitro* (Chapter 6).

Chapter 2

MATERIALS AND METHODS

2.1 Molecular biology

2.1.1 Bacterial culture media and reagents used

Sterilisation of bacterial culture media and other reagents used in the manipulation of DNA was carried out by autoclaving for 40 mins at 15psi and 121°C where indicated. All bacterial culture media and reagents used are detailed in Appendix I.

2.1.2 Bacterial strains used

Unless otherwise stated, the DH5α *Eschericia coli* strain was used in the generation of recombinant plasmid DNA.

2.1.3 Preparation of chemically competent DH5α bacterial cells

A 3 ml volume of LB broth (without antibiotic selection) was inoculated with a single colony of DH5α and incubated at 37°C overnight in a shaking incubator. 50 μl of this overnight culture was then used to inoculate a further 50 ml of LB broth, which was again incubated at 37°C until the optical density at l = 600nm (OD600nm) reached 0.3 to 0.6 (approximately 3 – 6 hours). The culture was centrifuged at 3000g for 10 mins and the resulting pellet was resuspended in 10 ml of ice-cold 100mM $CaCl_2$. This was incubated on ice for 1 hour and centrifuged as previously to pellet the cells. The pellet was resuspended in 2.5 ml ice-cold 100mM $CaCl_2$ and the competent cells were stored at 4°C for up to two weeks. Alternatively, for long-term storage, glycerol was added to a final concentration of 15% and the competent cells were aliquoted into 1.5 ml eppendorf tubes and frozen at 70°C until required.

2.1.4 Transformation of competent DH5α bacterial cells

Competent DH5α cells were kept on ice at all times and 100 – 500ng of plasmid DNA or 10 μl of a ligation reaction were added to 200 μl of cells and incubated on ice for 30 mins. The competent bacteria were then heat-shocked at 42°C for 90 secs in a water-bath. Subsequently, 0.5 ml of LB broth (without antibiotic selection) was added and the cells were incubated at 37°C for 30 mins. The transformation reactions were plated out onto selective LB agar plates as required and incubated overnight at 37°C without agitation.

2.1.5 Small-scale preparation of plasmid DNA (mini-preps)

An alkaline-lysis method was used for the small-scale preparation of plasmid DNA. 1.5 ml of the required overnight starter culture was centrifuged at 12,000g for 30 secs and the resulting supernatant removed completely. The bacterial pellet was resuspended thoroughly in 100 μl of Solution I (50mM glucose, 25mM Tris-HCl, pH 8.0 and 10mM EDTA) and 200 μl of Solution II (0.2M NaOH, 1% (w/v) SDS) was then added and mixed gently but thoroughly by inverting 6 to 8 times. A 150 μl volume of Solution III (3M potassium acetate, 11.5% (v/v) glacial acetic acid) was added to the viscous lysate and this was mixed thoroughly by vortexing the inverted tube followed by incubation on ice for 5 mins. The cloudy solution was centrifuged at 12,000g for 5 mins and the supernatant collected in a fresh 1.5 ml eppendorf tube. An equal volume of phenol:chloroform:isoamylalcohol (25:24:1) was added to the supernatant and following mixing was centrifuged at 12,000g for 2 mins. The upper aqueous layer was removed to another fresh 1.5ml eppendorf tube and 2 volumes of 100% AR quality ethanol (Hayman) were added and centrifuged at 12,000g for 5 mins to precipitate the plasmid DNA. The DNA pellet was washed with 1 ml of 70% EtOH and dried briefly at 40°C on a heating block. The dried pellet was dissolved in 50 μl TE.

2.1.6 Large-scale preparation of plasmid DNA (Cesium Chloride bulk preps)

Large-scale preparation of plasmid DNA was performed using a Cesium Chloride (CsCl) purification technique. A starter culture was used to inoculate 250 ml of

selective LB medium at a dilution of 1/1000 and this was incubated overnight at 37°C in an orbital shaker. The bacteria were harvested by pelleting cells at 3000g at 4°C for 8 mins. 1 ml of fresh lysozyme (0.1 g lysozyme (Sigma) to 100 µl of 1M Tris pH8, made up to 10 mls with dH_2O) was added directly onto the pellet. 4 mls of Solution I was added and pellets were disrupted and placed into sorval tubes. 10 mls of fresh Solution II was added to the tubes, and the samples were mixed and left for 5 mins. 7.5 mls of Solution III was added and the sorval tubes were left on ice for 5 mins before centrifuging at 23,000g for 15-30 mins at 4°C to pellet the protein. Supernatant was poured into a fresh sorval tube and 13.5 mls of isopropanol was added to each tube, shaken well and stored on ice. Tubes were spun at 20,000g for 30 mins at 4°C. The supernatant waste was poured off and the tubes were allowed to dry. 3 mls of 70% EtOH was added to each tube. The tubes were then rotated gently to wash the pellet and allowed to stand for 2 mins before carefully pouring off the ethanol and allowing tubes to dry thoroughly on tissue paper. 4 mls of T50:E10 was added to each tube along with 3-4 µl of RNAse (10 mg/ml) and the tubes were shaken for at least 1 hour, until the pellets dissolved.

CsCl gradient preparation

4.1g of Caesium chloride (CsCl, Roche) was accurately added to 12ml round-bottomed centrifuge tubes and 3.95g of the dissolved plasmid preparation was accurately added to the 12 ml tubes, which were then shaken until the CsCl had dissolved. 150 µl of Ethidium Bromide (EtBr) (10 mg/ml) was added to each tube, inverted a few times and put on ice for 5 minutes. The tubes were centrifuged at 17,000g for 10 minutes at 4°C. The plasmids were then carefully added to 5 ml Beckman tubes, weighed accurately and paired up according to weight. The tubes were centrifuged in a Beckman ultracentrifuge, overnight at 140,000g without a break at 22°C. Samples were then carefully removed from the centrifuge, so as not to disturb the gradient layers. The top of the Beckman tube was carefully pierced, using a needle and syringe, to relieve pressure. The DNA layer was removed from the tube using the needle and syringe and the tube and syringe were disposed of carefully. Distilled H_20 was added to make up 5g in weight

and the tubes were stored on ice. Isopropanol was added in a 1:1 ratio and the tubes were centrifuged for 25 mins at 17,000g. Supernatant was carefully removed, and the tubes were dried on tissue paper. 2 mls of 70% EtOH was added to wash the pellet quickly. The tubes were allowed to dry and 400 µl of TE Buffer (pH 8.0) was added to each tube and shaken until the pellet dissolved (at least 1 hour).

2.1.7 Phenol extraction of DNA

The dissolved plasmid solution was then placed in a 1.5 ml eppendorf and an equal volume of phenol was added and the sample was mixed vigorously until cloudy. This solution was centrifuged at 12,000g for two mins. The upper aqueous phase was removed into a fresh 1.5 ml eppendorf tube and an equal volume of phenol:chloroform:isoamylalcohol (25:24:1) was added and mixed well. Separation, by centrifugation at 12,000g was carried out as above, and the extraction was repeated until no sign of debris was visible at the interface between the phases. An equal volume of chloroform:isoamylalcohol (24:1) was then added and separation of the mixed phases was performed as before. DNA was precipitated from the final phase by ethanol precipitation.

2.1.8 Ethanol precipitation of DNA

A volume of 3M sodium acetate (pH 5.2), equal to 1/10 of the sample volume, was added along with 2.5 volumes of 100% EtOH AR quality (Hayman). The solution was mixed well and incubated at –20°C for at least 1 hour, and the DNA was pelleted by centrifugation at 12,000g for 30 mins. Following removal of the supernatant, the DNA pellet was washed with 70% EtOH, and dried and dissolved in an appropriate volume of TE buffer. DNA concentration was calculated on a spectrophotometer.

2.1.9 Construction of retroviral vectors

The PINCO retoviral vector (Appendix II) used in this study was a gift from Dr. Richard Darley, Dept. Haematology, UWCM. The pBabe puro, pBabe mTOR wt and pBabe mTOR S2035T vectors (Appendix II) used in this study were a gift from Prof.

George Thomas, Switzerland. The pBabe CNA wt and pBabe CNA V314R plasmids were constructed during this study using pBabe puro and PBJ5 CNA wt and PBJ5 CNA V314R plasmids (Appendix II). The PBJ5 CNA wt and PBJ5 CNA V314R plasmids were a gift from Dr. Joseph Heitman, Duke University.

2.1.9.1 Restriction endonuclease digestion

To construct the pBabe CNA wt and pBabe CNA V314R retroviral vectors, the pBabe puro plasmid was linearised with EcoRI digestion enzyme (New England Biolabs). The reactions were carried out in the required reaction volumes (generally 10-40 μl), containing 1/10th the final reaction volume of 10X reaction buffer, BSA (if required) and Units of restriction enzyme, according to the manufacturer's instructions. All reactions were incubated for 1 hour at 37°C. Restriction enzyme digestions were analysed by submerged horizontal agarose gel electrophoresis.

2.1.9.2 Alkaline phosphatase treatment of digested vector

Alkaline phosphatase treatment was used to remove free 5' phosphate groups and prevent the self-ligation of complementary overhangs present on plasmid DNA digested with only a single restriction enzyme. Following heat inactivation of single restriction enzyme digestion reactions at 70°C for 15 mins, calf intestinal alkaline phosphatase (CIP, 10 units) was added to the reaction and incubated at 37°C for 1 hour. Subsequently, 0.5 μl of 0.5M EDTA pH 8.0 was added and the reaction was heated to 75°C for 10 mins to inactivate the calf intestinal phosphatase. The alkaline phosphatase-treated vector was then purified (Section 2.1.9.3) and used in ligation reactions.

2.1.9.3 Purification of retroviral vector DNA

A QIAquick PCR purificication Kit (Qiagen) was used to purify the newly digested retroviral vector DNA, in preparation for cloning. This protocol is designed to purify single or double-stranded DNA fragments from PCR and other enzymatic reactions. Fragments are purified from primers, nucleotides, polymerases, and salts using QIAquick spin columns in a microcentrifuge. 5 volumes of Buffer PB was added

to 1 volume of the digestion reaction and mixed. A QIAquick spin column was placed in a 2 ml collection tube and the sample was applied to the column and centrifuged for 30-60 secs at 12,000g. The flow through was discarded, and the QIAquick column was placed back in the same tube. To wash, 750 μl of Buffer PE was added and the column was centrifuged for 30-60 secs at 12,000g. The flow through was discarded and the column centrifuged for a further 1 minute at maximum speed. The QIAquick column was placed in a clean 1.5 ml tube and the DNA was eluted by adding 50 μl of Buffer EB (10mM Tris-Cl, pH 8.5) to the centre of the membrane and centrifuging for 1 minute, as before.

2.1.9.4 Submerged horizontal agarose gel electrophoresis to excise insert

The pBJ5 carrier plasmids, containing the CNA wt and CNAV314R genes of interest, were restriction digested with EcoRI (Section 2.1.9.1) and an agarose gel electrophoresis was used for the resolution of DNA fragments. DNA agarose gels were prepared by dissolving electrophoresis grade agarose (Gibco, Invitrogen Corporation) in 1X TAE and heating in a microwave. Gels containing 1.2% or 2% (w/v) of agarose were generally used, depending on the size of the DNA fragments of interest and a 50 ml volume of agarose solution was required per gel (dimensions 10cm X 10cm). Agarose gels were cast and run using submerged horizontal electrophoresis tank apparatus (Flowgen). Prior to electrophoresis, DNA samples were mixed with 1/6 volumes of 6X DNA loading buffer (see Section 2.1.1) and loaded into the wells of an agarose gel submerged in 1X TAE, (see Section 2.1.1), along with a 1kb DNA ladder (MBI Fermentas). Agarose gels were run at 100V for 45 mins or until the loading buffer dye front reached the bottom of the gel. Gels were stained in a 0.5 μg/ml EtBr solution and visualised under ultraviolet light using a gel documentation system (Biorad).

2.1.9.5 Extraction of DNA insert fragments from agarose gels

The QIAquick gel extraction kit (Qiagen) was used to purify specific DNA fragments from agarose gels. The CNA wt and CNA V314R DNA fragments were excised from an agarose gel under UV light, and weighed in a 1.5ml eppendorf tube. A

volume of Buffer QG (sodium iodide, Qiagen) corresponding to 3X the weight of the agarose slice was added and heated at 50°C in a heating block for 10 mins or until the agarose was completely dissolved. After the gel slice had completely dissolved, the colour of the mixture was checked to confirm it was yellow (pH≤7.5, similar in colour to Buffer QG without the dissolved agarose). If the mixture was not yellow, 10 μl of 3M sodium acetate pH5.0 was added. 1 gel volume of isopropanol was added to the sample. A QIAquick spin column was placed in a 2ml collection tube and to bind the DNA, the sample was applied to the QIAquick column and centrifuged for 1 minute at 12,000g. The flow-through was discarded the QIAquick column was placed back in the same collection tube, washed with 0.75 ml of Buffer PE and centrifuged as before. The flow-through was again discarded and the QIAquick column was centrifuged as before. The QIAquick column was then placed in a clean 1.5 ml eppendorf. To elute the DNA, 50 μl of buffer EB (10mM Tris-Cl, pH8.5) was added to the centre of the QIAquick membrane and the tube was centrifuged for 1 minute at 12,000g.

2.1.9.6 Ligation of DNA and isolation of recombinant vector

Ligation reactions were set up to contain 2 μl 10X T4 DNA ligase buffer and 400 units T4 DNA ligase (both from New England Biolabs), 1 μl digested vector, 4 μl digested insert and 12.5 μl sterile distilled water to give a final volume of 20 μl. Control ligations were set up in parallel containing 4 μl distilled water instead of insert DNA. Ligation reactions were incubated at 16°C overnight and then used to transform competent DH5α bacteria (Section 2.1.4). Selected clones were used to inoculate small starter cultures, DNA was extracted using a plasmid miniprep protocol (Section 2.1.5) and DNA was screened for the correct orientation of the DNA fragment by restriction enzyme digestion.

2.1.9.7 Sequencing analysis of cloned DNA fragments

Following successful cloning, recombinant plasmids were sequenced to confirm the presence of the correct DNA fragment with the correct mutation. DNA sequencing reactions were set up containing 500 ng template DNA, 4 μl Big Dye ready reaction mix

(ABI Big Dye Sequencing kit, PE Applied Biosystems), 3.2pmole primer and distilled water was added to give a final volume of 10 μl. Reactions were overlaid with mineral oil and placed in a pre-programmed thermal cycler (Hybaid). The following cycling conditions were used for sequencing cloned DNA fragments: 96°C for 30 sec, 50°C for 15 sec and 60°C for 4 min (25 cycles). The mineral oil was then removed and the sequencing reactions were precipitated by adding 10μl 3M sodium acetate pH 5.2 and 250 μl 100% ethanol and incubating at room temperature for 15 min. The precipitated DNA was pelleted by centrifuging at 12,000g for 25 mins at room temperature and the resulting pellet was washed six times in 250 μl 70% EtOH. The reactions were dried on a vacuum drier and mixed with loading buffer. They were then separated on a 4% denaturing polyacrylamide gel which was run at 169kV, and analysed on an ABI prism 377 DNA sequencer. The drying of sequencing reactions and their analysis on the DNA sequencer were carried out by Joyce Hoy and Barry Francis at the UWCM core DNA sequencing facility. Sequencing results were analysed using the Lasergene Navigator software (DNAStar Inc.). Appendix II shows the sequences to confirm each plasmid. Table 2.2 shows the sequence of the primers used during the course of this study.

Table 2.2 Primer sequences

Primer name	**Primer sequence**
CNA fwd 5'-3'	GCATTTGGACCAATGTGTGA
mTOR fwd 5'-3'	CTAAGTCTACCACGACAGCCC

Primers were supplied by MWG Oligonucleotides.

2.2 Tissue culture

2.2.1 Materials used in routine tissue culture

RPMI-1640 without glutamine (Gibco, Invitrogen Corporation), 500 ml, was stored at 4°C.

DMEM without glutamine (Gibco, Invitrogen Corporation), 500 ml, stored at 4°C.

Foetal bovine serum (FCS, Gibco, Invitrogen Corporation) was stored in 50 ml aliquots at –20°C.

Calf serum (CS, Sigma) was stored in 50 ml aliquots at –20°C.

Human AB serum was obtained in 500 ml aliquots, from the Welsh Blood Transfusion Board and prepared as described in Section 2.2.6.

Glutamine 200mM (Gibco, Invitrogen Corporation) was stored in 5 ml aliquots at –20°C and used as 100X stock solution.

Penicillin/Streptomycin (Gibco, Invitrogen Corporation), 100 ml of 5000 IU/ml Penicillum G Sodium and 5000 μg/ml Streptomycin Sulfate, was stored in 10 ml aliquots at –20°C and used as a 50X stock solution.

Trypsin-EDTA (1X), (Gibco, Invitrogen Corporation), 0.05% Trypsin with EDTA-4Na. Stored long-term at –20°C and short-term at 4°C.

Phosphate-buffered saline (PBS) was made by dissolving 50 PBS tablets (Oxoid) in 5 litres of distilled water. 500 ml aliquots were sterilised by autoclaving and stored at room temperature.

Ficoll-Histopaque (Sigma), 500 ml, was stored at 4°C and used for the separation of mononuclear lymphocytes from whole blood as described in Section 2.2.4

Dimethyl sulfoxide (DMSO, Sigma) was stored at room temperature.

2.2.2 Cell lines used in this study

Cell lines used routinely throughout the project are shown in Table 2.3. Suspension cells were grown in RPMI-1640 (Gibco, Invitrogen Corporation) + 2mM L-glutamine, 100U penicillin/ml and 100 μg streptomycin/ml (hereafter referred to as complete RPMI)+ 10%FCS. Adherent cell lines were grown in DMEM (Gibco, Invitrogen Corporation) 2mM L-glutamine, 100U penicillin/ml and 100 μg streptomycin/ml (hereafter referred to as complete DMEM) +10% FCS or 10% CS.

Table 2.3 Cell lines routinely maintained

Cell line	Description	Growth Medium	Citation/source
Kit225	IL-2 dependent leukemic T-cell line	Complete RPMI +10 % FCS 20 ng/ml IL-2 (Chiron)	(Hori *et al.*, 1987) CRUK
LCL	EBV-transformed B-cell lines	Complete RPMI+ 10 % FCS	(Rowe *et al.*, 1992) Generated during the study (see Section 2.2.5)
Jurkat	Leukemic T-cell line, clone E6.1	Complete RPMI+ 10 % FCS	(Weiss *et al.*, 1984) European Collection of Animal Cell Cultures, Salisbury, UK
PH293[a]	Human embryonic kidney cell line (+ *gag-pol* and *env* retroviral genes)	Complete DMEM+ 10 % FCS	(Kinsella and Nolan, 1996) G. Nolan, Stanford University, Stanford, USA
Ω-E[b]	Omega E, ecotropic retroviral packaging line	Complete DMEM + 10% CS	(Morgenstern and Land, 1990) European Collection of Animal Cell Cultures, Salisbury, UK
Ψ-crip[b]	Psi –crip, amphotropic retroviral packaging line	Complete DMEM + 10% CS	(Danos and Mulligan, 1988) European Collection of Animal Cell Cultures, Salisbury, UK

(a) PH293 is a packaging line used in conjunction with the PINCO retroviral vector in a transient transfection protocol to produce amphotropic virus (can infect both human and murine cells).

(b) Ω-Eand Ψ-crip are packaging cell lines used in conjunction with the pBabe retroviral vector in a stable transfection to generate a stable cell line which produces ecotropic virus (infects murine cells only, Ω-E) or amphotropic virus (infects both murine and human cells, Ψ-crip).

2.2.3 Isolation of Peripheral blood lymphocytes from whole blood

Peripheral blood is the primary source of lymphoid cells for investigations of the human immune systems. Its use is facilitated by Ficoll-Histopaque (Sigma) density gradient centrifugation, a simple and rapid method of purifying peripheral blood lymphocytes (PBLs) that takes advantage of the density differences between mononuclear cells and other elements found in the blood sample. Mononuclear cells and platelets collect on top of the Ficoll-Histopaque layer because they have a lower density; in contrast, red blood cells and granulocytes have a higher density and collect at the bottom of the Ficoll-Histopaque. 125 ml of whole blood was mixed with an equal volume of PBS and distributed evenly among six 50 ml Falcon tubes. 10-15 ml of Ficoll Histopaque was layered carefully underneath the blood/PBS using a 50 ml syringe and Kwill filling tube. Tubes were centrifuged at room temperature at 700g (without a brake), for 25 mins. Tubes were carefully removed from the centrifuge and the white lymphocyte layer, at the Ficoll-histopaque interface was completely removed using a Pasteur pipette. The lymphocyte layer from three Falcon tubes were combined into one 50 ml Falcon tube and topped up to 50ml with PBS. This was repeated for the remaining three Falcon tubes. The two 50 ml Falcon tubes were centrifuged at 300g for 5 mins. Supernatant was removed and the pellets were resuspended and combined with 5ml tissue culture H_2O, to lyse any remaining red blood cells. This 5 ml cell suspension was topped up immediately with PBS and centrifuged at as before. The supernatant was removed and the pellet was washed twice more with PBS. After the final wash, the pellet was resuspended in 10 ml of RPMI and cell count was assessed using a haemocytometer.

2.2.4 Stimulation of freshly isolated PBLs

Following isolation the PBLs were resuspended at approximately $1X10^6$/ml concentration, unless otherwise stated. PBLs were stimulated with various stimuli depending on the experiment. All the T-cell stimuli used in this project are shown in Table 2.4.

Table 2.4 T-cell stimuli

Reagent	Description	Working Conc.	Supplier
Proleukin	Aldesleukin, a manufactured protein very similar to human IL-2, reconstituted in PBS or RPMI-1640 to 100 μg/ml stock conc.	20 ng/ml	Chiron
OKT3	Monoclonal antibody to the CD3 chain of the TCR	2.5 ng/ml	CRUK
Anti-CD28	Mouse anti-human monoclonal antibody recognising CD28 (stock conc. 1 mg/ml)	5 μg/ml	BD
PHA	Phytohaemagglutinin-L, the lectin extract from the red kidney bean (*Phaseolus vulgaris*) with high affinity for leukocyte receptors, reconstituted in PBS to 1 mg/ml stock conc.	1 μg/ml	Roche

2.2.5 Generation of EBV-transformed Lymphoblastoid Cell lines

50 ml of blood was obtained from a healthy donor and PBLs were isolated as described in Section 2.2.3. $5X10^6$ PBLs were resuspended in 1 ml of B95.8 EBV viral supernatant, and placed in a T25 cm^2 tissue culture flask. The remaining PBLs were frozen in $5X10^6$/ml aliquots. 4 mls of complete RPMI+ 10% FCS was added to the flask. 10 μl of Cyclosporin A (CsA) (50 μg/ml stock) was added to the flask. The flask was tilted and left in a 37°C incubator for at least a week. Complete RPMI + 10% FCS and CsA were added as required for a following week. Media was added/changed without CsA as required. When clumps began to appear, the flask was placed in an upright position and media added/changed as necessary. The generation of an LCL line took 4-6 weeks. LCL lines were maintained in complete RPMI+ 10%FCS.

2.2.6 Preparation of Human AB Serum

Human cytotoxic T-cells (CTLs) used in this study were grown in medium supplemented with 10% Human AB serum. The serum, obtained from the Blood

Transfusion Service, needed to be purified from contaminating lipids before it can be used in tissue culture. The serum was aliquoted into 20 ml ultracentrifuge tubes, ensuring the tubes were equally balanced. The tubes were spun in at 92,000g for 1 hour, at 4°C. In the tissue culture hood, the serum was aspirated into a TC flask, avoiding the lipid membrane. On average 20 ml should yield approximately 18 ml of lipid free serum. Once all of the serum had been centrifuged, the lipid free serum was pooled and centrifuged through a 0.45 μl bottle top filter. The serum was incubated in a waterbath at 55 °C for 30 mins, mixed, and aliquoted into 10ml fractions. The aliquots were stored at -20 °C until required.

2.2.7 Generation of EBV-specific cytotoxic T-cells

To generate the EBV-CTL lines, we used EBV-transformed B-cell lines from healthy donors as antigen presenting cells (APCs). The generation of these EBV-transformed B-cell lines or lymphoblastoid cell lines (LCLs), which display latency III pattern of gene expression, has already been described in Section 2.2.5. EBV-associated PTLD tumour cells generally express latency III gene expression, making the LCLs a good *in vitro* model of PTLD tumours. Because EBV is a ubiquitous and persistent virus, the majority of donors carry a high frequency of EBV-specific CTL precursors in their peripheral blood that can be readily reactivated and expanded *in vitro* using EBV-LCLs as APCs. The protocol used to generate the EBV-CTL lines follows.

Generation of EBV-specific cytotoxic T-cells

Day 0 PBLs islolated from whole blood, resuspended at $2X10^6$/ml
in complete RPMI-40+ 10%AB serum (AB media)
+
$1X10^6$ γ-irradiated (5000 rads) autologous LCLs in 0.5 ml AB media

↓

Day 4 1 ml of AB media containing 25 IU/ml IL-2 added

↓

Day 6 1 ml of media removed and replaced with 1ml AB media containing 10 IU/ml IL-2 added

↓

Day 7 T-cells harvested, counted and resuspended at $2X10^6$/ml
+ $1X10^6$/ml irradiated autologous LCLs

↓

Day 9 1 ml AB media containing 25 IU IL-2 added

↓

Day 13 Wells topped up with 1 ml AB media containing 10 IU IL-2 (unless performing chromium release assay Day 14)

↓

Day 14 Chromium release assay as described in Section 2.3
Remaining CTLs counted and resuspended at $2X10^6$/ml
+ $1X10^6$/ml irradiated autologous LCLs

Day 0 to Day 7 steps were repeated weekly for the duration of the CTL line

2.2.8 Generation of functional retrovirus

2.2.8.1 Reagents and Materials required

Sigma $CaPO_4$ transfection kit (Sigma), containing 2XHEPES-Buffered Saline (HeBS), pH7.05 (50mM HEPES, 280mM NaCl, 1.5mM $Na_2H\ PO_c$), 2.5M $CaCl_2$, Molecular Biology grade sterile H_20), stored at –20°C. $CaPO_4$ transfection is based upon the formation of a precipitate containing calcium phosphate and DNA. The precipitate adheres to the cell surface and is internalized.

Poly-L-Lysine (Sigma), 1% solution supplied ready to use in sterile H_2O, stored at 4°C.

Chloroquine (Sigma), Diphosphate salt, reconstituted in PBS, stored at 4°C and used at a final concentration of 25μM.

Polybrene (Sigma), reconstituted in sterile H_2O to 0.8 mg/ml (100X) and stored at 4°C. Added to the cell culture to make a final concentration of 8 μg/ml of DMEM.

Cryoflex (Fisher Scientific), Robust Plastic tubing, withstands liquid N_2 snap freezing.

Puromycin dihydrochloride (Sigma), from *Streptomyces albo-niger*. Protein synthesis inhibitor that can prevent growth of bacteria, protozoa, algae and mammalian cells. The resistance gene (puromycin acetyltransferase) gives very effective protection. 1 mg was reconstituted in 1 ml PBS (1 mg/ml) and 500 μl aliquots were stored at -20°C. Used as a selective agent at 1 μg/ml and 2.5 μg/ml final concentration.

Cloning cylinders (Fisher Scientific). 8X8mm glass cloning cylinders and 6X8mm glass cloning cylinders.

Silicone Grease (FLUKA, Sigma). 100 g silicone grease, aliquots were autolclaved to sterilise before use, for 40 minutes at 15psi and 121°C.

2.2.8.2 Transient tranfection in Phoenix 293 retroviral packaging cells

Producing functional PINCO virus from a plasmid involves transient transfection into Phoenix 293 (PH293) retroviral packaging cells. The goal is to obtain a high retroviral titre through high level of plasmid expression. The simplest transfection method is the calcium phosphate-mediated transfection protocol.

Day 0 A 75cm^2 vented TC flask (BD Falcon) was coated with a thin layer of Poly-L-lysine (approx. 5 ml) for a minimum of 30 mins at room temperature (RT). The Poly-L-lysine was aspirated off and 6X10^6 PH293 cells in 10-15ml complete DMEM + 10% FCS, were seeded in the flask, ensuring an even monolayer. This flask was placed in a 37°C incubator overnight.

Day 1 Last thing on this day, medium was replaced with 15 ml fresh complete DMEM 5 minutes before transfection, 25 μM of chlorquine was added to the monolayer. DNA precipitate was prepared according to the $CaPO_4$ kit instructions and the precipitate was added to the flasks dropwise, ensuring even distribution over the PH293 monolayer. The flask was returned to 37°C overnight, in a sealed box. From this point on the experiment was treated with caution as functional retroviral supernatant could now be produced.

Day 2 First thing on this day, the medium was replaced with 6-8 ml fresh complete DMEM and the incubation was continued overnight at 33°C, in a sealed box

Day 3 GFP fluorescence of PINCO transfection was assessed by fluorescent microscopy (Figure 2.1(a)). Supernatant was harvested into 1 ml freezing vials, packaged in cryoflex tubing, snap frozen in liquid N_2, and stored at -80°C in a sealed box. 6-8 ml fresh medium was added to the monolayer and the incubation was continued overnight at 33°C, in a sealed box. Supernatant was harvested as before and the medium replaced with fresh DMEM, until Day 7, when the monolayer began to come away from the flask.

(a) Transeint PINCO/PH 93 system

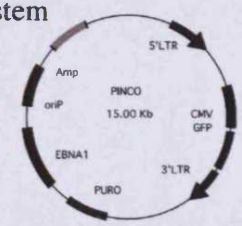

Hybrid EBV/Retroviral Vector
= PINCO GFP Plasmid
+
Phoenix 293 amphotropic packaging cell line

↓

Propagation of virus for human T-cell infection

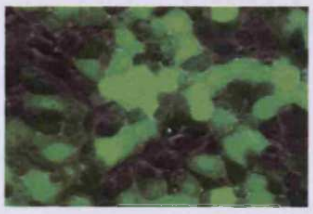

(b) Stable pBabe/ Ω-E/ Ψ-crip system

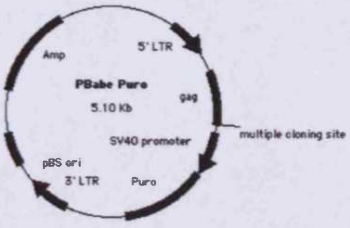

pBabe Retroviral Plasmid
+
Ω-E ecotropic packaging line

↓

Propagation of ecotropic virus

↓

Infection of Ψ-crip amphotropic packaging line

↓

Propagation of amphotropic virus for human T-cell infection

Figure 2.1 The generation of functional retroviral supernatant: 2 systems

(a) A transient transfection with PINCO and the amphotropic PH293 cell line is performed to generate functional PINCO retrovirus for human T-cell infection. (b) a stable Ω-E ecotropic packaging line is generated as an intermediate step in the generation of a Ψ-crip amphotropic packaging which produces the pBabe retrovirus for human T-cell infection.

2.2.8.3 Generation of stable retroviral packaging cell lines

The generation of stable amphotropic packaging cell lines is the method of choice to package the pBabe puro viral vector. The method involves an intermediate step during which a stable Omega E (ΩE) packaging line is generated, followed by the generation of a stable Psi crip (Ψcrip) amphotropic packaging cell line.

Omega E (ΩE) Ectotropic stage

Day 0 1-2X10^5 of ΩE cells were plated out in a 60mm tissue culture dish in 2-3 ml of complete DMEM +10% CS.

Day 1 4 hours before transfection the 60mm dish was re-fed with 3.6 ml of freshly opened, complete DMEM + 10% CS. The DNA precipitate was prepared according to the $CaPO_4$ kit instructions and added dropwise to the dish. The cells were returned to the incubator, in a sealed container and incubated overnight at 37°C. From this point, the experiment was treated with caution as functional retroviral supernatant could be produced.

Day 2 The precipitate was removed and the cells were washed twice in complete DMEM+ 10% CS. The cells were re-fed with 3 ml complete DMEM+ 10% CS and returned to the incubator overnight.

Day 3 Two days after transfection the cells were trypsinised and seeded in 75 cm^2 TC flasks at 1/10 and 9/10 dilutions made up to 10 ml with complete DMEM+ 10% CS.

Day 4 The medium was removed from each dish and replaced with 10 ml complete DMEM + 10% CS containing 2.5 μg/ml puromycin selection.

+ X days Cells were left to grow confluent, the supernatant was removed and replaced with puromycin free medium. The following day, the supernatant was removed,

snap frozen and stored at –80°C. The ΩE cells were harvested, frozen and stored in liquid N_2.

Psi crip (Ψcrip) Amphotropic stage

Day 0 1-2X10^5 of Ψcrip cells were plated out in a 60mm tissue culture dish in 5 ml of complete DMEM with 10% CS.

Day 1 1 hour prior to infection, the 60mm dish was re-fed with 5 ml of freshly opened, complete DMEM medium+10 % CS containing polybrene (8 μg/ml). The ecotropic superatant, from the ΩE transfection stage, was thawed at 37°C and filtered immediately through a 0.45 μM filter (treated wth caution). Polybrene was added to the viral supernatant (8 μg/ml) . The medium was removed from the 60mm dishes and the viral supernatant was added. The dishes were replaced to the incubator, in a sealed container, for four hours and 3 ml of complete DMEM +10 % CS was added. Dishes were incubated overnight at 37°C.

Day 2 The medium was removed and replaced with 5 ml complete DMEM+10 % CS.

Day 3 The Ψcrip cells were trypsinised, seeded into five 100mm tissue culture dishes in 1/2, 1/10, 1/50, 1/100 and 1/250 dilutions and topped up to 10 ml with complete DMEM+10 % CS.

Day 4 The medium was removed from each dish and replaced with 10 ml complete DMEM+10 % CS, containing 2.5 μg/ml puromycin.

+ X days Ψcrip cells were left to grow until numerous individual puromycin resistant colonies were evident, re-feeding as required with selection medium (The 1/2 dilution dish was allowed to grow to confluency and form a monolayer, of mixed Ψcrip

colonies, each producing virus of different efficiency. This mixed supernatant was harvested and snap frozen in liquid N_2). Once numerous individual puromycin resistant colonies were evident, they were isolated (minimum of 20) by trypsinisation within cloning cylinders (fixed to the dish with sterile silicone grease). These colonies were seeded in 60mm dishes in selection medium, allowed to grow to confluency and once confluent were passed to T25 cm^2 tissue culture flasks. Again the Ψcrip cells were allowed to grow confluent. At this point the supernatant was then removed and replaced with puromycin free medium. The cells were returned to the incubator.

X+1 Days Supernatant was removed, snap frozen in liquid N_2 and stored at –80°C in a sealed box. The Ψcrip cells were now harvested and frozen and stored in liquid N_2.

2.2.8.4 Titration of a retrovirus

PINCO virus

PINCO virus was titred according to a protocol used by Darley *et al.* in the Dept. of Haematology, UWCM. This involves an adapted version of the retroviral infection protcol described in Section 2.2.9, with the target cells being a Human Chronic Myelogenous Leukemia Cell line, K562 (ATCC). The wells of a 96 well TC plate were coated with 25 µl of retronectin (BioWhittaker) for two hours at RT and then replaced with 25 µl of 1% BSA/PBS for 30 mins at RT. This was then replaced with 100 µl of $2X10^5$ cells/ml in RPMI+10% FCS and incubated with 50 µl viral supernatant for two days at 37°C. A virus of known titre was used as standard. The percentage of GFP positive cells was assessed by flow cytometry after two days and the titre calculated as follows:

Titre (infectious units/ml) = % GFP +ve cells X $4X10^3$= total GFP +ve cells/ml virus X correction factor (calculated using standards % GFP)

pBabe puro virus

pBabe virus was titred according to a protocol used by Jones *et al.* in the Dept. of

Pathology, UWCM. $5X10^4$ A431 cells (human epidermal carcinoma cell line, ATCC) in 5ml of RPMI+10% FCS, were seeded in the wells of a six well plate. The following day, the virus was added in a 1/10 and a 1/100 dilution onto each plate in a 2 ml volume. The dish was replaced to the incubator and re-fed two days later with RPMI/10% FCS. The following day the cells were split into 1/100, 1/1000 and 1/10,000 dilutions in 100mm Petri dishes and replaced to the incubator overnight. The next day the medium was removed and replaced with 8 mls RPMI+10% FCS containing 2.5 μg/ml puromycin. The dishes were replaced to 37°C until discrete colonies began to form, re-feeding as required (10-14 days). The medium was then removed from the dishes, the cells were washed, soaked in 4% formal saline for 30 mins and stained with 10 % Geimsa stain (Sigma) for 30 mins. The stain was washed away with tap water, the colonies were counted and the viral titre was calculated according to the equation:

(No. Colonies X Dilution factor)/4=colony forming units/ml (cfu/ml)

2.2.9 Retroviral infection of human T-cells

2.2.9.1 Reagents and materials required

Retronectin (Takara Medicals, supplied by BioWhittaker), supplied as 0.5 mg of a recombinant human fibronectin fragment CD-296. Retronectin is the commercial form of the human fibronectin fragment protein of ≈ 63 kDa, which when coated onto the surface of either plates, petri dishes, or flaskes, significantly enhances retroviral-mediated gene transfer into mammalian cells. The lyophilised powder is reconstituted in 0.5 ml of sterile tissue culture grade water, allowed to rest at room temperature for 30 mins and then topped up to 5 ml with 50mM sodium carbonate buffer. 300 μl aliquots were stored at –20°C.

50mM sodium carbonate buffer pH 9.6. 160 mg Na_2CO_3 and 294 mg $NaHCO_3$ were dissolved in 100 ml tissue culture water, the pH was adjusted to pH 9.6 and the solution was filtered through a 0.2 μl m filter before use. Solution was stored at 4°C.

24-well non-tissue treated culture plates (Falcon, BD).

1%BSA/PBS 1g BSA (Sigma) added to 10 ml sterile PBS, dissolved thoroughly and filtered through a 0.2 μM filter. 1 ml aliquots stored at 4°C.

2.2.9.2 The 2-cycle retroviral infection protocol

This protocol involves infecting the T-cells in a two-cycle infection protocol with one-cycle per day. The reagent Retronectin and the centrifugation step used in the infection protocol are key features of this technique. See Figure 2.2 for a summary of the retroviral infection protocol.

Day 0 150 μl of retronectin solution was dispensed into required number of wells of 24-well untreated tissue culture plate, and placed on a rocker, for two hours, at RT. Retronectin was aspirated and replaced with 200 μl of 1% BSA/PBS and allowed to stand for 30 mins at RT. The required number of viral supernatant aliquots were removed from the –80°C storage and thawed immediately in a water bath (with caution). The aliquots were placed on ice and used immediately in infection. The BSA/PBS was removed and replaced with 1 ml of virus. The plates were sealed in bags and centrifuged at 3000g for two hours at RT. From each well in turn, the virus was discarded and immediately replaced with one wells worth of target cells ($2X10^5$ cells/ml) before any drying of the pre-coated wells could take place. The dish was then placed in a container. A 'tilt, mix, and lay flat gently' technique was used to ensure even coverage of the cells over the well. Since the virus in the plate was immobilised on the surface, the plate could gas up naturally in the incubator before affixing the lid to seal the container. The cells were incubated overnight at 37°C.

Day 1 The second cycle of the infection. The cells were transferred to a separate 24-well plate and were replaced to the incubator. Immediately, retrovirus was added to replace the cells and the plates were centrifuged again at 3000g for two hours at RT. The

virus was aspirated and immediately replaced with the original culture. The plates were replaced to the container and incubated overnight at 37°C. A 'tilt, mix ,and lay flat gently' technique was again used to ensure even coverage of the cells over the well.

Day 2 An aliquot of the cells was removed and assessed by flow cytometry for either GFP fluorescence (PINCO infection) and forward and side scatter of the cells (as an indication of the viability of the cultures). The GFP fluorescent cells were also visualised by fluorescent microscopy. From this point on, the cells were cultured according the requirements inherent to each cell type and assessed regularly by flow cytometry. For the pBabe puro infections, the selection medium was added (at a concentration determined by titration, see Section 2.2.9.3) and the puromycin resistant cells were grown out as described in the retroviral technology results of Chapter 4.

2.2.9.3 Titration of puromycin on Kit225 T-cells and primary human T-cells

Kit225 T-cells or primary human T-cells (which had been isolated three days previous and stimulated with anti-CD3 (OKT3, 2.5 ng/ml), anti-CD28 (5 μg/ml) and IL-2 (20 ng/ml)), were resuspended at $0.5X10^6$/ml in complete RPMI+10 % FCS, containing 20 ng/ml IL-2, and seeded in a 24-well plate. Puromycin was added to each well in increasing doses from 0.01 μg/ml to 10 μg/ml. The cells were incubated at 37°C overnight. The following day an aliquot of cells was removed and percentage of cell death was assessed as described in Section 2.3.3. This was repeated for three more days. Results showed that a minimum dose of 2.5 μg/ml of puromycin was required to kill 100% of Kit225 cells after two days selection and a minimum dose of 1 μg/ml puromycin was required to kill 100% of PBLs after two days selection.

Day 0

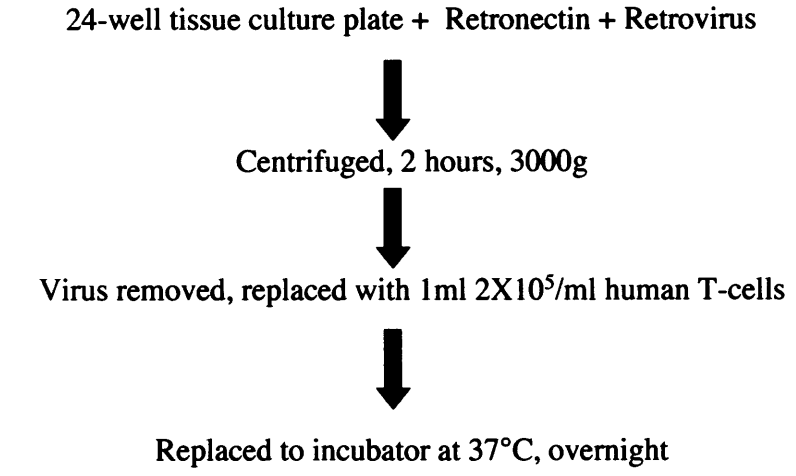

Day 1

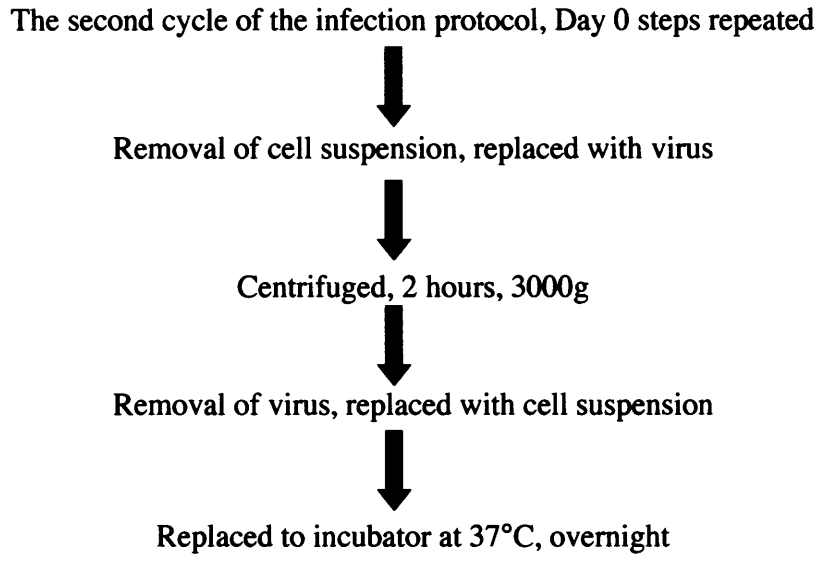

Day 2

Analysis of infected cells by Flow Cytometry

Figure 2.2 Retroviral infection of Human T-cells

Human T-cells were infected using a 2-cycle retroviral infection protocol which incorporates the use of Retronectin, a human fibronectin fragment, centrifugation of the retrovirus onto the tissue culture plate and 2-cycles of infection which involves repeating the centrifugation of the virus on the following day.

2.3 Investigation of human T-cells

2.3.1 Reagents and equipment required

Carboxyfluorescein diacetate, succinimidyl ester (5(6)-CFDA, SE) (CFSE), (Molecular Probes). 25 mg was reconstituted in 4.48 ml DMSO (to give10mM solution) and 50 µl aliquots were stored long-term at –80°C and short-term at –20°C. Cells were stained with 2.5 µM of CFSE.

Propidium Iodide (Sigma), (PI), 30X stock reconstituted in PBS and used at 50 µg/ml final concentration.

LY294002 (Calbiochem), 2-(4-Morpholinyl)-8-henyl-4H-1-benzopyran-4-one, a cell permeable, potent and specific phosphatidlyinositol 3-kinase (PI3K) inhibitor that acts on the ATP-binding site of the enzyme. Reconstituted in DMSO to a 50mM stock concentration and stored at –20°C. Dilutions made in RPMI-1640 and working concentrations of 1 µM to 20 µM used in experiments.

Rapamycin (Calbiochem), 100 µg was reconstituted in 1 ml DMSO (0.1 mg/ml stock) and stored at –20°C. 1/5 dilution working aliquots (20 µg/ml) were made up with RPMI and stored at –20°C. Experiments used 1 nM to 20 nM doses of rapamycin.

Cyclorsporin A (CsA, Novartis), Sandimmun, reconstituted in PBS to a stock concentration of 50 µg/ml and stored long-term at –20°C and short-term at 4°C. 0.25 µg/ml and 0.5 µg/ml concentrations used in experiments.

Tritiated thymidine (Amersham Biosciences), Methyl-^{3}[H] Thymidine, 1 mCi/ml, 37 mBq. Stored at 4°C.

Chromium 51 (Amersham Biosciences), 3.75 ug Cr/ml, 0.34 ml, 185 mBq. Made up in 1 ml RPMI-1640 before use, stored in a lead pot at 4°C.

Triton X100 (Fisher Chemicals), Octlyphenoxypolyethoxyethanol, stored at room temperature. 5% working dilutions were made in PBS and stored at 4°C.

Betaplate Scint (PerkinElmer), Liquid Scintillation Cocktail for assessment of Tritiated Thymidine levels on a Wallac, 1450 MicroBeta Liquid Scintillation Counter. .

Optiphase 'Supermix' (PerkinElmer). Scintillation cocktail for use in ^{51}Cr assays.

2% (w/v) Paraformaldehyde (PFA), was prepared by dissolving 10 g of paraformaldehyde (Sigma) in 500 ml of 1XPBS. This was done by overnight incubation in a water-bath at 50°C in a fume cupboard. Extreme care was taken not to allow the temperature to increase above 60°C due to the flash point of PFA. Once prepared, 2% PFA was stored at 4°C in the dark and as aqueous solutions of PFA can depolymerise to release formaldehyde, a known carcinogen in animals, caution was exercised at all times when in use. Retrovirally modified cells were resuspended in PFA to fix the cells before analysis by flow cytometry.

Cytometric Bead Array (CBA) Kit (BD Pharmingen), Human Th1/Th2 Cytokine CBA Kit for use with BD FACS brand Flow Cytometer (BD) and BD CBA analysis software (BD).

48-well Tissue Culture treated plates (Falcon, BD), Flat Bottomed, Low evaporation lid.

96-well tissue culture treated plates (CellStar, Greiner), U-shaped.

96-well Flexible Sample Plate (Wallac), Polyethylene terephtalate (PET), well volume 200 µl, for use with a Wallac, 1450 MicroBeta Liquid Scintillation Counter.

96-well Flexible Sample Plate Seal (Wallac), Sealing tape to seal 96-well Flexible Sample Plates (Wallac).

Printed Filtermat A (Perkin Elmer). Glass fibre filter mat, 90X120 mm, for use with a Wallac, 1450 MicroBeta Liquid Scintillation Counter.

Sample Bag (Perkin Elmer), to seal Printed Filtermat A (PerkinElmer), for use with Wallac, 1450 MicroBeta Liquid Scintillation Counter.

Becton Dickinson FACS brand Flow Cytometer (BD Pharmingen). CellQuest Analysis Software and BD Cytokine Bead Array analysis software used to analyse data generated from this machine.

Tomtec Harvester-96, Mach III (Tomtec, Hamden, CT).

Wallac Trilux 1450 Microbeta Liquid Scintillation Counter (Wallac).

2.3.2 Analysis of cell proliferation with carboxyfluorescein diacetate succinimidyl ester

Kit225 cells, PBLs or EBV-CTLs were washed twice in PBS and resuspended in 1 ml PBS for each 10^7 cells. Carboxyfluorescein diacetate succinimidyl ester (CFSE) (Kurts et al., 1997; Oehen and Brduscha-Riem, 1999) was added to give a final concentration of 2.5 μM. The cell suspension was mixed thoroughly and placed at 37°C for 5 minutes. The reaction was terminated by the addition of 50 ml of RPMI-1640 + 10% FCS. The sample was washed by centrifugation at 300g for 4 mins. The cells were washed twice more with PBS and resuspended in RPMI-1640 at $2x10^6$ cells/ml, in 6-well plates, prior to stimulation. The fluorescence of the cells was determined by flow

cytometry, acquiring data in the FL-1 channel on a BD FACS flow cytometer. Cells in the viable gate were analysed. The cell proliferation was determined by a decrease in cell fluorescence from Day 0 to the final time point of the experiment.

2.3.3 Cell counting and viability analysis

Cell Aliquots of 250 μl were removed from an experiment for analysis at appropriate times. A volume of 10 μl propidium iodide solution (PI, 50 μg/ml) was added in order to determine the levels of cell death in the samples. Cells in the live gate only, were counted for a defined time on the flow cytometer. The PI data to determine the percentage of cell death was analysed in the FL-3 channel, acquiring data on all cells, not just those in the live gate.

2.3.4 PI DNA staining

PI is a DNA dye that intercalates in the DNA helix and fluoresces strongly orange-red (Delmer *et al.*, 1995). Aliquots of confluent cells were centrifuged at 300g for four minutes. The cell pellet was resuspended in PBS, and centrifuged as before. This washing step was repeated once more. The cell pellet was fixed in cold 70% EtOH by adding dropwise to the cell pellet while vortexing. The cells were fixed for a minimum of 30 mins at 4°C. The EtOH was discarded and the samples were resuspended in PBS and centrifuged at 300g for four mins to wash the pellet. This was repeated twice more. To ensure only DNA was stained, cells were treated with RNAse (100 μg/ml) for 15 mins at room temperature. The cells were resuspended in PBS and centrifuged at 300g for four mins. The cells were then resuspended in propidium iodide (PI, 50 μg/ml) and analysed by flow cytometry. The percentage of cells with DNA in G0/G1, S or G2/M phase of the cell cycle was assessed in the FL-2 channel.

2.3.5 Analysis of cell proliferation by tritiated thymidine incorporation

Tritiated thymidine incorporation (^{3}[H]-thymidine) into DNA directly measures the DNA synthetic rate and therefore correlates with cell proliferation. Freshly isolated human T-cells were plated out (10^5 cells in 180 μl of complete medium) in triplicate, in

a 96-well round- bottomed plate and pre-treated with LY294002 and rapamycin at a range of doses alone or in combination for 30 minutes at 37°C. Cells were then stimulated with anti-CD3 antibody (OKT3 2.5 ng/ml) or anti-CD3 and anti-CD28 antibody (5 μg/ml) for three days and pulsed with tritiated thymidine (0.5 μCi per well; Amersham Life Sciences) for the last 16 hours of the experiment. Cultures were harvested onto glass fibre mats using a Tomtec Harvester-96, multiple sample cell-harvester and the filters sealed in sample bags filled with Betaphase scintillation fluid. ^{3}[H]-thymidine incorporation was assessed in a Wallac 1450 liquid scintillation counter. Data are expressed as mean counts per minute ± SEM.

2.3.6 Chromium release cytotoxicity assay

Unmodified or retrovirally modified CTLs were washed extensively with RPMI-1640+5% AB serum and resuspended in RPMI-1640+10% AB serum. CTLs were then added to wells of a 96-well round-bottomed tissue culture plate in 100 μl volumes in graded dilution to obtain the desired E:T ratios (with $10X10^5$ cells being the maximum number in a well and $3X10^3$ being the lowest). $1X10^6$ LCLs (autologous and allogeneic) were labelled for 90 mins at 37°C with 50 μCi of ^{51}Cr. 5 ml of RPMI-1640 was added and the samples were centrifuged at 300g for five mins. Supernatant was discarded carefully following radioactive waste disposal guidelines. Cell pellets were resuspended in 1 ml RPMI-1640+10% AB serum and replaced to the incubator for one hour to leach any excess ^{51}Cr. LCLs were then resuspended in RPMI-1640 and centrifuged at 300g for five mins. This was repeated. Cell pellets were then resuspended in RPMI-1640+10% AB serum and $2X10^3$ LCLs in 100 μl were added to each well of the 96-well plate. The maximum level of ^{51}Cr released from the LCLs was assessed by plating out a row of LCLs with $2X10^3$ per well in 100 μl and adding Triton-X. The level of ^{51}Cr released from the LCLs due to spontaneous lysis was assessed by plating out a row of LCL with $2X10^3$ per well in 100 μl and adding 100 μl of RPMI-1640+10% AB serum. The plates were incubated for four hours at 37°C. 20 μl of supernatant was removed from each well and added to 150 μl of Optimix scintillation fluid (Perkin Elmer) in a 96-well microtitre plate and sealed. The plates were shaken for five minutes before assessing ^{51}Cr levels in

a Wallac 1450 Liquid Scintillation Counter. The percentage lysis was determined by the following equation:

Percentage lysis= (E-S)/(M-S)X100

where E is the release from experimental samples, S is the spontaneous release, and M is the maximum release upon lysis with Triton-X. Data are presented as the mean percent lysis of triplicate samples +/- SEM. The Maximum release (M) counts per minute (cpm) and the spontaneous or background lysis (S) are noted in the relevant Figure legend for both autologous and allogeneic targets.

2.3.7 The assessment of cytokine production in retrovirally modified primary human T-cells

Cytokine production from retrovirally modified primary human T-cells was assessed using a Human Th1/Th2 Cytokine Cytometric Bead Array (CBA) Kit (BD Biosciences Pharmingen). PBLs were isolated from whole blood using a Ficoll gradient, and stimulated with anti-CD3 (OKT3, 2.5 ng/ml), anti-CD28 (5 μg/ml) and IL-2 (20 ng/ml) for three days. A 2-cycle retroviral infection was performed. PBLs were restimulated four days later with anti-CD3/IL-2 and puromycin (1 μg/ml) was added the following day. Once adequate cell numbers of puromycin resistant cells were available, the cytokine production from the PBLs was investigated. Cells were seeded at $1X10^6$/ml in a 48-well plate, pre-treated with CsA (0.25 μg/ml or 5 μg/ml doses) and stimulated with anti-CD3 (OKT3, 2.5 ng/ml) or anti-CD3 and anti-CD28 (5 μg/ml). Aliquots of supernatant were harvested after 8, 24 and 72 hours. A CBA assay was performed according to the manufacturers instructions, to assess the level of IL-5, IFNγ, IL-10, IL-2, IL-4 and TNF-α in the supernatant. The BD CBA system uses the sensitivity of fluorescence detection by flow cytometry to measure soluble analytes in a particle-based immunoassay. Six bead populations with distinct fluorescent intensities and coated with antibodies specific for IL-5, IFNγ, IL-10, IL-2, IL-4 and TNF-α proteins, were mixed together (5 μl of each bead/test, 30 μl total bead mix/test). The cytokine capture bead mixture was then mixed with the PE-conjugation detection antibodies (25 μl/test) and

then incubated for three hours at room temperature (protected from light) with recombinant standards (50 µl of each recombinant human IL-5, IFNγ, IL-10, IL-2, IL-4 and TNF-α protein) or test samples (50 µl) to form sandwich complexes. Samples were then washed with 1 ml wash buffer and centrifuged at 400g for five minutes. Supernatant was discarded and the bead pellet was resuspended in 300 µl of wash buffer. Following acquisition of sample data using the flow cytometer, the sample results were generated in graphical and tabular format using the BD CBA Analysis Software.

2.3.8 Detection of GFP expression by flow cytometry

The level of GFP expression from the PINCO modified T-cells was assessed by one-colour flow cytometry analysis. Cells were harvested by centrifuging at 300g, washed in PBS and fixed in 2% PFA/PBS. GFP fluorescence was then detected directly by flow cytometry and analysed with Cellquest Pro software (BD).

2.3.9 Staining of cell surface markers using immunofluorescence antibodies

CD3, CD4 and CD8 cell surface expression on primary human T-cells and EBV-CTLs was assessed using PE conjugated CD3 antibody (Serotec) and fluorescein isothiocyanate (FITC) conjugated CD4 and CD8 antibodies (Serotec). Cells were harvested by centrifuging at 400g, washed in PBS, resuspended at $10X10^6$/ml in chilled PBS/0.1% FCS and plated out in 100 µl volumes to a 96-well round-bottomed plate. The plate was centrifuged in a chilled centrifuge at 700g for two minutes. Supernatant was discarded and the cells were incubated with 2 µl of the required antibody (see Table 2.4) for 15 minutes at 4°C, protected from light. 100 µl of chilled PBS/0.1% FCS was added to the wells and the plates were centrifuged as before. This was repeated once more. Cells were then resuspended in 100 µl of PBS/0.1% FCS and analysed immediately by flow cytometry.

2.3.10 Mycoplasma testing

All reagents used in tissue culture protocols were mycoplamsa negative. All cell lines used routinely and all cell lines generated during the course of this project were negative for mycoplasma. Tests were carried out by Sian Llewellyn-Lacey in the MRC COOP Facility, Wales College of Medicine, Cardiff University. The method used for mycoplasma testing was the VenorGeM PCR kit which is currently the most sensitive available.

Table 2.5 Conjugated antibodies used in immunofluorescent experiments

Antibody	Description	Supplier
CD3:PE	Purified mouse IgG1 antibody to the human CD3 component of the TCR, conjugated to R. Phycoerythrin (RPE) 0.1 mg/ml	Serotec
CD4:FITC	Purified mouse IgG1 antibody to the human T-cell CD4 co-receptor, conjugated to fluroescein isothiocyanate isomer 1 (FITC) 0.1 mg/ml	Serotec
CD8:FITC	Purified mouse IgG1 antibody to the human T-cell CD8 co-receptor, conjugated to fluroescein isothiocyanate isomer 1 (FITC) 0.1 mg/ml	Serotec

2.4 Sodium Dodecyl Sulphate – Polyacryamide Gel Electrophoresis (SDS-PAGE) and Western blotting

2.4.1 Solutions and buffers used

2X Gel sample buffer (GSB) contained 100mM Tris-HCl pH 6.8, 20% glycerol, 0.2M dithiothreitol (DTT), 4% SDS, 0.02% bromophenol blue. Aliquots of 2X gel sample buffer were stored at –20°C.

Pre-stained molecular weight markers (Sigma) were supplied as ready-to-use protein markers and were stored in aliquots at –20°C.

Acrylamide solution (Merck) was purchased as a ready-mixed 40% stock containing acrylamide and *bis*-acrylamide at a ratio of 37.5:1 and stored at 4°C.

Ammonium persulphate (APS) was prepared as a 15% solution (w/v) in distilled water.

Resolving gel buffer was prepared as a 4X stock solution containing 1.5M Tris-HCl pH 8.8, 0.24% v/v NNN'N-tetramethyl-ethylenediamine (TEMED) and 0.4% SDS (w/v). This 4X stock solution was stored for up to one month at 4°C.

Stacking gel buffer was prepared as a 2X stock solution containing 0.25M Tris-HCl pH 6.8, 0.12% v/v NNN'N-tetramethyl-ethylenediamine (TEMED), 0.4% w/v SDS and stored for up to one month at 4°C.

Electrophoresis running buffer was prepared as a 10X stock solution containing 0.25M Tris-base, 1.92M glycine (Fisher), 1% SDS. The pH of the running buffer was at pH 8.3 and was not adjusted with HCl. This 10X stock solution was stored at room temperature.

Transfer buffer was prepared as a 1X working solution containing 25mM Tris-base, 192mM glycine, 20% v/v analysis grade methanol (Fisher) and stored at room temperature.

10X PBS was prepared by dissolving 50 PBS tablets (Oxoid) in 500 ml of distilled water, and this was stored at room temperature.

PBS-Tween was prepared by adding 100 ml of 10X PBS (1X PBS) and 500 μl (0.1% v/v Tween-20) of Tween-20 per litre of distilled water. This PBS-Tween was stored at room temperature.

Blocking buffer was prepared as a 1X working solution containing 0.2% I-block (Tropix), 0.1% v/v Tween-20 and 0.02% v/v NaN_2 in PBS. 200ml of distilled water were heated in a microwave until boiling and 25 ml of 10X PBS was added. 0.5 g of I-block purified casein was then dissolved in the hot PBS by stirring on a magnetic mixer. Following dissolution of the I-block, the solution was cooled and 250 μl of Tween-20 and 250 μl of 20% sodium azide were added. The blocking buffer solution was stored for up to 1 month at 4°C.

Alkaline phosphatase assay (APA) buffer was prepared as a 10X stock solution containing 1M diethanolamine (Tropix) pH 9.5 and 10mM MgCl2 and was stored for up to 1 month at 4°C.

CDP-Star development reagent (Tropix) was supplied as a ready-to-use solution and was stored at 4°C. It is an alkaline phosphatase substrate for use in chemiluminescent detection protocols and its corresponding chemical name is disodium 2-chloro-5-(4-methoxyspiro{-dioxetane-3, 2'-(5'-chloro)-tricyclo [3.3.1.13,7] decan}-4-yl-1-phenyl phosphate.

MESNA stripping buffer was prepared as a fresh 1X working solution as required and contained 62.5mM Tris-HCl pH 6.8, 2% w/v SDS and 50mM sodium 2-mercaptoethansulfonate (MESNA; Sigma).

SDS wash buffer was prepared as a 1X working solution containing 62.5mM Tris HCl pH 6.8 and 2% w/v SDS and was stored at room temperature.

2.4.2 Equipment used

Polyethylene lay flat film 204mm (Jencons)
Hybond-P polyvinylidene diflouride (PVDF) membrane (Amersham)
Chromatography paper 3MM Chr (Whatman)
P200 gel loading tips (Greiner)

Mini protean II SDS-PAGE apparatus (Biorad)

Mini protean 1mm glass plates, spacers, combs and stand (Biorad)

Trans-blot and Mini Trans-blot blotting apparatus (Biorad)

Powerpac 300 and 200/20 power supplies (Biorad)

X-omat LS Kodak film 18 X 24 cm (Amersham)

2.4.3 Preparation of whole cell extracts for SDS-PAGE

Cells were counted on a haemocytometer and resuspended in 50 μl of 1X PBS per $2X10^6$ cells. An equal volume of 2X gel sample buffer (GSB) was added and the cells were sonicated using a W0385 sonicator (Heatsystems-Ultrasonics Inc.). Following sonication, samples were heated at 100°C for 5 mins on a dry heating block.

2.4.4 Resolution of protein samples by SDS-PAGE

A 7.5% resolving gel required to resolve the mTOR protein, was prepared according to the recipe given in Table 2.6. This was poured into a mini protean gel apparatus and a layer of water-saturated butan-2-ol was pipetted over the gel. Resolving gels were left to set at room temperature for at least 45 mins.

Table 2.6 Composition of SDS-PAGE resolving gel used in this study

Reagent	7.5%
Resolving gel buffer	2.8 ml
Acrylamide solution	2.1 ml
15% APS	44 µl
Distilled H_20	6.3 ml

Once the resolving gel was set, the butan-2-ol layer was poured off and the surface of the gel was rinsed with distilled water with any remaining excess water absorbed with filter paper. Sufficient stacking gel for two mini-gels was prepared with 3.1ml distilled water, 3.9 ml stacking buffer, 0.8 ml acrylamide solution, 78 μl 15% APS and 8 μl NNN'Ntetramethyl- ethylenediamine (TEMED). This was poured over the

solidified resolving gel and a comb was inserted to form the wells of the gel. After setting the stacking gel for at least 20 mins, the wells were rinsed out with 1X electrophoresis running buffer and then a layer of running buffer was placed in the bottom of each well. Pre-stained molecular weight markers and protein samples were then loaded onto the gels by pipetting under this layer of running buffer. Further running buffer was used to bring the volume of the wells up to top of the gel and the gel was run in a mini protean II apparatus at 180V for 45 mins to 1 hour.

2.4.5 Transfer of resolved proteins onto polyvinylidene diflouride (PVDF) membranes

Polyvinylidene diflouride membranes were soaked in analysis grade methanol (Fisher) before use and then equilibrated in transfer buffer. Polyacrylamide gels were placed onto these membranes between two pieces of Whatman 3MM paper soaked in transfer buffer in a blotting cassette. Protein transfer was carried out at 50V for 3 hours (Mini- transblot apparatus, cooled with a container of ice). The blots were then washed three times for 10 mins in PBS-Tween.

2.4.6 Immunostaining of Western blots

Blots were blocked by placing in a sealed polyethylene bag with 15 ml of blocking buffer and incubating for a minimum of one hour at room temperature, with rocking. The blocking buffer was then removed and replaced with 10 ml primary anti-mTOR antibody (AbCam) at a 1/1000 dilution of stock (1 μg/ml), made up in blocking buffer, and incubated overnight at 4°C. The blot was then washed three times in PBS-Tween for at least 10 mins each. Subsequently, the blots were incubated with alkaline phosphatase-conjugated anti-rabbit secondary antibody diluted to 1/10,000 of stock reagent in blocking buffer, for 1 hour at room temperature. Blots were washed as previously and then given a final 10 mins wash in 1X alkaline phosphatase assay (APA) buffer. Any excess buffer was drained off and blots were incubated with CDP-Star (Tropix Inc.) for 5 mins. Again all excess liquid was removed and blots were exposed to a sheet of autoradiograph film (Kodak) through a polyethylene cover.

CHAPTER 3

Cell Proliferation studies of Human T-cells

3.1 Introduction

The objectives of this chapter were to investigate the proliferation of human T-cells in response to different stimuli; identify a T-cell stimulation strategy for high proliferation rates in primary human T-cells; and investigate the pharmacological agents rapamycin and LY294002. To monitor cell proliferation over time we used a carboxyfluorescein diacetate succinimidyl ester (CFSE) protein stain. CFSE spontaneously and irreversibly couples to both intracellular and cell-surface proteins by reaction with lysine side-chains and other available amine groups, making it a powerful probe for tracking cell proliferation and migration (Kurts et al., 1997; Oehen and Brduscha-Riem, 1999). When the cells divide, CFSE labelling is distributed equally between the daughter cells, which are therefore half as fluorescent as their parents. As a result, each successive generation in a population of proliferating cells is marked by a halving of cellular fluorescence intensity, that is readily discriminated by flow cytometry.

We first investigated the CFSE proliferation assay using the Kit225 cell T-cell line. Kit225 is an IL-2 dependent leukaemic T-cell line that has a regulated cell cycle proliferation pattern in response to IL-2. The line was established from a patient with T cell chronic lymphocytic leukemia (Hori *et al.*, 1987). Kit 225 cells express a large amount of IL-2 receptors constitutively and their growth is absolutely dependent on IL-2 (Hori *et al.*, 1987). No other stimuli, such as lectins or antigens, are required to maintain the responsiveness to IL-2. The Kit225 cells quiesce and accumulate in G1 phase of the cell cycle following the removal of IL-2 and upon addition of IL-2 the Kit225 cell line re-enters the cell cycle. This growth pattern is well characterised. The use of a T-cell system with a well-characterised proliferation pattern is useful in experiments to establish parameters of a technique or protocol

novel to the laboratory. Following on from these experiments, the proliferation of PBLs in response to different T-cell specific stimuli was assessed using the CSFE cell proliferation assay. PBLs can be readily activated *in vitro* with T-cell specific stimuli but the rate and degree of expansion is dependent on the stimulation used. Our objective was to determine a T-cell specific stimulation strategy that would result in optimal T-cell proliferation with minimal cell death in order to maximise infection potential in a retroviral infection protocol.

The effect of the immunosuppressant rapamycin, on human T-cell proliferation, was investigated in this chapter. Rapamycin, which was discovered through analysis of soil samples, is a lyphophilic macrolide produced by a strain of *Streptomyces Hygroscopicus* (Sehgal *et al.*, 1975; Vezina *et al.*, 1975). The work of Calne *et al.*, established rapamycin's role in the clinic and this natural microbial product has potent immunosuppressive activity (Watson *et al.*, 1999). Rapamycin inhibits a subset of PI3K pathways by inhibiting the molecule mTOR (Abraham and Wiederrecht, 1996). Experiments were performed using Kit225 cells as a model T-cell line system before moving onto to the PBL studies.

The effects of the PI3K inhibitor LY294002 on human T-cell proliferation was also investigated in this chapter. LY294002 is a competitive ATP binding site inhibitor, developed by Vlahos *et al.* (Vlahos *et al.*, 1994), that completely and reversibly inhibits PI3K (Downing *et al.*, 1996) and has been previously used in our laboratory to study the role of PI3K in lymphocyte cell cycle proliferation (Brennan *et al.*, 1997; Brennan *et al.*, 1999). The known functional effects of the PI3-kinases suggest possible therapeutic targets for a PI3-kinase inhibitor. Again, experiments were performed using Kit225 cells as a model T-cell line system before moving onto to the PBL studies. Following on from the rapamycin experiments and the LY294002 experiments, we also investigated the effects of a combination of LY294002 and rapamycin in the human T-cell.

3.2 Characterising the cell proliferation of human T-cells in response to different stimuli

To monitor cell proliferation over time we used carboxyfluorescein diacetate succinimidyl ester (CFSE) protein stain, which is a powerful probe for tracking cell proliferation and migration (Kurts et al., 1997; Oehen and Brduscha-Riem, 1999). As the cells divide the labelling is distributed equally between the daughter cells, thus the fluorescence moves left, down the log scale, as detected by flow cytometry. Before studying proliferation of primary human T-cells, we first applied this CFSE proliferation assay to Kit225 cells. This IL-2 dependent leukemic T-cell line has a regulated cell cycle proliferation pattern in response to IL-2 (Brennan *et al.*, 1997; Brennan *et al.*, 1999) and the Kit225 cells accumulate in G1 phase of the cell cycle following the removal of IL-2. Kit225 cells were washed out of IL-2 for 3 days and stained with the cell protein dye CFSE. Cells were then resuspended in growth medium with or without IL-2 (20 ng/ml) and fluorescence was analysed by flow cytometry for up to 4 days in the FL-1 channel. Gating of the live cells in the forward scatter/side scatter dot plots and applying this gate to the FL-1 histograms, restricted proliferation analysis to viable cells only, excluding an effect on cell survival. Representative flow cytometry histograms, measured after one day of IL-2 stimulation and four days stimulation, are illustrated in Figure 3.1. The percentage of cells that had proliferated was measured. The marker that was used to identify the proliferation of cells is indicated as M1. Figure 3.1 demonstrates that 62.1% of cells have proliferated in the IL-2 stimulated sample after four days stimulation. The results of Figure 3.1 illustrate that we can successfully monitor T-cell proliferation over time in a CFSE based proliferation assay.

We next assessed the proliferation of freshly isolated PBLs in response to various stimuli. PBLs can be readily activated *in vitro* with T-cell specific stimuli but the rate and degree of expansion is dependent of the stimulation used. It has been demonstrated that optimal T-cell stimulation requires signalling through the TCR, the IL-2R and the CD28 co-stimulatory receptor (Powell *et al.*, 1998). Our objective was to determine a T-cell specific stimulation strategy that would result in a high

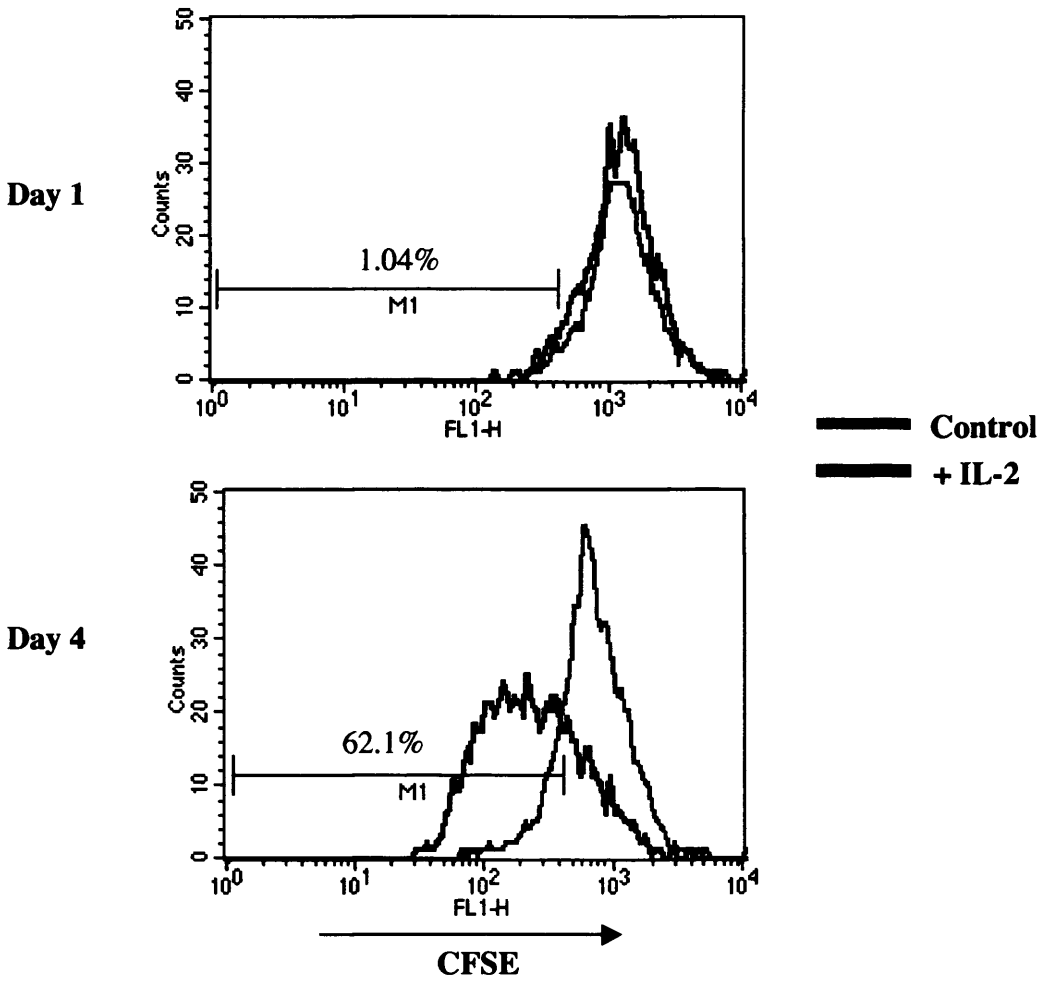

Fig 3.1 CFSE proliferation assay in the IL-2 dependent T-cell line, Kit225

Kit225 cells were washed out of IL-2 for 3 days to quiesce the cells, and stained with the cell protein dye CFSE. Cells were then resuspended in growth medium with or without IL-2 (20 ng/ml) and fluorescence was analysed by flow cytometry for up to 4 days post-stimulation. Data was acquired in the FL-1 channel. Representative flow cytometry histograms, measured after 1 day and 4 days, are illustrated. The marker (M1) that was used to identify the proliferation of cells is indicated. The live cells were gated in forward scatter/side scatter dot plots on the flow cytometer and this live gate was applied to the above histograms. Thus, only the percentage of cells that had proliferated within the live gate, was measured.

level of T-cell proliferation with minimal cell death. To elucidate optimal PBL stimulation for our purposes, we examined the use of Phytohaemagglutin (PHA) stimulation, which has proven effective in T-cell activation, IL-2 stimulation, antibody to the CD3 component of the TCR complex (anti-CD3) stimulation and anti-CD28 co-stimulatory stimulation. PBLs were isolated from whole blood by a Ficoll-gradient, and stained with the cell protein dye CFSE. Cells were then resuspended in growth medium with PHA (1 μg/ml); PHA and IL-2 (20 ng/ml); anti-CD3 (OKT3 2.5 ng/ml, CRUK); anti-CD3 and IL-2, anti-CD3 and anti-CD28 (BD,5 μg/ml); or anti-CD3 and anti-CD28 and IL-2. Aliquots were removed for analysis at day 4 and day 6. Representative flow cytometry histograms, measured after 4 days, are shown in Figure 3.2. The marker that was used to identify the percentage of proliferation of the cells is indicated as M1. Gating of the live cells in the forward scatter/side scatter dot plots and applying this gate to the FL-1 histogram restricted proliferation analysis to within the live gate only, excluding an effect on cell survival. Figure 3.2 demonstrated that PHA/IL-2 was effective in stimulating PBL proliferation but microscopic analysis revealed that the use of PHA to stimulate the PBLs resulted in a higher level of cell death. Stimulation of PBLs with anti-CD3/CD28/IL-2 resulted in proliferation of 47.96 % followed by anti-CD3/IL-2 stimulation, which yielded 44.04 %. Figure 3.3 demonstrates that stimulation of PBLs with anti-CD3/CD28/IL-2 resulted in optimal stimulation between 3 and 4 days following addition of the stimulation. Analysis of results from day 3 through to day 7 indicated that the percentage of PBLs that had proliferated more than doubled overnight from day 3 to day 4 (22.33%-47.33%) while the percentage of PBLs that had proliferated almost doubled over two days from day 4 to day 6 (47.73%-91.13%). The proliferation between day 6 and day 7 following PBL stimulation was not greatly increased. This data indicate that the highest rate of proliferation occurs between day three and day four days following PBL stimulation.

We used propidium iodide (PI) staining of the PBL DNA as a complementary technique to assess the effect of the various stimuli on the proliferation of PBLs. PI is a DNA dye that intercalates in the DNA helix and fluoresces strongly orange-red.

Fig 3.2 CFSE proliferation assay to assess the effect of various stimuli on the proliferation of PBLS

PBLs were isolated from whole blood and stained with the cell protein dye CFSE. Cells were resuspended in growth medium and stimulated as indicated. Aliquots were removed for analysis by flow cytometry at discrete timepoints. Data was acquired in the FL1 channel. Representative flow cytometry histograms, measured after 4 days, are illustrated. The marker (M1) that was used to identify the proliferation of cells is indicated. The live cells were gated in forward scatter/side scatter dot plots on the flow cytometer and this live gate was applied to the above histograms. Thus, only the percentage of viable cells that had proliferated was measured.

.

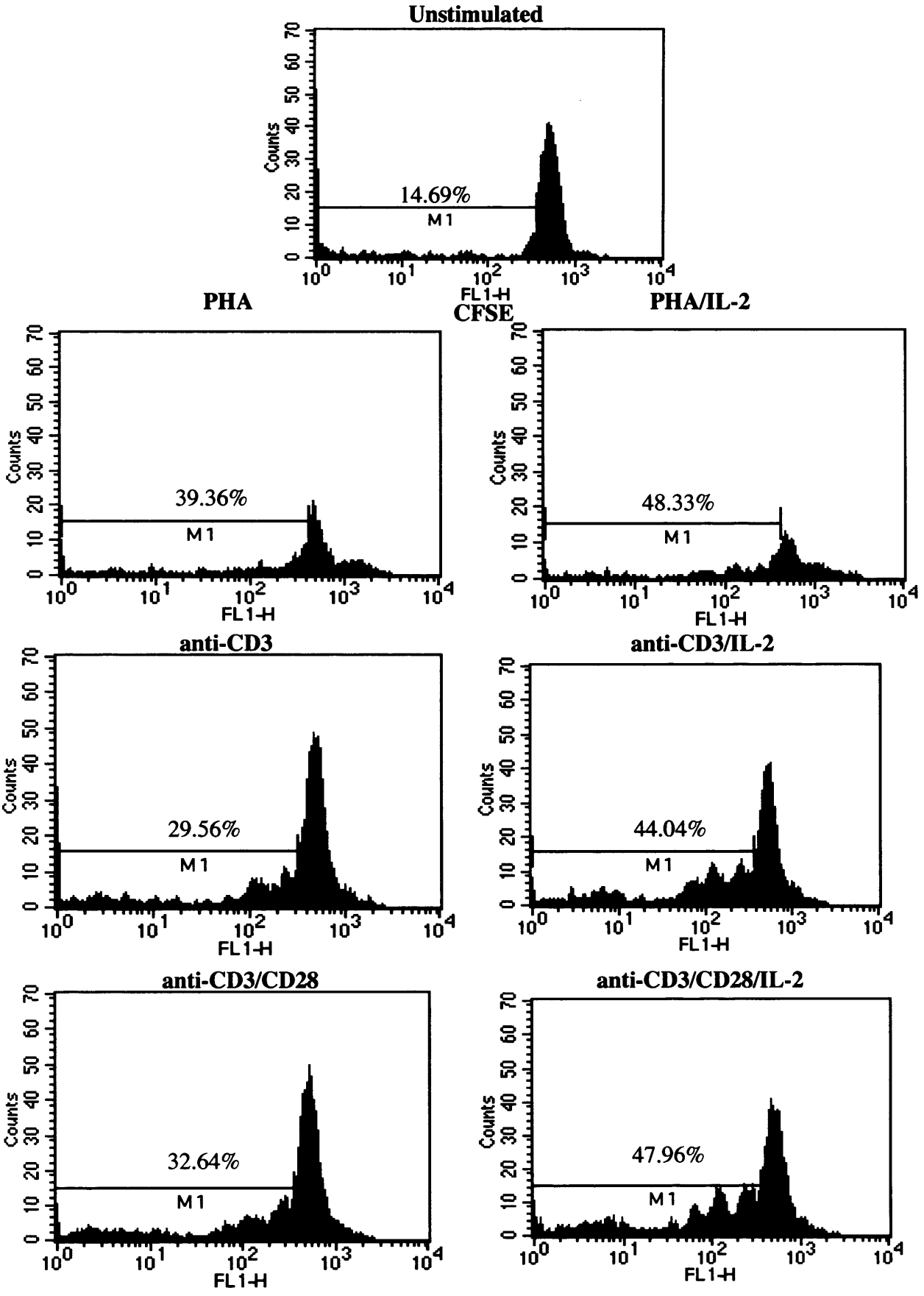

Fig 3.2 CFSE proliferation assay to assess the effect of various stimuli on the proliferation of PBLS

See opposite for figure legend text.

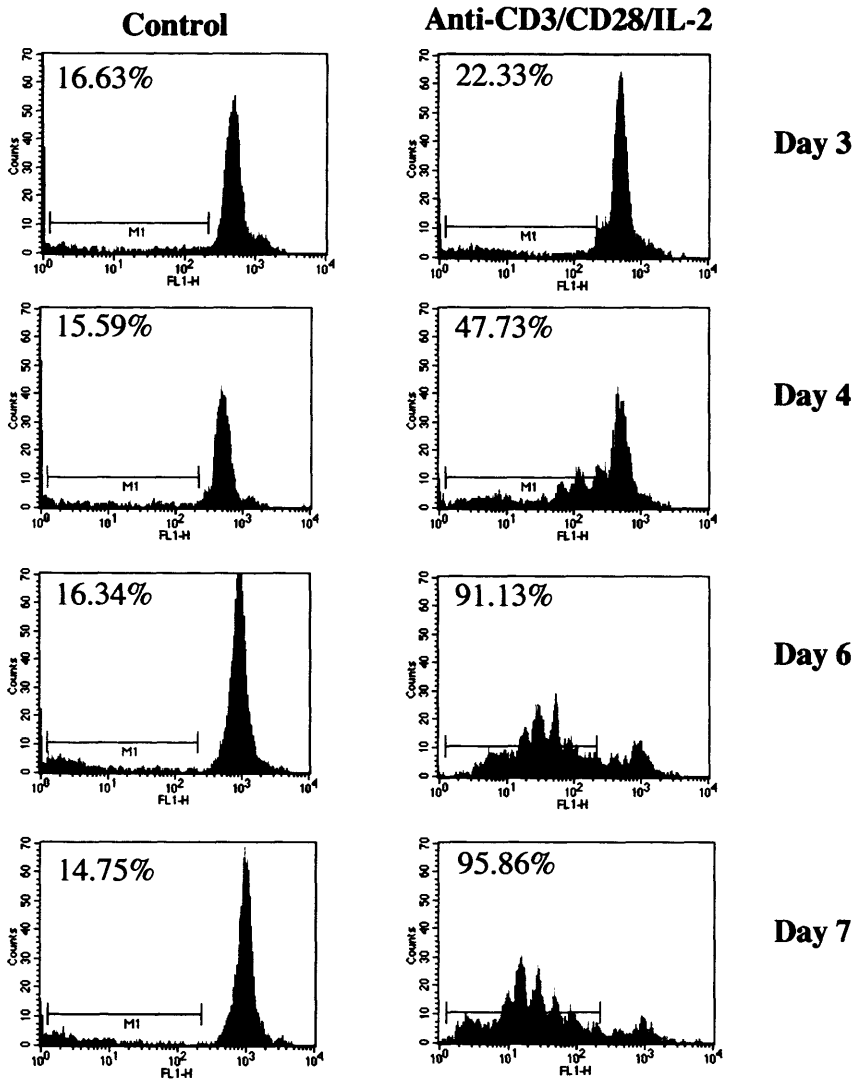

Fig 3.3 CFSE proliferation assay to assess the proliferation of PBLs in response to stimulus over time

PBLs were isolated from whole blood and stained with the cell protein dye CFSE. Cells were resuspended in growth medium and stimulated as indicated. Aliquots were removed for analysis by flow cytometry at discrete timepoints. Data was acquired in the FL1 channel. Representative flow cytometry histograms, measured after 4 days, are illustrated. The marker (M1) that was used to identify the proliferation of cells is indicated. The live cells were gated in forward scatter/side scatter dot plots on the flow cytometer and this live gate was applied to the above histograms. Thus, only the percentage of viable cells that had proliferated was measured.

PI staining can provide information about the percentages of cells in a population with DNA in G0/G1, S or G2/M phase of the cell cycle (Delmer *et al.*, 1995) and is a useful technique in determining the effect of particular stimuli on the cell cycle. It is possible to identify the proportions of cells that are in one of the three inter-phase stages of the cell cycle. The amount of DNA dye that is bound and the strength of the fluorescent signal it gives upon flow cytometric analysis is proportional to each cell's DNA content. The histograms generated can be separated into regions that represent cells within G0/1, S and G2/M phases of the cell cycle. Cells that are in the G0/1 phase (before DNA synthesis) have a defined amount of DNA (1X, a diploid chromosomal DNA content). During S phase (DNA synthesis), cells contain between 1X and 2X DNA levels. Within the G2 or M phases, cells have a 2X amount of DNA. This technique was used in parallel with the CFSE experiments to identify the stimulus that gave the most cell cycling (as determined by the percentage of cells in G0/1, S and G2/M phase). PBLs were isolated from whole blood and resuspended in growth medium with PHA (1 μg/ml); PHA and IL-2 (20 ng/ml); anti-CD3 (OKT3 2.5 ng/ml, CRUK); anti-CD3 and IL-2, anti-CD3 and anti-CD28 (BD, 5 μg/ml); or anti-CD3 and anti-CD28 and IL-2. Aliquots were harvested and fixed in 70% EtOH. The samples were PI stained with 50 μg/ml PI and analysed by flow cytometry. Markers were applied to the histograms as illustrated and the percentage of cells in G0/G1 phase (M1), S phase (M2) and G2/M phase (M3) of the cell cycle was assessed. The histograms of Figure 3.4 (a) are representative histograms and show control (unstimulated) PBLs and anti-CD3/CD28/IL-2 stimulated PBLs 6 days post-stimulation. The table in Figure 3.4 (b) represents the percentage of cells in G0/G1, S and G2/M phase for all of the stimuli tested. Figure 3.4 (b) shows that stimulation of PBLs with anti-CD3/CD28/IL-2 resulted in optimal stimulation with 61.7% of cells in G0/G1 phase of the cell cycle, 23.0% in S phase and 9.1% in G2/M phase.

(a)

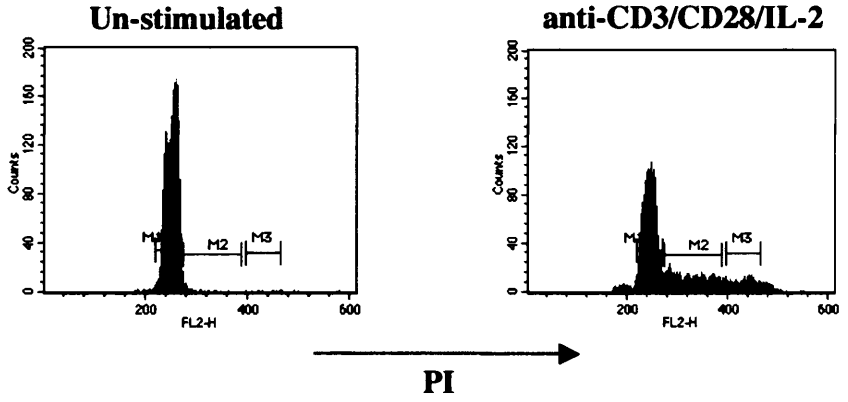

(b)

	G0/G1	S	G2/M
Control	97.2%	1.2%	0.3%
PHA	90.8%	4.7%	2.2%
PHA/IL-2	47.3%	19.4%	8.6%
anti-CD3	92.0%	1.8%	0.9%
anti-CD3/CD28	89.0%	5.2%	3.3%
anti-CD3/IL-2	64.2%	22.3%	8.0%
anti-CD3/CD28/IL-2	61.7%	23.0%	9.1%

Fig 3.4 Propidium iodide staining to assess the effect of various stimuli on the proliferation of PBLS

Propidium iodide (PI) staining of the PBL DNA was used as a complementary technique to assess the effect of the various stimuli on the proliferation of PBLs. PI is a DNA dye that intercalates in the DNA helix and fluoresces strongly orange-red. PI staining can provide information about the percentages of cells in a population with DNA in G0/G1, S or G2/M phase of the cell cycle and is a useful technique in determining the effect of particular stimuli on the cell cycle. PBLs were isolated from whole blood, resuspended in growth medium and stimulated with stimuli as indicated. Aliquots were harvested at appropriate timepoints and fixed in 70% EtOH. On the final day of the experiment, all of the samples were PI stained with 50 ng/ml PI and analysed by flow cytometry. (a) represents the control (unstimulated) PBLs and the anti-CD3/CD28/IL-2 stimulated PBLs after 6 days. Markers were applied to the histograms as illustrated and the percentage of cells in G0/G1 phase (M1), S phase (M2)and G2/M phase (M3) of the cell cycle was assessed. (b) The table represents the percentage of each stimulated PBL population in G0/G1, S and G2/M phase.

3.3 Combinations of LY294002 and rapamycin co-operate to inhibit IL-2 induced proliferation

Once a technique to monitor T-cell proliferation over time was established, we moved on to study the immunosuppressive compounds LY294002 and rapamycin. Rapamycin, an immunosuppressant, inhibits a subset of PI3K pathways by inhibiting the molecule mTOR (Abraham and Wiederrecht, 1996). We aimed to establish the effects of rapamycin on primary human T-cell proliferation as assessed by CFSE proliferation assays. We also performed experiments to establish the effects of LY294002 on human T-cells, in order to develop our understanding of the compound. LY294002 is a competitive ATP inhibitor of PI3K that is stable in aqueous solution (Vlahos *et al.*, 1994) and has been used previously in our laboratory to study the role of PI3K in lymphocyte cell cycle proliferation (Brennan et al., 1999). We first assessed the effects of LY294002 or rapamycin on IL-2 induced Kit225 cell proliferation. Quiesced Kit225 cells were stained with CFSE, treated with LY294002 or rapamycin at the concentrations shown and stimulated with IL-2 (20 ng/ml). Figure 3.5 (a) shows two dose response graphs combining cell proliferation data of Kit225 cells treated with LY294002 or rapamycin alone from 3 separate experiments. The concentrations of LY294002 used were 1μM, 5μM, 10μM and 20μM. The concentrations of rapamycin used were 1 nM, 5nM, 10 nM and 20 nM. This graph demonstrates that IL-2 induced Kit225 cell proliferation is inhibited by LY294002 and rapamycin in a concentration dependent manner and that 20μM and 20 ng/nl concentrations of LY294002 and rapamycin respectively are most effective in this inhibition.

Following on from these experiments we investigated the effects of a combination of LY294002 and rapamycin in the cell. We hypothesised that the effects of LY294002 and rapamycin may co-operate to cause enhanced inhibition of proliferation. This hypothesis was first investigated using Kit225 cells. Quiesced Kit225 cells were stained with CFSE, pre-treated with LY294002 or rapamycin in combination and stimulated with IL-2 (20 ng/ml). The concentrations of LY294002

(a)

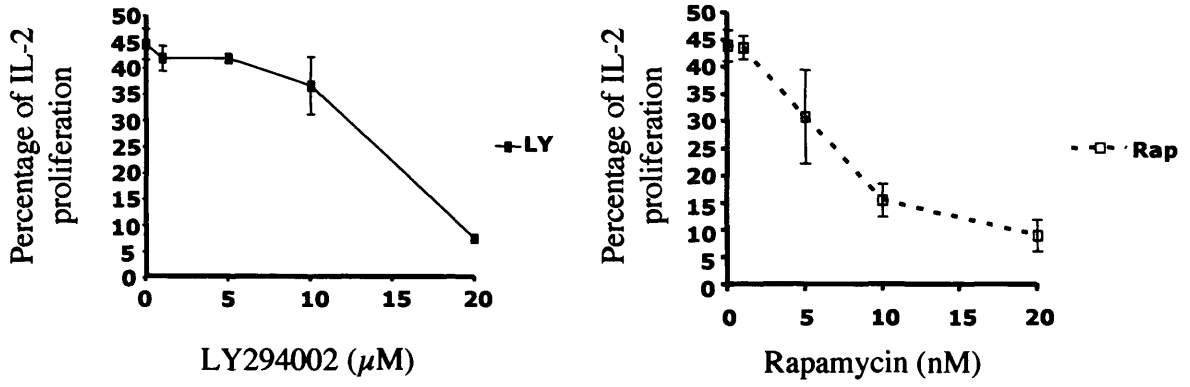

(b)

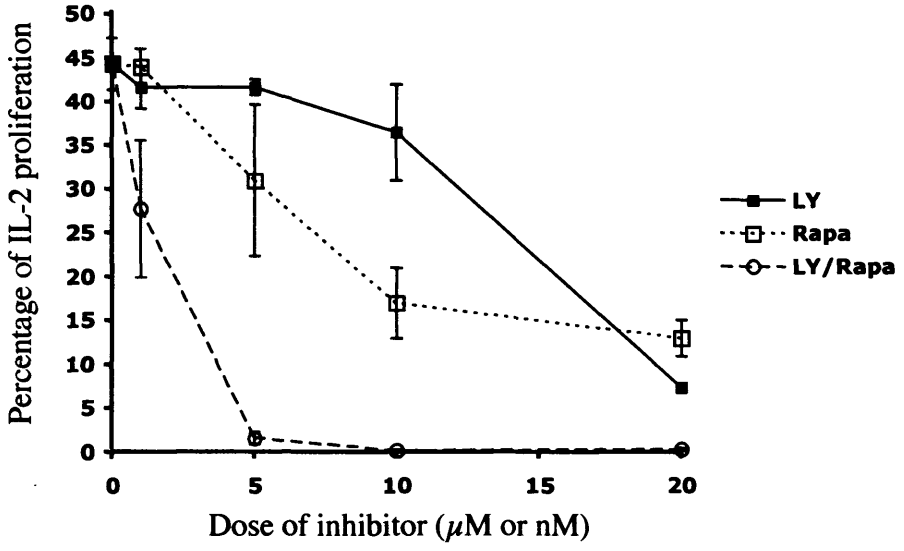

Fig 3.5 Combinations of LY294002 and rapamycin co-operate to inhibit IL-2 induced proliferation

Quiesced Kit225 cells were stained with a cell protein dye, CFSE. They were then treated with LY294002 or rapamycin at the concentrations shown and stimulated with IL-2 (20 ng/ml). (a) Dose response graph of the effects of LY294002 or rapamycin treatment on IL-2 induced proliferation of Kit225 cells after four days are indicated. The concentrations of LY294002 used were 1 μM, 5 μM, 10 μM and 20 μM. The concentrations of rapamycin used were 1 ng/ml , 5 ng/ml, 10 ng/ml and 20 ng/ml. The data from three separate experiments is shown in each graph (b) Dose response graph of the effects of a combination of LY294002 and rapamycin on IL-2 induced Kit225 proliferation is indicated comparing the effects to LY294002 and rapamycin alone. The data from 3 separate experiments is shown. The concentrations of LY294002 used were 1μM, 5μM, 10μM and 20μM (solid squares). The concentrations of rapamycin used were 1 ng/ml , 5ng/ml, 10 ng/ml and 20 ng/ml (open squares). LY294002 and rapamycin were combined at each of the above concentrations (open circles).

used were 1μM, 5μM, 10μM and 20μM and the concentrations of rapamycin used were 1 nM, 5nM, 10 nM and 20 nM. Figure 3.5 (b) shows a dose response graph combining cell proliferation data of Kit225 cells treated with LY294002 or rapamycin in combination from 3 separate experiments (open circles). For comparison, the graph also depicts the dose response using LY294002 (solid squares) and rapamycin (open square) separately. This graph suggested that LY294002 and rapamycin co-operate to inhibit IL-2 induced Kit225 T-cell proliferation and that this co-operation is most notable at 5μM LY294002 and 5nM rapamycin concentrations. Figure 3.6 shows a typical flow cytometry profile from this experiment. The numbers on the histograms denote the proposed number of population divisions the cells have undergone.

For more complex analysis of the data, the curves generated by the CFSE profile were analysed using the proliferation platform of the FlowJo software. This analysis allocates cells to populations that have divided, based on a best-fit root mean square function. FlowJo also returns various values that provide a measure of proliferation. Two of these measurements are Division Index and % Divided. Division Index is the average number of divisions that a cell (that was present in the starting population) has undergone. % Divided is the percentage of the cells of the original sample, which divided (assuming that no cells died during the culture). The allocation of cells to populations also allows a calculation of the number of cell divisions. Each cell in population 1 has divided once while each cell in population 2 has divided twice and so on. We have calculated these three measurements for Kit225 cells treated with LY294002 and rapamycin to allow the best quantitation of the effects of these inhibitors on the CFSE profiles. Each of these is indicated as histograms (Figure 3.7). All of the measurements show similar patterns. Paired T-tests were performed to determine if the samples were significantly different from those that have been treated with IL-2 alone. With $p<0.05$ indicated by one asterisk (*) and $p<0.01$ indicated by two asterisks (**). All three histograms show that 20 μM LY294002 and 20nM rapamycin significantly inhibited Kit225 cell proliferation. The lower concentrations, 5 μM LY294002 and 5nM rapamycin did not significantly

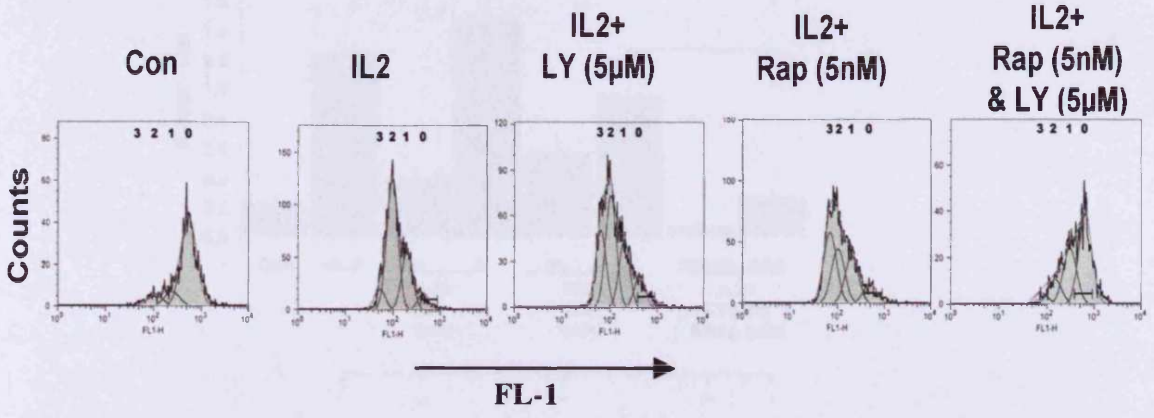

Fig 3.6 The co-operation of combinations of LY294002 and rapamycin to inhibit IL-2 induced proliferation is most notable at 5μM LY294002 and 5nM rapamycin doses

Quiesced Kit225 cells were stained with a cell protein dye, CFSE. They were then treated with LY294002 or rapamycin at the concentrations shown and stimulated with IL-2 (20 ng/ml). Representative flow cytometry histograms, measured after four days, are illustrated. The data was analysed using the proliferation platform of the FlowJo software. The numbers on the histograms denote the proposed number of population divisions the cells have undergone.

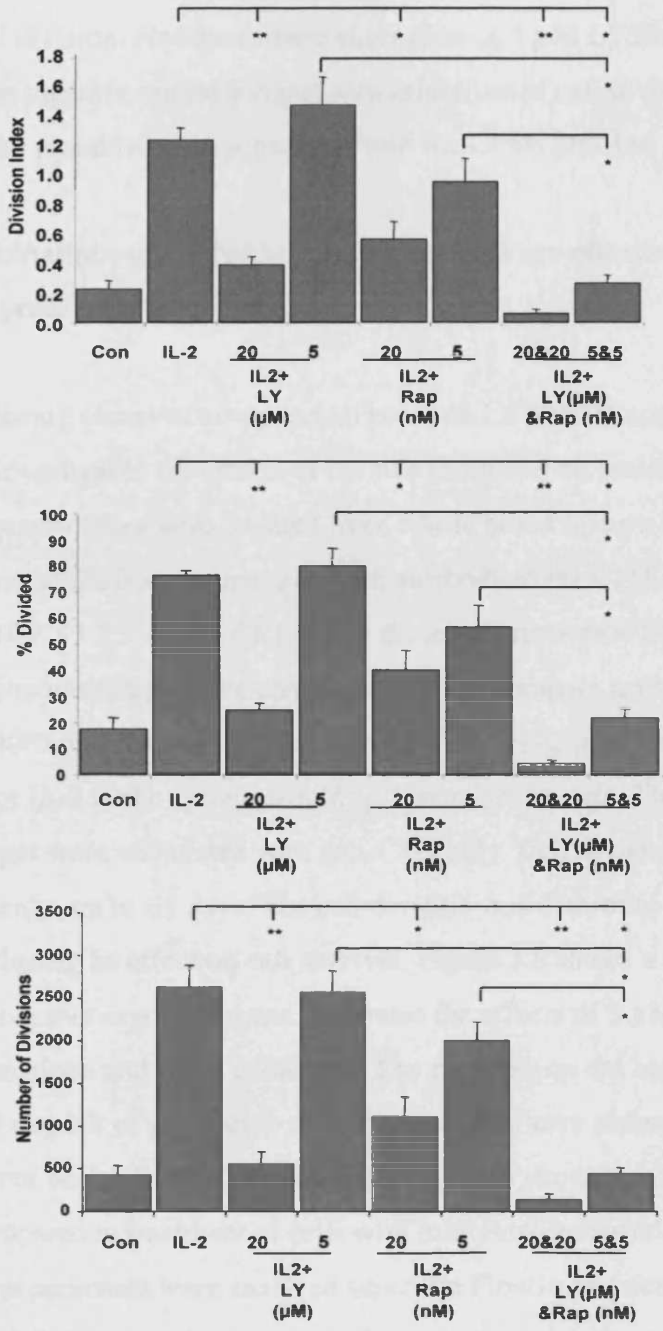

Fig 3.7 FlowJo analysis of the Kit 225 CFSE profiles

Quiesced Kit225 cells were stained with a cell protein dye, CFSE. They were then treated with LY294002 or rapamycin at the concentrations shown and stimulated with IL-2 (20 ng/ml). Fluroescence was measured by flow cytometry up to four days post-stimulation. The curves generated by the CFSE profile were analysed using the proliferation platform of the FlowJo software. The three measurements calculated (Division Index, % Divided and Number of Divisions) are indicated as histograms. The graphs were generated from three different experiments. The numbers under the axis represent inhibitor concentrations. The error bars represent the standard error from three experiments. Student's T-tests were used to ascertain if the results were significant with one asterisk indicating a significance level of $p<0.05$ and two asterisks indicating $p<0.01$.

affect cell division. However, the combination of 5 μM LY294002 and 5nM rapamycin together caused a significant inhibition of cell division as indicated by all three of the measurements generated from the CFSE profiles.

3.4 Combinations of LY294002 and rapamycin are effective at inhibiting CD3 induced proliferation

Having observed co-operation between LY294002 and rapamycin in Kit225 cells we investigated the effects of the two inhibitors on proliferation in PBLs. Human lymphocytes were isolated from whole blood using a Ficoll-gradient, labelled with CFSE and stimulated with antibody to the CD3 chain of the T-cell receptor (OKT3 2.5 ng/ml, CRUK). In these experiments, PBLs were also treated with the immunosuppressive compound CsA to compare immunosuppressive effects to LY294002 and rapamycin. CsA acts to inhibit IL-2 production so the addition of exogenous IL-2 to the system would compromise the data. Therefore PBLs in these experiments were stimulated with anti-CD3 only. Cell division was measured at various times, up to six days. The cell division was determined within the live gate only, excluding an effect on cell survival. Figure 3.8 shows a typical flow cytometry profile from this experiment and illustrates the effects of 5 μM LY294002 and 5 nM rapamycin alone and when combined. The numbers on the histograms denote the proposed number of population divisions the cells have undergone. The combined treatment of both LY294002 and rapamycin more strongly inhibited PBL division when compared to treatment of cells with inhibitors independently. Data from four separate experiments were analysed using the FlowJo proliferation platform and the number of divisions undergone in each population of cells was calculated. These were combined to generate the mean and standard error of the mean as shown in Figure 3.9. Paired student T-tests were performed to test if the differences between the combined treatments of LY294002 and rapamycin were significant when compared to the effects of the inhibitors used alone. The asterisk on Figure 3.9 indicates a significance level of $p<0.05$. Both inhibitors alone at concentrations of 5 μM LY294002 and 5 nM rapamycin reduced CD3 induced cell division although the

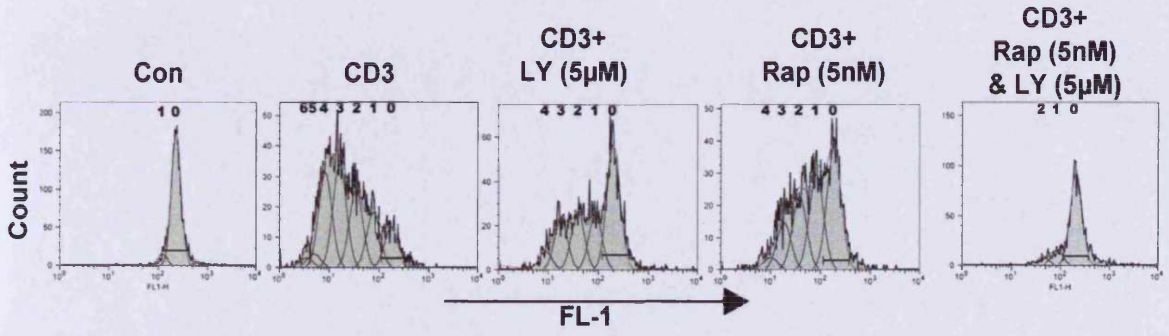

Fig 3.8 Combinations of LY294002 and rapamycin co-operate to inhibit cell division of Primary Human T-cells stimulated with anti-CD3

Primary Human T-cells isolated from whole blood were were stained with CFSE and pre-treated with LY294002 or rapamycin, or a combination of the two inhibitors at the doses indicated for 30 minutes prior to stimulation with an antibody to the CD3 chain of the T-cell receptor (OKT3, 2.5 ng/ml, CRUK). Representative flow cytometry histograms, measured after six days, are illustrated. The curves generated by the CFSE profile were analysed using the proliferation platform of the FlowJo software. The numbers on the histograms denote the proposed number of population divisions the cells have undergone.

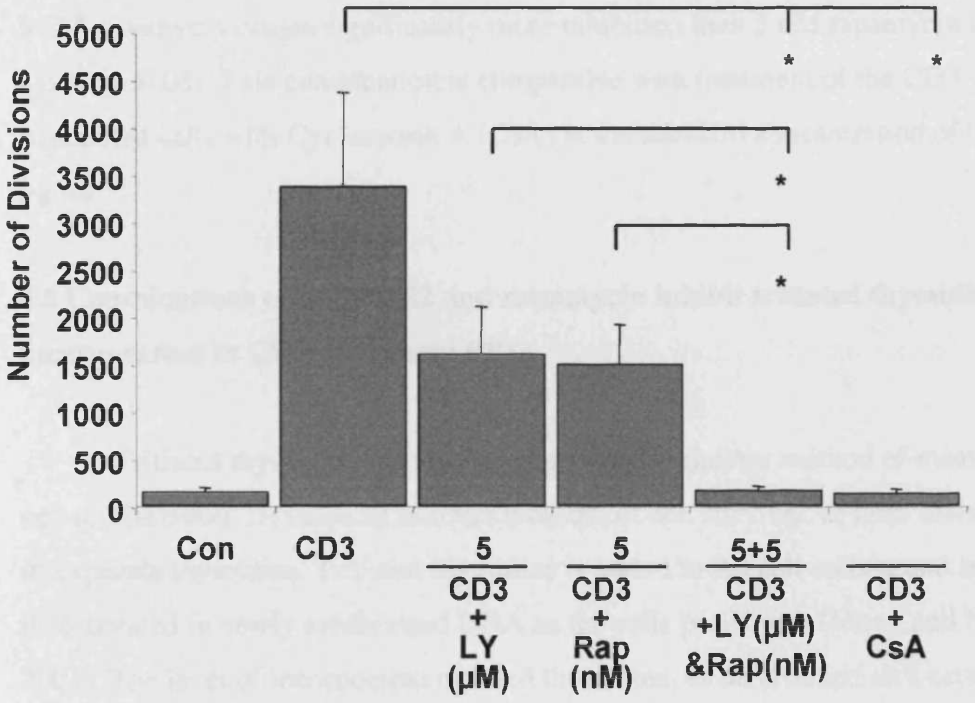

Fig 3.9 FlowJo analysis of the CFSE profiles of anti-CD3 stimulated PBLs

Primary Human T-cells isolated from whole blood were stained with CFSE and pre-treated with LY294002 or rapamycin, or a combination of the two inhibitors at the doses indicated for 30 minutes prior to stimulation with an antibody to the CD3 chain of the T-cell receptor (OKT3, 2.5 ng/ml, CRUK). The cells were analysed by flow cytometry after six days. The curves generated by the CFSE profile were analysed using the proliferation platform of the FlowJo software. This figure illustrates the graph generated using Number of Divisions as a measure of proliferation. The graph was generated from four different experiments. The numbers under the axis represent inhibitor concentrations. Cyclosporin A (CsA) at a standard dose of 0.5 μg/ml is used as a comparison. The error bars represent the standard error. Student's T-tests were used to ascertain the statistical significance of the results. Figure 3.8 indicates a significance level of $p<0.05$ (*).

.

changes were not significant (p=0.16, p=0.13 respectively), but the combined treatment of 5 μM LY294002 and 5 nM rapamycin caused a significant reduction of CD3 induced cell division ($p<0.05$, column 5 compared to columns 3 or 4). The graph also shows that the effects of the combined treatment of 5 μM LY294002 and 5 nM rapamycin causes significantly more inhibition than 5 nM rapamycin used alone ($p<0.05$). This combination is comparable with treatment of the CD3 stimulated cells with Cyclosporin A (CsA) at the standard concentration of 0.5 μg/ml.

3.5 Combinations of LY294002 and rapamycin inhibit tritiated thymidine incorporation in CD3 stimulated PBLs

Tritiated thymidine incorporation assays are another method of measuring cell proliferation. It is also an indirect measure of cell survival, as dead cells cannot incorporate thymidine. Tritiated thymidine is added to the cell culture and becomes incorporated in newly synthesised DNA as the cells proliferate (Moon and Nelson, 2001). The level of incorporated tritiated thymidine, as determined on a scintillation counter, is directly related to the proliferation of the cells at the time of the assay. We used tritiated thymidine incorporation cell proliferation assays as a complementary technique to the CFSE staining, to study the effects of LY294002 and rapamycin in combination on PBL proliferation. Assays to measure tritiated thymidine incorporation facilitate the use of a wider range of drug concentrations and combinations, and in addition to triplicate sample treatments, enable powerful statistical analysis.

We used four different combinations of LY294002 and two concentrations of rapamycin to further investigate the effects of combining these inhibitors. PBLs were isolated from blood and pre-treated with various concentrations and combinations of LY294002 and rapamycin for 30 minutes prior to stimulation with an antibody to the CD3 chain of the T-cell receptor (OKT3 2.5 ng/ml, CRUK). Cells were left for three days and then 0.5 μCi of tritiated thymidine was added to each well of a 96 well plate. The plate was harvested after sixteen hours and incorporation was measured by

liquid scintillation counting of tritium. Figure 3.10 (a) illustrates the percentage inhibition following pre-treatment with a range of concentrations of LY294002 in the absence and presence of rapamycin, from one experiment performed in triplicate. The same pattern of inhibition was seen in two further experiments. Both LY294002 and rapamycin, independently and combined, cause a reduction of incorporation of tritiated thymidine. Figure 3.10 (b) illustrates the results as a histogram and allows the visualization of CD3 alone and CD3 in the presence of inhibition. Student's T-tests were performed to determine if the effects of the combinations of LY294002 and rapamycin were significantly different to the inhibitors used alone. The combination of 2.5μM LY294002 and 1 nM rapamycin cause significantly more inhibition of CD3 induced thymidine incorporation than either inhibitor alone. Furthermore, the combination of 5μM LY294002 and 5 nM rapamycin also caused significantly more inhibition than the two inhibitors alone. Together this data show that combinations of LY294002 and rapamycin are more powerful for inhibiting CD3 induced lymphocyte proliferation.

3.6 LY294002 and rapamycin co-operate to inhibit proliferation induced by antibodies to CD3 and CD28

CD28 is the primary T-cell co-stimulatory receptor. Binding of its specific ligands enhances T-cell proliferation and IL-2 synthesis (Powell *et al.*, 1998). Our next objective was to compare the results observed in anti-CD3 stimulated PBLs to those obtained from anti-CD3/anti-CD28 stimulated PBLs. We examined the effects of combinations of LY294002 and rapamycin on PBLs stimulated with both an antibody to CD28 and antibody CD3 using both CFSE analysis of cell division and tritiated thymidine incorporation. A CD28 antibody clone (CD28.2, BD Biosciences) was used in these experiments as a strong co-stimulator for human T-lymphocytes. Similar to experiments described for CD3, PBLs were freshly isolated from human blood. For CFSE experiments, they were labelled for 5 minutes. The cells were pre-treated with the inhibitors for 30 minutes. They were then stimulated with an antibody to CD3 (OKT3, 2.5 ng/ml, CRUK) and an antibody to CD28 (BD

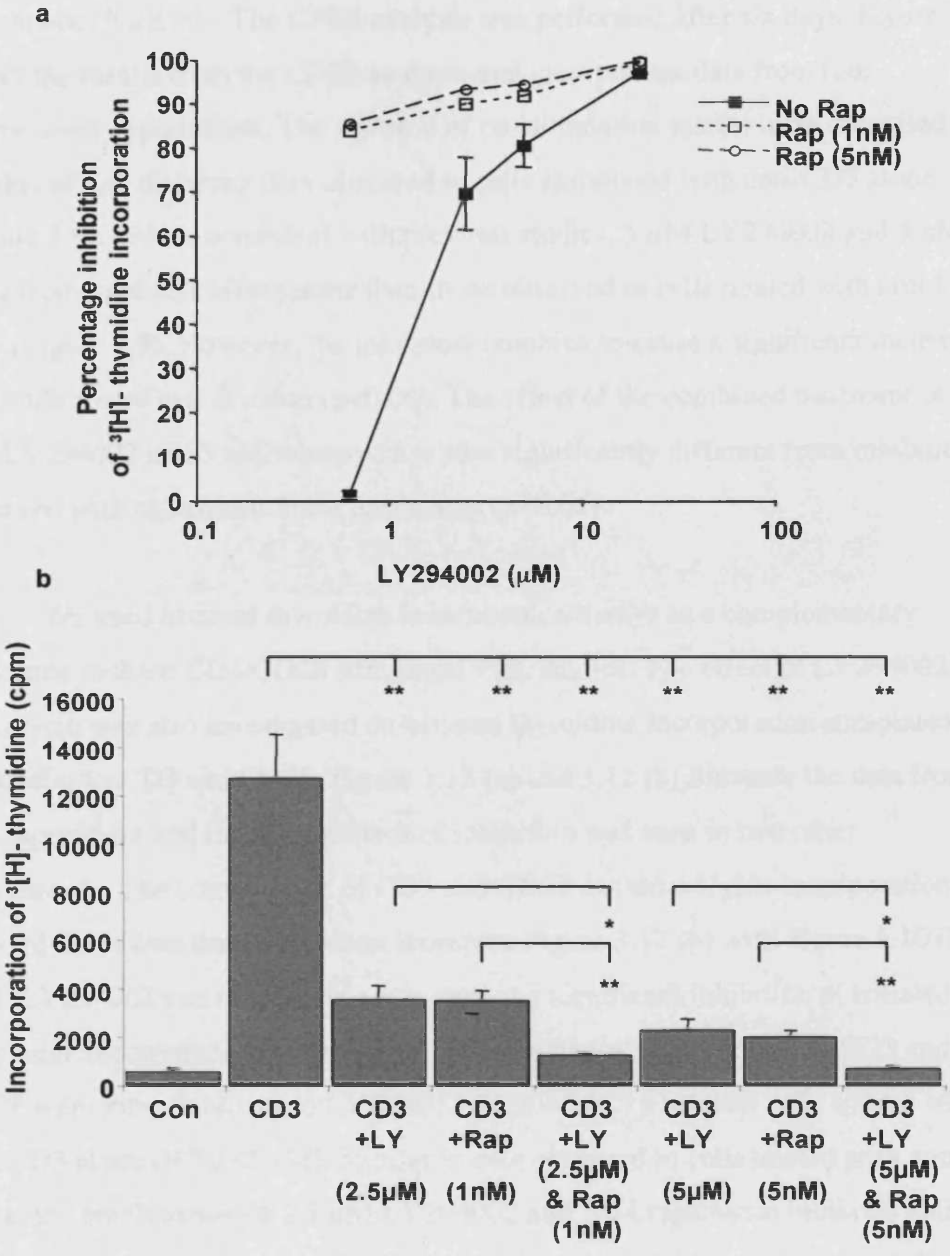

Fig 3.10 Combinations of LY294002 and rapamycin co-operate to inhibit thymidine incorporation in Primary Human T-cells stimulated with anti-CD3

PBLs isolated from whole blood were pre-treated with various doses and combinations of LY294002 and rapamycin for 30 minutes prior to stimulation with an antibody to the CD3 chain of the T-cell receptor for 4 days (OKT3, 2.5 ng/ml, CRUK). Cells were pulsed with 0.5μCi of tritiated thymidine for the last 16 hours of the experiment and the incorporation measured by liquid scintillation counting of tritium. (a) illustrates the range of doses of LY294002 in the absence and presence of rapamycin. (b) illustrates the results as a histogram, indicating the percentage inhibition of ^{3}[H]-thymidine incorporation, compared to anti-CD3 stimulated cells alone. A student's T-test determined any significant levels of inhibition.

Biosciences 5 μg/ml). The CFSE analysis was performed after six days. Figure 3.11 shows the results from the CFSE analysis and incorporates data from four independent experiments. The addition of co-stimulation results in an increased number of cell divisions than observed in cells stimulated with anti-CD3 alone (Figure 3.9). This is consistent with previous studies. 5 μM LY294002 and 5 nM rapamycin have less effect alone than those observed in cells treated with anti-CD3 only (Figure 3.9). However, the inhibitors combine to cause a significant increase in the inhibition of cell division ($p<0.01$). The effect of the combined treatment of 5 μM LY294002 and 5 nM rapamycin is also significantly different from inhibition observed with rapamycin 5 nM used alone ($p<0.01$).

We used tritiated thymidine incorporation assays as a complementary technique in these CD3/CD28 stimulated PBL studies. The effect of LY294002 and rapamycin was also investigated on tritiated thymidine incorporation stimulated by antibodies to CD3 and CD28. Figure 3.12 (a) and 3.12 (b) illustrate the data from one experiment and the same pattern of inhibition was seen in two other experiments. The combination of CD3 and CD28 caused a higher incorporation of tritiated thymidine than CD3 alone (compare Figure 3.12 (b) with Figure 3.10 (b)). Both LY294002 and rapamycin alone caused a significant inhibition of tritiated thymidine incorporation. Interestingly, cells treated with antibodies to CD3 and CD28 were more sensitive to LY294002 (IC50=0.625 μM) than cells treated with anti-CD3 alone (IC50=2 μM). Similar to data observed in cells treated with anti-CD3 alone, the combination of 2.5 μM LY294002 and 1nM rapamycin inhibited anti-CD3 and anti-CD28 treatment significantly more than either inhibitor alone ($p<0.01$). This is also the case for the combination of 5 μM LY294002 and 5 nM rapamycin. The concentrations used in Kit225 cells and PBLs treated with anti-CD3, 5 μM LY294002 and 5 nM rapamycin, also inhibited proliferation more significantly when combined than when used alone. Thus, combinations of LY294002 and rapamycin can combine to more effectively inhibit proliferation of lymphocytes stimulated through CD3 and CD28.

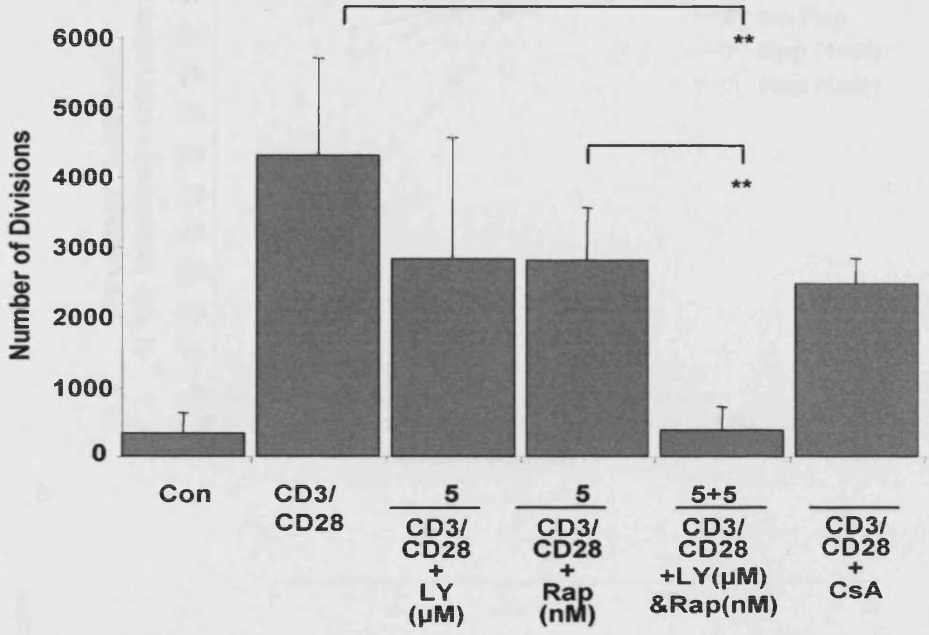

Fig 3.11 Combinations of LY294002 and rapamycin co-operate to inhibit proliferation in Primary Human T-cells stimulated with anti-CD3 and anti-CD28

Primary Human T-cells isolated from whole blood were were stained with CFSE and pre-treated with LY294002 or rapamycin, or a combination of the two inhibitors at the doses indicated for 30 minutes prior to stimulation with both an antibody to CD28 (5 μg/ml, BD Biosciences) and antibody to CD3 (OKT3, 2.5 ng/ml, CRUK). The cells were analysed by flow cytometry after six days. The curves generated by the CFSE profile were analysed using the proliferation platform of the FlowJo software. This figure illustrates the graph generated using Number of Divisions as a measure of proliferation. The graph was generated from four different experiments. The numbers under the axis represent inhibitor concentrations. Cyclosporin A (CsA) at a standard dose of 0.5 μg/ml is used as a comparison. The error bars represent the standard error. Student's T-tests were used to ascertain the statistical significance of the results.

a

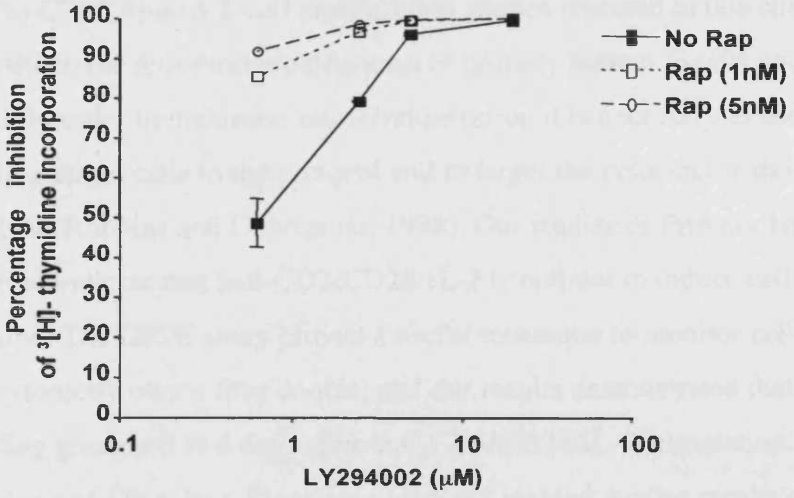

b

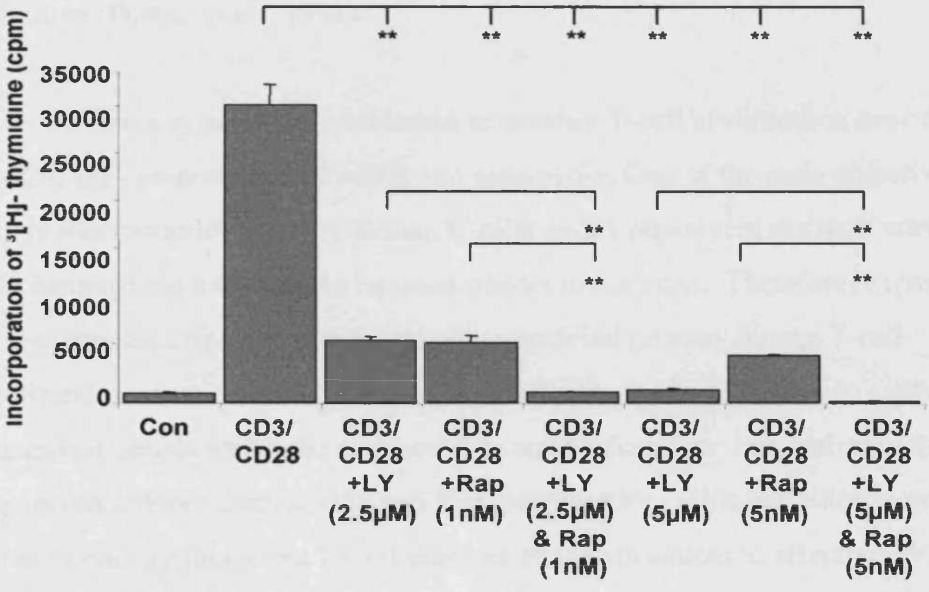

Fig 3.12 Combinations of LY294002 and rapamycin co-operate to inhibit ^{3}[H]-thymidine incorporation in Primary Human T-cells stimulated with anti-CD3 and anti-CD28

PBLs isolated from whole blood were pre-treated with various doses and combinations of LY294002 and rapamycin for 30 minutes prior to stimulation with both an antibody to CD28 (5 μg/ml, BD Biosciences) and antibody to CD3 (OKT3, 2.5 ng/ml, CRUK). Cells were pulsed with 0.5μCi of tritiated thymidine 3 days after stimulation, for the last 16 hours of the experiment and the incorporation measured by liquid scintillation counting of tritium. (a) illustrates the range of doses of LY294002 in the absence and presence of rapamycin. (b) illustrates the results as a histogram, indicating the percentage inhibition of ^{3}[H]-thymidine incorporation, compared to anti-CD3 stimulated cells alone. A student's T-test determined any significant levels of inhibition.

3.8 Discussion

The CFSE human T-cell proliferation studies reported in this chapter were a pre-requisite to the retroviral modification of primary human T-cells undertaken in Chapter 4. In order to maximise retroviral infection it is necessary to use optimally proliferating target cells in the protocol and to target the cells on the day of maximal proliferation (Robbins and Ghivizzani, 1998). Our studies of Primary Human T-cell proliferation indicate that anti-CD3/CD28/IL-2 is optimal to induce cell proliferation. The CFSE assay proved a useful technique to monitor cell proliferation by flow cytometry over a time course, and our results demonstrated that the PBLs are proliferating greatest 3 to 4 days after anti-CD3/CD28/IL-2 stimulation. The cell cycle analysis of DNA by a PI staining protocol yielded similar results and illustrates the usefulness of complementary techniques. Our data is in agreement with the literature (Powell *et al.*, 1998).

Once a system was established to monitor T-cell proliferation over time, we studied the compounds LY294002 and rapamycin. One of the main objectives of this thesis was to modify primary human T-cells with a rapamycin resistant retrovirus and demonstrate a rapamycin resistant phenotype *in vitro*. Therefore, experiments to investigate the effects of rapamycin on unmodified primary human T-cell proliferation were necessary before the effectiveness of a retrovirus to confer rapamycin resistance on the cell, could be established. Our data indicated that rapamycin inhibits both Kit225 and PBL proliferation. This inhibition is greatest at 20 nM concentrations, but 10 nM concentrations are almost as effective. We also investigated the inhibitory effects of the PI3K inhibitor LY294002. Our studies showed that there is a difference in the susceptibility of Kit225 and primary T-cells, to LY294002. 5μM LY294002 had very little effect on the proliferation of Kit225 cells while 2.5μM LY294002 inhibits the proliferation of PBL stimulated with anti-CD3 (Figure 3.10) or anti-CD3 with anti-CD28 (Figure 3.12). This is also the case with for rapamycin where PBLs are more sensitive than Kit225 cells.

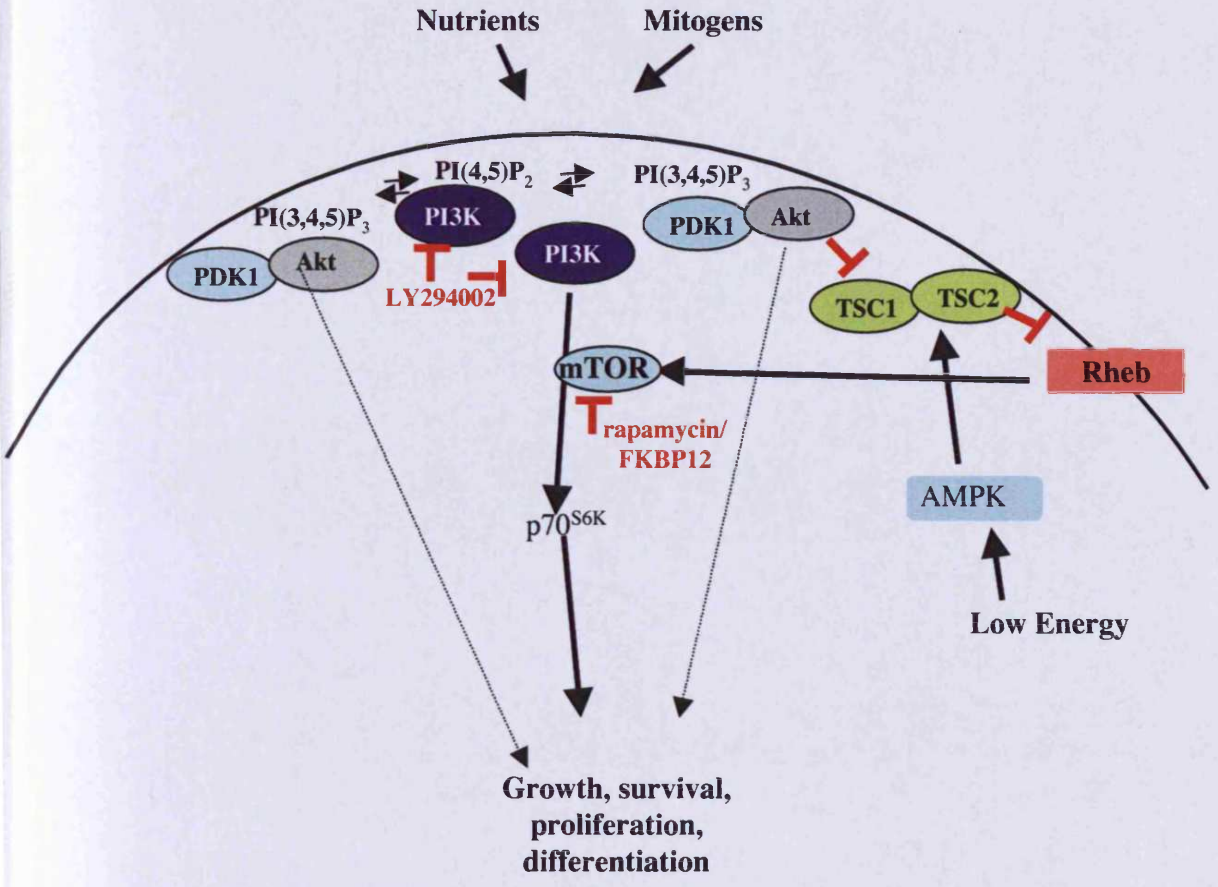

Figure 3.13 Hypothesis for the co-operation of LY294002 and rapamycin to inhibit T-cell proliferation: inhibition of overlapping and parallel pathways.

Rapamycin inhibits a subset of PI3K pathways but mTOR may be integrating other pathways too. Mammalian cell proliferation is stimulated by a combination of nutrients and growth factors and there is evidence that mTOR might mediate signalling in response to both stimuli (Kim *et al.*, 2002). The regulation of mTOR by growth factors is through the PI3K pathway. PIP_3 recruits Akt to the membrane where it is phosphorylated by PDK1. Activataed Akt phosphorylates TSC2 resulting in the inhibition of the TSC1/2 complex. Rheb is a small GTPase that is inactivated by TSC1/2 and is a positive regulator of mTOR (Li *et al.*, 2004). mTOR is also thought to integrate signals relating to energy levels in the cell. Under low energy conditions, mTOR is inhibited: the AMP-activated protein kinase (AMPK) phosphorylates the TSC2 protein, enhancing the ability of the TSC1/TSC2 complex to inhibit mTOR (Inoki *et al.*, 2003). Thus there are many distinct possibilites for the parallel pathways LY294002 and rapamycin are inhibiting.

Our exeperiments also showed that PBLs treated with antibodies to CD3 and CD28 were more sensitive to LY294002 (IC50=0.625 μM) than cells treated with anti-CD3 alone (IC50=2 μM). Given that a mixed lymphocyte population was used in the experiments, it is possible that B7.1 or B7.2 ligand expressing non-T-cells in the PBL mixture may have contributed natural co-stimulatory signals to the T-cells in the absence of anti-CD28 MAbs. The fact that the cells (stimulated with anti-CD3 alone and possibly stimulated through CD28 by B7.1 or B7.2 ligand binding) were less sensitive to LY294002 treatment suggests that such stimulation is differential to that of T-cells stimulated with anti-CD3 and anti-CD28 antibodies. It has been demonstrated that several signalling cascades are activated by CD28 *in vitro* including the $p21^{ras}$ pathway (which leads to the activation of a MAP kinase cascade), the PLC pathway (leading to increase in intracellular $Ca2^{+}$) and the PI3K pathway. Evidence has suggested that the signals transmitted to the cell from ligand binding are differential to signals transmitted to the cell as a result of anti-CD28 MAb binding and that activation of the downstream signalling events mentioned above, such as $Ca2^{+}$ flux and activation of the MAP kinase cascade are differentially activated accordingly (reviewed in (Ward, 1996). It is also worth noting that the ability of anti-CD28 Abs to elicit downstream signalling is dependent on the epitope recognised by the MAb (Nunes *et al.*, 1993) and that different CD28 MAb clones have different patterns of activation (eg. in their ability to induce IL-2 release and increase intracellular $Ca2^{+}$ levels), implying that there exists functionally distinct subregions in the CD28 molecule. An important example is that certain CD28 MAbs can activate the $p21^{ras}$ pathway while others cannot (Nunes *et al.*, 1994). However CD28 does not detectably activate $p21^{ras}$ pathway following natural ligand (B7.1) binding. Thus the choice of antibody and the interpretation of the experimental data is important with regard to the physiological releveance of the results.

Our data indicated that combinations of LY294002 and rapamycin combine to give a stronger inhibition of cell proliferation in Kit225 cells than when the inhibitors are used alone. The CFSE cell proliferation data and tritiated thymidine data showed that combinations of lower concentrations of both inhibitors are more effective in both anti-CD3 stimulated PBLs and anti-CD3/CD28 PBLs than either

inhibitor alone. Immunoblotting experiments were carried out by collaborating colleagues in the laboratory (See Appendix IV, publication (Breslin *et al.*, 2005). Our data suggest that LY294002 and rapamycin are targeting both overlapping and parallel pathways. We have shown that S6 phosphorylation is altered by both LY294002 and rapamycin in Kit225 cells and T-cell blasts. In both cell types, LY294002 can co-operate with rapamycin at doses where rapamycin completely ablates S6 phosphorylation suggesting that LY294002 is affecting other pathways. Rapamycin inhibits a subset of PI3K pathways but TOR may be integrating other pathways too. There is evidence that TOR responds to nutrient levels in yeast (Barbet *et al.*, 1996). In mammalian cells, proliferation is stimulated by a combination of nutrients and growth factors. Accumulating evidence indicates that TOR might mediate signalling in response to both stimuli. In the presence of raptor, the newly identified TOR interacting protein, mTOR kinase activity is increased when stimulated with leucine (Kim *et al.*, 2002). TOR is also thought to respond to a mitochondrial signal, but this signal may be as a result of amino acids synthesized in the mitochondria (Crespo *et al.*, 2002). Thus there are many distinct possibilities for the parallel pathways LY294002 and rapamycin are inhibiting. Figure 3.13 illustrates the LY294002 and rapamycin inhibition of both overlapping and parallel pathways and represents our hypothesis of LY294002 and rapamycin co-operation to inhibit T-cell proliferation. Changes in the levels of cell cycle proteins were also investigated using specific antibodies. The data obtained showed that the expression of key cell cycle regulatory proteins, cyclin D2 and cyclin D3 and phospho pRb, are inhibited by the combination of LY294002 and rapamycin. See Appendix IV, publication (Breslin *et al.*, 2005).

This work suggests that inhibition of T-cell proliferation using a combination of a PI3K inhibitor and rapamycin could be beneficial as an alternative immunosuppressive regime. The synergistic effects of rapamycin and CsA have been documented in both experimental and clinical settings (Kahan, 2002; Kahan *et al.*, 1992) and the known functional effects of the PI3-kinases in the immune system suggest possible immunotherapeutic targets for a PI3-kinase inhibitor. However, the therapeutic use of PI3K inhibitors is controversial because of the potential toxicity of

broad-spectrum PI3-kinase inhibitors such as LY294002 (Fruman, 2004; Ward and Finan, 2003). The use of PI3-kinse inhibitors in the clinic will not be feasible until highly isoform specific compounds are developed for clinical use.

CHAPTER 4

The Retroviral Modification of Human T-cells

4.1 Introduction

The objective of this chapter was to develop a system for the genetic modification of primary human T-cells. We chose retroviral infection as a powerful method of genetic modification. Retroviral vectors based on the Moloney Murine Leukemia Virus (MoMLV) backbone have become the primary tool for gene delivery into mammalian cells in clinical trials. We aimed to establish an efficient and reproducible retroviral infection system, with a view to applying this technology to modify primary T-cells with genes of interest. Retroviral infection was not established in our department, and we first needed to transfer the technology from other sources of expertise. To assess infection efficiency, we needed to use a retrovirus, which would confer a marker indicating successful infection in the target cell. To facilitate ease of transfer of the technology, two retroviral systems already in use in this university were investigated. One system uses a PINCO vector and a Phoenix 293 (PH293) packaging line (Darley *et al.*, 2002; Tonks *et al.*, 2003), and the other uses a pBabe puro vector and a ψ-crip packaging line (Bond *et al.*, 2004; Bond *et al.*, 1999; Jones *et al.*, 2000). The transfer of two distinct retroviral systems to our laboratory would facilitate a more comprehensive retroviral technology transfer, and enable us to determine which system was most applicable to modify the target cells of this project, human T-cells.

The PINCO-PH293 system involves transient transfection of the PH293 packaging cell line, a transformed human embryonic kidney cell line containing the *gag-pol* and *env* genes, with a PINCO vector based on the MoMLV virus backbone (Kinsella and Nolan, 1996). The PINCO vector has been modified using two elements from EBV, oriP and EBNA-1, to confer stable episomal maintenance capabilities to the retroviral construct (Kinsella and Nolan, 1996) and a GFP marker

gene, (Grignani *et al.*, 1998). Transient transfection of PH293 cells with PINCO yields functional virus and infection of target cells with the PINCO virus, allows high efficiency transduction and stable expression of the GFP marker in target cells (Grignani *et al.*, 1998). Darley *et al.* (Dept. of Haematology, UWCM) have used this system to study the role of Ras mutations in myeloid leukaemia (Darley *et al.*, 2002; Tonks *et al.*, 2003). They have modified $CD34^+$ progenitor cells with a PINCO retrovirus expressing a mutant Ras gene, and studied proliferation in Ras expressing cells, by flow cytometry (Darley *et al.*, 2002; Tonks *et al.*, 2003). Our objective was to transfer, from the Dept. of Haematology, the expertise and knowledge required to apply this PINCO-Phoenix technology to our T-cell target system.

The next objective was to characterise transduction of T-cells using a vector conferring drug resistance in the cell, as a marker of infection. The pBabe puro system used, involves the transduction of target cells with a puromycin resistance gene, and the pBabe plasmid is also based on the MoMLV virus (Morgenstern and Land, 1990). The pBabe puro system is different to the PINCO system because the pBabe puro vector does not have the EBV genes required to maintain the plasmid episomally, limiting the use of transient transfection to generate functional virus. Stable producer cell lines are developed, based on the stable chromosomal integration of the vector within packaging cells. Jones *et al.* (Dept. of Pathology, UWCM) use this stable pBabe puro system to modify normal human fibroblast cells and primary follicular epithelial cells, in the study of cellular senescence (Bond *et al.*, 2004; Bond *et al.*, 1999; Jones *et al.*, 2000). An ecotropic packaging line, ΩE, is used as an intermediate in the production of stable ψ-crip amphotropic packaging lines (Bond *et al.*, 2004; Bond *et al.*, 1999; Jones *et al.*, 2000). Our objective was to transfer, from the Dept. of Pathology, the pBabe puro technology and apply it to our T-cell target system.

Using a strategy that proved useful in Chapter 3, we commenced our experiments with the modification of the IL-2 dependent Kit225 T-cell line, with both the PINCO retrovirus and the pBabe puro retrovirus. Once the technical parameters involved in obtaining efficient retroviral infection were established with

the Kit225 cell line infections, the next objective was the retroviral modification of primary human T-cells (PBLs) and Epstein-Barr virus specific cytotoxic T-cells (EBV-CTLs) with both the PINCO retrovirus and the pBabe puro retrovirus.

4.2 Genetic modification of the Kit 225 T-cell line with a GFP retrovirus

We commenced the retroviral experiments by targeting the IL-2 dependent T-cell leukaemic line, Kit225. The first objective was to establish the technical parameters involved in obtaining optimal retroviral infection efficiency, and infection of the IL-2 dependent Kit225 T-cell line, whose growth pattern is well characterised, would facilitate this. Kit225 retroviral infection has previously been reported with HIV-1 based retroviral vectors (Branch *et al.*, 2002), however no reported studies have modified Kit225 cells with a MoMLV based retroviral vector.

Functional retroviral supernatant was obtained by transient transfection of PINCO plasmid in the PH293 packaging cell line. We adopted a PINCO retroviral infection protocol with which the successful genetic modification of $CD34^+$ primary human cells has been demonstrated (Tonks *et al.*, 2003). The protocol combines a number of methods found to enhance infection including coating the 24-well plate with a human fibronectin fragment (Retronectin, BioWhittaker); a 2-cycle retroviral infection on consecutive days to increase infection efficiency (Tonks *et al.*, 2003); and a more recent adaptation involving centrifugation of the retrovirus onto the Retronectin coated plate before adding the target cells (Tonks *et al.*, 2004). Retronectin is a commercially available human fibronectin fragment and has been shown to enhance retroviral gene transfer into primary human T-cells, probably due to the co-localization of retrovirus and target cell on specific fragments of the molecule (Hanenberg *et al.*, 1997; Hanenberg *et al.*, 1996; Stockschlader *et al.*, 1999). The wells of a 24-well plate were coated with Retronectin for 2 hours. Following removal of the Retronectin, the viral supernatant was added to the wells and the plates were centrifuged at 3000g for two hours at room temperature. As a control, a 'mock' infection well was set up whereby complete medium was added to a well instead of virus supernatant. The viral supernatant or the medium was then

removed from the wells and $2X10^5$ Kit225 cells/ml complete RPMI/10% FCS containing 20 ng/ml IL-2 was added to each well. The plates were placed at 37°C overnight. As the infection protocol is 2-cycle, the following day, target cells were removed from the plates (to a new 24-well plate) and immediately replaced with virus supernatant. Centrifugation of the retrovirus onto the 24-well plates was repeated as before. The target cells were placed to the incubator for the duration of the spin. The viral supernatant was then removed from the wells and the target cells re-added. The plates were placed at 37°C overnight.

Cells were analysed by flow cytometry from two days post-infection. Cells from the live gate, as determined by forward and side scatter dot plots were analysed in the FL1 channel to establish the percentage of GFP positive cells in the viable population. The cells were also visualised by fluorescent microscopy. Figure 4.1 shows GFP modified Kit225 cells. The fluorescent photograph (Figure 4.1 (a)) showed the GFP positive cells overlaid on the brightfield image, day 4 post-infection. The dot plot of Figure 4.1(b) showed an infection efficiency of 73.4% for the retrovirally infected Kit225 cells. Over twelve experiments this infection efficiency ranged from 36.7% to 78% depending on the batch of virus used, with an average of 60.57% ± 11.1%. Kit225 GFP positive cells were monitored long-term for over two months with little change in GFP levels from those observed two days post-infection. For example, in one experiment the percentage of GFP positive cells ranged from 61% three days post-infection to 65.7% 75-days post infection. This indicated that the expression of the transgene did not confer any growth advantage on the Kit225 cells. These results demonstrate that we have successfully modified a T-cell line with a GFP expressing retrovirus. We have also demonstrated maintained expression of the transgene long-term with no discernible differences to the parent line phenotype.

4.3 Genetic modification of Primary Human T-cells with a GFP retrovirus

Having demonstrated successful modification of a T-cell line with a GFP retrovirus we investigated whether we could modify primary human T-cells.

(a)

Kit 225+PINCO

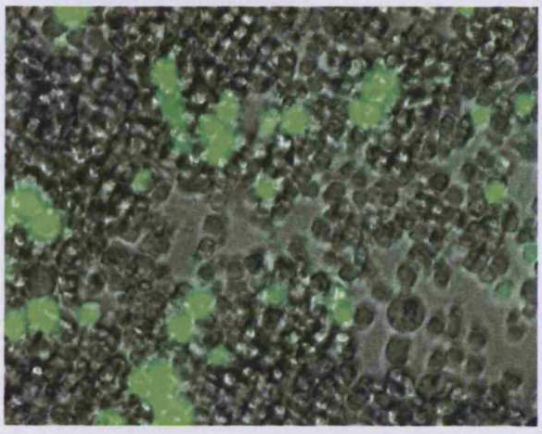

(b)

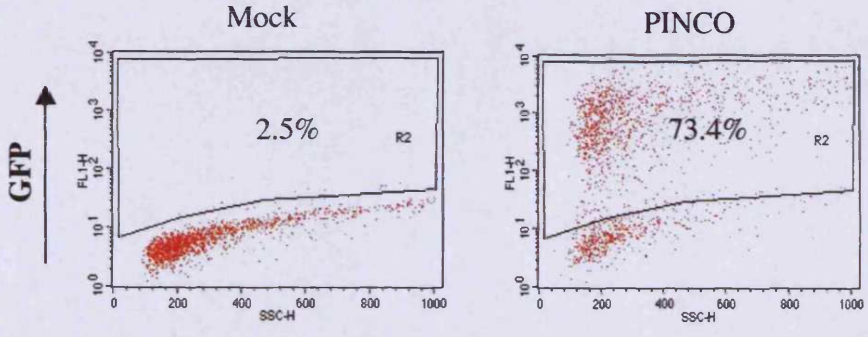

Figure 4.1 Genetic modification of Kit225 with a GFP retrovirus.

Functional PINCO retrovirus was obtained by transient transfection of PINCO plasmid in the PH293 retroviral packaging cell line. Retroviral supernatant was used to infect $2X10^5$ IL-2 dependent Kit225 cells in a 2-cycle infection protocol. Cells were analysed by flow cytometry. The cells were also visualised on a fluorescent microscope. (a) The fluorescent photograph shows the GFP positive cells overlaid on the brightfield image, day 4 post-infection. (b) The dot plot shows GFP positive cells in the FL-1 channel, 4 days post infection.

Infection of primary T-cells is different to the modification of an established T-cell line. Whereas the Kit225 T-cell line is constitutively growing in the presence of IL-2, the infection of freshly isolated primary human T-cells requires optimal stimulation through the TCR and the IL-2 receptor. Co-stimulation through the addition of anti-CD28 monoclonal antibody can also enhance the level of stimulation. As retroviral infection must occur at a time when the cells are optimally dividing the assessment of cell proliferation or cell cycle status of the PBLs is useful post-stimulation to facilitate optimal infection.

Our observations in Chapter 3 indicated that stimulation of freshly isolated PBLs with anti-CD3, anti-CD28 and IL-2 resulted in high cell proliferation and that the most cell proliferation occurred three to four days post-stimulation. We applied this knowledge in our investigation of the PINCO retroviral infection of PBLs. PBLs were isolated from whole blood by a Ficoll-gradient and stimulated with anti-CD3 (OKT3 2.5 ng/ml, CRUK), anti-CD28 (5 μg/ml, BD) and IL-2 (20 ng/ml) for three or four days. The infection protocol described for Figure 4.1 was carried out with $2X10^5$ cells/ml PBL cell suspension in complete medium substituted with 20 ng/ml IL-2, as the target cells. The 24-well plates were placed at 37°C overnight. Again, a 2-cycle infection protocol was used. Cells was analysed by flow cytometry following infection. Cells from the live gate, as determined by forward and side scatter dot plots were analysed in the FL1 channel to establish the percentage of GFP positive cells in the viable population. The cells were also visualised by fluorescent microscopy.

For the purposes of the primary cell retroviral modification, the timepoints from this point refer to 'days post-isolation' of the PBLs, rather than 'days post-infection' to facilitate analysis of the data in the context of the lifespan of the PBLs. Figure 4.2 shows GFP fluorescence twelve days post-isolation of CD3/CD28/IL-2 stimulated PBLs, and shows an infection efficiency of 55% for the retrovirally infected PBLs. Over eight experiments this infection efficiency ranged from 15.2% to 55%, depending on the both the batch of virus used and the cell proliferation rate

(a)

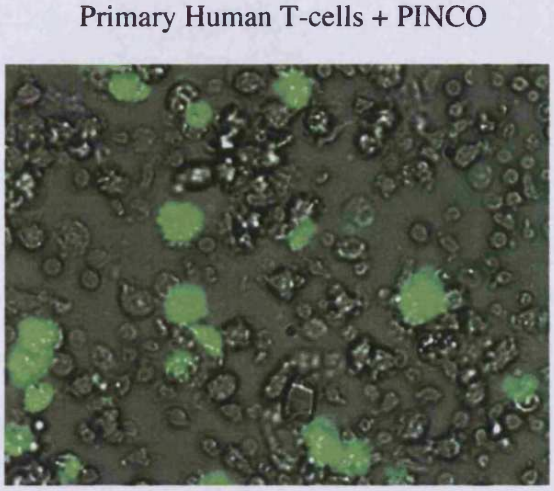

(b)

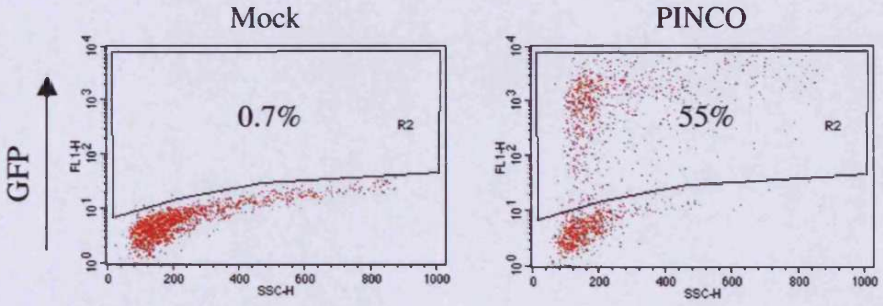

Figure 4.2 Genetic modification of primary human T-cells with a GFP retrovirus.

Human PBLs were isolated from whole blood by a Ficoll gradient and stimulated with anti-CD3 (OKT3, 2.5 ng/ml, CRUK), anti-CD28 (5 μg/ml, BD Biosciences) and IL-2 (20 ng/ml) for four days. Functional PINCO retrovirus was obtained by transient transfection of PINCO plasmid in the PH293 retroviral packaging cell line. Retroviral supernatant was used to infect $2X10^5$ PBLs, four days post-isolation, in a 2-cycle infection protocol. Cells were analysed by flow cytometry. The cells were also visualised on a fluorescent microscope. (a) The fluorescent photograph shows the GFP positive cells overlaid on the brightfield image, day 6 post-isolation. (b) The dot plot shows GFP positive cells, in the FL-1 channel, 6 days post isolation.

on the day of infection. The average percentage of GFP positive cells was 29.9% ± 16.5%. These results demonstrate that we can successfully modify a primary human T-cell with a GFP expressing retrovirus. Comparisons with the Kit225 infection efficiency data, which showed an average infection efficiency of 60.57% ± 11.1%, demonstrated that the Kit225 cells infected more efficiently than PBLs. This increased infection efficiency of Kit225 cells compared to PBLs was observed consistently in all of our retroviral infections.

4.4 Investigating GFP modified PBLs

The maintenance of retroviral transgene expression has been demonstrated long-term in PBLs (Di Florio *et al.*, 2000) and is an important aspect of successful genetic modification. We monitored GFP fluorescence in PINCO modified PBLs long-term, in order to establish whether transgene expression changed over time, and whether expression of the transgene conferred any growth advantage on the PBLs. In addition we used immunofluorescent flow cytometry staining to phenotypically characterise the infected cells.

The infected cells were analysed by flow cytometry from six days post-isolation for 43 days. Cells from the live gate, as determined by forward and side scatter dot plots were analysed in the FL1 channel to establish the percentage of GFP positive cells in the viable population. Figure 4.3 (a) depicts the results obtained from tracking the retrovirally infected PBL population of Figure 4.2, for a 43-day period. The GFP fluorescence increased from 30.4% to 55% from day 6 to day 8 post-isolation, and was 51.4% on day 43. The increase in GFP positive cells from day 6 to day 8 is representative of the results observed in all PINCO primary T-cell infections. The maintenance of the percentage of GFP positive PBLs between 50-60% over the 43-day time course demonstrates that the retroviral modification of PBLs with a GFP retrovirus does not confer any growth advantage on the PBLs. The infected PBLs were immunofluorescent stained at day 27 of this experiment. We used PE conjugated CD3, CD4 and CD8 antibodies which fluoresce in the FL-2

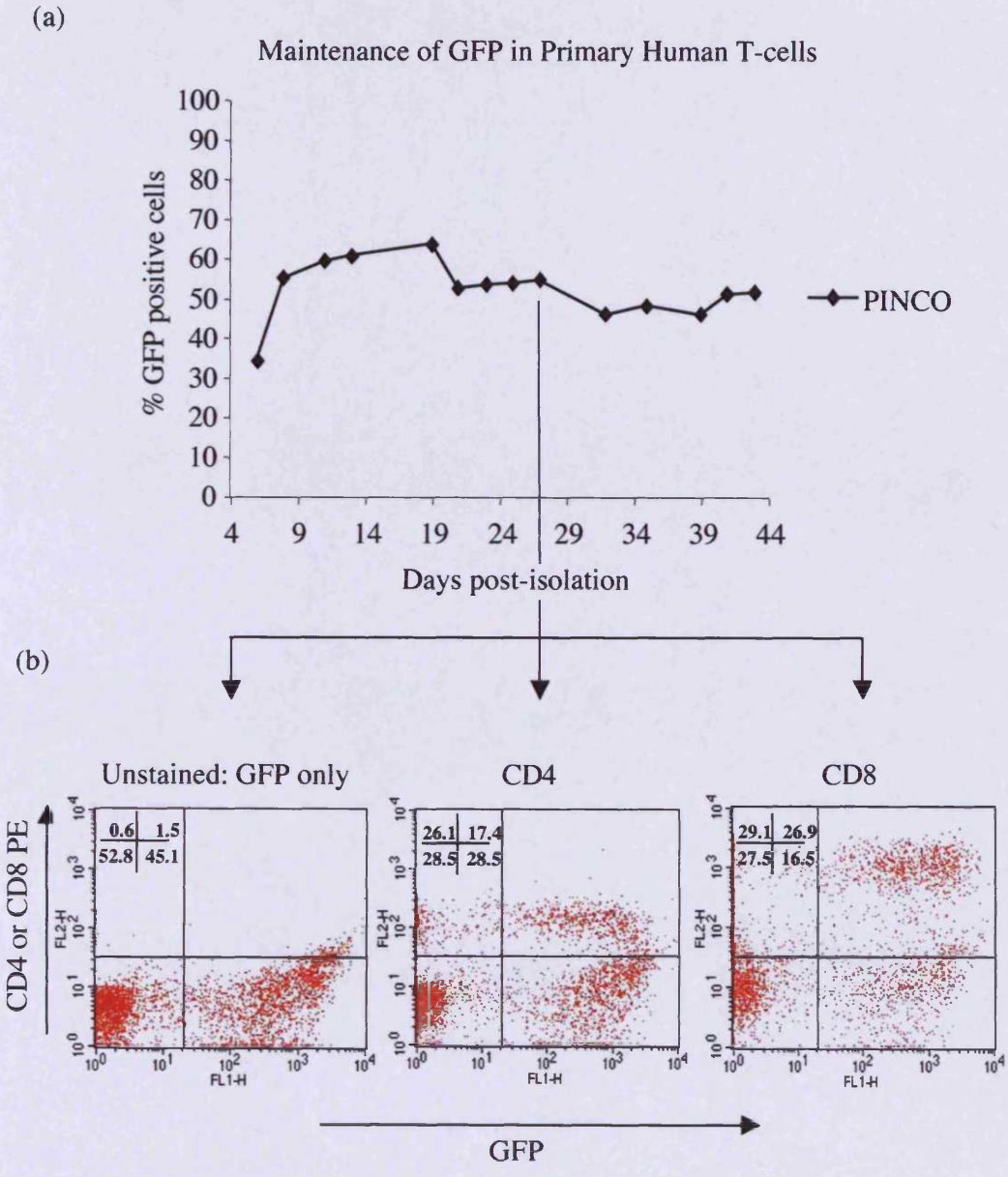

Figure 4.3 Investigation of GFP modified PBLs

The GFP modified population of Figure 4.2 was monitored by flow cytometry for 43 days post-isolation (a) shows the percentage of GFP positive PBLs in the culture over a 43 day period post-isolation. (b) The infected PBLs were immunofluorescent stained at day 27 post-isolation of this experiment using PE conjugated CD3, CD4 and CD8 antibodies. The percentage of PBLs positive for CD4, CD8 and GFP are indicated in quadrants for each histogram.

channel, in order to facilitate the analysis of FL-1 fluorescent GFP positive cells in the PE stained T-cell populations. Figure 4.3 (b) shows that the population was 43.5% $CD4^+$ cells and 56 % $CD8^+$ T-cells. Of the 43.4% $CD4^+$ cells, 17.4% were GFP positive and of the 56 % $CD8^+$ T-cells, 26.9% were GFP positive. This indicates that both $CD4^+$ T-cells and $CD8^+$ T-cells were modified with a GFP retrovirus.

4.5 The generation of EBV-specific Cytotoxic T-cells

In addition to the retroviral modification of PBLs, another objective in this study was to modify EBV-CTLs. It was first necessary to demonstrate that we could successfully generate EBV-CTL lines in the laboratory before we could retrovirally modify the cells. Because EBV is a ubiquitous and persistent virus, the majority of donors carry a high frequency of EBV-specific CTL precursors in their peripheral blood that can be readily reactivated and expanded *in vitro*. To generate the EBV-CTL lines, we used EBV-transformed B-cell lines from healthy donors as antigen presenting cells. These EBV-transformed B-cell lines are known as lymphoblastoid cell lines (LCLs) and display latency III pattern of gene expression. EBV-associated PTLD tumour cells generally express latency III gene expression, making the LCLs a good *in vitro* model of PTLD tumours. EBV-CTL lines generated *in vitro* demonstrating specificity against EBV-LCLs, have proven useful in the prophylactic therapy of PTLD and in the treatment of established tumours in transplant recipients (Rooney *et al.*, 1998a).

We generated three EBV-CTL lines 1,2 and 3 from three separate donors in this project. Each cell line itself was generated a minimum of three times with similar results each time. To stimulate the donor blood we used EBV-LCL lines autologous to Donor 1,2 and 3 respectively. Two of the three LCL lines had previously been generated in the department. We generated the third LCL line during the course of this project. This was achieved by infecting B-cells derived from a healthy volunteer with a laboratory strain of the EBV virus, as described in the methods. The new LCL line was successfully established after 6 weeks of culture.

The first step in the generation of the EBV-CTLs was the isolation of the lymphocytes from the whole blood of a healthy volunteer using a Ficoll gradient. These lymphocytes were seeded in a 24-well plate at $2X10^6$ cells/ml in complete RPMI supplemented with 10% human AB serum. $1X10^6$ of autologous γ-irradiated LCLs in 0.5 ml complete RPMI supplemented with 10% human AB serum were immediately added. The cultures were placed at 37°C. 25IU/ml IL-2 was added on Day 4 and 10 IU/ml IL-2 was added on Day 6. The cells were re-stimulated on Day 7 with autologous irradiated LCLs. This protocol was repeated weekly for the duration of the line. ^{51}Chromium-release killing assays were performed, as described in the methods, to investigate the EBV-specificity of each line (Figure 4.4). Autologous LCLs labelled with ^{51}Cr were the target cells and allogeneic LCLs labelled with ^{51}Cr, were used as a negative control. The ratio of effector CTLs to LCL targets ranged from 50:1 to 1.6:1 in the assays. The levels of ^{51}Cr released into the supernatant upon incubation of the CTLs and ^{51}Cr labelled LCLs relates to the percentage of specific lysis of the LCLs, which was determined using a calculation shown in the methods. Cultures were classified as positive if a biologically meaningful level of HLA-restricted killing was shown i.e. specific lysis 10% greater than that for the negative allogeneic control (Wills *et al.*, 1996). A clear difference in CTL lysis of donor LCLs and allogeneic LCLs can be seen for all three lines shown in Figure 4.4. For example, for EBV-CTL line 1, 43.7% specific lysis was shown against donor LCLs compared to 8.8% lysis of allogeneic targets. The results showed the successful generation of three HLA restricted EBV-CTL lines.

Immunofluorescent antibodies; PE conjugated CD3 antibody and FITC conjugated CD4 and CD8 antibodies, were used to phenotypically investigate the EBV-CTL lines. Figure 4.5 shows the results from EBV-CTL line 2. The results indicated that 4.5% of the population was $CD4^+$ while 87.5% was $CD8^+$. These results, taken together with Figure 4.4 show that HLA-restricted EBV-CTL lines were successfully generated. Once established, the EBV-CTLs were maintained long-term with weekly antigenic re-stimulation with irradiated autologous LCLs and addition of IL-2 at discrete timepoints. For example, in the case of Donor 1, two separately generated EBV-CTL lines were maintained for greater than 54 and 41

Figure 4.4 Generation of EBV-CTLs.

PBLs were isolated from the whole blood of healthy donors, using a Ficoll gradient. PBLs were resuspended at $2X10^6$/ml and stimulated with $1X10^6$/ml irradiated autologous LCL. IL-2 was added on discrete days and irradiated autologous LCL stimulation was repeated weekly. EBV-specificity was assessed by ^{51}Cr assay using ^{51}Cr-labelled autologous and allogeneic LCLs as targets for the effector EBV-CTLs. The effector:target cell ratio decreased from 50:1 to 1.6 in all the assays. Figure 4.4 shows three separate EBV-CTL lines generated from three healthy donors at 13 days (a), 21 days (b) and 21 days (c) post-isolation. Average maximal lysis and spontaneous lysis values were based on an average of 12 replicates. (a) Autologous LCL: average of 861 cpm ± 25 maximal lysis (=M) and 223 cpm ± 6 spontaneous lysis (=S). Allogeneic LCL: M=1743 cpm ± 57, S=338 cpm ± 10. (b) Autologous LCL: M= 4030 cpm ± 75, S= 722 cpm ± 31. Allogeneic LCL: M= 1362 cpm ± 28, S=204 cpm ± 4. (c Autologous LCL: M= 1985 cpm ± 41, S= 317 cpm ± 14. Allogeneic LCL: M= 4062 cpm ± 56, S=788 cpm ± 28. The mean specific lysis ± SEM are shown from triplicate wells and was based on the equation (E-S)/(M-S)X100-see chpt 2, page 83.

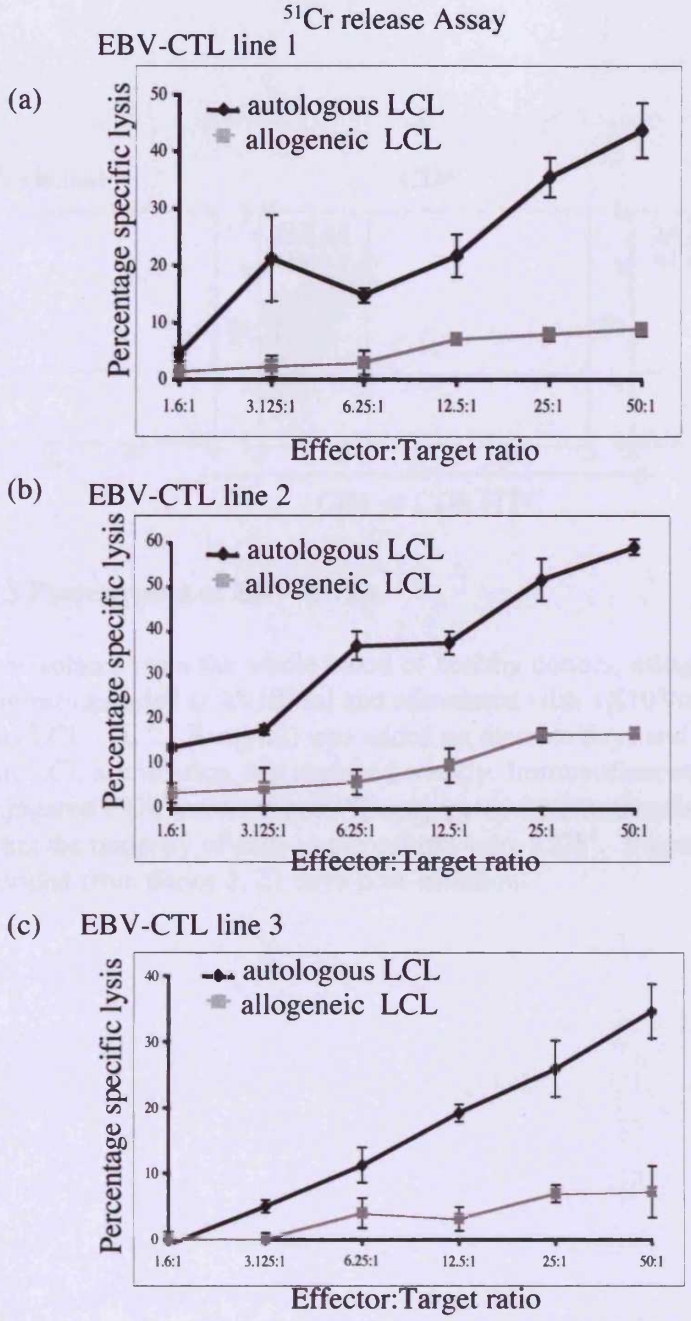

Figure 4.4 Generation of EBV-CTLs (Figure legend opposite)

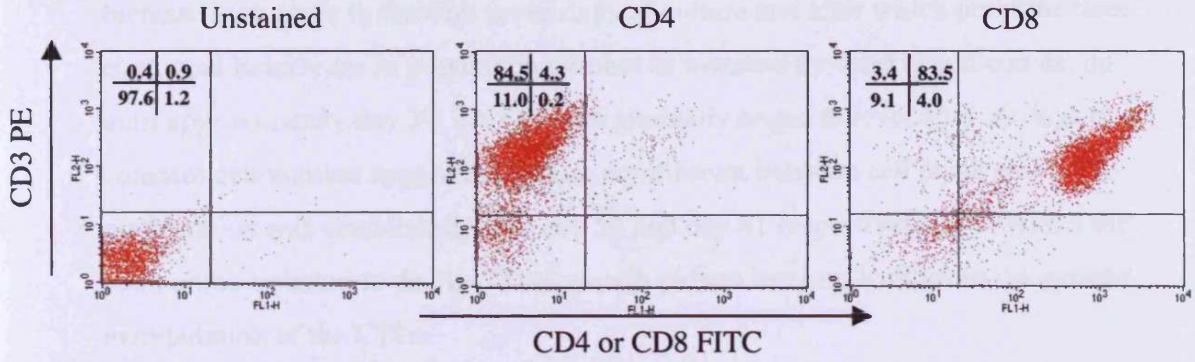

Figure 4.5 Phenotyping of EBV-CTLs.

PBLs were isolated from the whole blood of healthy donors, using a Ficoll gradient. PBLs were resuspended at $2X10^6$/ml and stimulated with $1X10^6$/ml of irradiated autologous LCL. IL-2 (20 ng/ml) was added on discrete days and irradiated autologous LCL stimulation was repeated weekly. Immunofluorescent staining with FITC conjugated CD8 and CD4 and PE conjugated CD3 antibodies, was used to confirm that the majority of cells in the culture were $CD8^+$. Figure 4.5 shows EBV-CTL generated from donor 2, 21 days post-isolation.

days respectively, after which the level of cell death increased dramatically in the cultures. A similar growth pattern was observed with both lines in that little or no increase took place in the first seven days of culture and after which point the lines continued to increase in population number as assessed by weekly cell counts, up until approximately day 30. This growth gradually began to level after 30 days to a constant cell number suggesting that an equilibrium between cell death and proliferation was established, until day 54 and day 41 respectively, after which the cell numbers started to decline. This growth pattern has implications in the genetic manipulation of the CTLs.

4.6 Genetic modification of EBV-CTLs with a GFP retrovirus

Once the EBV-specific CTL lines had been successfully generated, our next objective was to genetically modify the EBV-CTLs with GFP retrovirus. Genetic modification of CTLs is different to the retroviral infection of an established T-cell line such as Kit225 and is different to the infection of PBLs. We had determined the technical infection issues such as the most suitable stimulation for PBLs, and the appropriate day post-stimulation to infect PBLs in order to reach maximal GFP levels in PBL infections. However, the EBV-CTLs are different to freshly isolated PBLs in that they are a polyclonal antigen specific line and require weekly EBV-antigenic re-stimulation. These differences between the PBLs and the CTLs meant that the most appropriate day to infect the cells had to be determined for the CTLs. Infection of the cell culture too early may result in the retrovirus infecting non-specific $CD4^+$ or $CD8^+$ cells present in the lymphocyte population, thereby decreasing the infection efficiency of the EBV-specific $CD8^+$ precursor cells which will establish the EBV-CTL line. However, infection of the EBV-CTLs too late in their lifespan may also limit the infection efficiency as the cells will begin to slow down in their growth as described in Section 4.5.

Weekly counting of the CTL lines and labelling of the cells with CFSE indicated that the cells were proliferating at an optimal pace two to three days after stimulation (with irradiated autologous LCLs) on day 7, 14 and 21. Figure 4.6 (a)

(a)

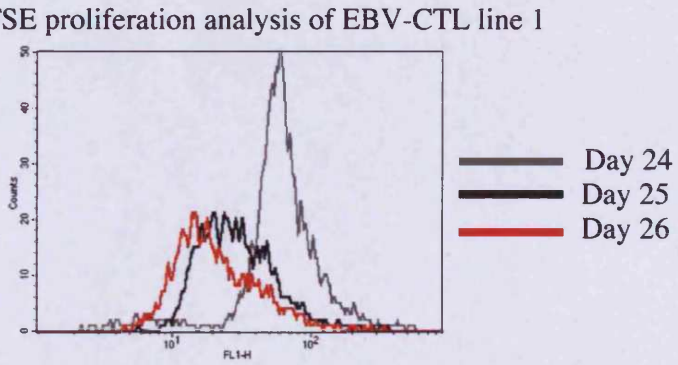

(b)

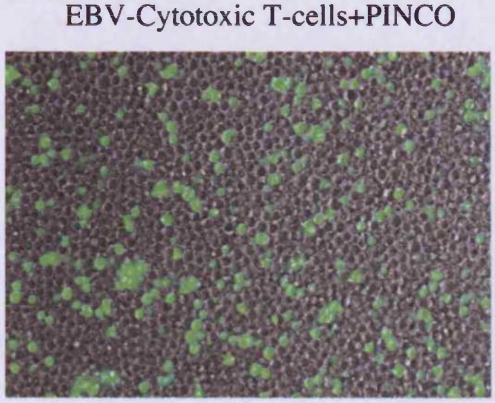

(c)

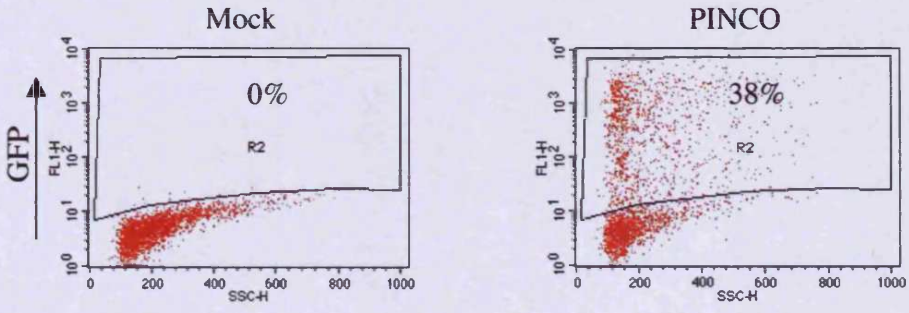

Figure 4.6 Genetic modification of EBV-CTLs with a GFP retrovirus.

CFSE cell proliferation analysis of EBV-CTLs was carried out. EBV-CTLS were stained with CFSE, stimulated with irradiated LCL and monitored by flow cytometry (a) shows the Donor 1 EBV-CTL line of Figure 4.4 (a), which was labelled with CFSE and re-stimulated on day 21 and analysed by flow cytometry from day 24 to day 26. Day 24 post-isolation, $2X10^5$/ml of these CTLs were modified with PINCO in a 2-cycle retroviral infection. (b) The GFP fluorescent cells were visualised on a fluroescent microscope and analysed by flow cytometry. This photograph shows the GFP positive cells overlaid on the brightfield, 49 days post-isolation (c) shows the percentage of GFP positive cells day 49 post-isolation.

illustrates an EBV-CTL line generated from Donor 1 that displayed 50% specific lysis at Day 21 and was re-stimulated with irradiated autologous LCLs on this day. An aliquot of this cell line was labelled with CFSE immediately prior to stimulation on day 21 and cell proliferation was assessed from day 24 to day 26. CFSE results indicated that that proliferation of the CTLs between day 24 and day 25 of the line was highest. The 2-cycle retroviral infection protocol with PINCO retrovirus was carried out on day 24 of the EBV-CTL culture. The infection time points will be referred to as the day post-isolation of the EBV-CTLs (day 0 of infection = day 24 EBV-CTL line). The photograph in Figure 4.6 (b) shows the GFP fluorescence of a successfully modified EBV-CTL line on day 49 post-isolation. The dot plots in Figure 4.6 (c) show an infection efficiency of 38% on day 49 of the EBV-CTL line. This had changed little from the 39.2% observed at day 27. Combined, these results demonstrate that we have successfully modified EBV-CTLs with a GFP retrovirus.

4.7 Investigation of EBV-modified CTLs

Polyclonal EBV-CTL lines have a finite lifespan and maintained expression of a transgene long-term as the cells divide and reach senescence is an important consideration in gene therapy. The GFP positive EBV-CTL line from Figure 4.6 was assayed for GFP expression from day 27 to day 56 of the EBV-CTL line. The expression of the transgene did not appear to confer any growth advantage on the EBV-CTL population as there was little change in the 39.2% GFP positive cells from day 27 onwards as shown in Figure 4.7 (a). The same GFP modified EBV-CTL line was stained with immunofluorescent antibodies on day 52 of this experiment using PE conjugated CD3 and CD8 antibodies. Figure 4.7 (b) shows that the population was 98.5 % $CD8^+$ T-cells, of which 34.1% were GFP positive. Combined, these results prove that genetically modified EBV-CTLs can be maintained long-term with no loss of transgene expression.

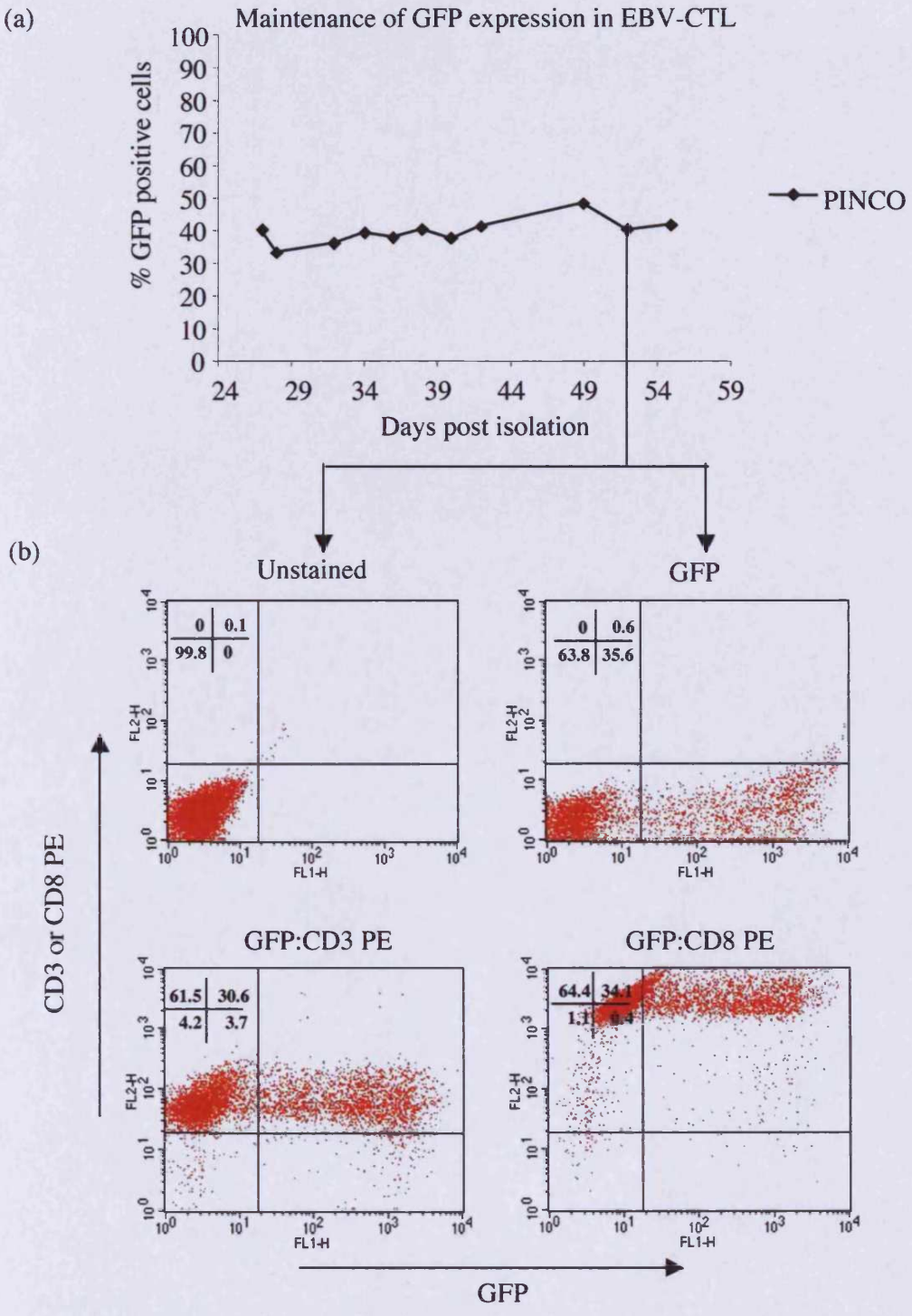

Figure 4.7 Investigation of GFP modified EBV-CTLs

(a) The GFP positive EBV-CTL line from Figure 4.6 was assayed for GFP expression for 29 days. This GFP modified EBV-CTL line was immunofluorescent stained with PE conjugated CD3 and CD8 antibodies, 52 days post-isolation. (b) shows the percentage of GFP positive, CD3 positive and CD8 positive cells in the GFP modified population.

4.8 Genetic modification of the Kit 225 T-cell line with a pBabe puro retrovirus

The previous results established that we could genetically modify the Kit225 T-cell line, primary human T-cells and EBV-CTLs, with a GFP retrovirus and demonstrate maintained transgene expression over time. The next objective was to modify these T-cell types with a retrovirus containing a drug selection marker. We used a pBabe puro vector, another retroviral plasmid again based on the MoMLV retrovirus. This retrovirus delivers a puromycin resistant gene to the target cell and successfully modified target cells will grow in the presence of puromycin.

A similar strategy to that used in the PINCO infections was followed, and the study was commenced by targeting the Kit225 T-cell line. The pBabe puro virus was packaged in the transient PH293 packaging cell line. Once functional pBabe puro virus supernatant was obtained, the two-cycle infection protocol described earlier for the PINCO retroviral infections, was employed. Again, a mock infection well was set up in parallel. Five days post-infection, the Kit225 cells were cultured and puromycin drug selection was added on this day at a concentration of 2.5 μg/ml (as calculated by titration of puromycin on unmodified Kit225 cells). An aliquot of the cells was taken daily and forward and side scatter was assessed by flow cytometry to determine the percentage of cells in the live gate. Four days after adding selection it was observed that there were dead and live cells in the culture. Cells were maintained by culturing with fresh RPMI/IL-2 containing puromycin as required.

Eight days post-selection, all of the mock-infected cells were dead (Figure 4.8) and there were 48.6% live cells remaining in the pBabe puro modified culture. Eight days post-selection the live cells were separated from the dead cells in a low speed centrifugation spin and resuspended in fresh RPMI/IL-2/puromycin. A pure population of Kit225 puromycin resistant cells was obtained which displayed no growth differences to the parent line. Experiments were performed in which both lines were washed out of IL-2 for three days and then labelled with CFSE to monitor any proliferation. The puromycin resistant cell line remained IL-2 dependent like the

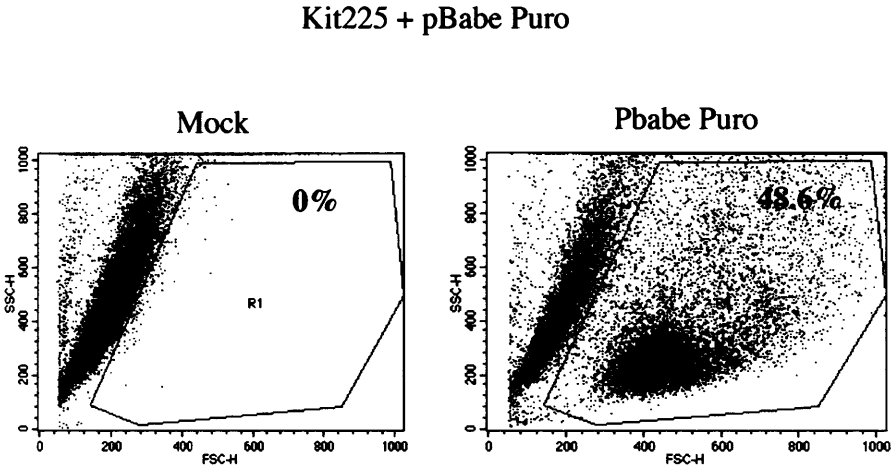

Figure 4.8 Genetic modification of Kit225 with a pBabe puro retrovirus. Kit225 cells were infected in a 2-cycle retroviral infection to generate pBabe puro modified Kit225 cells. A mock infection was set up in parallel. An R1 gate was used to assess the percentage of viable cells in the forward and side scatter dot plots of the cultures. Figure 4.8 shows the results after 8 days under puromycin selection.

parent cell line. The transgene was expressed over a long period of time, as the cell lines were grown in puromycin for over four months continuously.

4.9 Genetic modification of primary human T-cells with a pBabe puro retrovirus

The next objective was to establish if this system was applicable to primary human T-cells. The GFP infection system was useful in establishing quickly that we could efficiently modify PBLs, but with the puromycin retrovirus we could theoretically obtain a pure population of cells transduced with the retrovirus without the need for FACS sorting. Up to this point in the study, we had transiently transfected the pBabe puro virus in the PH293 packaging line, to generate virus. However, the generation of stable packaging cell lines is the method of choice to generate efficient pBabe puro virus. The pBabe puro plasmid does not have the EBV genes found in PINCO to maintain the plasmid episomally, and transient transfections in PH293 cells can potentially limit the titre of the virus. Additionally, previous results had revealed that the PINCO infection efficiencies in PBLs were less efficient than infection of Kit225 cells. Thus, to enable the pBabe puro modification of a higher number of PBLs, optimal viral supernatant was required. The packaging system was changed from the transient PH293 system to the stable producer line system described in the introduction to this chapter. The chosen system used two packaging cells lines, the ecotropic packaging cell line ΩE is used in an intermediate step and this is followed by the use of the amphotropic packaging cell line, ψ-crip (Morgenstern and Land, 1990). The supernatant generated from the ΩE cell line was used to infect the ψ-crip packaing line, as described in the methods, to generate a puromycin resistance stable producing packaging cell line.

Once functional viral supernatant was obtained we employed the same infection strategy used to modify the PBLs with the PINCO retrovirus. Cells were stimulated for three to four days and infected in a 2-cycle infection. GFP was used to assess infection efficiency initially. Experiments indicated that re-stimulation of the PBLs three or four days following isolation, with anti-CD3 and IL-2, and the

addition of puromycin (1 μg/ml) the following day was the most effective approach to outgrow the puromycin resistant cells. Once puromycin was added the cells were monitored daily. The PBLs were maintained in puromycin with the addition of IL-2 every three days and re-stimulation with anti-CD3 weekly. Figure 4.9 illustrates a schematic of the whole procedure from isolation of the PBLs from whole blood, through to the generation of pBabe modified PBLs.

The dot plots in Figure 4.10 (a) show the results obtained day 18 post-isolation. The mock cells were all dead but there were 81.6% live cells in the pBabe puro culture. On average there was 68%±13% of PBLs live cells 18 days post-isolation. The pBabe puro modified PBLs of Figure 4.9 (a) were stained with immunofluorescent antibodies on day 18 post-isolation, to phenotypically characterise the puromycin resistant T-cell population. We used PE conjugated CD3 antibody and FITC conjugated CD4 and CD8 antibodies. Figure 4.10 (b) demonstrates that 34.2% of the cell population was $CD4^+$ and 72.5% was $CD8^+$. The puromycin resistance was maintained for 43 days post isolation. These results indicate that we can successfully modify PBLs with a drug selection virus and maintain the transgene expression long-term.

4.10 Genetic modification of EBV-CTLs with a pBabe puro retrovirus

Our next objective was to establish if we could modify the EBV-CTLs with a puromycin resistant retrovirus and maintain the cells long-term in puromycin. First we had to generate the EBV-CTL line as described in 4.4. Once the EBV-CTL line was established, a similar strategy to the modification of PBLs with pBabe puro was adopted, whereby establishing the best day to infect the CTLs and the best day to add selection, was required. We carried out experiments whereby CTLs were re-stimulated at various timepoints after EBV-specificity was established on Day 21, and selection was added the following day. However infection efficiency wasn't high and the generation of puromycin resistant CTLs proved difficult. To circumvent this, we devised a strategy involving the modification of the CTLs earlier in the EBV-CTL generation protocol. This involved the re-stimulation of the CTL line on

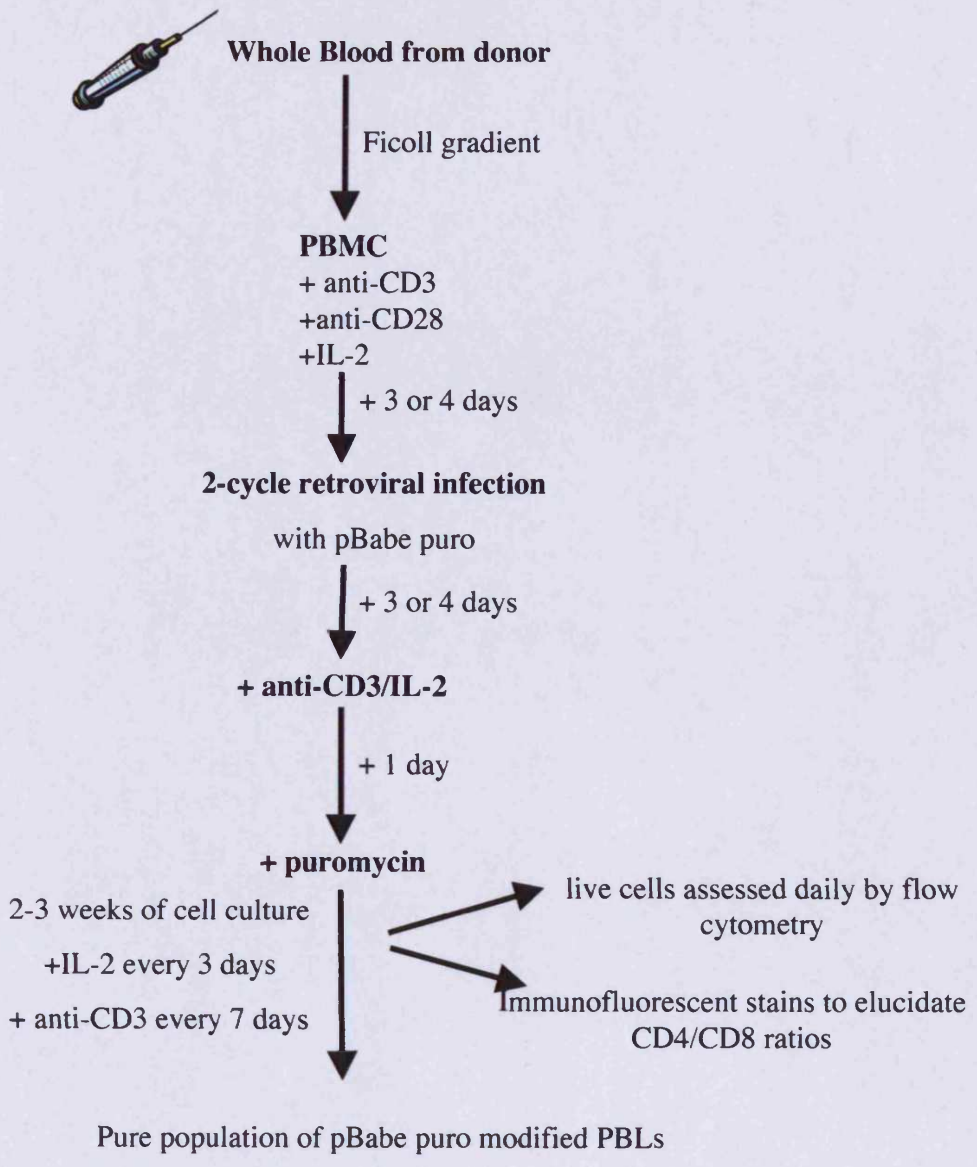

Figure 4.9 Schematic of the generation of pBabe puro modified PBLs. This diagram illustrates the entire procedure from isolation of the PBLs from whole blood to the generation of the modified PBLs.

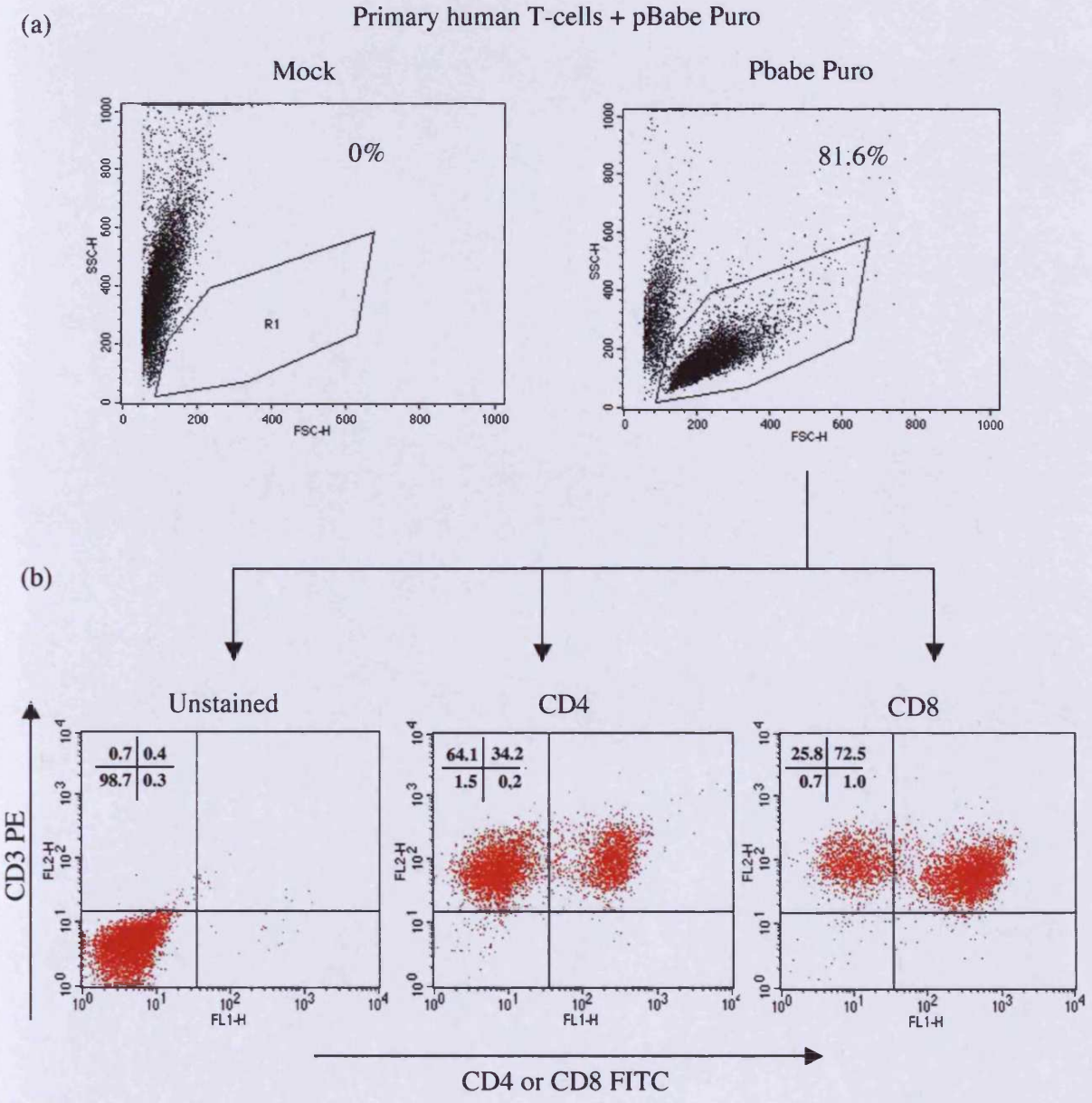

Figure 4.10 Genetic modifiation of PBLs with pBabe Puro. PBLs were isolated from whole blood using a Ficoll gradient and stimulated with anti-CD3 (OKT3, 2.5 ng/ml), anti-CD28 (BD, 5 μg/ml), and IL-2 (20ng/ml). PBLs were infected day 3 post-isolation with pBabe puro virus in a 2-cycle infection. The cells were restimulated day 7 post-isolation with anti-CD3 and IL-2 and 1 μg/ml puromycin was added the following day. Forward and side scatter analysis determined the percentage of viable puromycin resistant cells in the population 18 post-isolation, results are shown in Figure 4.10 (a). These pBabe puro modified PBLs were immunofluorescent stained with PE conjugated CD3 antibody and FITC conjugated CD4 and CD8 antibodies day 18 post-isolation and analysed by flow cytometry. The results are shown in Figure 4.10 (b).

day 7 with irradiated autologous LCLs, addition of IL-2 on day 9 and infection with pBabe puro on day 10. The EBV-CTL line was re-stimulated again on day 13 or 14 and puromycin drug selection was subsequently added the following day (day 14 or 15 of the CTL line) at 1 μg/ml. The cells were monitored daily for percentage of live cells in the culture. The schematic in Figure 4.11 illustrates the entire procedure from the isolation of PBLs and the generation of EBV-CTLs from the whole blood of a healthy donor, through to the generation of pBabe puro modified CTLs.

Figure 4.12 (a) shows a pBabe puro modified EBV-CTL line on day 24. This line was generated from donor 1 as described in 4.4 and infected with pBabe puro on day 10 of the CTL line. The line was re-stimulated on day 14 and selection was added on day 15. After 10 days under selection, there were 28.9% live cells in the pBabe puro modified CTL culture while all of the mock cells were dead. On average the percentage of live cells after puromycin drug selection was 18%±3%, and these data show that puromycin resistant EBV-CTL lines were successfully generated. The line shown in Figure 4.12 (a) was maintained for 41 days. We also maintained the unmodified EBV- CTL line in a parallel culture with the modified line, with no observed differences in cell numbers as observed by cell counts between the two lines (data not shown). The pBabe puro modified line of Figure 4.12 (a) was immunofluroescence stained and analysed by flow cytometry on day 27, to phenotypically characterise the culture. We used PE conjugated CD3 antibody or FITC conjugated CD4 or CD8 antibodies. The results in Figure 4.12 (b) for the pBabe puro modified line show that 89.3% of the culture is $CD8^+$ compared to 6.1% $CD4^+$. The results were comparable to those for the unmodified line whereby 91.7% of the cells were $CD8^+$ and 7.7% are $CD4^+$. These results demonstrated that we had successfully modified a $CD8^+$ line with a pBabe puro virus and that there are some $CD4^+$ cells in this culture.

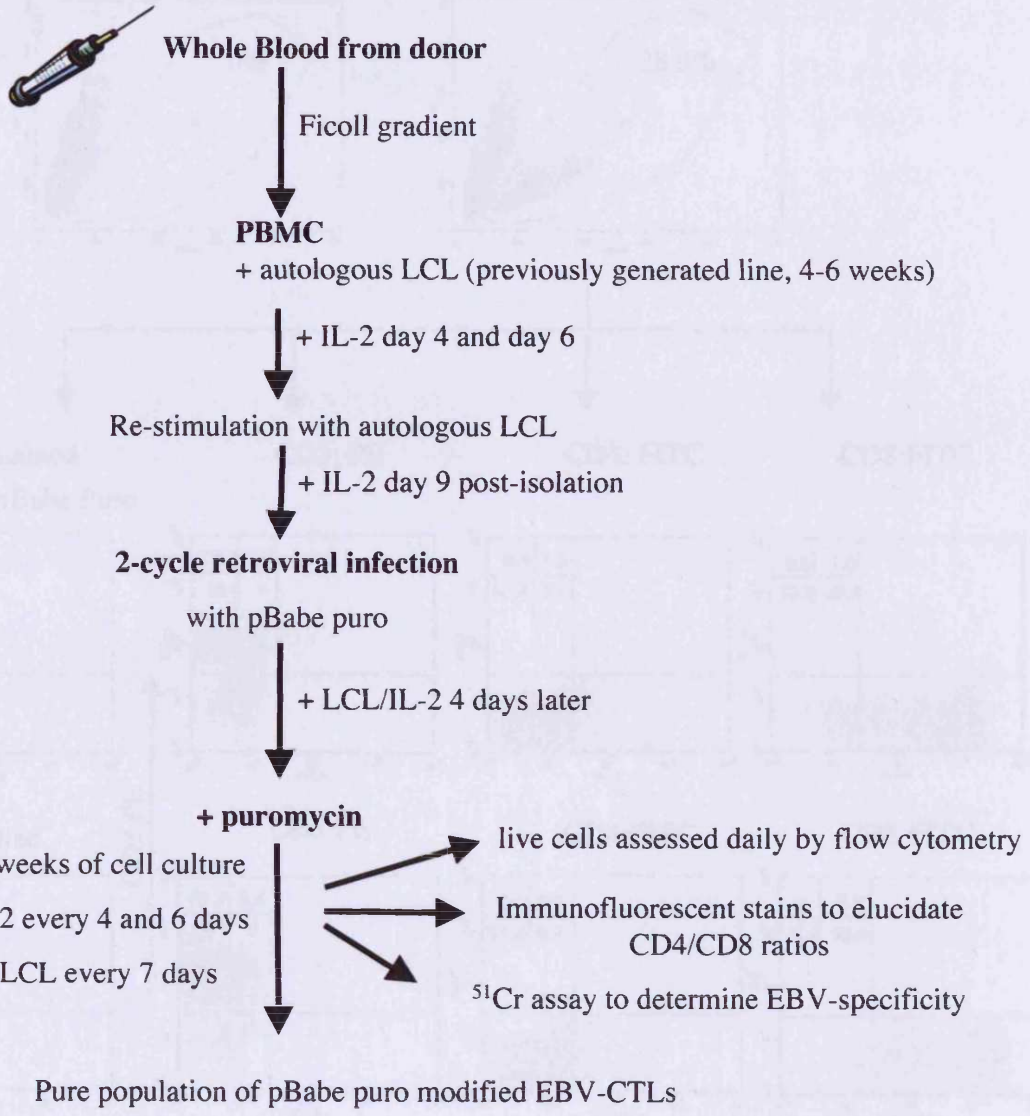

Figure 4.11 Schematic of the generation of pBabe puro modified CTLs. This diagram illustrates the entire procedure from the isolation of the PBLs from whole blood and the generation of EBV-CTLs, to the generation of the modified PBLs.

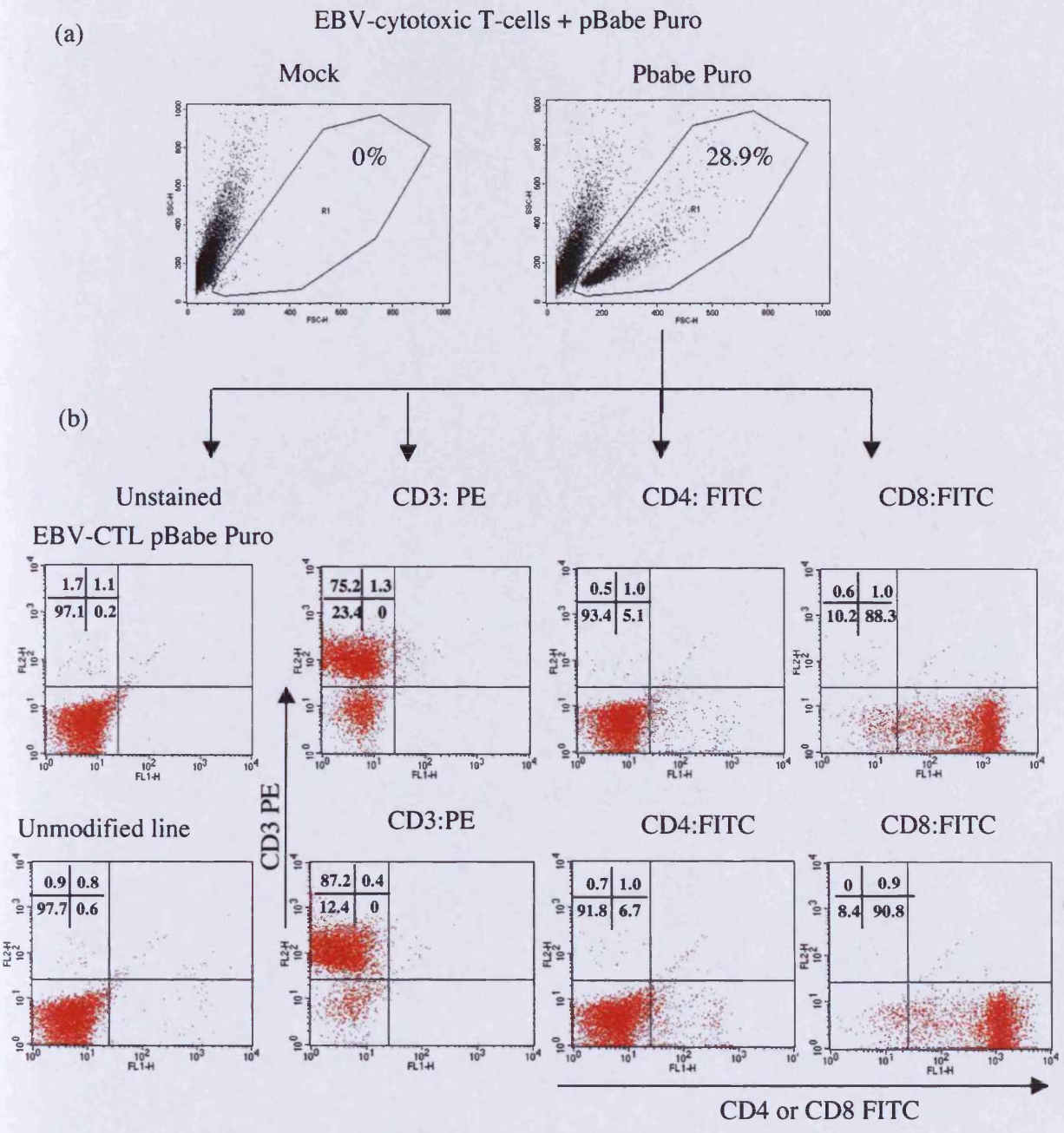

Figure 4.12 Genetic modification of EBV-CTLs with a pBabe Puro retrovirus. PBLs were isolated from the whole blood of Donor 1 using a Ficoll gradient, seeded at $2X10^6$/ml and stimulated with autologous irradiated LCLs. IL-2 was added at discrete timepoints and weekly LCL restimulation was used to generate an EBV-CTL line. This line infected with pBabe puro on day 10 of the CTL line. The line was restimulated on day 14 and selection was added on day 15. After 10 days under selection, the percentage of live cells was assessed and is shown in Figure 4.12 (a). Both the pBabe modified line and the unmodified CTL line were immunofluorescent stained with PE conjugated CD3 antibody or FITC conjugated CD4 and CD8 antibodies on day 27 post-isolation, and analysed by flow cytometry. The results are shown in Figure 4.12 (b)

To investigate the EBV-specificity of the modified CTLs, chromium release assays as described in 4.4, were carried out on the pBabe puro modified EBV-CTLs, using autologous EBV-LCLs and allogeneic LCLs as targets. Figure 4.13 (a) shows the results of a chromium release assay performed on a pBabe puro modified EBV-CTL line, generated from donor 1 and assayed for EBV-specificity on day 28 of the line. At an E:T ratio of 50:1 the pBabe puro modified line displays 33.5% specific lysis against autologous LCL and 14.4% against the allogeneic LCL line. The unmodified line was also assessed for EBV-specificity in the assay. Figure 4.13 (b) shows the results of the chromium assays performed on the unmodified EBV-CTL line. At an E:T ratio of 50:1 the unmodified line displays 40.5% specificity against autologous LCL and and 23.7% against the allogeneic LCL line. This shows that we have successfully generated pBabe puro EBV-CTLs that display HLA-restricted killing.

(a) EBV-CTLs + pBabe puro

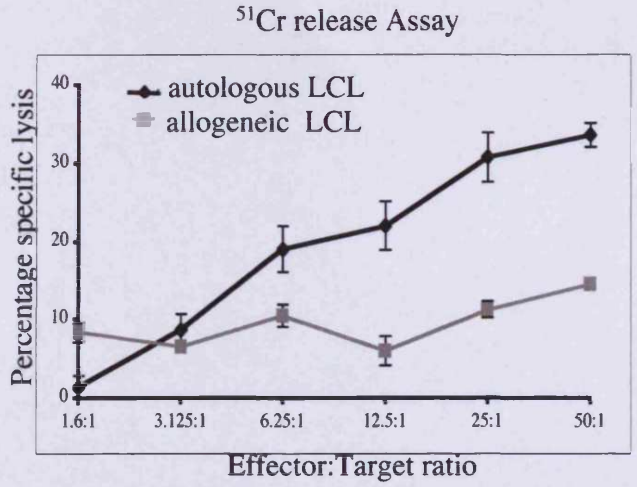

(b) Unmodified EBV-CTLs

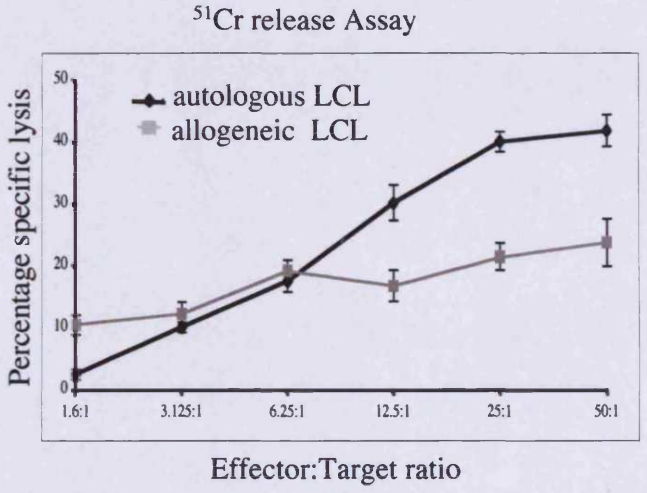

Figure 4.13 Assessment of EBV-specificity in pBabe puro modified CTLs.
PBLs were isolated from the whole blood of Donor 1 using a Ficoll gradient, seeded at $2X10^6$/ml and stimulated with autologous irradiated LCLs. IL-2 was added at discrete timepoints and weekly LCL restimulation was used to generate an EBV-CTL line. This line infected with pBabe puro on day 10 of the CTL line. The line was restimulated on day 14 and selection was added on day 15. The resistant cells were assayed for EBV-specificity day 28 of the line. Figure 4.13 (a) shows the results over a range of E:T ratios using autologous LCLs and allogeneic LCLs as targets. The unmodified line was also assayed on the same day using the same targets and the results are shown in Figure 4.13 (b). The mean specific lysis ± SEM are shown from triplicate wells and was based on the equation (E-S)/(M-S)X100-see chpt 2, page 83. Average maximal lysis (M) and spontaneous lysis values (S) were based on an average of 12 replicates. The same controls/targets were used to calculate (a) and (b) mean specific lysis. . Autologous LCL: average of 3955 cpm ± 78 maximal lysis (=M) and 223 cpm ± 6 spontaneous lysis (=S). Allogeneic LCL: M=1746 cpm ± 69, S=265 cpm ± 18.

4.12 Discussion

This chapter shows that we have successfully adapted the retroviral technology transferred from the Dept. of Haematology, UWCM; and the Dept. of Pathology, UWCM, to modify human T-cells. The application of the strategy established in Chapter 3, which investigated Kit225 T-cell lines first before commencing the primary T-cell work, proved useful in this chapter. In addition, the primary T-cell proliferation results of Chapter 3 were necessary to achieve successful retroviral infection in this chapter. Comparing the two different retroviral systems we studied, there are advantages to a drug selection system rather than a GFP marker system. One advantage is that the CFSE cell proliferation assay, applied earlier in this chapter to assess the optimal day to infect the PBLs and EBV-CTL lines, could still be employed. Both CFSE and GFP fluoresce in the FL-1 channel limiting the application of this assay to monitor GFP transduced cells. Another advantage of the pBabe puro retroviral system is that the pBabe vector is smaller than the PINCO vector (5.1 kb Vs 15 kb), which may prove advantageous in cloning a large gene of interest into the retroviral plasmid.

The infection efficiencies we achieved in PBLs compare favourably to numerous previous reports of freshly isolated T-cell infections where efficiencies often less than 10% have been reported (Blaese *et al.*, 1995; Heslop *et al.*, 1996b; Rooney *et al.*, 1995a). Infection efficiencies similar to the levels (29.9% ± 16.5%) we achieved of approximately 30% have been reported when the fibronectin protein was employed in the protocol (Introna *et al.*, 1998). We found that the infection of PBLs three or four days after stimulation with anti-CD3, anti-CD28 and IL2, was the most effective protocol for both GFP and pBabe puro infections. The stimulation of the pBabe puro culture four or five days following infection, and the addition of puromycin the following day was optimal to generate puromycin resistant PBLs. Our findings are consistent with reports in the literature that suggest that CD28 co-stimulation improves the generation of functional gene-modified T-cells by enhancing cell growth. It has also been reported that skewing of the TCR can occur following stimulation with anti-CD3 and IL-2 alone and that co-stimulation with

anti-CD28 can prevent this and retain the clonal diversity and antigen specific $CD4^+$ and $CD8^+$ T-cells in a culture (Ferrand *et al.*, 2000; Movassagh *et al.*, 2000). In one experiment, anti-CD3/CD28/IL-2 stimulated PBL cultures infected with PINCO, had 55% GFP fluorescent cells while anti-CD3/IL-2 stimulated PBL cultures from the same donor and infected with the same batch of virus, had 41% GFP fluorescent cells. This suggests that the anti-CD3/CD28/IL-2 stimulated PBLs infect better than the anti-CD3/IL-2 stimulated PBLs. Taken together, our experiments show that Kit225 T-cells infect most efficiently, followed by anti-CD3/CD28/IL-2 stimulated PBLs and anti- CD3/IL-2 stimulated PBLs.

The experiments investigating the modification of EBV-CTLs, showed that infection of EBV-CTLs three days after re-stimulation with irradiated LCLs yielded the highest infection efficiency. In the pBabe puro virus infections, a lengthy *in vitro* selection procedure was required, and we found that infection earlier in the generation of the EBV-CTL line, on day 10, was optimal to generate puromycin resistant CTLs. Our EBV-CTL infection efficiencies compared quite favourably to the literature where infection efficiencies as low as 0.1% have been reported (Heslop *et al.*, 1996a; Zhou *et al.*, 2003). We found that a small percentage of modified $CD4^+$ T-cells were maintained long-term. Rooney *et al* suggest that the presence of $CD4^+$ T-cells in the EBV-CTL modified lines may be beneficial to the *in vivo* expansion and long-term persistence of adoptively transferred T-cells (Rooney *et al.*, 1998a). This is based on findings that $CD4^+$ T-cells play a crucial role in establishing and maintaining $CD8^+$ T-cell mediated anti-viral immunity. Figure 4.13 indicated that the EBV specificity of the CTLs did not decrease following pBabe puro retroviral modification. This is in agreement with the evidence in the literature, which suggests that the retroviral modification of EBV-CTL lines does not affect function or specificity (Bonini *et al.*, 1997; Rooney *et al.*, 1998a).

Our results indicate that Kit225 T-cell lines infect better than either PBL or EBV-CTL lines and that the infection efficiency in the PBLs, and in the EBV-CTL lines depends on variables including the cell cycle status of the cells. Evidence suggests that factors other than proliferation are also important for optimal retroviral

gene transfer and that the distribution of the amphotropic receptor (Miller *et al.*, 1994) on target cells may also be a source of variation in infection protocols. PIT-2 is a 652-amino acid type III sodium phosphate cotransporter, and the receptor for amphotropic MoMLVs (Goff, 2001). Activation of cell surface PIT-2 molecules is required for efficient amphotropic retroviral infection. Differences in the levels of PIT-2 expression between different cell types may be a source of variation of infection efficiency in our experiments. The synthesis, stability and activation of the PIT-2 receptor is regulated by posttranslational modifications of cell surface molecules induced by phosphate, and the entry of amphotropic retroviruses mediated by PIT-2, requires the presence of active forms of the molecule at the cell surface (Goff, 2001; Rodrigues and Heard, 1999). Thus in addition to variation in cell surface expression between cell types, differences in the PIT-2 modifications induced by phosphate, among different cell types, may lead to variation in the susceptibility to retroviral infection.

There are options aside from adjusting the culture system of the target cells, which can be employed to obtain efficient retroviral infection. Reports of infection efficiencies in primary human T-cells as high as 80% to 95% have been made (Movassagh *et al.*, 2000; Pollok *et al.*, 1998). In the case of these very high transduction efficiencies, the retroviral system is modified so that the retrovirus envelope is a gibbon ape leukaemia virus (GALV) envelope rather than a MLV amphotropic viral envelope. The receptors for amphotropic MoMLV and the GALV are both expressed in most tissues but at different levels (Kavanaugh *et al.*, 1994; Uckert *et al.*, 1998) and the GALV envelope has been shown to be more effective in T-cell infection (Lam *et al.*, 1996; Movassagh *et al.*, 2000; Yang *et al.*, 1999). However, such retroviral vector modifications are beyond the boundaries of this study.

The objectives outlined at the beginning of this chapter have been achieved. The retroviral technology has been successfully transferred to our laboratory and we have demonstrated the genetic modification of Kit225 T-cells, PBLs and EBV-CTLs with both a GFP expressing retrovirus and a puromycin resistance expressing

retrovirus to levels of efficiency, which compare favourably to the literature. More importantly, we have demonstrated maintenance and expression of the marker transgenes long-term in the Kit225 T-cells, PBLs and EBV-CTLs with no discernible phenotypic differences to the unmodified cells. The next step is the modification of these T-cells with a gene of interest and the demonstration of a phenotype *in vitro*.

CHAPTER 5

Generation of rapamycin resistant human T-cells

5.1 Introduction

The objective of this chapter was to modify human T-cells with a transgene to confer rapamycin resistance. The genetic modification of adoptively transferred T-cells with transgenes to improve the function of the cells *in vivo* has been demonstrated by a number of groups (Bonini *et al.*, 1997; Riddell *et al.*, 1996b; Rooney *et al.*, 1995a). However, the effectiveness of adoptively transferred T-cells can be limited by the fact that they must function in an immunosuppressive environment in post-transplant patients. Rapamycin inhibits certain signal transduction pathways coupled to the IL-2 R of T-cells (Powers and Walter, 1999) and may potentially limit the function and longevity of adoptively transferred T-cells . We aim to combine the technology established in Chapter 3 and Chapter 4 to efficiently modify human T-cells with a retrovirus, which will confer rapamycin resistance in T-cells.

The target of rapamycin protein (TOR) protein has an important role in the control of cell growth and proliferation in eukaryotic cells, and contains several distinct and evolutionarily conserved structural domains. The FKBP12/rapamycin binding domain (FRB) of mTOR, upstream of the kinase domain, contains a critical serine residue 2035 which is required for the FKBP12-rapamycin inhibition of TOR, and is homologous to serine 1972 and serine 1975 of yeast TOR1 and TOR2 respectively (Chen *et al.*, 1995; Stan *et al.*, 1994). A simplified schematic, illustrating the conserved domains of mTOR and a S2035 mutation is shown in Figure 5.1.

Serine mutations in residues S1972 and S1975 in the TOR1 and TOR 2 yeast proteins respectively, have been investigated for their ability to confer rapamycin

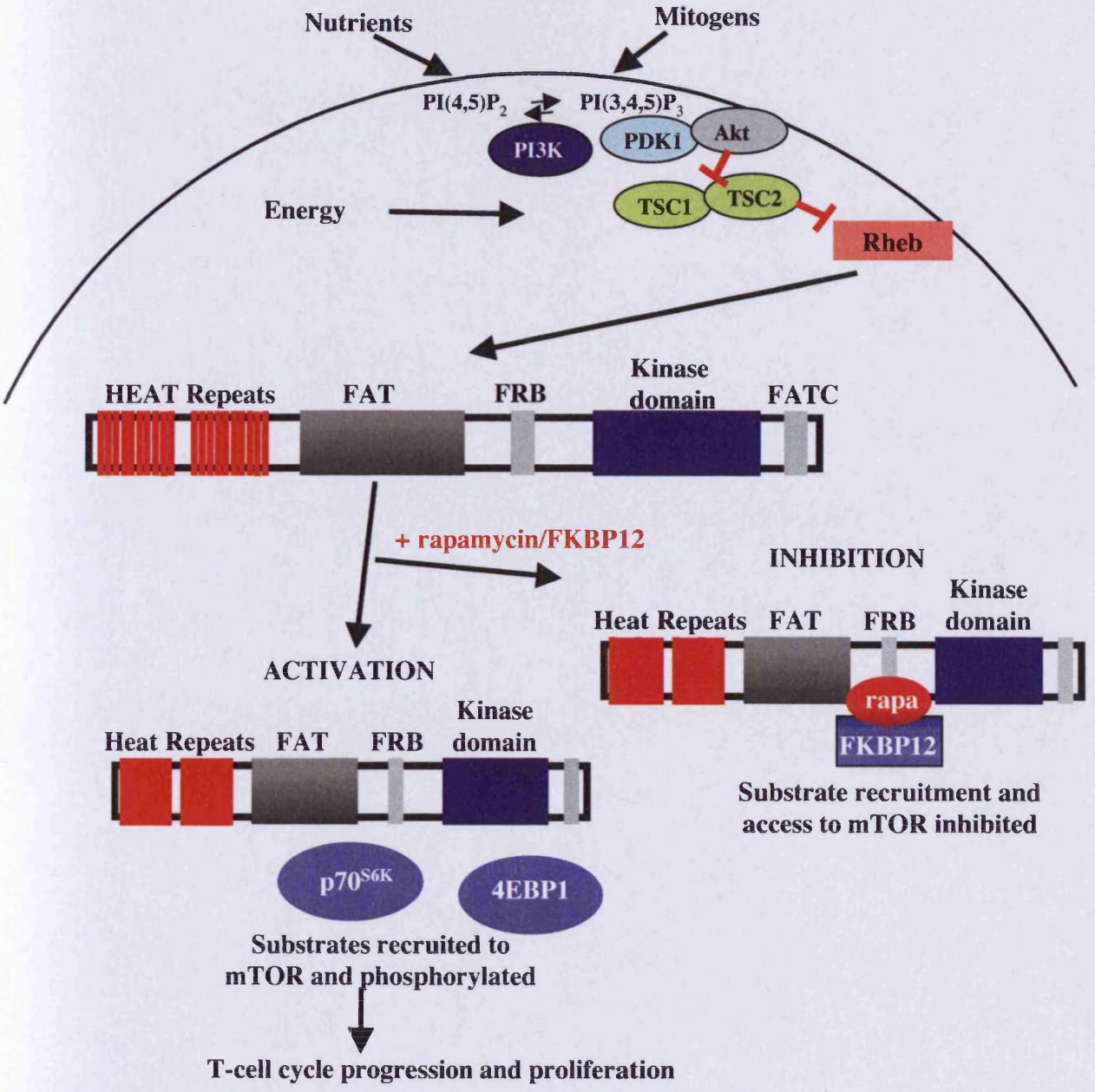

Figure 5.1 mTOR structure and function

The functional domains conserved in TOR proteins are depicted, including the N-terminal 20 tandem HEAT repeats, the central FAT domain, FKBP12-rapamycin binding domain (FRB), the kinase domain and the FATC domain. mTOR activity is regulated by mitogens, nutrient levels and energy levels in the cell. The regulation of mTOR by growth factors is through the PI3K pathway. PIP_3 recruits Akt to the membrane where it is phosphorylated by PDK1. Activataed Akt phosphorylates TSC2 resulting in the inhibition of the TSC1/2 complex. Rheb is a small GTPase that is inactivated by TSC1/2 and is a positive regulator of mTOR (Li *et al.*, 2004). Substrates such as $p70^{S6K}$ and 4EBP1 are recruited to mTOR by scaffolding proteins such as raptor and mLST8. The substrates gain access to the kinase domain of mTOR and become phosphorylated leading to a host of downstream signalling events and cell cycle proliferation. The binding of rapamycin/FKBP12 to the FRB domain causes dissociation of scaffolding proteins from mTOR, prevents the recruitment and activation of mTOR substrates to the protein, and prolongs G1 cell cycle progression

resistance on yeast cells (Zheng *et al.*, 1995). TOR is a central mediator of nutrient levels in the yeast cell and loss or inhibition of TOR function by treating the yeast cells with rapamycin, mimics nutrient deprived conditions (Fingar and Blenis, 2004). Zheng *et al.* introduced an arginine substitution at the conserved residue S1972 in the TOR 1 locus and S1975 in the TOR 2 locus of the SK1 laboratory yeast strain. In biochemical analysis they demonstrated that these mutations disrupted the ability of FKBP12-rapamycin to bind to TOR and investigation of the growth of the modified yeast strains in culture, showed that the mutations conferred a resistance to the effects of rapamycin (Zheng *et al.*, 1995).

Similarly, mutations of the corresponding serine 2035 residue in mTOR, abolish the FKBP12-rapamycin binding activity of the protein (Chen *et al.*, 1995). Binding assay analysis studies have shown that the mutation of S2035 to any residue containing a larger side chain, abolishes binding activity probably through steric hindrance or induced conformational change (Chen *et al.*, 1995). Cell proliferation studies have also demonstrated that such mutations in the FKBP12/rapamycin binding domain conferred rapamycin resistance on T-cells (Dumont *et al.*, 1995). Dumont *et al.* isolated rapamycin resistant clones of the YAC-1 T-cell lymphoma and investigated the molecular basis of their rapamycin resistance. Their data indicated that the FRB domain is critical for FKBP-12/rapamycin binding in T-cells and mutations in this region can confer rapamycin resistance in T-cells (Dumont *et al.*, 1995)..

The modification of primary human T-cells, to express a mutant mTOR protein with a substitution in the critical S2035 residue, has not been demonstrated to date. The aim of our study is to confer rapamycin resistance by modifying primary human T-cells to express such a mutant mTOR protein with the overall objective being to improve the function of primary human T-cells in an immuosuppressive environment. To modify the PBLs, we use a pBabe puro retroviral plasmid containing an mTOR transgene with a point mutation in the wild-type mTOR sequence, resulting in an amino acid change from serine to threonine (pBabe mTOR S2035T). We also modify PBLs with a pBabe virus with only the puromycin

resistant transgene (pBabe puro, Chapter 4), and a pBabe virus with the wild-type mTOR gene (pBabe wt mTOR) and results are compared to those from the pBabe mTOR S2035T modified cells.

5.2 Modification of Kit225 cells with pBabe mTOR viruses

In the previous chapter we successfully modified Kit225 cells, PBLs and EBV-CTLs with a pBabe puro puromycin resistant retrovirus. The next objective was to modify target cells with a pBabe puro virus carrying a rapamycin resistant mTOR gene (pBabe mTOR S2035T), and to demonstrate a function *in vitro*. We also modified T-cells with a retrovirus containing the wild-type sequence of mTOR (pBabe wt mTOR) and a pBabe puro retrovirus and compared results to the mTOR S2035T modified T-cells. Similar to the strategy employed in Chapter 4, the Kit225 T-cell line was the initial target, to determine if we could modify a T-cell line with a gene of interest, maintain the line long-term and demonstrate a function *in vitro*. We used the transient PH293 packaging system in order to produce functional control pBabe puro, pBabe wt TOR and pBabe mTOR S2035T viruses. Once functional viral supernatatant was obtained, a 2-cycle retroviral infection was performed (as described in Chapter 4) with control pBabe puro virus, pBabe wt mTOR virus and pBabe mTOR S2035T virus. The modified cells were placed under puromycin drug selection (2.5 μg/ml) after five days, and were then maintained in puromycin and IL-2 and monitored daily.

Figure 5.2 shows the panel of modified Kit225 T-cells after 8 days under selection. The pBabe puro viral supernatant generated more infected Kit225 cells than either the pBabe wt mTOR or the pBabe mTOR S2035T viral supernatant. The dot plots in Figure 5.2 show that there were 48.9% live cells in the pBabe puro modified culture, 2.2% live cells in the pBabe wt mTOR modified culture and 4.3% live cells in the pBabe mTOR S2035T culture, after 8 days selection. As the Kit225 cell line is constitutively growing in IL-2, the puromycin resistant cells proliferated

(a)

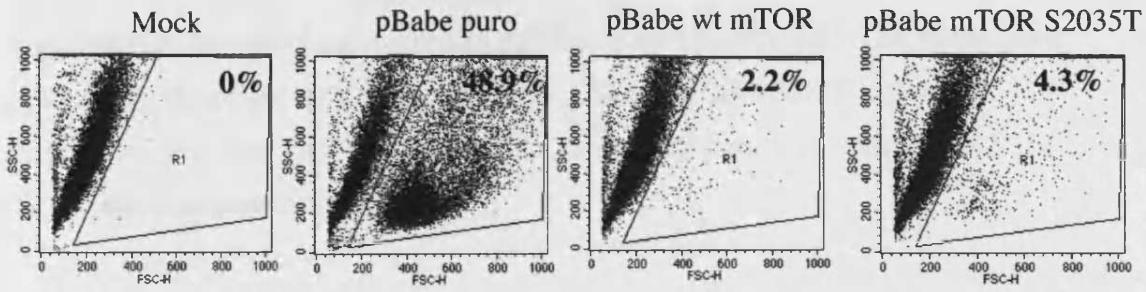

(b)

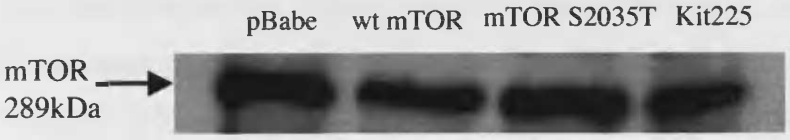

Figure 5.2 Genetic modification of Kit225 cells with pBabe mTOR viruses. Kit225 cells growing in IL-2 (20 ng/ml) were infected in a 2-cycle retroviral infection with RPMI only, pBabe puro virus, pBabe wt mTOR virus or pBabe mTOR S2035T virus. Puromycin (2.5 μg/ml) was added after five days and the cultures were maintained in IL-2 and puromycin and monitored for viability by flow cytometry. Figure 5.1 (a) shows the forward and side scatter dot plot analysis results after eight days under puromycin drug selection. The R1 gate was used to determine the percentage of viable cells in the population. The expression levels of mTOR in each modified cell line was analysed and compared to the expression of mTOR in the parent Kit225 line. Total cell lysates were generated and run on an SDS-PAGE gel. Proteins were transferred to PVDF membranes at 50V for three hours and the membranes were then probed with an anti-mTOR rabbit polyclonal primary antibody and detected with a secondary anti-rabbit antibody and chemiluminescent substrate detection methods. Figure 5.1 (b) shows the levels of mTOR in the pBabe puro, pBabe wt mTOR, pBabe mTOR S2035T modified Kit225 cells lines and the Kit225 parent cell line.

rapidly to generate pBabe puro, pBabe wt mTOR and pBabe mTOR S2035T modified lines. Regular removal of dead cells from the cultures with low speed centrifugation generated pure populations of modified Kit225 cells. The pBabe puro control line, the pBabe wt TOR line, and the pBabe mTOR S2035T line were cultured for over four months in puromycin, indicating that expression of the puromycin transgene is maintained.

mTOR expression levels were analysed in the pBabe puro, pBabe wt mTOR and pBabe S2035T modified Kit225 lines and were compared to the levels of mTOR in the parent Kit255 line. This was achieved using SDS-PAGE, immunoblotting and chemiluminescent detetection techniques. Total cell lysates were generated for the pBabe puro, pBabe wt mTOR and pBabe S2035T Kit225 cell lines and for the Kit225 parent cell line, as described in the methods. These samples were run on a 7.5% SDS-PAGE gel and transferred to PVDF membrane at 50V for three hours. The membranes were then probed with an anti-mTOR rabbit polyclonal primary antibody and a secondary anti-rabbit antibody and detected with chemiluminescent substrate detection methods. Figure 5.1 (b) shows the levels of mTOR in the pBabe puro, pBabe wt mTOR, pBabe mTOR S2035T modified Kit225 cells lines and the Kit225 parent cell line. The expression levels of mTOR are similar in all four of the cell lines. This demonstrates that modification of Kit225 cells with a retrovirus expressing mTOR does not lead to increased expression of mTOR in the cell. Because the samples were run on such a low percentage gel (7.5%), only large proteins were retained, thus actin and tubulin proteins were no longer on the gel and a loading control could not be demonstrated.

5.3 Investigation of mTOR modified Kit225 lines

The aim of the modifying the Kit225 cells with a mutant mTOR gene was to investigate a rapamycin resistant phenotype. So far we had generated three stable Kit225 lines; pBabe puro, pBabe wt mTOR and pBabe mTOR S2035T modified Kit225 lines. The next objective was to design experiments to investigate rapamycin resistance. Cell proliferation experiments in the presence or absence of rapamycin,

over four days were performed in the pBabe mTOR S2035T line and results were compared to the pBabe puro and pBabe wt mTOR lines. Cells were first washed out of IL-2 for three to four days to quiesce the lines. Quiescence of the cell lines is useful for cell proliferation experiments. Kit225 T-cells are IL-2 dependent and depriving the cells of IL-2 causes the cell cycle to halt in G1 phase. The cells in the population quiesce, and are at a similar cell cycle stage when setting up the experiment. Quiesced cells were then stained with CFSE as described in the methods and resuspended in complete medium at $2X10^6$/ml in 6-well plates. Appropriate wells were pre-treated with various concentrations of rapamycin for 30 minutes at 37°C and stimulated with 20 ng/ml IL-2. Cell proliferation was monitored daily by flow cytometry.

Figure 5.3 (a) shows the results of the pBabe puro, pBabe wt mTOR and pBabe mTOR S2035T lines, which will now be referred to as 'Set 1'. The histograms are flow cytometry results four days after CFSE labelling, and are representative of six separate experiments on Set 1. The greater the shift in fluorescence to the left of the histogram the greater the proliferation of the cell population. The grey line shows unstimulated Kit225 cells that undergo very little proliferation and do not demonstrate a decrease in fluorescence. The black line shows IL-2 stimulated cells and the red line indicates 10 nM rapamycin/IL-2 treated cells. Results show that rapamycin resistance is demonstrated in the pBabe mTOR S2035T Kit225 cell line. More of the rapamycin treated cells in the pBabe mTOR S2035T histogram are shifted to the left compared to rapamycin treated cells in both the pBabe puro and the pBabe wt mTOR lines. The CFSE fluorescence of the rapamycin/IL-2 treated pBabe mTOR S2035T line looks similar to that of cells treated with IL-2 only. In both other cell lines, the cells treated with rapamycin/IL-2 look similar to control, unstimulated cells.

Figure 5.3 (b) shows the combined results from six separate experiments graphically. The graph was generated using fluorescence results four days after CFSE labelling from each experiment. The geometric mean fluorescence of the rapamycin treated cells, the IL-2 treated cells and the unstimulated cells were used to

(a)

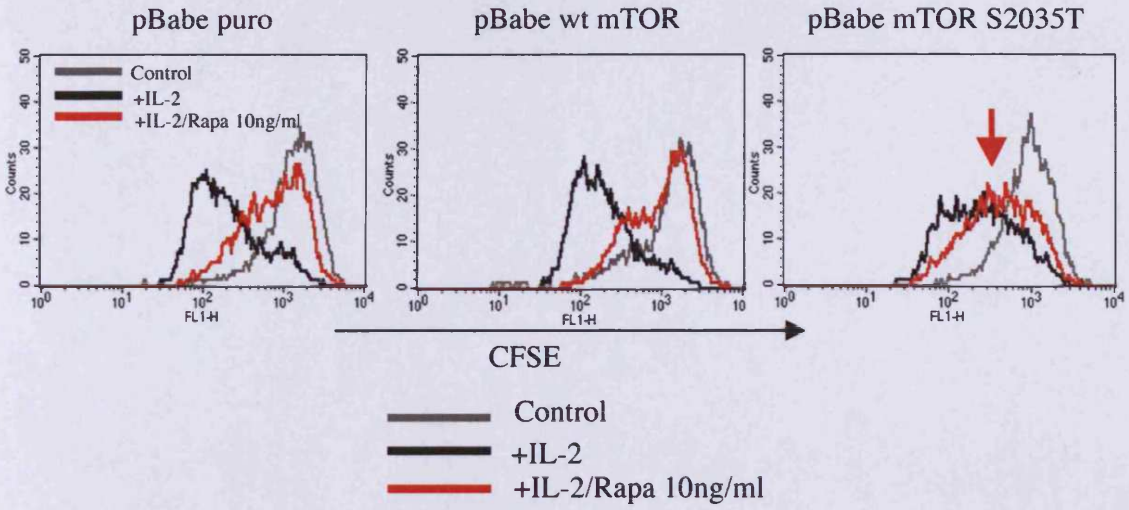

(b)

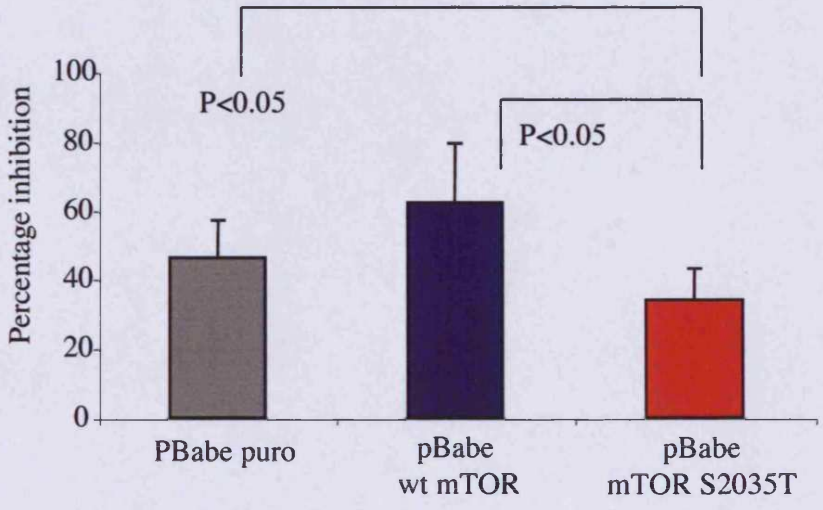

Figure 5.3 Investigation of pBabe mTOR modified Kit225 lines. pBabe puro, pBabe wt mTOR and pBabe mTOR S2035T lines of Set 1 were quiesced for three days and stained with CFSE. Samples were pre-treated with rapamycin at various doses and stimulated with IL-2 (20 ng/ml). Cell proliferation was monitored over a four day period. (a) A representative experiment illustrating the results observed in six separate experiments is shown. Results are shown four days after CFSE labelling. The light grey line represents unstimulated Kit225 cells, the black line represents IL-2 stimulated cells and the red line indicates rapamycin (10 ng/ml) /IL-2 treated cells. (b) illustrates the combined results from these six experiments graphically. The graph was generated using results four days after CFSE labelling from each experiment. We used the geometric mean fluorescence to calculate a percentage inhibition of proliferation value for rapamycin treated cells. Student's T-test was used to determine any statistical significance.

calculate a percentage inhibition of proliferation value (see equation) and we then compared this percentage inhibition value of each of the three lines to each other. A high geometric mean fluorescence indicates little cell proliferation.

$$\frac{\text{Rapamycin/IL-2 treated Geo. mean fluorescence} - \text{IL-2 treated Geo. mean fluorescence}}{\text{Unstimulated Geo. mean fluorescence} - \text{IL-2 treated Geo. mean fluorescence}} \times 100$$

The graph in Figure 5.3 (b) shows that rapamycin resistance is evident in the pBabe mTOR S2035T line, as this line was inhibited less by rapamycin treatment (34% inhibition) compared to the pBabe wt mTOR modified cell line, which was inhibited by 62%. A paired Student's T-test showed that the percentage inhibition in the pBabe mTOR S2035T line is significantly different to both the pBabe puro and the pBabe wt mTOR lines ($p<0.05$).

Three further complete sets of modified Kit225 lines were generated in the same manner. One of the features of the retrovirus is stable integration into the host genome. However this integration is not sequence specific and there is a possibility that should the virus integrate in a different region of the host genome, the phenotype conferred on the cells would differ. The expression levels of mTOR were analysed in the three further sets of mTOR modified Kit225 lines in the same way as described for Set 1. Figure 5.4 (a) shows the results. The mTOR expression levels of pBabe puro, pBabe wt mTOR and pBabe mTOR S2035T are similar between Set 2 and Set 4, and in Set 3 the expression levels of mTOR in the pBabe puro modified Kit225 line is slightly lower than that in the pBabe wt mTOR or pBabe mTOR S2035T line.

Proliferation, in the presence or absence or rapamycin, was measured as before (Figure 5.4 (b)). Histograms are shown four days after CFSE labelling for each experiment. Results are representative of three separate experiments performed on each of the three sets of modified Kit225 lines. Results showed that the retroviral infection of Kit225 cells with a pBabe mTOR S2035T virus did not generate rapamycin resistant cells every time. In Set 3 the pBabe mTOR S2035T line showed

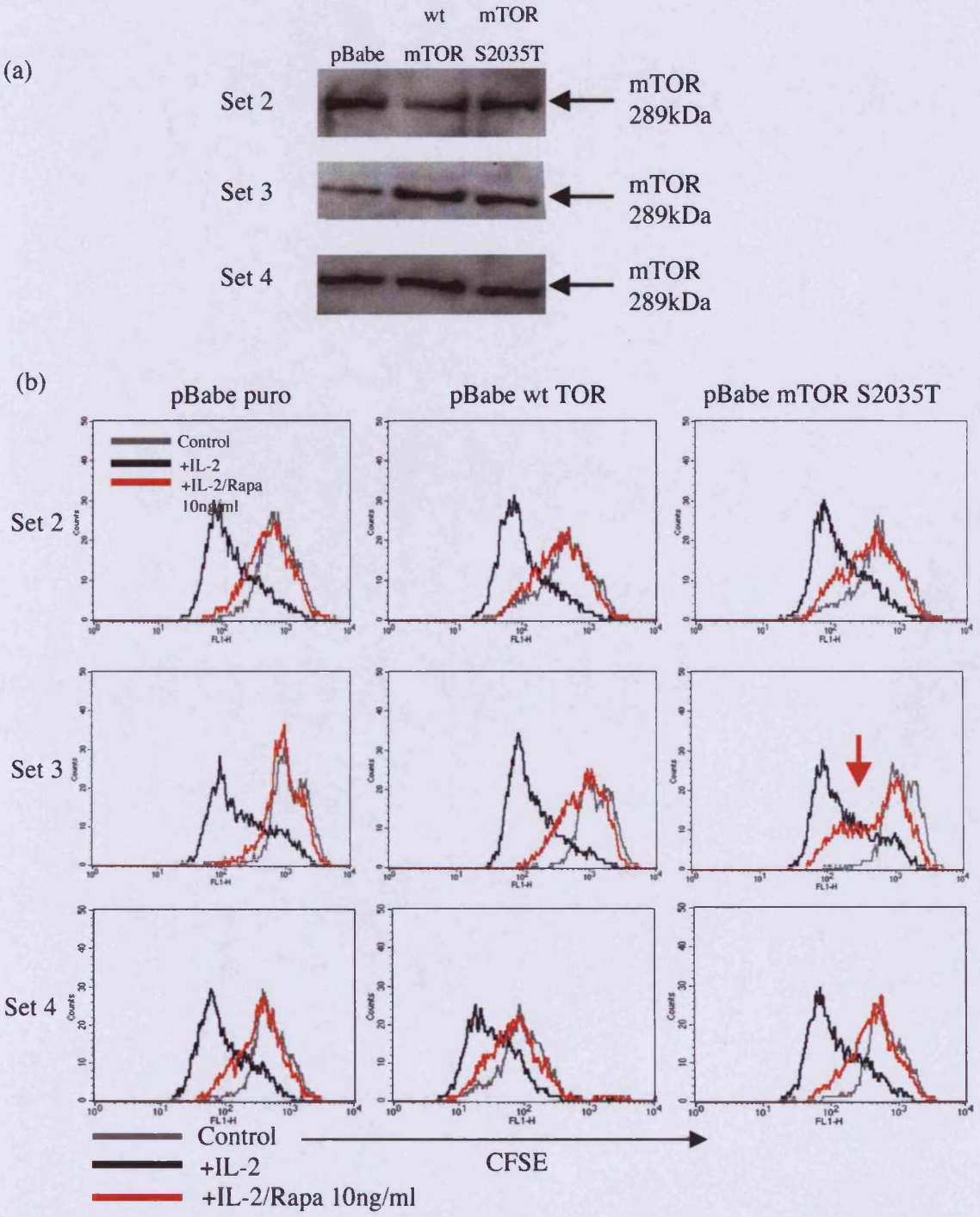

Figure 5.4 Investigation of pBabe mTOR modified Kit225 lines of Set 2, Set 3 and Set 4. Three further sets of mTOR Kit225 lines were generated as for Set 1. (a) The expression levels of mTOR in each modified cell line was analysed as before. (b) pBabe puro, pBabe wt mTOR and pBabe mTOR S2035T lines of Set 2, Set 3 and Set 4 were quiesced for three days and stained with CFSE. Samples were pretreated with rapamycin at various doses and stimulated with IL-2 (20 ng/ml). Cell proliferation was monitored over a four day period. A representative experiment for each Set 2, Set 3 and Set 4 is shown four days after CFSE labelling. The light grey line represents unstimulated Kit225 cells, the black line represents IL-2 stimulated cells and the red line represents rapamycin (10 ng/ml) /IL-2 stimulated cells.

rapamycin resistance. However, the pBabe mTOR S2035T lines of Set 2 and Set 4 did not. The graphical analysis of these experiments is shown in Figure 5.5 and uses the percentage inhibition calculation explained in Figure 5.3. Each graph is a combination of three separate experiments. Student's T-test revealed that the percentage inhibition of the rapamycin treated pBabe mTOR S2035T line of Set 3 was significantly different to both the pBabe puro and the pBabe wt mTOR lines of Set 3. The differences in Set 2 and Set 4 were not statistically significant. These data show that rapamycin resistant T-cells can be generated but that it does not occur with every infection.

5.4 Modification of Primary Human T-cells with pBabe mTOR S2035T

Our results indicated that rapamycin resistance was possible and the next objective was to establish if this was applicable to primary human T-cells. The transient PH293 transfection system generated control pBabe puro viral supernatant sufficient to infect PBLs and grow out puromycin resistant cells. However, the transiently produced pBabe wt mTOR and the pBabe mTOR S2035T virus supernatants were not adequate to infect PBLs due to low titre. We observed that a threshold level of at least 10% of live PBLs after eight days drug selection was required if the modified PBLs were to survive. Thus, we changed to the stable producer line system discussed in Chapter 4, in order to obtain high titre pBabe viral supernatant for infection. Stable packaging lines were generated for the packaging of the pBabe wt mTOR and the pBabe mTOR S2035T viruses, as described in the methods (Chapter 2). All viruses were tested on Kit225 cells to determine if infectious virus was present in the viral supernatants. The stably produced pBabe mTOR S2035T virus supernatant was more effective than the transiently produced viral supernatant (27.6% Vs 4.3% live cells in the culture after 8 days under selection). However, generation of a stable packaging line to produce pBabe wt mTOR virus with a high enough titre to generate pBabe wt mTOR PBLs was unsuccessful. Therefore subsequent infections involve only the pBabe puro control virus and the pBabe mTOR S2035T virus.

Set 2

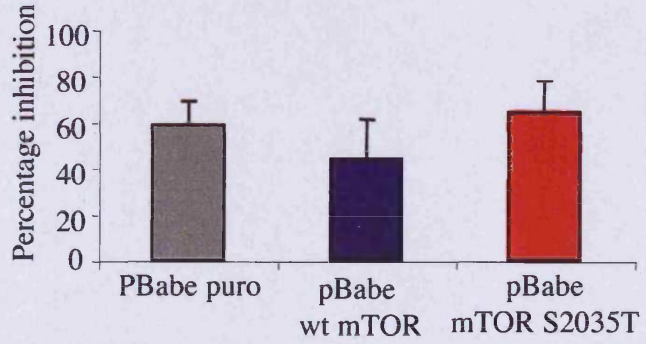

Set 3

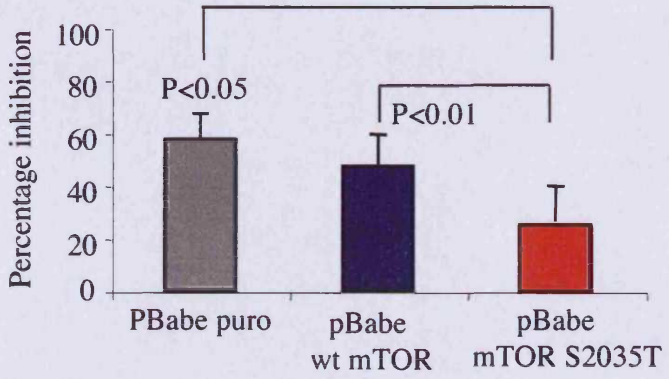

Set 4

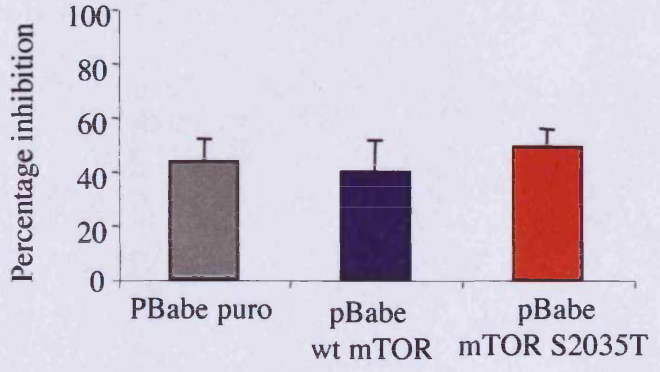

Figure 5.5 Investigating pBabe mTOR modified Kit225 lines of Set 2, Set 3 and Set 4. pBabe puro, pBabe wt mTOR and pBabe mTOR S2035T lines of Set 2, Set 3 and Set 4 were quiesced for three days and stained with CFSE. Samples were pretreated with rapamycin at various doses and stimulated with IL-2 (20 ng/ml). Cell proliferation was monitored over a four day period. Figure 5.5 illustrates the graphical analysis of the CFSE cell proliferation experiments for Set 2, Set 3 and Set 4 four days after CFSE labelling. Each graph was generated using three experiments. The geometric mean fluorescence was used to calculate a percentage inhibition of proliferation value for rapamycin treated cells. Student's T-test determined any statistical significance.

Once the pBabe mTOR S2035T viral supernatant was obtained we employed the same infection strategy used to modify PBLs with the pBabe puro control virus in Chapter 4. PBLs were stimulated for three to four days following isolation, and infected in a 2-cycle infection with either pBabe puro virus or pBabe mTOR S2035T virus. Experiments showed that re-stimulation of the PBLs three or four days after infection with anti-CD3/IL-2 and the addition of puromycin the following day was optimal to select and grow puromycin resistant PBLs. The percentage of live cells in the culture was monitored daily. The PBLs were maintained in puromycin with the addition of IL-2 every 3 days and re-stimulation with anti-CD3 weekly.

Figure 5.6 shows PBLs modified with pBabe mTOR S2035T virus. Parallel infections with PINCO virus were performed and GFP fluorescence levels day 6 post-infection were 35% (data not shown), which indicated a successful infection protocol. The results in Figure 5.6 (a) were obtained 17 days post-isolation and showed that the mock cells were all dead, there were 81.6% live cells in the pBabe puro culture and there were 70.6% live cells in the pBabe mTOR S2035T culture. This was one of the best infection efficiencies obtained with the pBabe mTOR S2035T virus, and on average there were 35.2% ± 9.5% of live cells in the pBabe mTOR S2035T PBL culture 17 days post-isolation. We used immunofluorescent staining with PE conjugated CD3 antibody and FITC conjugated CD4 and CD8 antibodies to phenotypically characterise the modified PBLs. Figure 5.6 (b) shows the results of staining the pBabe mTOR S2035T PBLs of Figure 5.6 (a) day 17 post-isolation. We also compared these results to the pBabe puro modified PBLs. Of the pBabe mTOR S2035T modified PBLs, 34.1% of the cells were $CD4^+$ and 74.7% of the cells were $CD8^+$. In the pBabe line 34.2% of the $CD3^+$ cells are $CD4^+$ and 72.5% of the $CD3^+$ are $CD8^+$. Both the pBabe puro modified PBLS and the pBabe mTOR S2035T modified PBLs were maintained in puromycin for 43 days post-isolation. These data show that we can successfully modify PBLs with a drug selection virus containing a gene of interest and maintain these PBLs in puromycin long term.

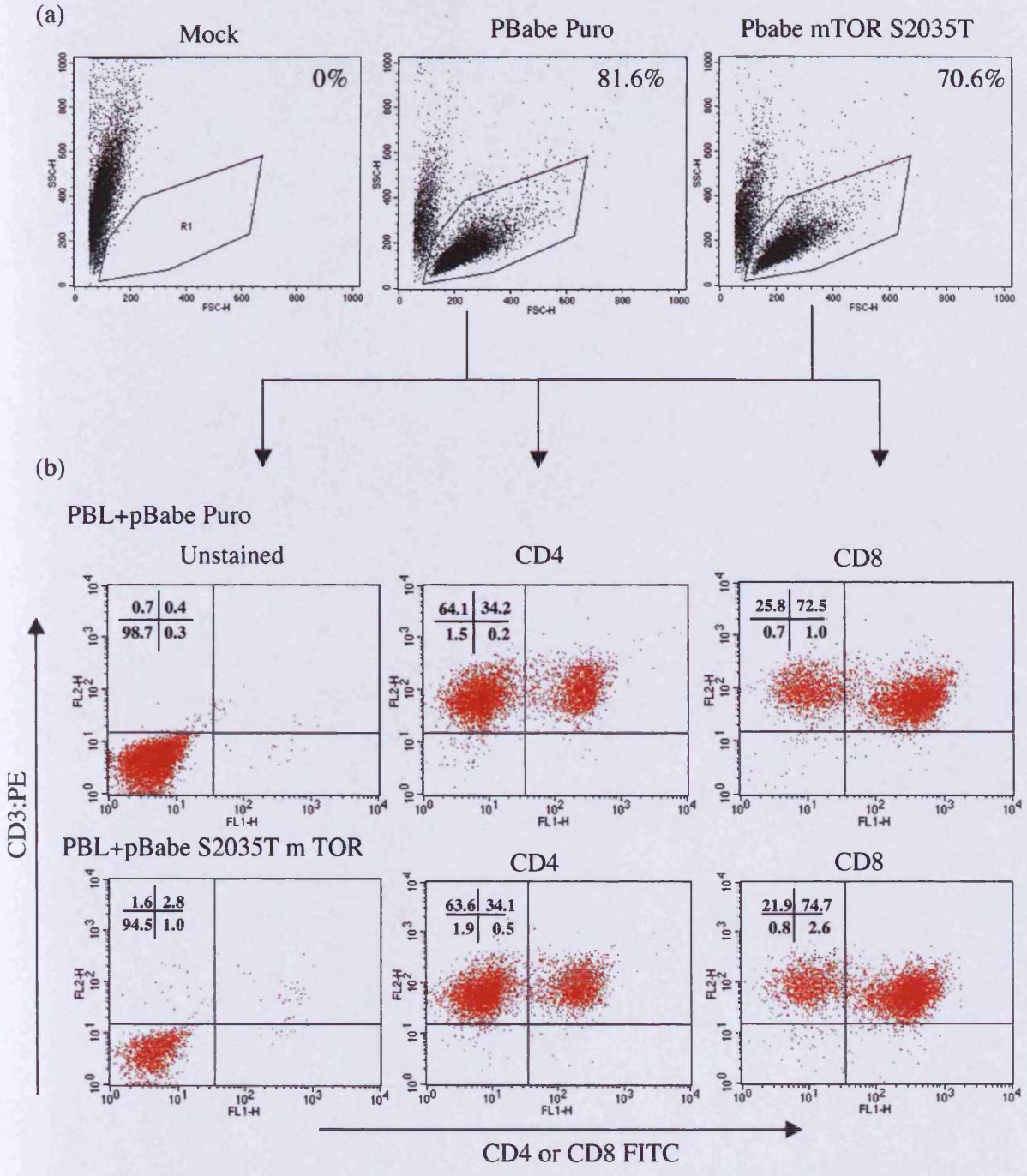

Figure 5.6 Genetic modification of PBLs with pBabe puro and pBabe mTOR S2035T and phenotypic analysis. PBLs were isolated from blood using a Ficoll gradient and stimulated with anti-CD3(2.5 ng/ml), anti-CD28 (5 μg/ml) and IL-2 (20 ng/ml) for three days. A 2-cycle infection was performed with RPMI, pBabe puro or pBabe mTOR S2035T. PBLs were re-stimulated on day 7 post-isolation and puromycin (1 μg/ml) was added. (a) shows mock infected, pBabe puro and pBabe mTOR S2035T infected PBLs 17 days post-isolation. The R1 gate determined the percentage of viable cells in the population. (b) These PBLs were immunofluorescent stained 17 days post-isolation with PE conjugated CD3 antibody and FITC conjugated CD4 and CD8 antibodies and analysed by flow cytometry. The percentages of anitbody positive and negative cells for each dot plot are illustrated in each quadrant.

5.5 Investigation of pBabe mTOR S2035T modified PBLs

We designed experiments to investigate whether the introduction of the mTOR S2035T gene generated rapamycin resistant PBLs. It took three to four weeks of cell culture post-isolation to obtain adequate PBL cell numbers to carry out CFSE cell proliferation experiments. Once adequate cell numbers were available, pBabe puro PBLs and pBabe mTOR S2035T PBLs were stained with CFSE, seeded at $1X10^6$/ml in 48-well plates and pre-treated with rapamycin at various concentrations for 30 minutes. Appropriate wells were then stimulated with anti-CD3 and IL-2. Fluorescence was monitored from 3 days after the day of CFSE labelling and cell stimulation, for up to two weeks. Figure 5.7 shows a schematic of the experimental procedure from isolation of the PBLs from whole blood through to setting up an experiment to determine rapamycin resistance. The proliferation experiment to investigate rapamycin resistance in PBLs was carried out three times using PBLs modified with pBabe puro and pBabe mTOR S2035T from three different infections.

The CFSE histograms in Figure 5.8 show the results of one of the experiments. The histograms show cells treated with anti-CD3/IL-2 only (black line) or pre-treated with rapamycin followed by treatment with anti-CD3/IL-2 (red line). In this particular experiment the modified cells were used 22 days post-isolation. If the cells were rapamycin resistant, the red line (rapamycin treated) would be similar in fluorescence to the black line (anti-CD3/IL-2 treatment). In this experiment no rapamycin resistance was demonstrated in the pBabe mTOR S2035T modified cells.

The graphs in Figure 5.9 show three experiments, separately, for both the pBabe mTOR S2035T PBLs and the corresponding pBabe puro PBLs. The flow cytometry histograms denote the CFSE fluorescence obtained seven days following CFSE labelling. The unstimulated samples died by day 5 of each experiment so could not be analysed. The corresponding bar graph shows the geometric mean fluorescence from the flow cytometry histograms. This allows visualisation of the effects of rapamycin in a quantitative fashion. Incorporated CFSE, and therefore the fluorescence detected, was maximal before the cells divided and decreased upon cell

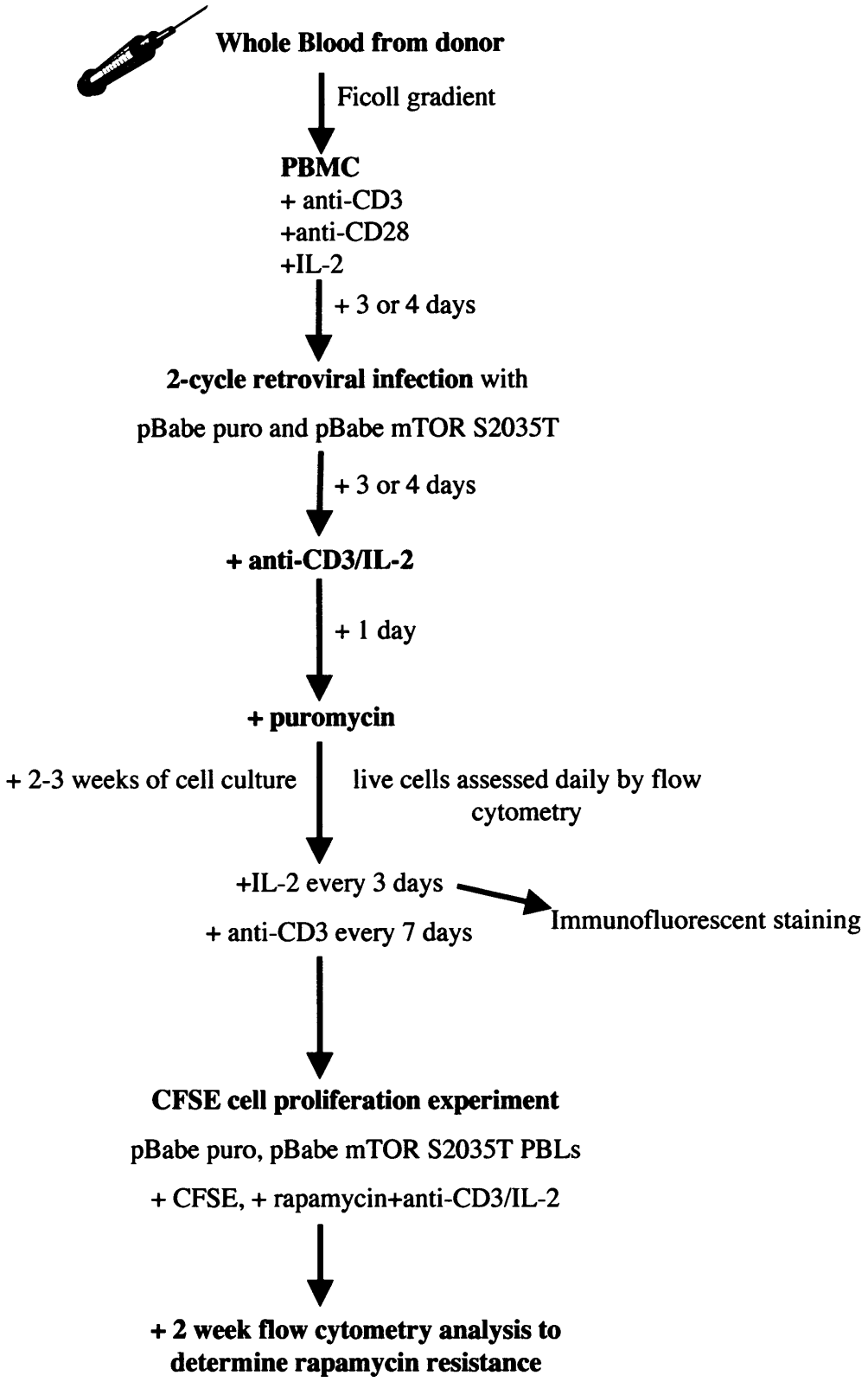

Figure 5.7 Schematic of the investigation of pBabe mTOR S2035T modified PBLs. This diagram illustrates the entire procedure from isolation of the PBLs from whole blood to the analysis of the modified PBLs following rapamycin treatment in a cell proliferation experiment.

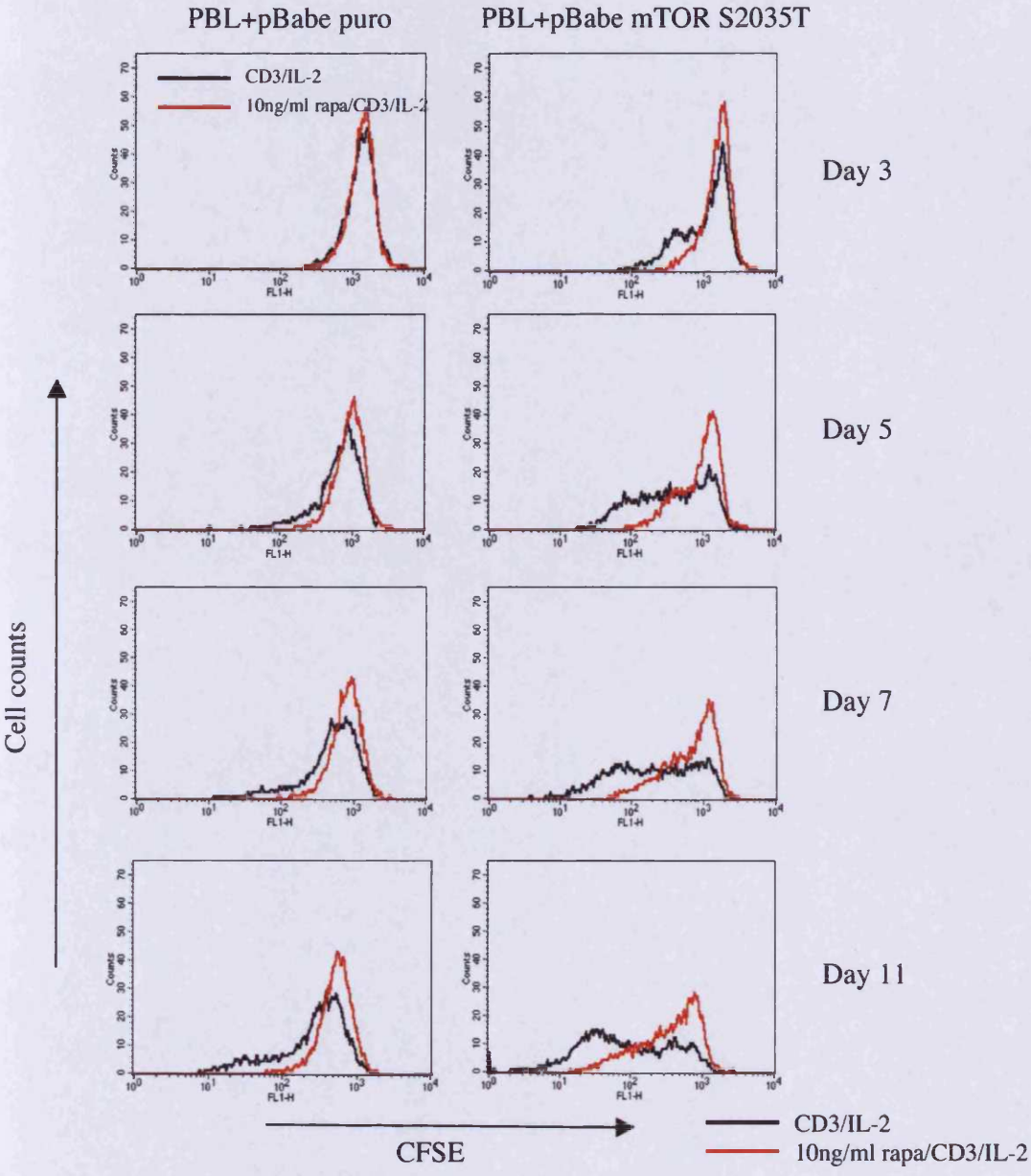

Figure 5.8 CFSE cell proliferation analysis of pBabe puro modified and pBabe mTOR S2035T modified PBLs. PBLs were isolated from blood using a Ficoll gradient and stimulated with anti-CD3(OKT3, 2.5 ng/ml), anti-CD28 (5 μg/ml) and IL-2 (20 ng/ml) for 3 days. A 2-cycle infection was performed with pBabe puro and pBabe mTOR S2035T. PBLs were re-stimulated on day 7 post-isolation and puromycin (1 μg/ml) was added the following day. PBLs were maintained in IL-2 and puromycin and restimulated with anti-CD3 weekly. pBabe puro and pBabe mTOR S2035T PBLs were then stained with CFSE. Samples were pretreated with rapamycin at various doses and stimulated with anti-CD3 (OKT3, 2.5 ng/ml) and IL-2 (20 ng/ml). Cell proliferation was monitiored over a two week period. A representative experiment is shown from three days after CFSE labelling to eleven days after CFSE labelling. The black line represents anti-CD3/IL-2 stimulated cells and the red line indicates rapamycin (10ng/ml) /IL-2 stimulated cells.

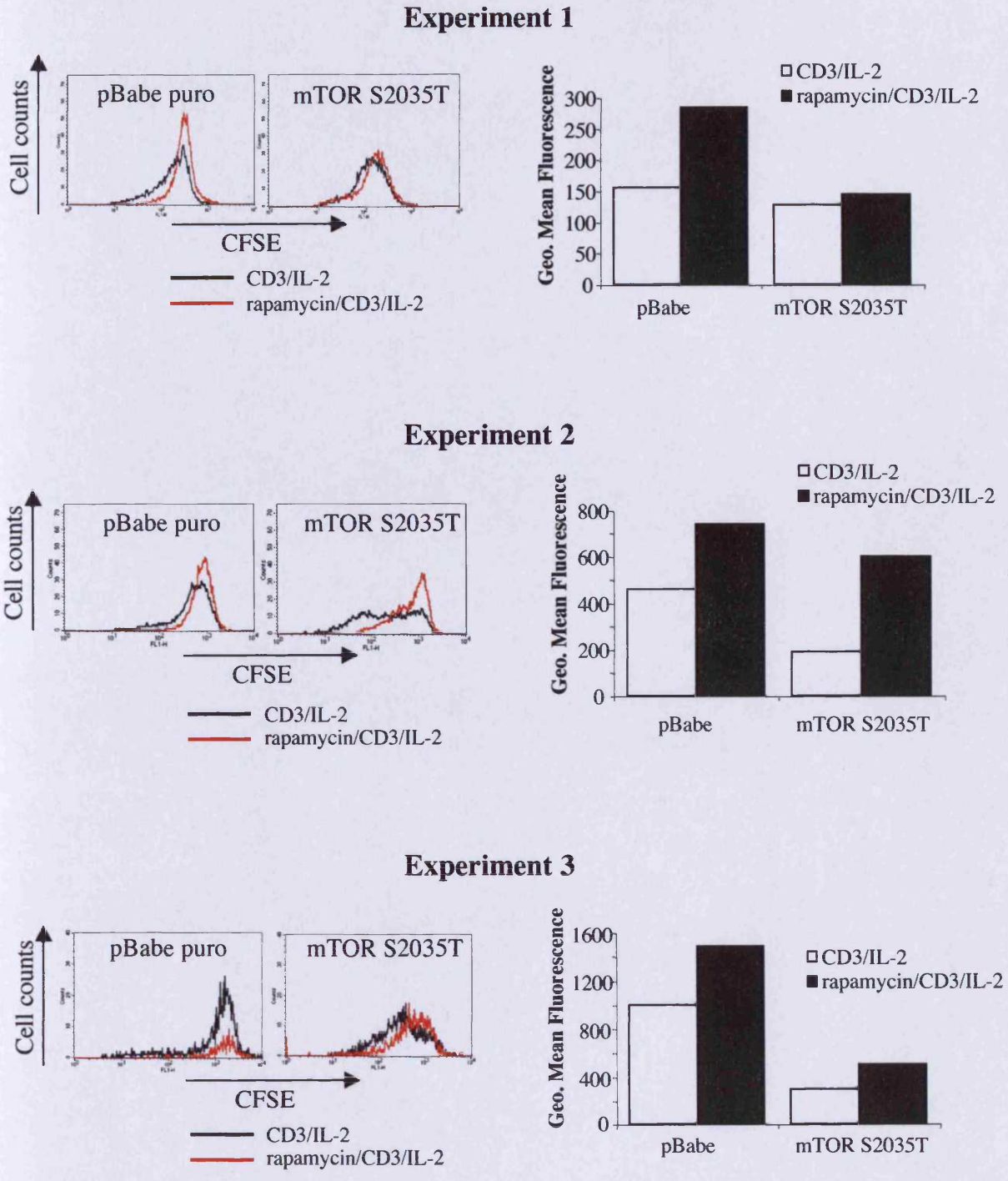

Figure 5.9 Investigation of pBabe puro and pBabe mTOR S2035T modified PBLs. This figure depicts the CFSE cell proliferation data from three separate PBL experiments. (a) shows Experiment 1 geometric mean fluorescence results seven days after CFSE labelling for pBabe mTOR S2035T PBLs and pBabe puro PBLs treated with either CD3/IL-2 only or 10 ng/ml rapamycin/CD3/IL-2, in histogram and bar graph format for. (b) shows the corresponding results for Experiment 2. (c) shows the corresponding results for Experiment 3.

division. The data show rapamycin resistance in Experiment 1. Rapamycin did not alter the geometric mean fluorescence of the cells modified with mTOR S2035T compared to the cells without rapamycin treatment, indicating that cell division was not affected following rapamycin treatment. The fluorescence of pBabe puro modified PBLs remained high following rapamycin treatment, indicating that less cell division occurred. Experiment 2, however, as also shown in Figure 5.9, did not show any rapamycin resistance with the fluorescence of rapamycin treated cells being higher than anti-CD3/IL-2 stimulated PBLs in both pBabe puro modified and pBabe mTOR S2035T modified PBLs. Experiment 3 shows a small degree of rapamycin resistance with a the difference in fluorescence in mTOR S2035T modified cells either treated with rapamycin or with anti-CD3/IL-2 only, being less than that observed in pBabe puro modified cells. Together this data shows that rapamycin resistant primary human T-cells can be generated. However, it does not occur in all cases, similar to our results in Kit225 cells.

Careful analysis of the data, generated from the three different experiments, showed that primary human T-cells infected with a pBabe mTOR S2035T virus had a growth advantage over PBLs infected with pBabe puro control virus. In all of the experiments performed, we observed a difference in the proliferation of the anti-CD3/IL-2 stimulated pBabe mTOR S2035T PBLs compared to the anti-CD3/IL-2 stimulated pBabe puro PBLs, over the course of each experiment. The bar graphs in Figure 5.9 show that the proliferation advantage demonstrated by the pBabe mTOR S2035T modified PBLs, was more dramatic in Experiment 2 and 3 than Experiment 1 (compare untreated white columns of pBabe mTOR S2035T to pBabe puro PBLs in each experiment of Figure 5.9). The line graph of Figure 5.10 depicts the geometric mean fluorescence of anti-CD3/IL-2 stimulated pBabe mTOR S2035T PBLs (red line) over seven days and compares results to the pBabe puro PBLs. The experiment shown in this graph is representative of the growth advantage shown by pBabe mTOR S2035T PBLs in three experiments. A paired student's T-test determined that for three experiments combined, the geometric mean fluorescence of the anti-CD3/IL-2 stimulated pBabe mTOR S2035T PBLs was significantly lower

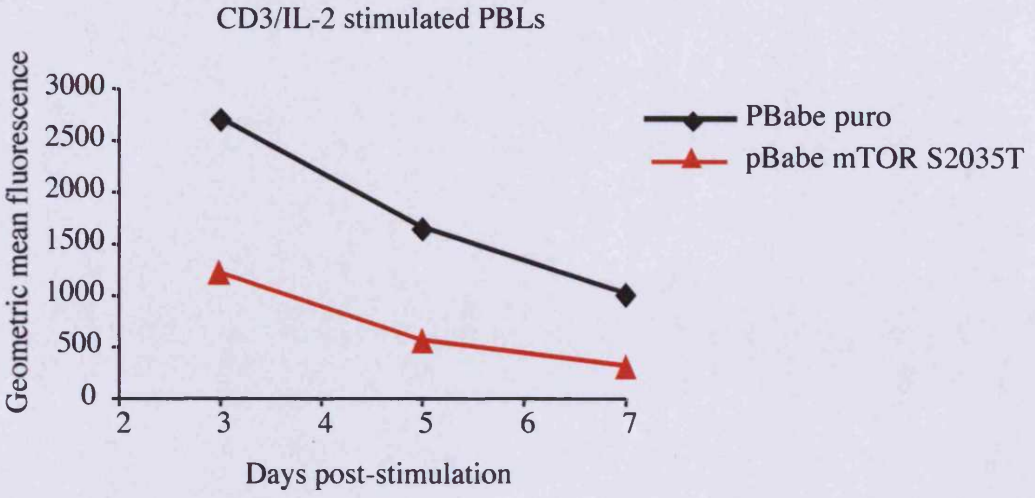

Figure 5.10 Investigation of pBabe puro modified and pBabe mTOR S2035T modified PBLs.

The graph shows the geometric mean fluorescence for anti-CD3/IL-2 stimulated pBabe mTOR S2035T modified PBLs over seven days (red line) and compares results to the pBabe puro modified PBLs (black line).

than the anti-CD3/IL-2 stimulated pBabe puro PBLs over the course of the seven days ($p<0.05$).

5.6 Modification of EBV-CTLs with rapamycin resistant mTOR

We next modified EBV-CTLs with the pBabe mTOR S2035T retrovirus. Genetic modification of EBV-CTLs first involves the generation of the EBV-CTL line as described in 4.4. Once the CTLs were established, we followed the strategy devised in the previous chapter for the modification of EBV-CTL with a drug selection virus. This involved the re-stimulation of the CTL line on day 7, as per the protocol, the addition of IL-2 on day 9 and the infection of the EBV-CTLs on day 10 with the pBabe mTOR S2035T virus and the pBabe puro virus for comparison. The EBV-CTL line was re-stimulated on day 13 or 14 and puromycin (1 μg/ml) selection was subsequently added the following day (4-5 days post-infection). The cells were monitored daily by flow cytometry to assess the percentage of viable cells in the population.

Figure 5.11 (a) shows an EBV-CTL line on day 24 of the CTL line. This line has been under selection for ten days and was generated from Donor 1 as described in 4.4. After ten days under selection, there were 28.9% live cells in the pBabe puro culture, and 10% live cells in the pBabe mTOR S2035T culture. On average there were 10.8% ±12% live cells in the pBabe mTOR S2035T CTL cultures after ten days under selection. We successfully grew out puromycin resistant pBabe mTOR S2035T EBV-CTL lines in parallel with pBabe puro modified EBV-CTL lines. The lines shown in Figure 5.11 (a) were maintained for 41 days. We used PE conjugated CD3 antibody, FITC conjugated CD8 antibody or CD4 antibody to phenotypically characterise the pBabe mTOR S2035T modified line. Samples were analysed by flow cytometry. Results were compared to the pBabe puro modified lines. Figure 5.11 (b) shows the flow cytometry data on day 27 of the CTL line. In the pBabe mTOR S2035T modified line, 77.3% of the cells were $CD8^+$ and 3.8% of the total culture was $CD4^+$. In the pBabe puro modified line, 81.9% of the cells were $CD8^+$ and 3.3% of the total culture was $CD4^+$. These results demonstrate that we have

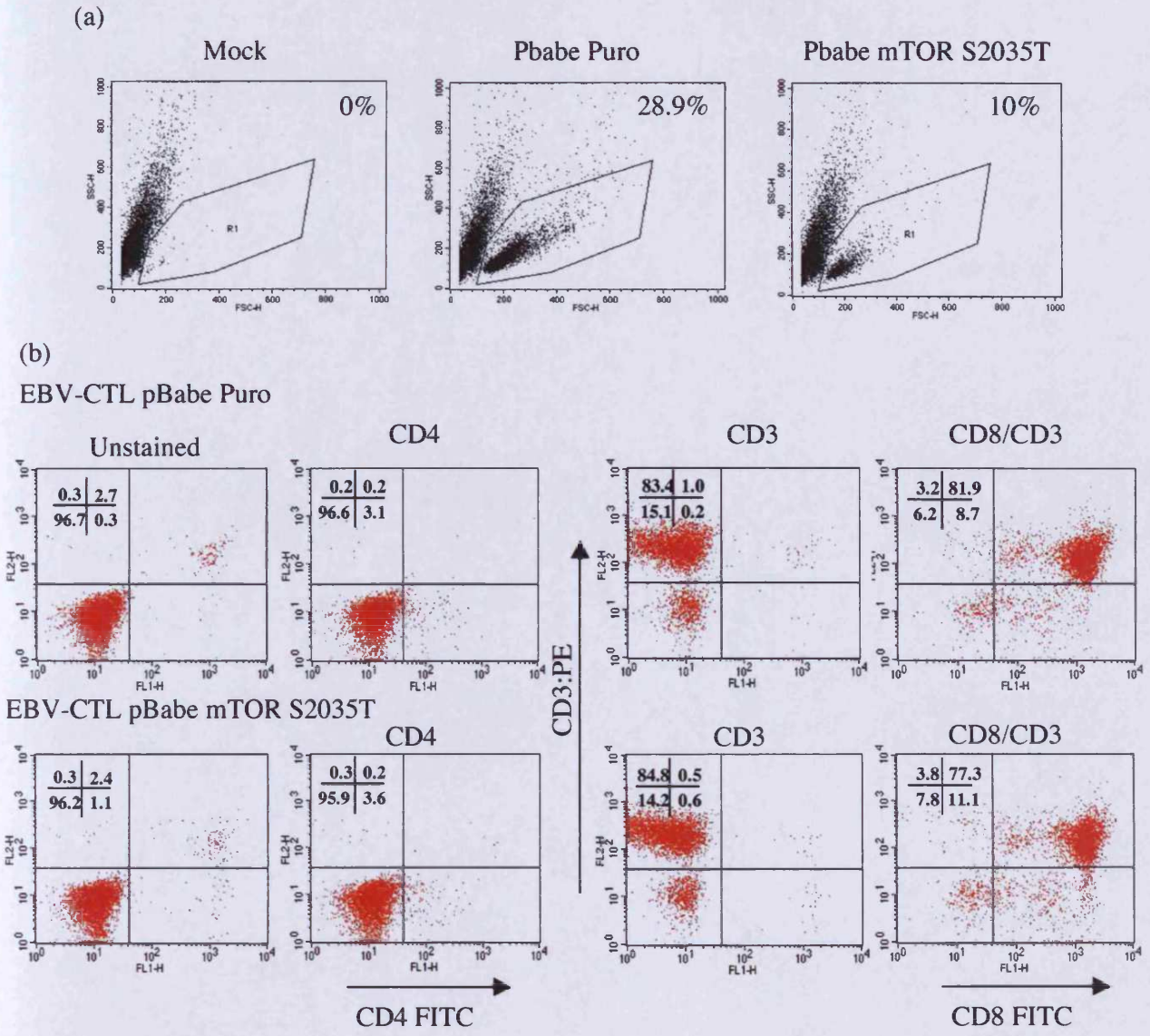

Figure 5.11 Genetic modification of EBV-CTLs with pBabe puro and pBabe mTOR S2035T and phenotypical analysis. PBLs were isolated from the blood of a healthy volunteer and stimulated with irradiated autologous EBV-LCL and IL-2 at discrete timepoints to generate an EBV-CTL line. A 2-cycle retroviral infection was carried out 10 days post-isolation with RPMI, pBabe puro and pBabe mTOR S2035T viruses. CTLs were restimulated with irradiated autologous LCL on day 14 and puromycin (1 μg/ml) added on day 15 post-isolation. Cells were maintained in puromycin and IL-2 and re-stimulated weekly with LCLs. (a) represents mock infected, pBabe puro and pBabe mTOR S2035T infected CTLs 24 days post-isolation. The R1 gate determined the percentage of viable cells in the population. (b) shows EBV-CTLs which were immunofluorescent stained 27 days post-isolation with PE conjugated CD3 antibody , and or FITC conjugated CD8 or CD4 antibody and analysed by flow cytometry. The percentages of antibody positive and negative cells are illustrated for each dot plot.

(a) EBV-CTLs + pBabe mTOR S2035T

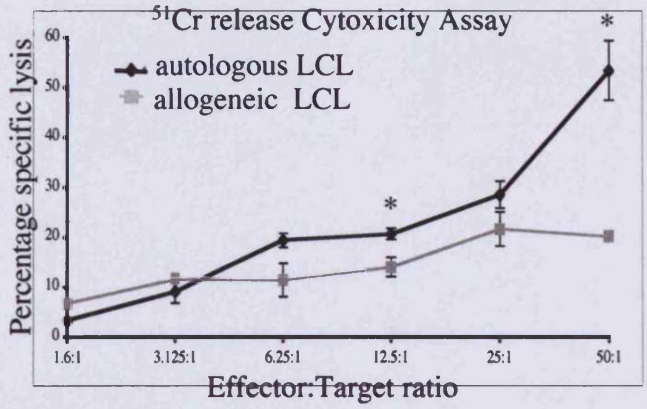

(b) EBV-CTLs + pBabe puro

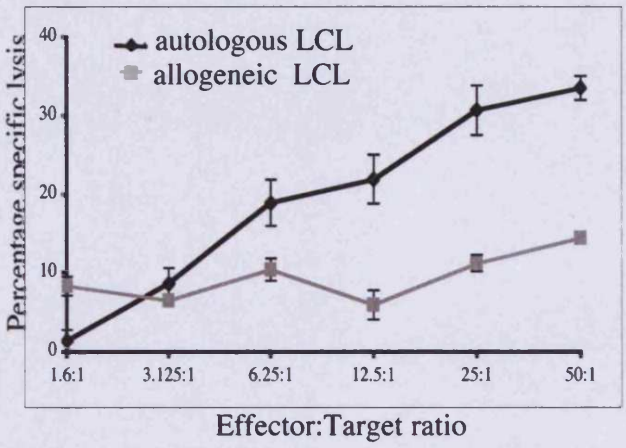

(c) Unmodified EBV-CTLs

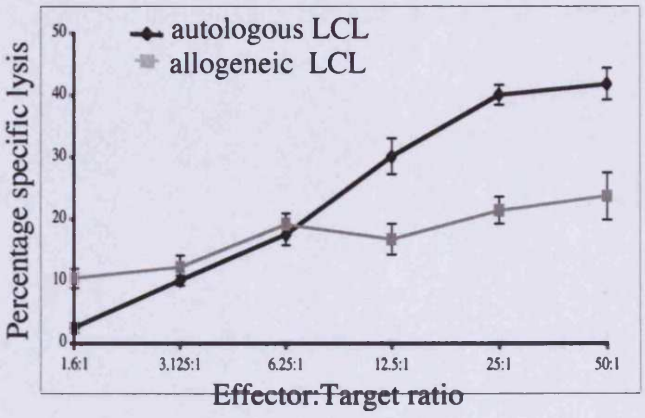

Figure 5.12 Assessment of EBV-specificity in pBabe puro and pBabe mTOR S2035T modified CTLs (Figure legend opposite)

1X10 ^{6}/ml in 48-well plates and pretreated with rapamycin at various concentrations for 30 minutes. Appropriate wells were then stimulated with irradiated autologous LCL and IL-2. Fluorescence was monitored from three days after CFSE labelling and LCL/IL2 stimulation, for a two-week period, to assess cell proliferation. The schematic of Figure 5.13 illustrates the entire experimental procedure from the isolation of PBLs and generation of EBV-CTLs from a donor's blood, through to the investigation of rapamycin resistance in the pBabe mTOR S2035T modified CTLs. The proliferation experiment to investigate rapamycin resistance in CTLs was carried out three times using CTLs modified with pBabe puro and pBabe mTOR S2035T.

Figure 5.14 depicts the results for three experiments separately. The flow cytometry histograms denote the CFSE fluorescence obtained three days following CFSE labelling. These histograms show cells treated with LCL/IL-2 only (black line) or pre-treated with rapamycin followed by treatment with LCL/IL-2 (red line). If the cells were rapamycin resistant, the red line (rapamycin treated) would be similar in fluorescence to the black line (anti-CD3/IL-2 treatment). The corresponding bar graphs show the geometric mean fluorescence from the flow cytometry histograms. Again, this allows visualisation of the effects of rapamycin in a quantitative fashion. As for the PBL analysis, incorporated CFSE, and therefore the fluorescence detected, was maximal before the cells divided and decreased upon cell division. The data showed no rapamycin resistance, with the fluorescence of rapamycin treated cells being higher than LCL/IL-2 stimulated CTLs in both pBabe puro modified and pBabe mTOR S2035T modified CTLs, in the three experiments. This data shows that the modification of EBV-CTLs with a pBabe mTOR S2035T virus did not generate rapamycin resistant CTLs.

Careful analysis of the data, generated from the three different experiments, showed that LCL/IL-2 stimulated pBabe mTOR S2035T CTLs showed a growth advantage over pBabe puro CTLs. This growth advantage of pBabe mTOR S2035T CTLs over pBabe puro CTLs was evident three days after CFSE labelling in all three experiments, with differences becoming smaller at later timepoints in one experiment

and lost completely in two further experiments. This growth advantage for three experiments is also shown in Figure 5.14 (compare untreated white columns of pBabe mTOR S2035T to pBabe puro CTLs in each experiment). A paired student T-test, examining the geometric mean fluorescence three days after CFSE labelling over three experiments, indicated that the difference between LCL/IL-2 stimulated pBabe mTOR S2035T CTLs was significantly lower than that of pBabe puro CTLs ($p<0.01$) on this timepoint.

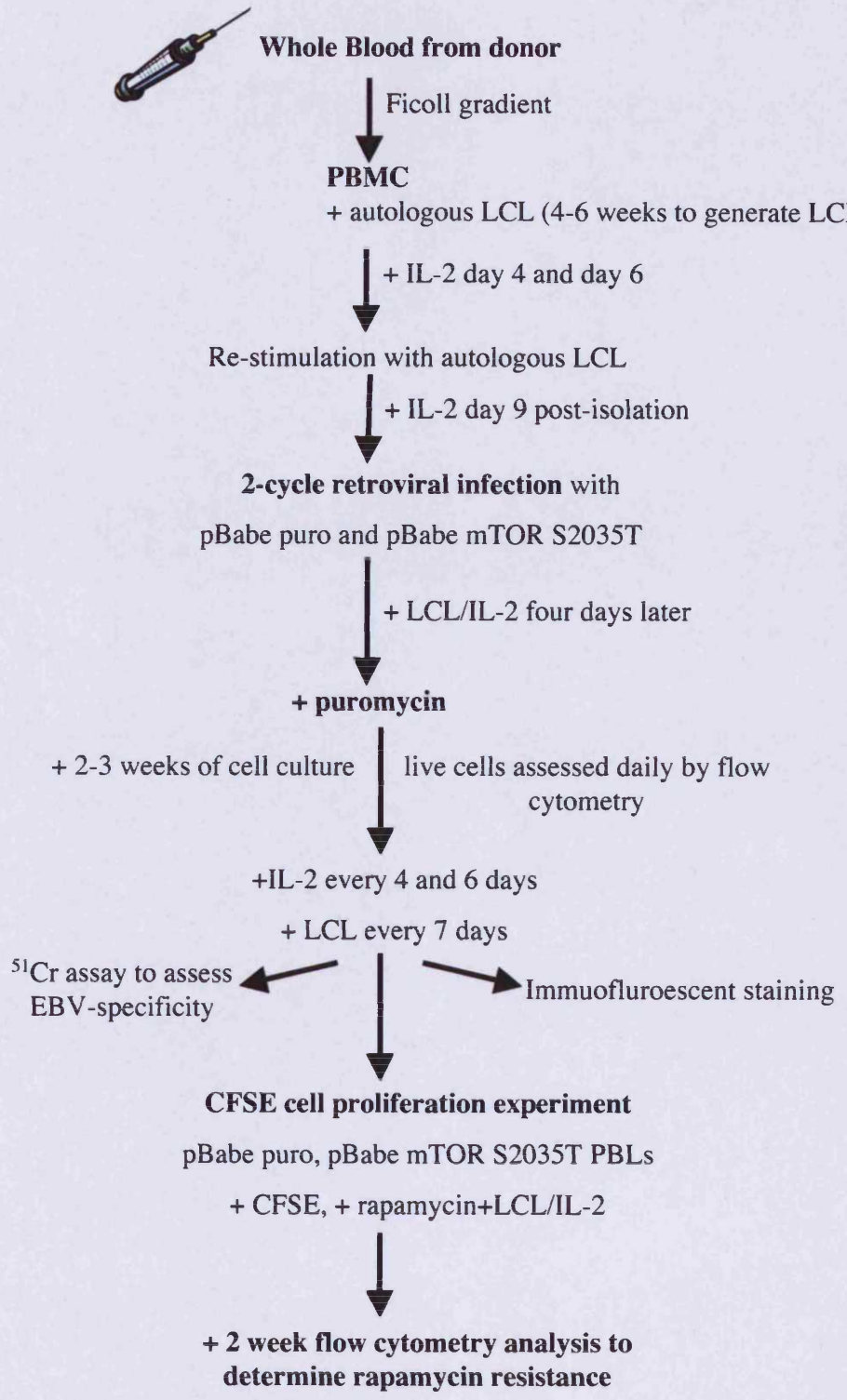

Figure 5.13 Schematic of the investigation of pBabe mTOR S2035T modified CTLs. This diagram illustrates the entire procedure from isolation of the PBLs from whole blood and the generation of the EBV-CTL line, to the analysis of the modified CTLs following rapamycin treatment in a cell proliferation experiment.

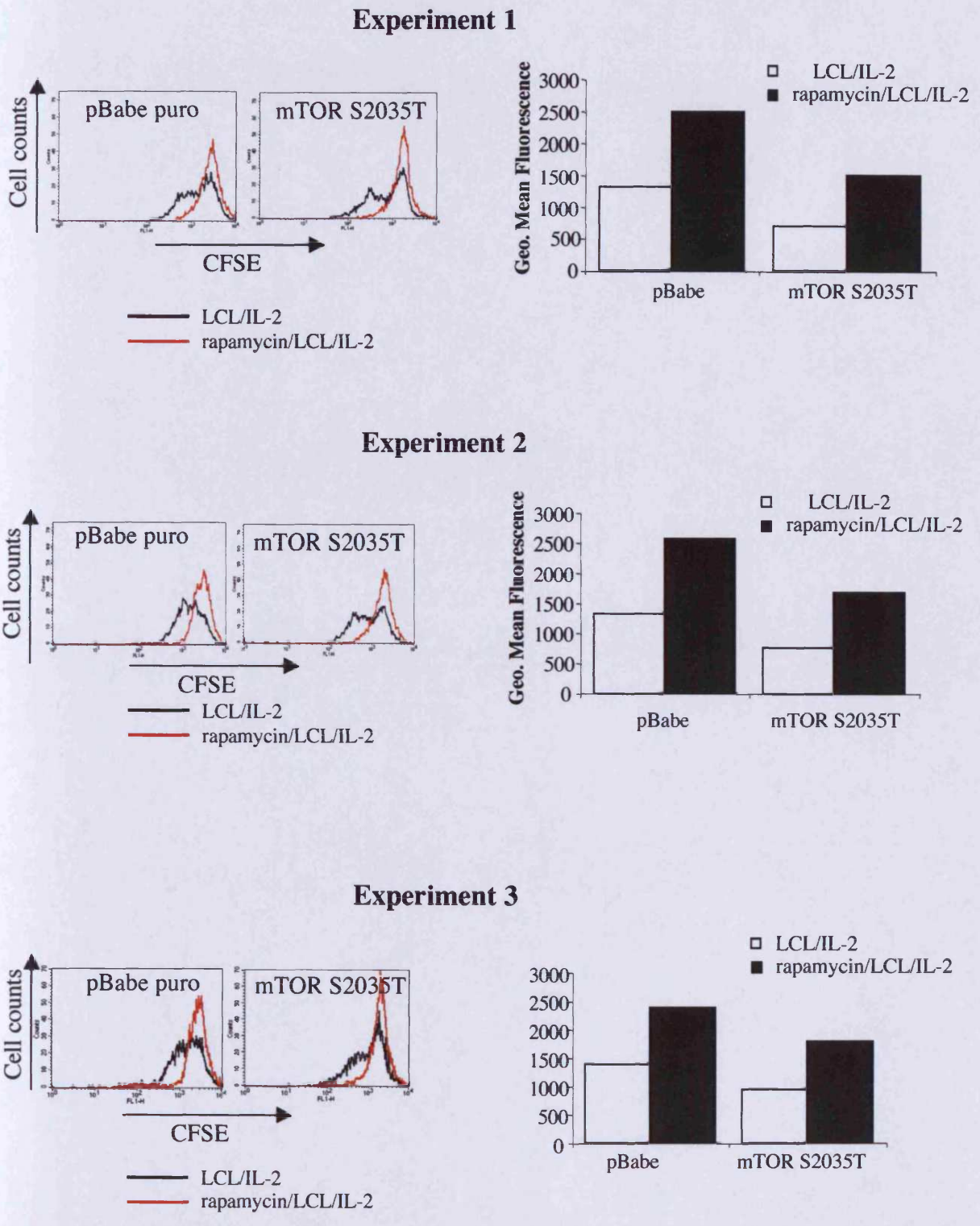

Figure 5.14 Investigation of pBabe puro and pBabe mTOR S2035T modified CD8⁺ T-cell proliferation. This figure depicts the CFSE cell proliferation data from three separate experiments. (a) shows Experiment 1 geometric mean fluroescence results of pBabe S2035T mTOR CTLs and pBabe puro CTLs treated with either LCL/IL-2 only or 10ng/ml rapamycin/LCL/IL-2, in histogram and bar graph format, three days after CFSE labelling. (b) shows the corresponding results for Experiment 2 and (c) shows the corresponding results for Experiment 3.

5.8 Discussion

In this study we demonstrated rapamycin resistance in Kit225 cells and primary human T-cells, modified with a pBabe mTOR S2035T virus. The S2035 residue is critical for FKBP12/rapamycin binding (Chen *et al.*, 1995; Dumont *et al.*, 1995) and corresponds to the S1972 and S1975 residues of the yeast proteins TOR1 and TOR2 respectively. In yeast, mutations in this residue confer virtually complete sporulation resistance to low concentrations of rapamycin (Zheng and Schreiber, 1997). Biochemical studies have demonstrated that a mutation of the corresponding residue S2035 in mTOR also abolishes binding of rapamycin/FKBP12 (Chen *et al.*, 1995). In a study to investigate the molecular mechanism of rapamycin inhibition, Dumont *et al.* examined mTOR mutations in a YAC-1 T-cell lymphoma line. They carried out mutagenesis experiments and generated YAC-1 rapamycin resistant mutants by culturing the YAC-1 cells with an alkylating agent. Tritiated thymidine incorporation cell proliferation studies of the T-cells showed that the rapamycin resistance was consistent with a mutation downstream from the rapamycin/FKBP12 complex, in the serine 2035 residue of the FRB domain of mTOR (Chen *et al.*, 1995; Dumont *et al.*, 1995). While Dumont *et al.* successfully demonstrated that mutations in the FRB domain confer rapamycin resistant in a T-cell line, rapamycin resistance in primary human T-cells through the expression of a S2035 mTOR protein, has not been reported to date. The strength of our study lies in the fact that it involves the modification of primary human T-cells with a pBabe mTOR S2035T virus and the data show that this virus can confer rapamycin resistance in primary T-cells but that it does not occur in every infection.

Rapamycin resistance in pBabe mTOR S2035T modified T-cells was clearly demonstrated in two out of the four sets of modified Kit255 lines (Figure 5.3 and Figure 5.5) and one of the three pBabe S2035T modified PBL cultures (Experiment 1, Figure 5.9). A slight degree of rapamycin resistance was shown in one further pBabe mTOR S2035T modified PBL culture (Experiment 3, Figure 5.9). A possible explanation for this 50% success rate is that the integration site of the retrovirus in the T-cell genome may vary for each infection. There is a possibility that should the

virus integrate in a different region of the host genome, the phenotype conferred on the cells would differ. This could be due to transgene silencing. The insertion of retroviral DNA can trigger transcriptional silencing of the inserted sequences via mechanisms that involve methylation of DNA within regulatory regions (Wolffe and Matzke, 1999). Transcriptional silencing of the mTOR transgene may have occurred in pBabe mTOR S2035T modified T-cells displaying no rapamycin resistance. However, the puromycin resistance was maintained in these cells, which shows that the puromycin resistant gene is still being expressed. This can be explained by the fact that the gene of interest (mTOR in our case) in the pBabe plasmid, is under the control of the upstream 5' LTR promoter, while expression of the puromycin resistant gene, is driven by the SV40 promoter (See Appendix II) (Morgenstern and Land, 1990). Studies have shown that transcriptional silencing is generally directed against 5'LTR promoter of the retrovirus (Wei *et al.*, 1999). Advances in retroviral vector design have aimed to overcome such transgene silencing problems, and have led to the development of novel families of vectors containing an engineered LTR, facilitating increased expression and decreased DNA methylation (Challita *et al.*, 1995).

Modification of EBV-CTLs with pBabe mTOR S2035T virus did not generate rapamycin resistant CTLs (Figure 5.14). While the PBL data indicated that the modification of T-cells with pBabe mTOR S2035T virus did not generate rapamycin resistant cells every time, the data did clearly show rapamycin resistance in PBLs in one experiment and a smaller degree of resistance in another (Figure 5.9). The CTLs used in our study are a polyclonal CTL line, enriched for EBV specific $CD8^+$ T-cells whereas the PBL cultures are a mixture of both $CD4^+$ and $CD8^+$ T-cells. Modifying an established CTL line, to express an exogenous transgene may be different to the modification of PBLs. It has been suggested that a retrovirally modified cell recognises structural features diagnostic of retroviral integration and that this recognition promotes DNA methylation of adjacent sequences (Bestor and Tycko, 1996). It is possible that the CTLs respond differently to transduction with an exogenous transgene than PBLs and a variation in the recognition of viral integration may lead to different effects on transgene expression in CTLs compared to PBLs.

Strategies such as altering the 5'LTR promoter in the viral vector may overcome these problems. With regard to the pBabe mTOR S2035T modified CTLs, another important point to highlight is the fact that the statistical analysis of Figure 5.12(a) suggested that the modification of EBV-CTLs with mTOR S2035T may alter CTL function and/or HLA-restricted specificity. Further studies may clarify these suggestions and determine if such a possible effect on CTL function/specificity is specific to the mTOR S2035T gene or as a consequence of transducing the CTL genome with such a large gene (7kb).

Our results showed that modification of human T-cells with pBabe mTOR S2035T virus conferred a proliferative advantage on both PBLs and CTLs. The Kit225 anti-mTOR immunoblotting, did not show any increased expression in mTOR modified lines compared to pBabe puro lines or parent Kit225 lines, indicating that modification of human T-cells with an mTOR expressing virus does not lead to overexpression of the protein. Changes in the conserved serine residue 2035 could lead to conformational changes in the mTOR protein, altering its role in the cell. In addition, mutation of conserved serine residues may lead to a gain in function for the kinase domain of the protein. Although serine 2035 is a critical residue in the rapamycin-binding domain not the kinase domain of mTOR, it is located next to the kinase domain of the protein. Zheng *et al.* postulate that in yeast cells, analogous sequences to S1972 and its flanking sequences are found in the regulatory domains of serine/threonine kinases such as PKC (Zheng *et al.*, 1995). The important role of mTOR as a central mediator of nutrient, mitogen and energy signals in T-cells (Hay and Sonenberg, 2004) means that a gain in kinase function may increase the effectiveness of the T-cell *in vitro*. The proliferative advantage conferred by the pBabe mTOR S2035T virus in both PBLs and EBV-CTLs, observed in our experiments, may also increase the proliferative capacity of the T-cells *in vivo*.

In summary, our data suggest that infection of T-cells with pBabe mTOR S2035T is a possible strategy to increase the proliferative capacity of T-cells in an immunosuppressive environment. The cytotoxicity data raised some interesting

questions. The data indicated that the function of the pBabe mTOR S2035T modified CTL line was impaired. Future cytotoxicity studies, involving the examination of the CTL function in the presence of rapamycin may clarify whether or not this strategy will lead to more effective CTL function in addition to the observed increase in proliferative capacity in an immunosuppressive environment.

CHAPTER 6

Generation of Cyclosporin A resistant Human T-cells

6.1 Introduction

The immunosuppressive drug cyclosporin A (CsA), blocks the rejection of transplanted organs by inhibiting signalling pathways required for T-cell activation (Liu *et al.*, 1991) and has revolutionised the world of transplant medicine. However, CsA has been shown to limit the proliferation and efficacy of CTLs (Kiziroglu and Miller, 1990; Weiss et al., 1986) and the drug can potentially limit the function and longevity of adoptively transferred CTLs in an immunosuppressive environment. The modification of T-cells with a CsA resistant transgene may increase the efficacy and longevity of human T-cells. Our objective in this chapter was to extend the rapamycin resistance studies of Chapter 5 to the immuosuppressive drug, CsA, and modify human T-cells with a retrovirus containing a transgene to confer CsA resistance on the T-cell.

CsA exerts its immunosuppressive effects by inhibiting calcineurin (Liu *et al.*, 1991), a protein phosphatase that has been shown to be a major player in T-cell activation through the regulation of NFAT, a transcription factor required for the expression of T-cell cytokine genes (Liu *et al.*, 1991). The catalytic subunit, CNA comprises four regions, a catalytic domain, a CNB binding segment, a calmodulin-binding segment, and a C-terminal autoinhibitory helix (Martinez-Martinez and Redondo, 2004). Figure 6.1 (a) illustrates a simplified schematic of the domain structure of both CNA and CNB and Figure 6.1 (b) illustrates the activation of the calcineurin complex. Catalytic activity is inhibited by a complex of CsA bound to its immunophilin cyclophilin A, and CNB is required for this interaction. The cyclophilin/CsA complex contacts both chains of calcineurin in two distinct patches: the primary interface and the secondary interface, blocking substrate access to the catalytic site (Figure 6.1 (b)).

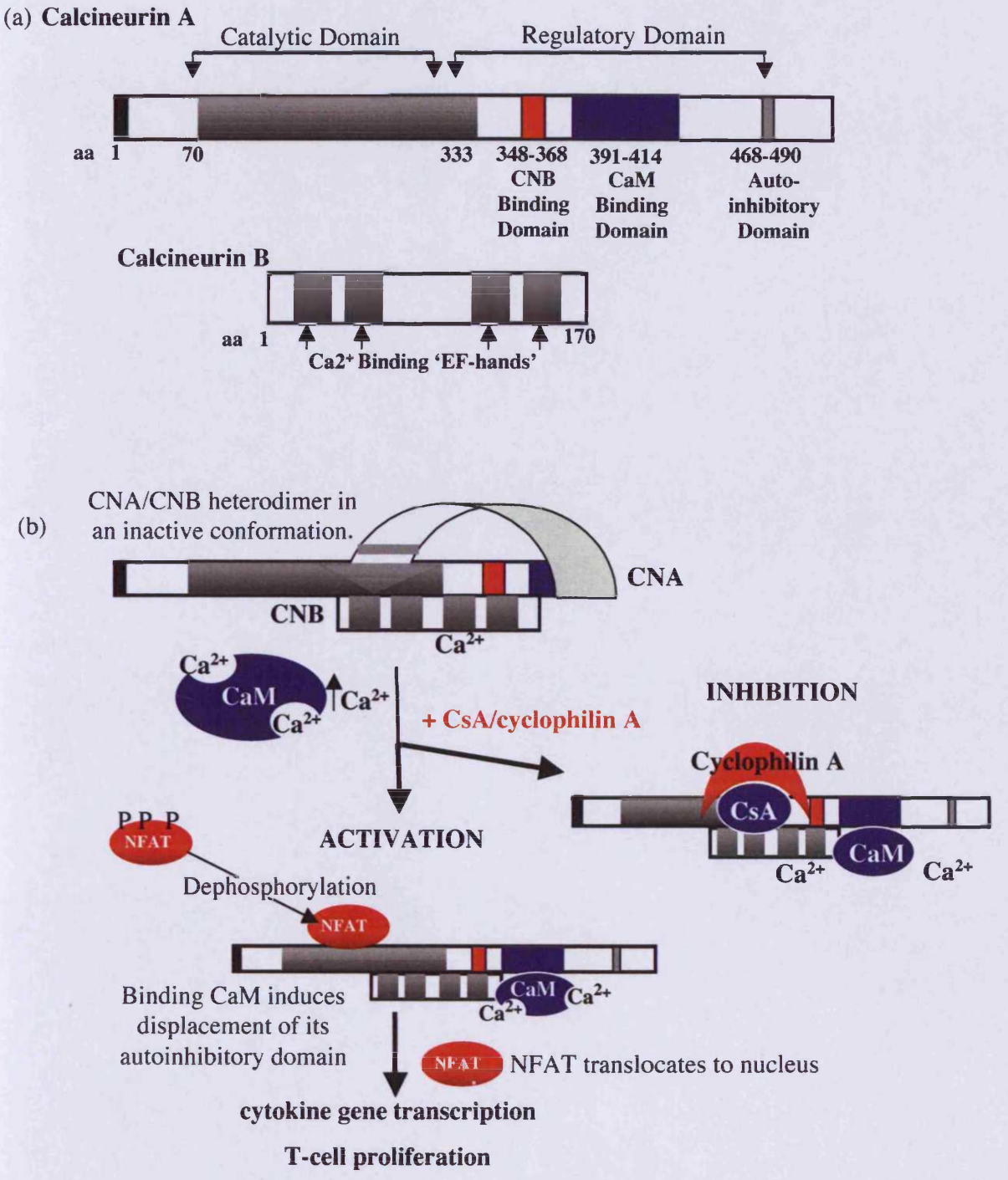

Figure 6.1 The Calcineurin complex structure and function

(a) Functional domain organisation of CNA and CNB subunits. (b) In an unstimulated cell, calcineurin forms a CNA/CNB inactive heterodimer, A stimulation such as antigen recognition by the TCR, causes an increase in intacellular Ca^{2+}, which activates calmodulin (CaM) and CNB to bind to Ca^{2+}. Activated CaM binding to calcineurin leads to a conformational change which allows the autoinhibitory domain of CNA to move away from the catalytic active site, opening access for NFAT to bind and become dephosphorylated. NFAT translocates to the nucleus and cytokine gene transcription and cell proliferation are initiated. In the presence of CsA/cyclophilin, access to the catalytic site is blocked, inhibiting the dephosphorylation of NFAT (adapted from Martinez-Martinez *et al*, 2004).

Zhu *et al.* have investigated two mutations in CNA, one in the primary interface (Y341F) and the other in the secondary interface (V314R), which confer resistance to CsA by blocking binding by the cyclophilinA/CsA complexes (Zhu *et al.*, 1996). Their studies demonstrated that these mutations render the T-cell receptor signal transduction cascade, CsA resistant in human Jurkat T-cells (Zhu *et al.*, 1996). Jurkat T-cells were co-transfected with a plasmid expressing the mutant CNA V314R gene, and an NFAT reporter plasmid bearing multiple NFAT response elements upstream of an SEAP reporter gene. The data showed that the transfection of Jurkat T-cells with the mutant CNA V314R gene rendered T-cell signalling virtually resistant to CsA inhibition, increasing the IC50 for CsA action 250-fold. Their findings demonstrated that this mutation, which had previously proved effective in rendering yeast cells resistant to CsA (Cardenas *et al.*, 1995) was also functional in a human T-cell line, and suggest a means to render cells resistant to CsA.

The expression of a V314R mutant CNA protein, to confer CsA resistance, has yet to be demonstrated in primary human T-cells. The aim of this chapter was to retrovirally modify primary human T-cells with a pBabe puro plasmid containing a CNA transgene, with a valine to arginine point mutation at residue 314 of the CNA subunit (pBabe CNA V314R), which abolishes the binding of the CsA/cyclophilin complex. A pBabe puro virus was also used in our experiments, and results compared to those from the pBabe CNA V314R modified PBLs. The overall objective was to modify primary human T-cells with this CNA V314R transgene and investigate a phenotype *in vitro*.

6.2 Genetic modification of a Primary Human T-cells with a pBabe CNA V314R retrovirus

To generate the CsA resistant retrovirus, a CNA mutant gene containing a valine to arginine substitution at residue 314 of the gene (V314R), was cloned into a pBabe puro empty vector. Successful generation of the pBabe CNA V314R constructs was confirmed by sequencing (Appendix II) and restriction digestion

analysis. Following this, we adopted the stable Ψ-crip packaging system to produce functional pBabe CNA V314R viruses for infection. pBabe puro control virus supernatant was also used in the infections. Once the pBabe CNA V314R viral supernatant was obtained we modified PBLs in a 2-cycle retroviral infection. Primary human T-cells isolated from whole blood using a Ficoll gradient, were stimulated with anti-CD3 (OKT3, 2.5 ng/ml), anti-CD28 (5 μg/ml) and IL-2 (20 ng/ml). After three to four days stimulation, PBLs were infected with either pBabe puro control virus or pBabe CNA V314R virus. The PBLs were re-stimulated three to four days after infection with anti-CD3/IL-2, and puromycin (1 μg/ml) was added the following day. The percentage of live cells in the culture was monitored daily by flow cytometry. The PBLs were maintained in puromycin with the addition of IL-2 every three days and re-stimulation with anti-CD3 weekly.

Figure 6.2 (a) shows pBabe puro and pBabe CNA V314R modified PBLs 17 days post-isolation. The mock cells are all dead, there are 78.7% live cells in the pBabe puro culture and there were 70.9% live cells in the pBabe CNA V314R PBLs culture. On average there were 66%±8% of live cells in the pBabe CNA V314R PBLs cultures 17 days following isolation. pBabe CNA V314R modified cells were immunofluorescent stained with PE conjugated CD3 antibody and FITC conjugated CD4 and CD8 antibody, and analysed by flow cytometry to phenotypically characterise the modified cells. Figure 6.2 (b) shows the results of immunofluorescent staining of pBabe CNA V314R PBLs 17 days post-isolation. The pBabe puro modified PBLs were also immunofluorescent stained for comparison. Of the pBabe CNA V314R PBLs, 31.3% of the cells were $CD4^+$ and 75.7% of the cells were $CD8^+$. In the pBabe puro modified PBLs 34.2% of the cells were $CD4^+$ and 72.5% of the cells were $CD8^+$. Live cells were observed in cultures for six weeks post isolation. These results showed that we can successfully modify PBLs with a pBabe CNA V314R virus and maintain these PBLs in puromycin long term.

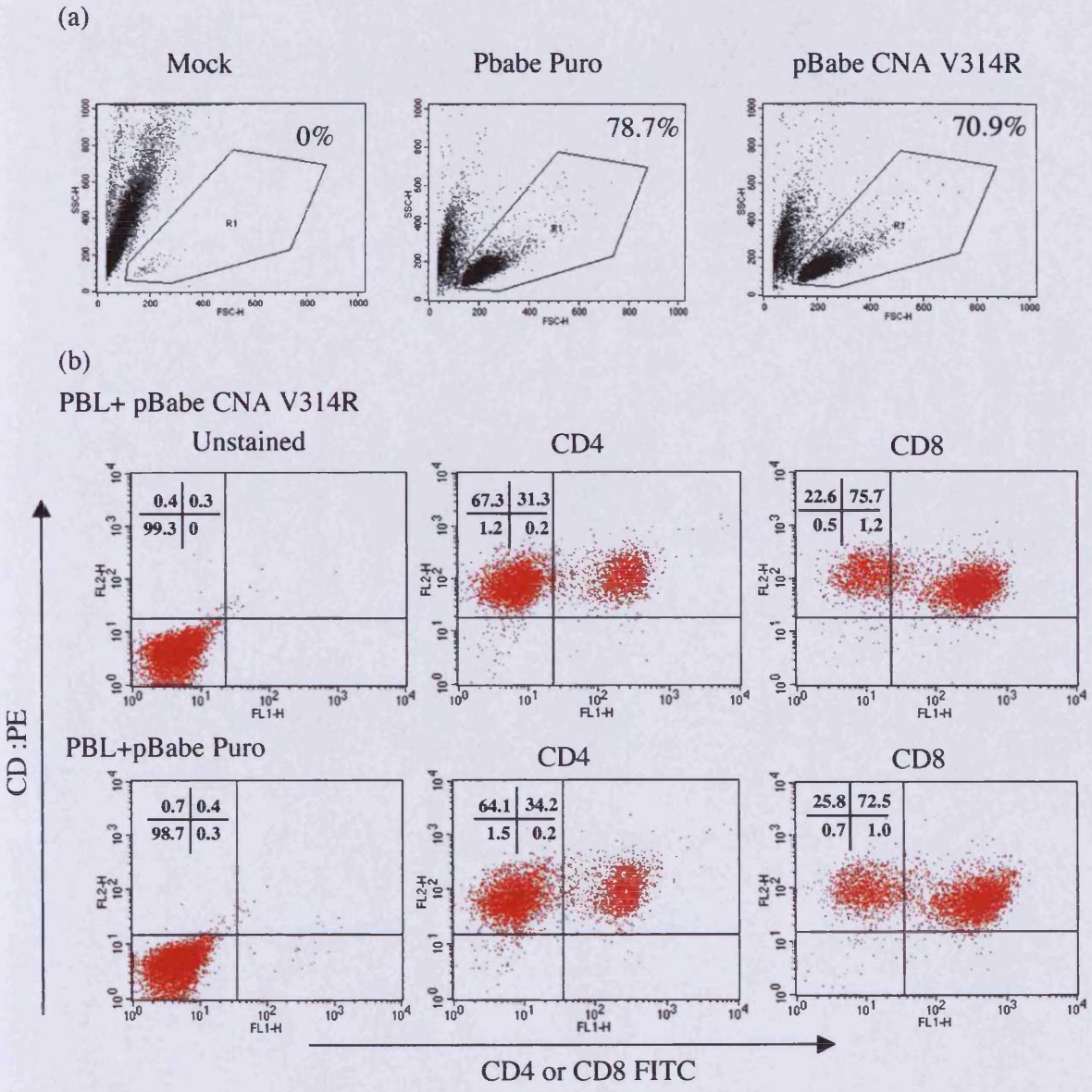

Figure 6.2 Genetic modification of PBLs with pBabe puro and pBabe CNA V314R

PBLs were isolated from whole blood using a Ficoll gradient, and stimulated with anti-CD3 (OKT3, 2.5 ng/ml), anti-CD28 (5 μg/ml) and IL-2 (20 ng/ml) for three days. A 2-cycle retroviral infection was performed with pBabe CNA V314R and pBabe puro. PBLs were restimulated four days later with anti-CD3/IL-2 and puromycin (1 μg/ml) was added the following day. Live cells were assessed by flow cytometry. (a) shows the forward and side scatter dot plots of mock infected, pBabe puro and pBabe CNA V314R modified PBLs 17 days post-isolation. The percentage of cells in the live gate (R1) is shown. (b) Modified PBLs were immunofluorescent stained with PE conjugated CD3 antibody and FITC conjugated CD4 and CD8 antibodies, 17 days post-isolation. The percentage of cells positive for PE and FITC are indicated in the quadrants.

6.3 Investigation of cytokine production from retrovirally modified PBLs

To assess the pBabe CNA V314R modified PBLs, we monitored cytokine production from pBabe CNA V314R modified PBLs and compared the results to the pBabe puro modified PBLs. NFAT family members play a key role in the transcriptional activation of cytokine genes such as IL-2, IL-4, IL-5, Interferon-γ (IFN-γ) and Tumour Necrosis Factor (TNF) (Campbell *et al.*, 1996; De Boer *et al.*, 1999; Rao *et al.*, 1997). CsA has been shown to inhibit cytokines such as IL-2, Interferon-γ (IFN-γ), and TNF (Andersson *et al.*, 1992; Thomson, 1992). Thus, the expression of the mutant CNA V314R protein should prevent CsA mediated inhibition of cytokine production.

Three to four weeks of cell culture post-isolation were required in order to obtain adequate cell numbers to carry out experiments. Figure 6.3 illustrates the strategy developed to analyse cytokine production, from isolation of the PBLs from whole blood on Day 0 through to the set up of the experiment to investigate the pBabe CNA V314R modified PBLs. A human Th1/Th2 cytokine bead array (CBA) assay kit was used, to quantitatively measure IL-2, IL-4, IL-5, IL-10, TNF-α and IFN-γ protein levels in the modified PBLs. The CBA system uses the sensitivity of fluorescence detection by flow cytometry to measure soluble analytes in a particle-based immunoassay. The BD CBA Kit uses six groups of different particles stably labelled with a fluorescent dye whose emission wavelength is read at FL-3. Each group of beads is labelled with a discrete level of fluorescent dye so that the groups can be distinguished by their mean fluorescent intensity upon flow cytomety analysis (Figure 6.4). The beads are coupled with antibodies specific for each of the 6 cytokines IL-2, IL-4, IL-5, IL-10, TNF-α and IFN-γ. The antibody-coupled beads are analogous to the solid-capture phase of an Enzyme-linked ImmunoSorbent Assay (ELISA) assay. The high-affinity antibodies capture cytokine proteins of interest that may be present in the test sample. A PE-fluorescent antibody is then added to detect the captured protein. The wavelength of which (≈ 585 nm, detected in the FL-2 channel) is discrete from the fluorescence signal emitted by the CBA beads (≈ 650 nm, detected in the FL-3 channel). Serial dilutions of a standard analyte solution (containing a mixture of protein standards with known concentrations) are employed

Whole Blood from donor

Ficoll gradient

PBMC
+ anti-CD3/ anti-CD28/ IL-2

+ 3 or 4 days

2-cycle retroviral infection with
pBabe puro and pBabe CNA V314R

+ 3 or 4 days

+ anti-CD3/IL-2

+ 1 day

+ puromycin

+ 2-3 weeks of cell culture

live cells assessed daily by flow cytometry

+IL-2 every 3 days
+ anti-CD3 every 7 days

Immunofluorescence staining

Set up experiment: +/-pretreatment with CsA
+/- stimulation

Supernatant harvested 8, 24 and 72 hours

CBA assay and flow cytometry analysis to assess cytokine production

Figure 6.3 Schematic of the investigation of pBabe puro and pBabe CNA V314R modified PBLs.

This diagram illustrates the entire procedure from isolation of the PBLs from whole blood to the analysis of the cytokine production from the modified PBLs in a CBA assay.

(a)

Bead	Specificity
(Brightest) A1	IL-2
A2	IL-4
A3	IL-5
A4	IL-10
A5	TNF
(Dimmest) A6	IFN-γ

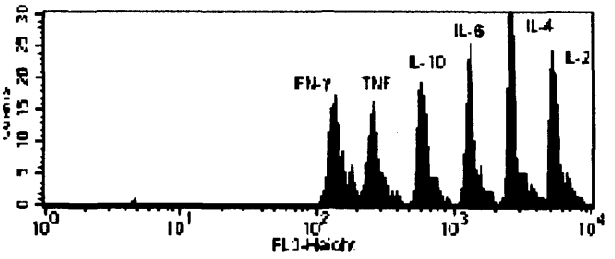

(b)

1. Reconstitute Human Th1/Th2 Cytokine Standards in Assay Diluent and Dilute Standards by serial dilutions

↓

2. Mix 10 μl/test of each Human Cytokine Capture Bead suspension **and** transfer 50 μl of mixed beads to each assay tube

↓

3. Add PE Detection Reagent (50 μl/test) and Standard Dilutions and test samples to the appropriate sample tubes (50 μl/tube)

(protect from light) ↓ 3 hour incubation at RT*

↓

4. Wash samples with 1 ml Wash Buffer and centrifuge

↓

5. Add 300 μl of Wash Buffer to each assay tube, analyze samples

Note: *Cytometer Setup Bead Procedure; as per manual

Figure 6.4: The BDA Th1/Th2 CBA Kit

The BD CBA Kit uses six groups of different particles stably labelled with a fluorescent dye whose emission wavelength is read at FL-3. The beads are coupled with antibodies specific for each of the 6 cytokines IL-2, IL-4, IL-5, IL-10, TNF-α and IFN-γ. Each group of beads is labelled with a discrete level of fluorescent dye so that the groups can be distinguished by their mean fluorescent intensity upon flow cytomety analysis (a). Figure 6.4 (b) describes the CBA assay set-up procedure. (a) and (b) are adapted from www.bdbiosciences.com.

to generate standard curves for each cytokine being detected. The levels of analytes captured by the discrete bead groups (distinguished by their discrete FL-3 fluorescent intensity levels) are measured. The level of analyte is directly proportional to the bound detection antibody MFI signal (FL-2). The concentration of each test sample is then determined using the standard curves generated in the assay, and the data is compiled in tabular format by BD CBA Analysis Software provided. Cytokine concentrations as high as 10,000 pg/ml and as low as 5 pg/ml can be detected in these assays. Figure 6.4 and Figure 6.5 illustrate the CBA assay protocol and a detailed description is available in the appropriate figure legend.

The cytokine profiles using PBLs from two different donors (Donor 1 and Donor 2) were assessed. PBLs modified with pBabe puro virus and pBabe CNA V314R virus were seeded at a $1X10^6$ cells/ml in 48-well plates. Appropriate wells were pre-treated with two concentrations of CsA (0.25 μg/ml and 0.5 μg/ml) and stimulated with anti-CD3 (OKT3, 2.5 ng/ml). IL-2 stimulation was omitted from these experiments. The aim was to investigate the effects of CsA on cytokine production, thus adding exogenous IL-2 into the experimental system would have compromised the data. Aliquots of supernatant were harvested from each well (taking care not to harvest any cells) at 8, 24 and 72 hours post-stimulation, and frozen at –80°C until required. Substantial data was generated from the cytokine analysis of the samples, which was then analysed at various levels. The table in Figure 6.5 (b) illustrates an example of the raw fluorescence (FL-2) data generated in the protocol. All data presented from Figure 6.6 onwards is depicted graphically as the concentration of cytokine determined from the Standard Curves generated during the experiment by the CBA Software (extrapolated from the MFI of each individual sample).

Figure 6.6, the first level of analysis, shows the concentration of all six cytokines produced from pBabe puro modified PBLs stimulated with anti-CD3 at 8 hours, and 72 hours, for both donors. Where values are shown, they were calculated with a standard curve and standardised to International NIBSC/WHO Standards using BD CBA/NIBSC/WHO conversion factors (BD Biosciences). Therefore, the values can be considered accurate despite the levels looking low compared to more

(a)

Protein (pg/ml)	Top standard	1:2 Diln	1:4 Diln	1:8 Diln
IFN-γ	5000	2500	1250	625

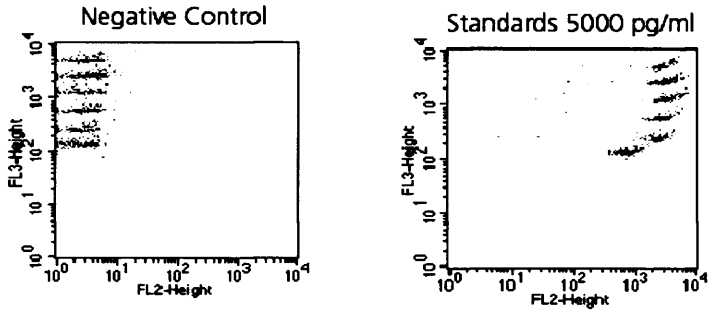

(b)

Sample	FL2-MFI	IFN-γ Sample pg/ml
pBabe PBL +anti-CD3/CD28/IL-2	71.0	810.4

Figure 6.5: Determination of cytokine concentration in a sample

Serial dilutions of a standard analyte solution (containing a mixture of protein standards with known concentrations) are employed to generate standard curves for each cytokine being detected. The levels of analytes captured by the discrete bead groups (distinguished by their discrete FL-3 fluorescent intensity levels) are measured. The level of analyte is directly proportional to the bound detection antibody MFI signal (FL-2). (a) The histograms in (a) are representative of the raw data generated in such an assay, and illustrate the FL-2 MFI for all 6 of the standard cytokines undiluted (Top standard). The IFN-γ standard are the dimmest beads. The BDA standards are of a known fluorescence, therefore the mean fluorescence intensity values (MFI) generated for the serial dilutions of BDA standards are used to generate standard curves in the assay. The table in Figure 6.5 (a) shows a representative example of the concentrations of the IFN-γ standard at a selection of dilutions. The concentration of each test sample is determined using the standard curves generated in the assay, and the data is compiled in tabular format by BD CBA Analysis Software provided. Cytokine concentrations as high as 10,000 pg/ml and as low as 5 pg/ml can be detected in these assays. (b) is an example of the raw data for one sample generated in the experiments. The MFI of the pBabe PBL anti-CD3/CD28/IL-2 stimulated sample taken 72 hours after stimulation is converted to pg/ml sample concentration of IFN-γ using the standard curves described in (a). Figure (a) is adapted from www.bdbiosciences.com.

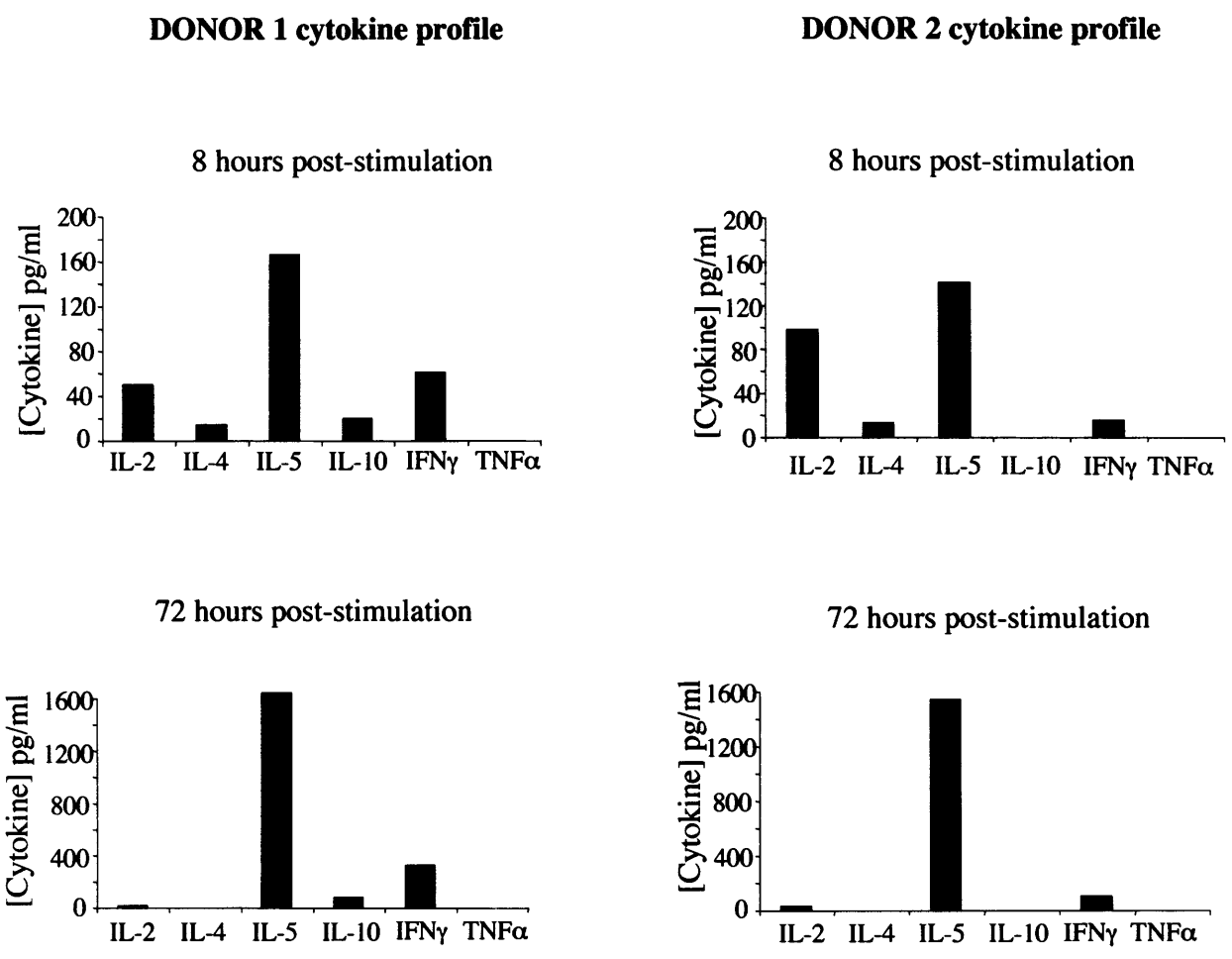

Figure 6.6 CBA is used to measure cytokines produced from retrovirally modified PBLs

PBLs were isolated from whole blood using a Ficoll gradient, and stimulated with anti-CD3 (OKT3, 2.5 ng/ml), anti-CD28 (5 μg/ml) and IL-2 (20 ng/ml) for three days. A 2-cycle retroviral infection was performed with pBabe CNA V314R and pBabe puro. PBLs were restimulated four days later with anti-CD3/IL-2 and puromycin (1 μg/ml)was added the following day. Once adequate cell numbers of puromycin resistant cells were available, the cytokine production from the PBLs was investigated. Cells were seeded at $1X10^6$/ml in a 48-well plate, pre-treated with CsA and stimulated with anti-CD3(OKT3, 2.5 ng/ml). Supernatant was harvested after 8, 24 and 72 hours. A CBA assay was performed, according to the manufacturers instructions, to assess the level of IL-5, IFNγ, IL-10, IL-2, IL-4 and TNFα in the supernatant. Figure 6.4 shows the levels of all six cytokines (pg/ml) at 8 hours and 72 hours from anti-CD3 stimulated pBabe puro modified PBLs from both donors.

abundant cytokines, for example IL-4 compared to IL-5. Five cytokines were detected at 8 hours for Donor 1 and four were detected at 72 hours (IL-2, IL-5, IL-10 and IFN-γ), whereas for Donor 2 four cytokines were detected at 8 hours and three were detected at 72 hours (IL-2, IL-5 and IFN-γ). For both donors, the levels of IFN-γ and IL-5 increased from 8 hours to 72 hours, while the levels of IL-2 and IL-4 decreased. After 72-hours, IL-5, IFN-γ and IL-2 were above the minimal level of detection for both donors, so we focused our analysis on these three cytokines. Thus, this analysis identified the most useful cytokines for the investigation of retrovirally modified PBLs. We then analysed the data to compare cytokine production in the absence and presence of CsA from modified PBLs. The graphs in Figure 6.7 show that IFN-γ and IL-5 cytokine production from the pBabe puro modified PBLs was decreased following CsA treatment, while surprisingly, CsA treatment did not cause a decrease in IL-2 levels from the cells. Thus, we concluded that the analysis of IL-2 levels produced by the modified PBLs, could not be used to assess CsA resistance and we focused analysis on the cytokines IFN-γ and IL-5.

During the experiment, we monitored untreated retrovirally modified PBLs, and retrovirally modified PBLs stimulated with anti-CD3 only (OKT3 2.5 μg/ml) or anti-CD3 and anti-CD28 (0.5 μg/ml). We were interested to compare the cytokine profiles of PBLs from each treatment. Figure 6.8 shows IFN-γ and IL-5 levels at 8 and 24 hours post-treatment. The levels of IFN-γ and IL-5 produced from untreated and anti-CD3 treated were similar in the case of both donors. The levels of cytokine from anti-CD3/anti-CD28 treated pBabe modified PBLs were marginally higher than those from anti-CD3 stimulated PBLs in Donor 1 and were similar to anti-CD3 stimluated PBLs in Donor 2. This is also the case at 72 hours and this similarity in concentrations from untreated, anti-CD3 stimulated and anti-CD3/28 stimulated PBLs, was also evident for the other cytokines assayed. These results demonstrated that retrovirally modified PBLs that were untreated, anti-CD3 stimulated and anti-CD3/28 stimulated all produced similar levels of cytokine.

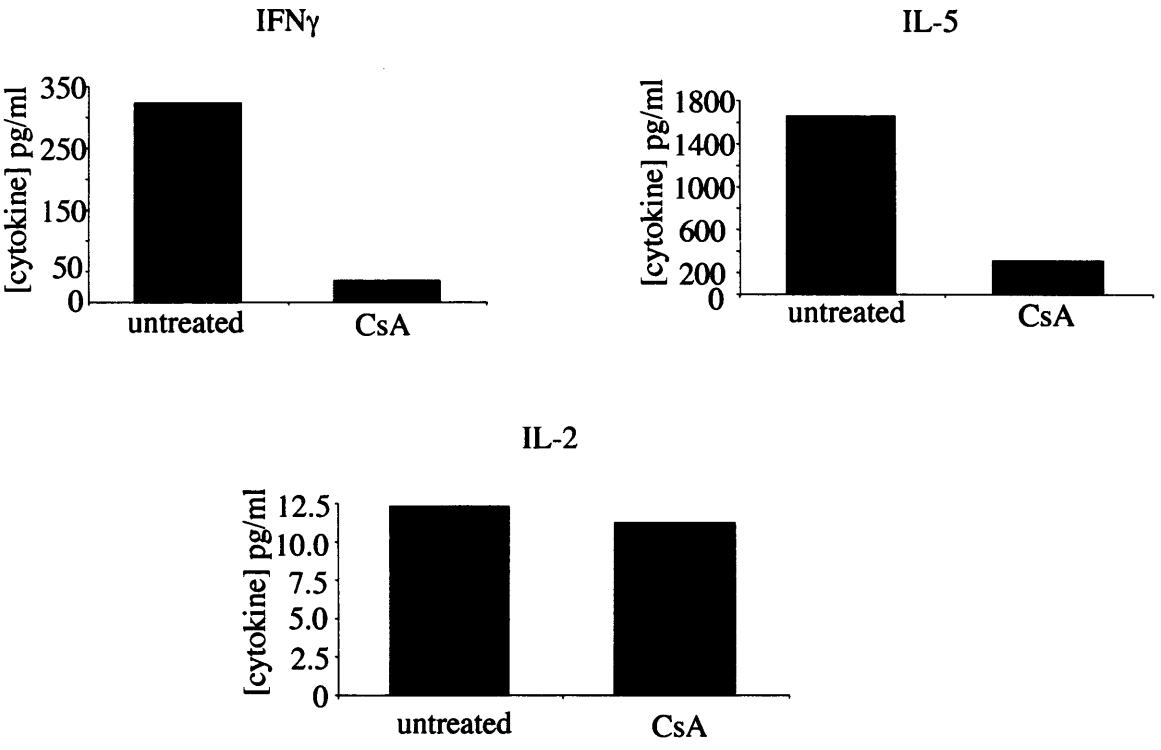

Figure 6.7 The effects of CsA on cytokine production in retrovirally modified PBLs

The CBA data was analysed to compare cytokine production in the absence and presence of CsA from pBabe puro modified PBLs. Figure 6.5 shows IFN-γ, IL-5 and IL-2 cytokine production at 72 hours, from anti-CD3 stimulated pBabe puro modified PBLs from Donor 1, in the absence of presence of 0.5 μg/ml CsA.

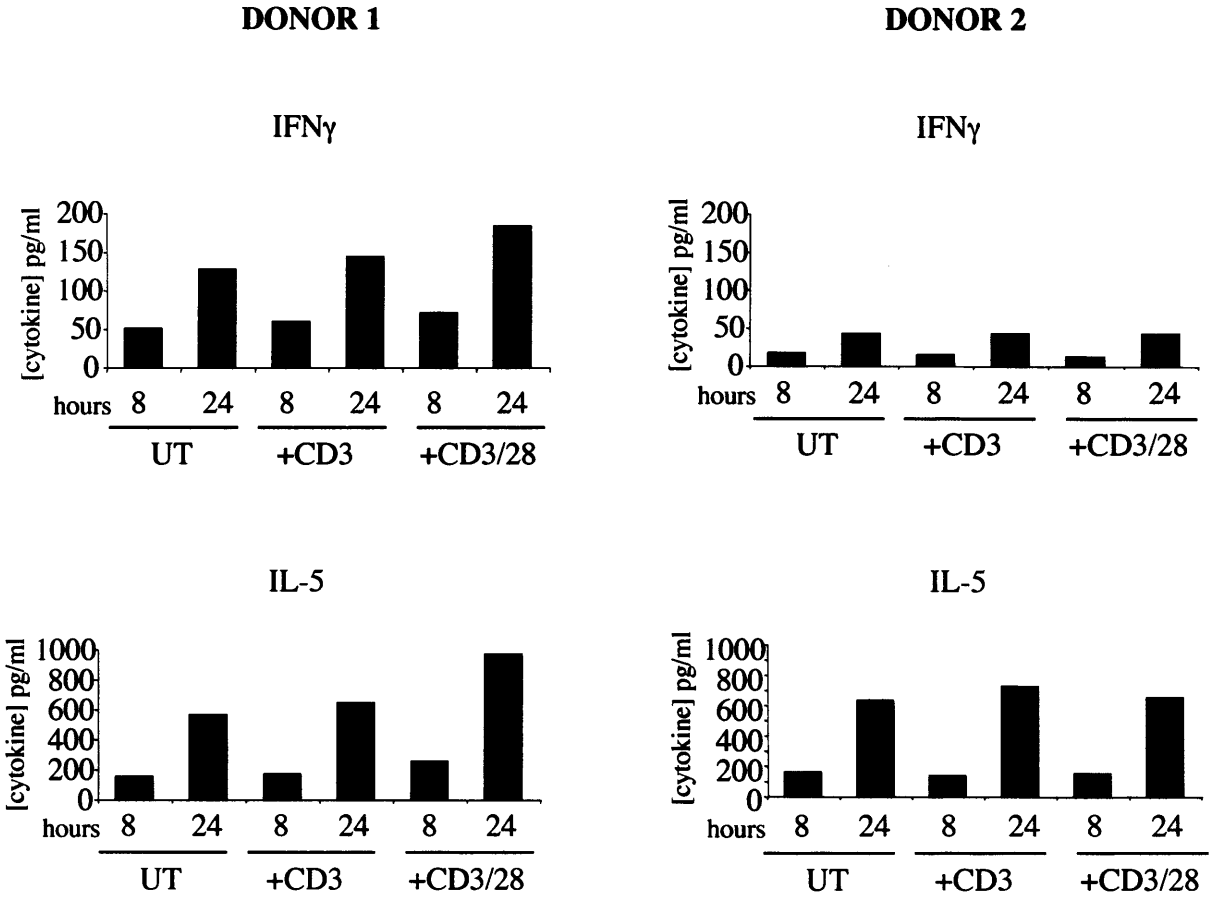

Figure 6.8 Assessment of the level of IFNγ and IL-5 produced from modified PBLs.

Modified PBLs were either untreated, stimulated with anti-CD3 (2.5 ng/ml) or anti-CD3 and anti-CD28 (5 μg/ml). Figure 6.6 shows the levels of IFNγ and IL-5 from pBabe puro modified PBLs from both donors, at 8 and 24 hours post-treatment.

6.4 Investigation of CsA resistance in pBabe CNA V314R modified PBLs

With the parameters of the assay system clearly defined, we analysed the data generated from our experiment to investigate whether cytokine production was CsA resistant in pBabe CNA V314R modified PBLs. Figure 6.9 shows the concentration of IFN-γ and IL-5 at 72 hours from Donor 1 and Donor 2. The results for Donor 1 show that both IFN-γ and IL-5 were slightly higher in pBabe CNA V314R PBLs following CsA treatment, than the level of IFN-γ and IL-5 from pBabe puro PBLs. However, no dramatic resistance to the inhibitory effects of CsA on cytokine production in pBabe CNA V314R PBLs, was demonstrated in Donor 1. For Donor 2, the level of IFN-γ is also higher in pBabe CNA V314R PBLs following CsA treatment, than the level of IFN-γ from the pBabe puro PBLs following CsA treatment. However, no dramatic resistance to the inhibitory effects of CsA on IFN-γ production from pBabe CNA V314R PBLs, was evident in the data for Donor 2. The IL-5 graph for Donor 2 shows that the level of IL-5 is dramatically higher in the pBabe CNA V314R PBLs following CsA treatment than the level of IL-5 produced from the pBabe puro PBLs following CsA treatment. More importantly, the data showed that the levels of IL-5 produced from the pBabe CNA V314R PBLs following CsA treatment, were at least equivalent to the IL-5 produced from the untreated pBabe CNA V314R PBLs. This demonstrates a CsA resistance in the pBabe CNA V314R modified PBLs from Donor 2, to the inhibitory effects of CsA on IL-5 production.

In addition to the question of CsA resistance, careful analysis of the data revealed that the modification of PBLs with a pBabe CNA V314R retrovirus leads to increased cytokine production. We compared cytokine levels from pBabe puro PBLs and pBabe CNA V314R PBLs for untreated, anti-CD3 and anti-CD3/28 treated samples. Again, the CBA assay results for both donors were compared. Figure 6.10 shows the results for IFN-γ and IL-5 production over a 72-hour time-course. The graphs show that the level of IFN-γ produced from the pBabe CNA V314R PBLs was greater than that from pBabe puro modified PBLs for both donors. The graphs also demonstrated that, for Donor 2 but not Donor 1, the level of IL-5 produced from pBabe CNA V314R PBLs, was greater than that from pBabe puro PBLs. This was

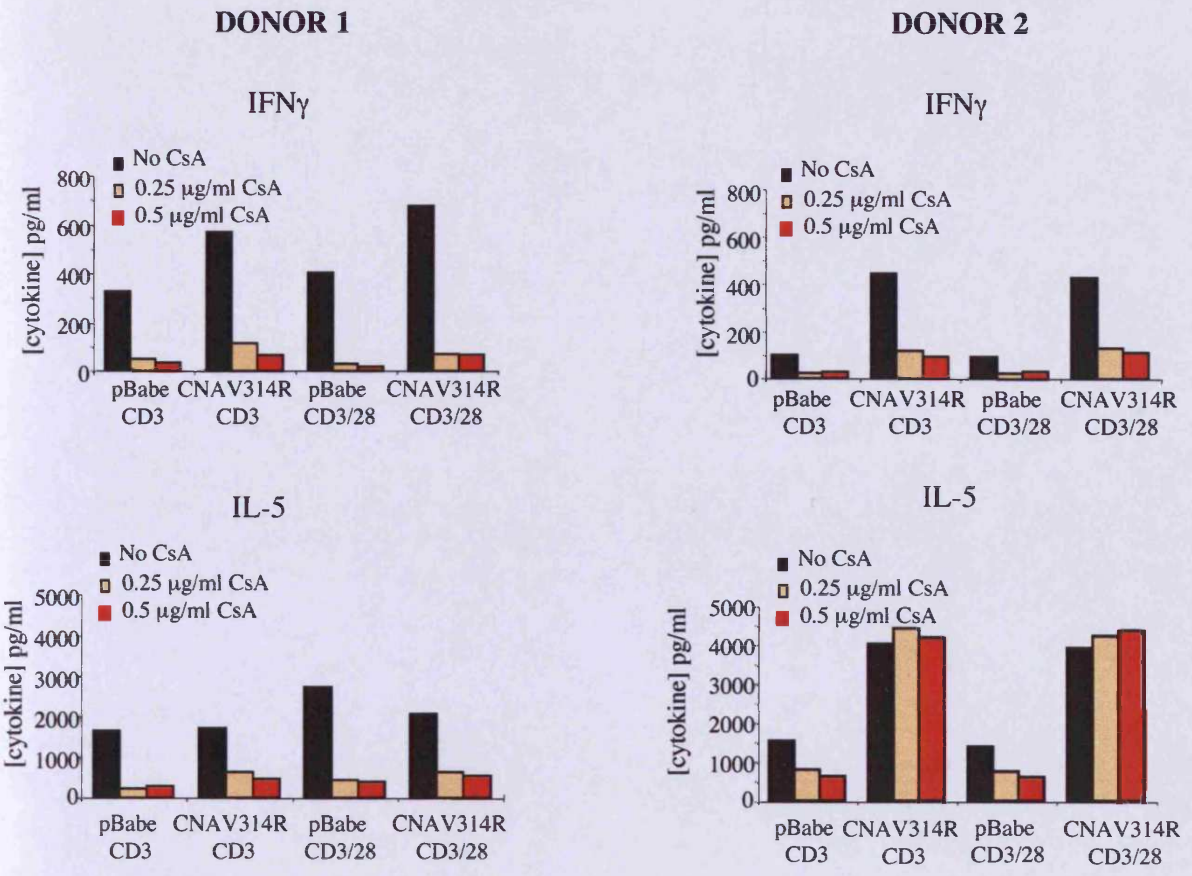

Figure 6.9 Investigation of CsA resistance in pBabe CNA V314R modified PBLs

pBabe CNA V314R modified PBLs were investigated for CsA resistance and results were compared to pBabe puro modified PBLs. Figure 6.7 shows the concentration of IFN-γ and IL-5 at 72 hours from anti-CD3 or anti-CD3/28 stimulated pBabe CNA V314R PBLs and pBabe puro PBLs in the presence (0.25 µg/ml or 0.5 µg/ml) or absence of CsA, from both Donor 1 and Donor 2.

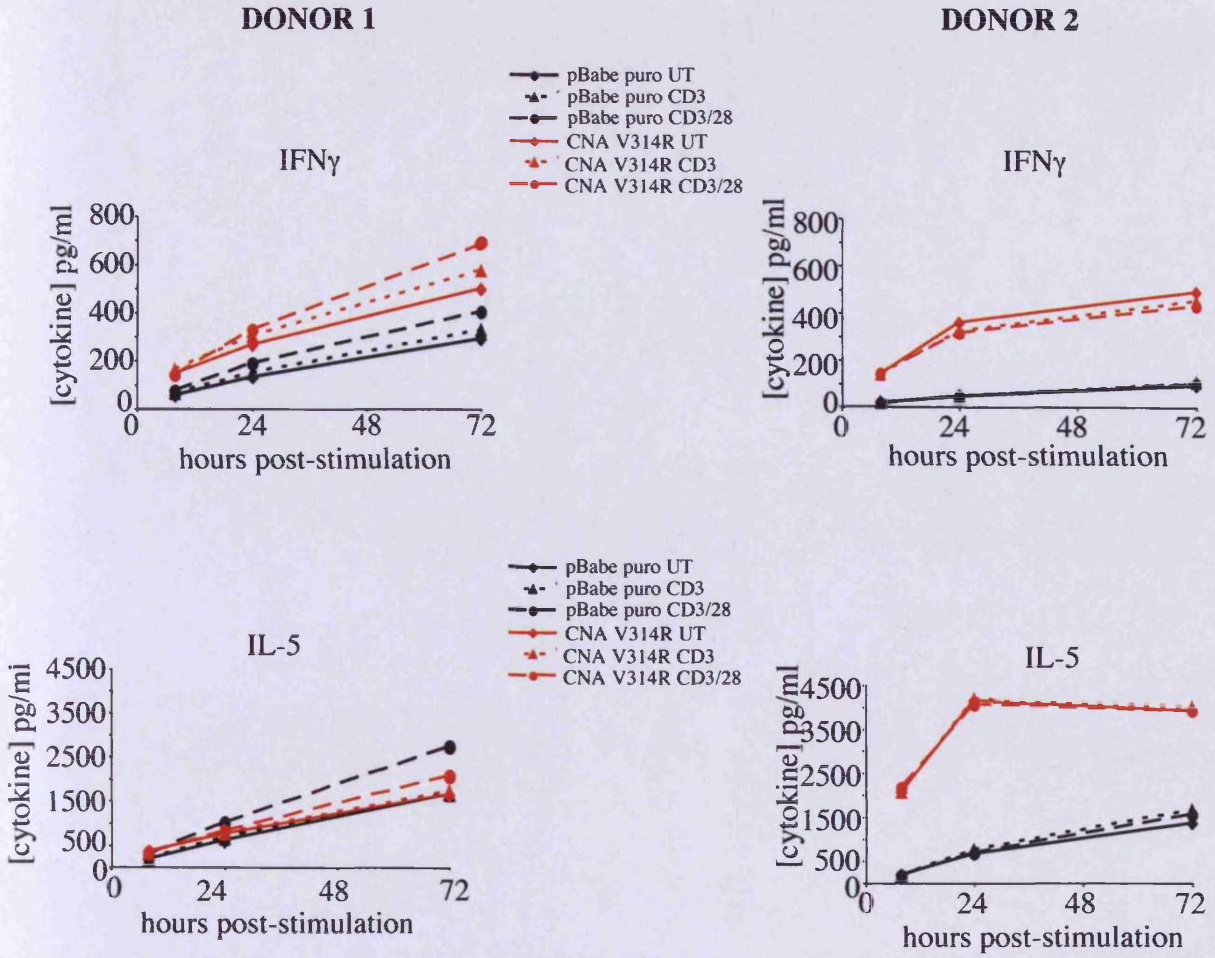

Figure 6.10 Increased cytokine production in pBabe CNA V314R modified PBLs

The levels of IFNγ and IL-5 produced over 8, 24 and 72 hours, from pBabe puro modified and pBabe CNA V314R modified PBLs from both donors are shown. PBLs were either untreated, stimulated with anti-CD3 (2.5 ng/ml) or stimulated with anti-CD3 and anti-CD28 (5 μg/ml).

also evident for all of the other cytokines assayed from Donor 2 PBLs but not Donor 1 PBLs. Taken together, our results indicated that the pBabe CNA V314R modified PBLs from both donors had an increased IFN-γ cytokine production, and that the pBabe CNA V314R PBLs from Donor 2, but not Donor 1, had an increased cytokine production for all of the other cytokines assayed.

6.6 Analysis of cytokine production from PBLs modified with other retroviruses

To investigate if altered cytokine production was unique to cells modified with pBabe CNA V314R PBLs, we measured cytokine production from PBLs modified with two other retroviruses. They were the pBabe mTOR S2035T virus, previously described in Chapter 5, and a pBabe hTERT virus, which expresses human telomerase (Wallis *et al.*, 2004). PBLs were infected simultaneously with either pBabe puro, pBabe CNA V314R, pBabe mTOR S2035T or pBabe hTERT virus and selected in puromycin. Figure 6.11 (a) shows the panel of puromycin resistant cells used in the experiment. All of the mock-infected cells are dead.

The experiments with pBabe mTOR S2035T and pBabe hTERT virally infected PBLs were performed in parallel with the experiments with PBLs infected with pBabe puro and pBabe CNA V314R. A CBA assay was used to assess cytokine profiles. Figure 6.11 (b) shows the levels of IFN-γ and IL-5 production from pBabe puro, pBabe CNA V314R, pBabe mTOR S2035T and pBabe hTERT modified PBLs from both donors, at 8, 24 and 72 hours. For both donors, the levels of IFN-γ produced from the pBabe CNA V314R PBLs and the pBabe mTOR S2035T PBLs were greater than those produced from the pBabe puro or pBabe hTERT PBLs. Looking at IL-5 for Donor 1, the levels of IL-5 from pBabe mTOR S2035T PBLs were greater than the other viruses. This difference was most evident at 72 hours. For Donor 2, the levels of IL-5 from pBabe CNA V314R PBLs and pBabe mTOR S2035T PBLs were greater than the levels of IL-5 from pBabe puro or pBabe hTERT. Thus genetic modification of PBLs, with viruses expressing modified CNA and modified mTOR, causes increased cytokine production.

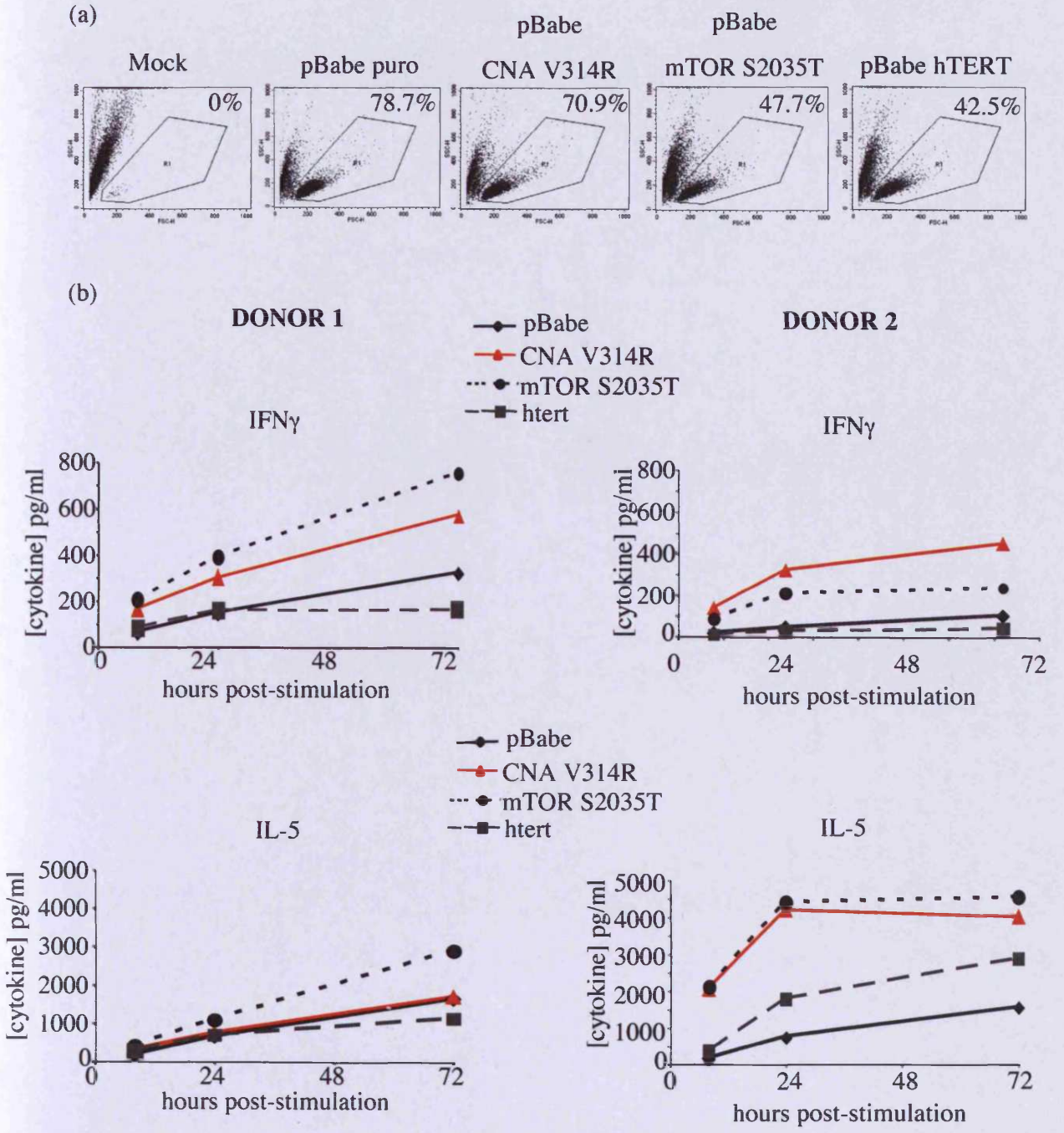

Figure 6.11 Investigation of cytokine production from PBLs modified with other retroviruses

To investigate if altered cytokine production was unique to cells modified with pBabe CNA V314R PBLs, we measured cytokine production from PBLs modified with two other retroviruses, pBabe mTOR S2035T virus and pBabe hTERT, and compared results to pBabe puro and pBabe CNA V314R PBLs. Figure 6.9 (a) shows the forward and side scatter dot plots of the panel of modified PBLs 17 days post-isolation. The percentage of cells in the live gate (R1) is shown. Figure 6.9 (b) shows the levels of IFNγ and IL-5 produced at 8, 24 and 72 hours, from anti-CD3 stimulated PBLs modified with all four retroviruses, for both donors.

6.7 Discussion

The immunofluorescent phenotyping and the CBA data demonstrated the infection of both cytotoxic $CD8^+$ T-cells and $CD4^+$ T-cells with a pBabe CNA V314R retrovirus. Immunofluorescent staining and analysis by flow cytometry, demonstrated that both pBabe puro modified PBLs, and pBabe CNA V314R modified PBLs cultures contained $CD8^+$ and $CD4^+$ T-cells. IFN-γ is the typical cytokine produced by $CD8^+$ T-cells. IL2, IFN-γ and TNF-α are cytokines produced by Th1 helper $CD4^+$ T- cells, while IL-5, IL-4, IL-10 and TNF-α, are cytokines typically produced by Th2 helper $CD4^+$ T-cells. In the CBA assays, analysis of the cytokine levels produced from modified PBLs show that $CD8^+$, Th1, and Th2 cytokines were produced from the modified PBLs. Taken together, these results demonstrate that we have successful retrovirally modified all three T-cell subsets; $CD8^+$, Th1 $CD4^+$ and Th2 $CD4^+$ T-cells with a pBabe CNA V314R retrovirus. It should be noted at this point that because the retroviral protocol involved the infection of a mixed lymphocyte population there may have been some non-T-cells infected with the retrovirus during the course of the retroviral infection protocol and these other cells (e.g macrophage, B-cells) may have contributed to the levels of cytokines observed the the samples. The presence of these non-T-cells in the PBL mixture may also have provided co-stimulatory signals to the T-cells in the population, which could explain why the levels of cytokine observed from the anti-CD3 stimulated and the anti-CD3/28 stimulated PBLs were quite similar. While this is possible, it is highly unlikely. The immunofluorescent flow cytometry analysis indicated that the majority of the cells in the culture were T-cells (Figure 6.2). In addition, the infected cells were cultured for greater than 3 weeks using T-cell specific stimuli.

In this study we only saw CsA resistance for one cytokine, IL-5, in cells from one donor. The observation that CsA resistance was only observed for one donor agrees with our study of rapamycin resistance, where we only observed resistance in approximately 50% of cases. This may be due to viral integration sites altering gene expression, as discussed in Chapter 5 (Wolffe and Matzke, 1999). However, why one cytokine was resistant to CsA while others were not is a bit more difficult to explain.

IL-5 transcription may be regulated differently to the other cytokines measured. NFAT is involved in the transcriptional regulation of a number of cytokines including IL-2, IL-4, IL-5 and IFN-γ, measured in our study (Campbell *et al.*, 1996; De Boer *et al.*, 1999; Rao *et al.*, 1997). Four of the five NFAT sites in the IL-2 promoter, essential for IL-2 regulation, have been found to bind both NFAT and the transcription factor AP-1 (Rooney *et al.*, 1995b). The binding of both NFAT and AP-1 to the conserved P sequence and the conserved IL-4 CLEO sequence in the IL-4 promoter is critical for IL-4 promoter activity and gene expression (Hodge *et al.*, 1995; Miyatake *et al.*, 1991; Rooney *et al.*, 1995b). Inhibition of NFAT activity would inhibit the production of cytokines critically dependent on NFAT binding for transcription. Like IL-2 and IL-4, the IL-5 promoter also has NFAT binding consensus sites; the P sequence and the IL-5 CLEO sequence. De Boer *et al.* showed that, unlike the other cytokines, AP-1 binds to the IL-5 CLEO region but NFAT does not (De Boer *et al.*, 1999). With regard to the P sequence, NFAT and AP-1 both bind, and De Boer have shown that the binding of NFAT to this region of the IL-5 promoter is critical for IL-5 expression in human T-cells (De Boer *et al.*, 1999). However, there is conflicting evidence, and other data show that the P-sequence may not be not important for IL-5 gene transcription (Siegel *et al.*, 1995). Thus, the apparent CsA resistance we observed, for IL-5, for one donor, may not be as a result of a resistant calcineurin/NFAT pathway but rather because the transcription of IL-5 is not crucially dependent on NFAT activity. However, this is unlikely and does not fully explain the observations, since no CsA resistance in IL-5 production was observed in either pBabe puro PBLs from the same donor or the pBabe puro and pBabe CNA V314R PBLs from Donor 1. While future experiments are required to fully clarify the results obtained in this study, overall our data suggest that the pBabe CNA V314R virus conferred CsA resistance on the PBLs and that ultimately, the role of CsA in regulating cytokine production is more complicated than suggested by work to date.

Aside from the question of CsA resistance, careful analysis of the data revealed that the modification of PBLs with a pBabe CNA V314R retrovirus confers an increased cytokine production phenotype on the PBLs. A functional change in the

mutant calcineurin, may explain the increased cytokine production observed in pBabe CNA V314R modified PBLs. The binding of the CsA/Cyclophilin A complex is dependent on key residues in the catalytic region of CNA. Yan *et al.* generated V314 mutants in order to study the importance of such residues in calcineurin phosphatase activity and their data showed that a mutation of the V314 residue significantly increased the phosphatase activity of the CNA subunit, in addition to altering the CsA/cyclophilin interaction, and the CNB subunit interaction (Yan and Wei, 1999). Further experiments confirmed a confirmational change in the V314 mutant protein and the data suggested that the change of activity and function of V314 was due to such conformational changes affecting the interaction between the CNA subunit and the CNB subunit (Xiang *et al.*, 2003). In our experiments, the expression of a mutant calcineurin in the modified PBLs may have altered the cytokine production observed in the pBabe CNA V314R modified PBLs compared to pBabe puro modified PBLs. The increased cytokine production was observed consistently, in both donors, with regard to IFN-γ production. An overall objective of this study is to genetically modify T-cells, with a view to enhancing the efficacy and function of these adoptively transferred T-cells to fight EBV-infection in post-translant patients (Rooney *et al.*, 1998a). IFN-γ is a cytotoxic cytokine, typically produced by cytotoxic T-cells. The increased production of IFN-γ in the retrovirally modified T-cells, indicates that the modification of human T-cells with a pBabe CNA V314R virus may be a useful strategy to improve the efficacy and anti-viral function of these T-cells in adoptive transfer.

The investigation of additional retroviruses in the study yielded some interesting results. We were interested to determine if the increased cytokine production observed following the modification of PBLs with the pBabe CNA V314R retrovirus was also evident in PBLs modified with other retroviruses. The results showed that the modification of PBLs with both a pBabe CNA V314R virus and a pBabe mTOR S2035T virus led to IFN-γ production greater than that from either pBabe puro PBLs or pBabe hTERT PBLs. This result was consistently demonstrated for both donors. Again, the increased production of IFN-γ in the retrovirally modified T-cells, indicates that the modification of human T-cells with a

pBabe CNA V314R virus or a pBabe mTOR S2035T virus, may be a useful strategy to improve the efficacy and anti-viral function of these T-cells in adoptive transfer.

Chapter 7

Final Discussion

The application of gene therapy to improve the efficacy and survival of T-cells remains a major goal in the development of an optimal immunotherapeutic strategy to treat cancers and infections. One of the main aims of this thesis was to genetically modify human T-cells with a retrovirus that would improve the efficacy and longevity of the cells in an immunosuppressive environment. While immunosuppressive resistant lymphocytes were not generated in all cases, potentially more effective cells were generated. The modified cells demonstrated functional differences in three distinct ways: immunosuppression resistance, a growth advantage and an increased cytokine production.

Resistance to rapamycin was demonstrated in Kit225 cells and primary human T-cells modified with the pBabe mTOR S2035T retrovirus. The resistant phenotype was not observed for every infection. However, the rapamycin resistance that was demonstrated suggests that the mTOR S2035T transgene may enhance the longevity and function of adoptively transferred T-cells in a rapamycin immunosuppressive environment. PBLs modified with pBabe CNA V314R also showed resistance to the inhibitory effects of CsA, for one cytokine (IL-5) from one donor. As discussed previously transgene silencing may explain why immunosuppressive resistance was not observed in all cases. However, the observed growth advantage and increased cytokine production argues against transgene silencing occurring. The growth advantage was observed consistently in all pBabe mTOR S2035T modified cells, including those that did not demonstrate drug resistance. Increased cytokine production was also observed in pBabe CNA V314R and pBabe mTOR S2035T modified cells that did not demonstrate drug resistance. Comparable levels of increased cytokine production was not observed for cells modified with pBabe hTERT suggesting that the phenomenon is not conferred by all transgenes.

The CFSE cell proliferation data clearly showed that the modification of human T-cells with a pBabe mTOR S2035T virus leads to a growth advantage in the cell. The mTOR protein is a crucial regulator of cell growth and proliferation and controls protein synthesis through a number of downstream targets. mTOR itself is regulated by growth factors, nutrient levels and amino acid levels in the cell (Hay and Sonenberg, 2004). Mutations in the mTOR protein may lead to alterations in both the regulation of mTOR by its upstream components and the regulation of the downstream signalling targets of mTOR. McMahon *et al.* demonstrated that a S2035 mutation leads to rapamycin resistance as expected, but that the mutation also affected the substrate sites phosphorylated by mTOR, leading to the conclusion that the FRB domain may participate in substrate recognition in addition to FKBP12/rapamycin binding (McMahon *et al.*, 2002). Additionally, a mutation in mTOR may alter the association of the recently identified raptor and mLST8 proteins (jaHara *et al.*, 2002; Oshiro *et al.*, 2004), which serve as a scaffold for the association of mTOR with its substrates, leading to a different phenotype in the pBabe mTOR S2035T modified cells.

The CBA experiments demonstrated that the modification of primary human T-cells with both pBabe mTOR S2035T and pBabe CNA V314R viruses leads to increased cytokine production compared to pBabe puro or a pBabe hTERT modified PBLs. The increased cytokine production observed in the pBabe mTOR S2035T modified PBLs may be as a result of a change in the function of the protein in the cell compared to wild type mTOR. The substrates of mTOR $p70^{S6K}$ and 4EBP-1 are both regulators of mRNA transcription and any alteration in the phosphorylation of these substrates could alter the cytokine profile of the cell. Likewise, a change in the function of the mutant calcineurin, may explain the increased cytokine production observed in pBabe CNA V314R modified PBLs and studies have shown that a mutation of the V314 residue increases the phosphatase activity of the CNA subunit due to confirmational changes in the mutant protein (Xiang et al., 2003; Yan and Wei, 1999). The increased cytokine profile was observed consistently, in both donors, with regard to IFNγ production. IFNγ is a cytokine typically produced by

cytotoxic T-cells and Th1 $CD4^+$ T-cells and IFNs are involved in numerous immune interactions during viral infections. Whether NFAT proteins play a role in regulating transcription of the IFNγ gene remains to be clarified. Potential NFAT binding sites in the IFNγ promoter have been identified, which contribute to the Ca^+ inducibilty and CsA sensitivity of IFNγ production (Campbell *et al.*, 1996) and studies have shown that IFNγ production in murine T-cells is regulated by NFAT1 (Kiani et al., 2001; Porter and Clipstone, 2002). Taken together, the current evidence indicates that NFAT proteins play a role in regulating the transcription of IFNs. An overall objective of this study was to genetically modify T-cells, with a view to enhancing the efficacy and function of adoptively transferred T-cells to treat EBV-associated PTLD. The increased production of IFNγ, suggest that the modification of human T-cells with a immunosuppressant resistant transgene such as CNA V314R or mTOR S2035T may be a useful strategy to improve the efficacy and anti-viral function of these T-cells in adoptive transfer. However, it is important to note here that the cytotoxicity data generated for pBabe S2035T EBV-CTLs in this project demonstrated that the modification of EBV-CTLs with mTOR S2035T may alter CTL function and/or specificity. Future experiments to clarify this finding would be a useful advancement of this project.

The pBabe hTERT modified PBLs proved useful to compare the data from the pBabe mTOR S2035T and pBabe CNA V314R PBLs to PBLs modified with another transgene, but PBLs modified with a wild-type mTOR gene or a wild-type CNA gene could have been a more useful comparison. However, the generation of stable ψ-crip packaging lines to produce functional wild-type viruses proved unsuccessful. Why this was the case, when the pBabe mTOR S2035T and the pBabe CNA V314R virus packaging lines were successfully made and generated virus of sufficient titre to modify primary T-cells, is not clear. The wild type mTOR gene is very large (7 kb) and this may have limited both proliferation of the packaging line and efficient packaging of the retroviral particle. However, the mutant mTOR gene is also 7kb and thus transgene size is not the only issue. Additionally, the wild type and the mutant CNA genes are of equal size, and at 1.8kb are much smaller than the mTOR transgenes, again indicating that the size of the gene is not the key limiting

factor. The pBabe puro transfection results indicated that stable transfection with both the mTOR and CNA wild-type retroviral plasmids had an inhibitory effect on cell proliferation of the packaging cell line, whereas stable transfection with the mutant plasmids did not. Further investigation with future experiments would be useful in elucidating the problems associated with the generation of the stable wild-type packaging lines. Modifications of the retroviral vector (discussed below) or the use of alternate packaging cell lines may be requied to circumvent such limitations. Transient transfection in PH293 cells did yield pBabe wt mTOR virus but it was not sufficient to modifiy PBLs. Stable chromosomal integration of the viral genome does not take place in PH293 transient transfection (Grignani *et al.*, 1998) and this may explain why the generation of wild-type virus was not completely limited. Despite the low titre, pBabe wt mTOR Kit225 lines were successfully made. Experiments showed that these cell lines had a similar phenotype to the pBabe puro modified line in the presence of rapamycin, and that any rapamycin resistance shown was unique to the pBabe mTOR S2025T modified lines.

While this project clearly demonstrates the successful transfer and adaptation of retroviral technology to infect human T-cells, it also demonstrates that there are technical considerations to the application of a retroviral system to gene therapy. There are a number of areas in which the system could possibly be improved in order to enhance the results. One limitation is that gene transfer protocols using retroviruses require optimal T-cell activation and generally involve the use of CD3 and IL-2 (Movassagh *et al.*, 2000). This may affect the efficacy of the modified T-cell. Sauce *et al.* examined the impact of an *ex vivo* gene transfer protocol on the anti-EBV potential of gene-modified T-cells (Sauce *et al.*, 2002). Their results showed that genetically modified EBV-CTLs had impaired anti-EBV potential and suggest that this is a result of both culture dependent and selection-dependent mechanisms. Ferrand *et al.* also showed that the use of CD3 and IL-2 for the optimal activation of T-cells was associated with reduced T-cell receptor diversity (Ferrand et al., 2000). To circumvent these limitations, recent studies have developed engineered APCs in an attempt to improve *in vitro* stimulation. A study undertaken by Maus *et al.* involved the TNF receptor family member 4-1BB (CD137) co-

stimulatory molecule, which preferentially activates $CD8^+$ T-cells *in vitro*, and which was initially identified in receptor screens of activated lymphocytes (Maus *et al.*, 2002). The 4-1BB ligand is expressed by activated APCs and previous studies have shown that 4-1BB is a co-stimulatory molecule in the activation of T-cells and its signalling is independent from CD28 signalling (Saoulli *et al.*, 1998). Maus *et al.* engineered articifical APCs to express the co-stimulatory molecule human 4-1BB ligand and demonstrated that the addition of this 4-1BB ligand to the APCs used to stimulate the T-cells, maintained TCR diversity and reduced apoptosis of $CD8^+$ T-cells (Maus *et al.*, 2002).

Aside from the improvement of culture conditions in order to enhance the system, low gene transfer efficiency can also be attributed to limitations with the retrovirus itself and is also a challenge of the retroviral system. In our experiments, the time required to outgrow adequate numbers of genetically modified T-cells for experiments, was a drawback of the system. If a higher number of cells could have been infected initially this would have circumvented the time consumption. *In vitro*, random Brownian motion is thought to bring retroviruses and target cells into close proximity, initiating adhesion and virus entry. Approaches to increase this binding have been developed which include increasing the virus titre through concentration of harvests from packaging cell lines (Paul et al., 1993) and centrifugation of retrovirus and target cells (which we employed) (Kotani et al., 1994). Another approach which we also employed, involved the co-localization of the retrovirus and target cell on fibronectin fragments allowing the specific interaction of the viral surface protein with its cell receptor to occur more frequently (Hanenberg et al., 1996). It would have been interesting to determine if it was possible to increase the virus titre obtained from packaging cell lines through concentration of harvests, and this is a method which could be pursued to enhance the viral titres obtained in this project, with a view to decreasing the time required to outgrow adequate T-cell number.

Low gene transfer efficiency can also be attributed to the design of the retroviral vectors. Recently, significant improvement in retroviral vector design has

enhanced their application in viral gene therapy. One improvement has been the use of heterologous envelopes from other viruses in the production of retroviral vectors to enhance the infectivity of the virus. Van Der Loo demonstrated that retroviruses pseudotyped with the envelope of the gibbon ape leukaemia virus (GALV) transduced human haematopoetic cells more efficiently than retroviruses expressing the amphotropic envelope protein (van der Loo et al., 2002). Another major advancement has been the engineering the regulatory regions of the retroviral vector to improve transgene expression in specific target cells (Challita et al., 1995). Challita *et al.* demonstrated multiple modifications in elements of the LTR of retroviral vectors lead to increased expression in embryonic carcinoma cells. In many situations, transgene expression is often silenced by incorporation into condensed and transcriptionally inactive chromatin (Mountain, 2000). This is a limitation to gene therapy and the use of chromatin opening elements which can modify the structure of chromatin and prevent transgene silencing are currently being explored to circumvent this problem (Fraser and Grosveld, 1998). Future experiments to advance this project could investigate the improvement of T-cell activation, packaging cell systems, vector design and culture systems. This may increase infection efficiency of target T-cells and shorten the period required to outgrow retrovirally modified cells for experiments. While further modifications of the system were beyond the scope and objectives of this project, the exploration of such modifications could lead to a significant enhancement of the system.

Despite the widespread application of retroviral vectors in cellular immunotherapy, the safety of retroviral-based systems is a concern. It is estimated that 10% of the mammalian genome comprises endogenous proviruses and other retroelements accumulated during evolution (Temin, 1985). These endogenous retroelements may represent a source of functional viral sequences and may serve as donors in recombination with a vector genome. Such recombination has strong implications for the use of retroviral vector mediated gene delivery (Broeke and Burny, 2003). Insertional mutagenesis is also a potential risk associated with retroviral vectors. The risk of tumourogenesis as a result of insertional mutagenesis in gene transfer procedures was believed to be low. However, the finding that two of

the ten patients in the 2000 SCID trial developed T-cell leukaemia, questioned this belief (Cavazzana-Calvo *et al.*, 2000). The leukaemia arose due to vector insertions near the regulatory region of the LMO2 gene, which encodes a transcription factor essential for the regulation of normal haematopoiesis (McCormack and Rabbitts, 2004). The findings questioned the notion that retroviruses randomly integrate into host genomes and suggested that retroviruses insert preferentially into certain genome sites. However subsequent research indicated that the oncogenesis was more likely due to context dependent factors such as the young age of the patients and the huge expansion the cells underwent *in vivo* and these findings restored confidence in the safety of retroviral vectors in gene therapy (Berns, 2004).

Other retroviral vectors are being explored as alternatives to the MoMLV vector in gene therapy e.g. HIV-1, which has proven advantageous over the conventional MoMLV virus in phase I therapeutic trials (Dropulic, 2001; Lever, 2000). The main advantage of the lentiviral vector is that it can infect both non-dividing and post-mitotic cells, making it useful for gene delivery to neurons and muscle cells. Lentiviral vectors don't tend to integrate in 5' promoter regions, decreasing the chances of activating full-length cellular transcripts. The lentiviral vector system is currently being investigated by colleagues in our department as a potential tool in the genetic modification of NK cells. The extension of these investigations to T-cells would be a useful extension to this retroviral project. However, it is important to note that their application in gene theray may be limited as they have been reported to produce a high copy number per cell (Woods *et al.*, 2003), which may increase the risk of insertional mutagenesis. Foamy viruses, of the spumavirus retroviral family, also have potential as gene delivery vectors (Goff, 2001) as they can infect non-dividing cells and have a broad host and tissue tropism (Josephson *et al.*, 2004). They have the largest genome of all the retroviruses making them attractive for delivery of large transgenes and they have not been associated with any human pathology. Regardless of the category of retroviral vector exploited, the retroviruses remain one of the most popular and effective vectors of choice in gene therapy. The ongoing retoviral vector developments may enable future studies

to circumvent the problems of low titre and infection rates and possibly low transgene expression, which made this project more challenging.

Aside from the immunotherapy studies, the investigation of the effects of rapamycin and LY294002 on primary human T-cell proliferation, which was not the main focus of the project, generated interesting data. Our data demonstrated that LY294002 and rapamycin co-operate to inhibit T-cell proliferation and suggest that inhibition of T-cell proliferation using a combination of a PI3K inhibitor and rapamycin could be beneficial as an alternative immunosuppressive regime. Along with gene knockout studies, LY294002 has proved invaluable in elucidating the role of PI3K in the immune system but the compound does not discriminate between different isoforms in the PI3K family. As a result the therapeutic use of PI3K inhibitors is controversial. The first isoform-selective PI3K inhibitor, for p110δ, has been described by the ICOS corporation (Sadhu *et al.*, 2003a; Sadhu *et al.*, 2003b) and it has been suggested that these isoform-selective agents may be useful for anti-inflammatory or anti-cancer therapies. A broad spectrum PI3Kinase inhibitor such as LY294002 will never be used in the clinic, because of the potential toxicity associated with it. However, highly isoform specific compounds may make the therapeutic use of PI3K inhibitors feasible in the future. Our data, which shows that inhibition of PI3K and TOR can co-operate, suggests that these isoform-selective agents may be useful for combination therapies. Such combination therapies may allow lower doses to be administered and as such may avoid the serious side effects of immunosuppressive agents, such as nephrotoxicity, neurotoxicity, and hyperlipidemia.

In conclusion, this project has supported the concept of using retroviral gene therapy to enhance adoptive T-cell transfer therapies. The results reinforce the importance of the TOR and calcineurin pathways in regulating T-cell proliferation. The study also highlights the benefits of targeting these pathways for immunosuppression and investigating and exploiting these pathways to improve immunotherapy.

Bibliography

Abonour, R., Williams, D.A., Einhorn, L., Hall, K.M., Chen, J., Coffman, J., Traycoff, C.M., Bank, A., Kato, I., Ward, M., Williams, S.D., Hromas, R., Robertson, M.J., Smith, F.O., Woo, D., Mills, B., Srour, E.F. and Cornetta, K. (2000) Efficient retrovirus-mediated transfer of the multidrug resistance 1 gene into autologous human long-term repopulating hematopoietic stem cells. *Nat Med*, **6**, 652-658.

Abraham, R.T. and Wiederrecht, G.J. (1996) Immunopharmacology of rapamycin. *Annu Rev Immunol*, **14**, 483-510.

Aiuti, A., Slavin, S., Aker, M., Ficara, F., Deola, S., Mortellaro, A., Morecki, S., Andolfi, G., Tabucchi, A., Carlucci, F., Marinello, E., Cattaneo, F., Vai, S., Servida, P., Miniero, R., Roncarolo, M.G. and Bordignon, C. (2002) Correction of ADA-SCID by stem cell gene therapy combined with nonmyeloablative conditioning. *Science*, **296**, 2410-2413.

Alfieri, C., Birkenbach, M. and Kieff, E. (1991) Early events in Epstein-Barr virus infection of human B lymphocytes. *Virology*, **181**, 595-608.

Alton, E.W., Middleton, P.G., Caplen, N.J., Smith, S.N., Steel, D.M., Munkonge, F.M., Jeffery, P.K., Geddes, D.M., Hart, S.L., Williamson, R. and et al. (1993) Non-invasive liposome-mediated gene delivery can correct the ion transport defect in cystic fibrosis mutant mice. *Nat Genet*, **5**, 135-142.

Aman, M.J., Lamkin, T.D., Okada, H., Kurosaki, T. and Ravichandran, K.S. (1998) The inositol phosphatase SHIP inhibits Akt/PKB activation in B cells. *J Biol Chem*, **273**, 33922-33928.

Ambinder, R.F. (1990) Human lymphotropic viruses associated with lymphoid malignancy: Epstein-Barr and HTLV-1. *Hematol Oncol Clin North Am*, **4**, 821-833.

Andersson, J., Nagy, S., Groth, C.G. and Andersson, U. (1992) Effects of FK506 and cyclosporin A on cytokine production studied in vitro at a single-cell level. *Immunology*, **75**, 136-142.

Auger, K.R., Carpenter, C.L., Cantley, L.C. and Varticovski, L. (1989) Phosphatidylinositol 3-kinase and its novel product, phosphatidylinositol 3-phosphate, are present in Saccharomyces cerevisiae. *J Biol Chem*, **264**, 20181-20184.

Balla, T. (2001) Pharmacology of phosphoinositides, regulators of multiple cellular functions. *Curr Pharm Des*, **7**, 475-507.

Baltimore, D. (1970) RNA-dependent DNA polymerase in virions of RNA tumour viruses. *Nature*, **226**, 1209-1211.

Barata, L.T., Henriques, R., Hivroz, C., Jouanguy, E., Paiva, A., Freitas, A.M., Coimbra, H.B., Fischer, A. and da Mota, H.C. (2001) [Primary immunodeficiency secondary to ZAP-70 deficiency]. *Acta Med Port*, **14**, 413-417.

Barbet, N.C., Schneider, U., Helliwell, S.B., Stansfield, I., Tuite, M.F. and Hall, M.N. (1996) TOR controls translation initiation and early G1 progression in yeast. *Mol Biol Cell*, **7**, 25-42.

Barry, M. and Bleackley, R.C. (2002) Cytotoxic T lymphocytes: all roads lead to death. *Nat Rev Immunol*, **2**, 401-409.

Bassuk, A.G., Anandappa, R.T. and Leiden, J.M. (1997) Physical interactions between Ets and NF-kappaB/NFAT proteins play an important role in their cooperative activation of the human immunodeficiency virus enhancer in T cells. *J Virol*, **71**, 3563-3573.

Bayer, A.L., Yu, A., Adeegbe, D. and Malek, T.R. (2005) Essential role for interleukin-2 for CD4(+)CD25(+) T regulatory cell development during the neonatal period. *J Exp Med*, **201**, 769-777.

Beck, J.M., Blackmon, M.B., Rose, C.M., Kimzey, S.L., Preston, A.M. and Green, J.M. (2003) T cell costimulatory molecule function determines susceptibility to infection with Pneumocystis carinii in mice. *J Immunol*, **171**, 1969-1977.

Berkowitz, R., Fisher, J. and Goff, S.P. (1996) RNA packaging. *Curr Top Microbiol Immunol*, **214**, 177-218.

Berns, A. (2004) Good news for gene therapy. *N Engl J Med*, **350**, 1679-1680.

Berridge, M. (2004) Conformational coupling: a physiological calcium entry mechanism. *Sci STKE*, **2004**, pe33.

Bestor, T.H. and Tycko, B. (1996) Creation of genomic methylation patterns. *Nat Genet*, **12**, 363-367.

Beugnet, A., Wang, X. and Proud, C.G. (2003) Target of rapamycin (TOR)-signaling and RAIP motifs play distinct roles in the mammalian TOR-dependent phosphorylation of initiation factor 4E-binding protein 1. *J Biol Chem*, **278**, 40717-40722.

Bevan, M.J. (2004) Helping the CD8(+) T-cell response. *Nat Rev Immunol*, **4**, 595-602.

Bi, L., Okabe, I., Bernard, D.J. and Nussbaum, R.L. (2002) Early embryonic lethality in mice deficient in the p110beta catalytic subunit of PI 3-kinase. *Mamm Genome*, **13**, 169-172.

Bi, L., Okabe, I., Bernard, D.J., Wynshaw-Boris, A. and Nussbaum, R.L. (1999) Proliferative defect and embryonic lethality in mice homozygous for a deletion in the p110alpha subunit of phosphoinositide 3-kinase. *J Biol Chem*, **274**, 10963-10968.

Bitsch, A. and Bruck, W. (2002) Differentiation of multiple sclerosis subtypes: implications for treatment. *CNS Drugs*, **16**, 405-418.

Bjornsti, M.A. and Houghton, P.J. (2004) The TOR pathway: a target for cancer therapy. *Nat Rev Cancer*, **4**, 335-348.

Black, D., Bogomolniy, F., Robson, M.E., Offit, K., Barakat, R.R. and Boyd, J. (2005) Evaluation of germline PTEN mutations in endometrial cancer patients. *Gynecol Oncol*, **96**, 21-24.

Blaese, R.M., Culver, K.W., Miller, A.D., Carter, C.S., Fleisher, T., Clerici, M., Shearer, G., Chang, L., Chiang, Y., Tolstoshev, P. and et al. (1995) T lymphocyte-directed gene therapy for ADA- SCID: initial trial results after 4 years. *Science*, **270**, 475-480.

Blattman, J.N., Grayson, J.M., Wherry, E.J., Kaech, S.M., Smith, K.A. and Ahmed, R. (2003) Therapeutic use of IL-2 to enhance antiviral T-cell responses in vivo. *Nat Med*, **9**, 540-547.

Bogedain, C., Wolf, H., Modrow, S., Stuber, G. and Jilg, W. (1995) Specific cytotoxic T lymphocytes recognize the immediate-early transactivator Zta of Epstein-Barr virus. *J Virol*, **69**, 4872-4879.

Bollard, C.M., Kuehnle, I., Leen, A., Rooney, C.M. and Heslop, H.E. (2004) Adoptive immunotherapy for posttransplantation viral infections. *Biol Blood Marrow Transplant*, **10**, 143-155.

Bollard, C.M., Rossig, C., Calonge, M.J., Huls, M.H., Wagner, H.J., Massague, J., Brenner, M.K., Heslop, H.E. and Rooney, C.M. (2002) Adapting a transforming growth factor beta-related tumor protection strategy to enhance antitumor immunity. *Blood*, **99**, 3179-3187.

Bond, J., Jones, C., Haughton, M., DeMicco, C., Kipling, D. and Wynford-Thomas, D. (2004) Direct evidence from siRNA-directed "knock down" that p16(INK4a) is required for human fibroblast senescence and for limiting ras-induced epithelial cell proliferation. *Exp Cell Res*, **292**, 151-156.

Bond, J.A., Haughton, M.F., Rowson, J.M., Smith, P.J., Gire, V., Wynford-Thomas, D. and Wyllie, F.S. (1999) Control of replicative life span in human cells: barriers to clonal expansion intermediate between M1 senescence and M2 crisis. *Mol Cell Biol*, **19**, 3103-3114.

Bonini, C., Ferrari, G., Verzeletti, S., Servida, P., Zappone, E., Ruggieri, L., Ponzoni, M., Rossini, S., Mavilio, F., Traversari, C. and Bordignon, C. (1997) HSV-TK gene transfer into donor lymphocytes for control of allogeneic graft-versus-leukemia. *Science*, **276**, 1719-1724.

Boonen, G.J., van Dijk, A.M., Verdonck, L.F., van Lier, R.A., Rijksen, G. and Medema, R.H. (1999) CD28 induces cell cycle progression by IL-2-independent down-regulation of p27kip1 expression in human peripheral T lymphocytes. *Eur J Immunol*, **29**, 789-798.

Borel, J.F., Feurer, C., Gubler, H.U. and Stahelin, H. (1976) Biological effects of cyclosporin A: a new antilymphocytic agent. *Agents Actions*, **6**, 468-475.

Branch, D.R., Valenta, L.J., Yousefi, S., Sakac, D., Singla, R., Bali, M., Sahai, B.M. and Ma, X.Z. (2002) VPAC1 is a cellular neuroendocrine receptor expressed on T cells that actively facilitates productive HIV-1 infection. *Aids*, **16**, 309-319.

Brazelton, T.R. and Morris, R.E. (1996) Molecular mechanisms of action of new xenobiotic immunosuppressive drugs: tacrolimus (FK506), sirolimus (rapamycin), mycophenolate mofetil and leflunomide. *Curr Opin Immunol*, **8**, 710-720.

Brennan, P., Babbage, J.W., Burgering, B.M., Groner, B., Reif, K. and Cantrell, D.A. (1997) Phosphatidylinositol 3-kinase couples the interleukin-2 receptor to the cell cycle regulator E2F. *Immunity*, **7**, 679-689.

Brennan, P., Babbage, J.W., Thomas, G. and Cantrell, D. (1999) p70(s6k) integrates phosphatidylinositol 3-kinase and rapamycin- regulated signals for E2F regulation in T lymphocytes. *Mol Cell Biol*, **19**, 4729-4738.

Breslin, E.M., White, P.C., Shore, A.M., Clement, M. and Brennan, P. (2005) LY294002 and rapamycin co-operate to inhibit T-cell proliferation. *British Journal of Pharmacology*, **144**, 791-800.

Brodie, S.J., Lewinsohn, D.A., Patterson, B.K., Jiyamapa, D., Krieger, J., Corey, L., Greenberg, P.D. and Riddell, S.R. (1999) In vivo migration and function of transferred HIV-1-specific cytotoxic T cells. *Nat Med*, **5**, 34-41.

Broeke, A.V. and Burny, A. (2003) Retroviral Vector Biosafety: Lessons from Sheep. *J Biomed Biotechnol*, **2003**, 9-12.

Bu, J.Y., Shaw, A.S. and Chan, A.C. (1995) Analysis of the interaction of ZAP-70 and syk protein-tyrosine kinases with the T-cell antigen receptor by plasmon resonance. *Proc Natl Acad Sci U S A*, **92**, 5106-5110.

Bunnell, B.A., Muul, L.M., Donahue, R.E., Blaese, R.M. and Morgan, R.A. (1995) High-efficiency retroviral-mediated gene transfer into human and nonhuman primate peripheral blood lymphocytes. *Proc Natl Acad Sci U S A*, **92**, 7739-7743.

Burkitt, D. (1958) A sarcoma involving the jaws in African children. *Br J Surg*, **46**, 218-223.

Calne, R.Y., White, D.J., Thiru, S., Evans, D.B., McMaster, P., Dunn, D.C., Craddock, G.N., Pentlow, B.D. and Rolles, K. (1978) Cyclosporin A in patients receiving renal allografts from cadaver donors. *Lancet*, **2**, 1323-1327.

Campbell, P.M., Pimm, J., Ramassar, V. and Halloran, P.F. (1996) Identification of a calcium-inducible, cyclosporine sensitive element in the IFN-gamma promoter that is a potential NFAT binding site. *Transplantation*, **61**, 933-939.

Cardenas, M.E., Muir, R.S., Breuder, T. and Heitman, J. (1995) Targets of immunophilin-immunosuppressant complexes are distinct highly conserved regions of calcineurin A. *Embo J*, **14**, 2772-2783.

Carpinteiro, A., Peinert, S., Ostertag, W., Zander, A.R., Hossfeld, D.K., Kuhlcke, K., Eckert, H.G., Baum, C. and Hegewisch-Becker, S. (2002) Genetic protection of repopulating hematopoietic cells with an improved MDR1-retrovirus allows administration of intensified chemotherapy following stem cell transplantation in mice. *Int J Cancer*, **98**, 785-792.

Cavazzana-Calvo, M., Hacein-Bey, S., de Saint Basile, G., Gross, F., Yvon, E., Nusbaum, P., Selz, F., Hue, C., Certain, S., Casanova, J.L., Bousso, P., Deist, F.L. and Fischer, A. (2000) Gene therapy of human severe combined immunodeficiency (SCID)-X1 disease. *Science*, **288**, 669-672.

Cereseto, A. and Giacca, M. (2004) Integration site selection by retroviruses. *AIDS Rev*, **6**, 13-21.

Challita, P.M., Skelton, D., el-Khoueiry, A., Yu, X.J., Weinberg, K. and Kohn, D.B. (1995) Multiple modifications in cis elements of the long terminal repeat of retroviral vectors lead to increased expression and decreased DNA methylation in embryonic carcinoma cells. *J Virol*, **69**, 748-755.

Chang, C.D., Mukai, H., Kuno, T. and Tanaka, C. (1994) cDNA cloning of an alternatively spliced isoform of the regulatory subunit of Ca2+/calmodulin-dependent protein phosphatase (calcineurin B alpha 2). *Biochim Biophys Acta*, **1217**, 174-180.

Chantry, D., Vojtek, A., Kashishian, A., Holtzman, D.A., Wood, C., Gray, P.W., Cooper, J.A. and Hoekstra, M.F. (1997) p110delta, a novel phosphatidylinositol 3-kinase catalytic subunit that associates with p85 and is expressed predominantly in leukocytes. *J Biol Chem*, **272**, 19236-19241.

Chatila, T., Castigli, E., Pahwa, R., Pahwa, S., Chirmule, N., Oyaizu, N., Good, R.A. and Geha, R.S. (1990) Primary combined immunodeficiency resulting from defective transcription of multiple T-cell lymphokine genes. *Proc Natl Acad Sci U S A*, **87**, 10033-10037.

Chen, J., Zheng, X.F., Brown, E.J. and Schreiber, S.L. (1995) Identification of an 11-kDa FKBP12-rapamycin-binding domain within the 289-kDa FKBP12-rapamycin-associated protein and characterization of a critical serine residue. *Proc Natl Acad Sci U S A*, **92**, 4947-4951.

Cheng, L.E., Ohlen, C., Nelson, B.H. and Greenberg, P.D. (2002) Enhanced signaling through the IL-2 receptor in CD8+ T cells regulated by antigen recognition results in preferential proliferation and expansion of responding CD8+ T cells rather than promotion of cell death. *Proc Natl Acad Sci U S A*, **99**, 3001-3006.

Clarke, S.J., McStay, G.P. and Halestrap, A.P. (2002) Sanglifehrin A acts as a potent inhibitor of the mitochondrial permeability transition and reperfusion injury of the heart by binding to cyclophilin-D at a different site from cyclosporin A. *J Biol Chem*, **277**, 34793-34799.

Clayton, E., Bardi, G., Bell, S.E., Chantry, D., Downes, C.P., Gray, A., Humphries, L.A., Rawlings, D., Reynolds, H., Vigorito, E. and Turner, M. (2002) A crucial role for the p110delta subunit of phosphatidylinositol 3-kinase in B cell development and activation. *J Exp Med*, **196**, 753-763.

Clipstone, N.A. and Crabtree, G.R. (1992) Identification of calcineurin as a key signalling enzyme in T-lymphocyte activation. *Nature*, **357**, 695-697.

Coghlan, V.M., Perrino, B.A., Howard, M., Langeberg, L.K., Hicks, J.B., Gallatin, W.M. and Scott, J.D. (1995) Association of protein kinase A and protein phosphatase 2B with a common anchoring protein. *Science*, **267**, 108-111.

Cosimi, A.B., Burton, R.C., Colvin, R.B., Goldstein, G., Delmonico, F.L., LaQuaglia, M.P., Tolkoff-Rubin, N., Rubin, R.H., Herrin, J.T. and Russell, P.S. (1981) Treatment of acute renal allograft rejection with OKT3 monoclonal antibody. *Transplantation*, **32**, 535-539.

Cousens, L.P., Orange, J.S. and Biron, C.A. (1995) Endogenous IL-2 contributes to T cell expansion and IFN-gamma production during lymphocytic choriomeningitis virus infection. *J Immunol*, **155**, 5690-5699.

Cox, C., Naylor, B.A., Mackett, M., Arrand, J.R., Griffin, B.E. and Wedderburn, N. (1998) Immunization of common marmosets with Epstein-Barr virus (EBV) envelope glycoprotein gp340: effect on viral shedding following EBV challenge. *J Med Virol*, **55**, 255-261.

Crabtree, G.R. (1999) Generic signals and specific outcomes: signaling through Ca2+, calcineurin, and NF-AT. *Cell*, **96**, 611-614.

Crespo, J.L., Powers, T., Fowler, B. and Hall, M.N. (2002) The TOR-controlled transcription activators GLN3, RTG1, and RTG3 are regulated in response to intracellular levels of glutamine. *Proc Natl Acad Sci U S A*, **99**, 6784-6789.

D'Hondt, V., Symann, M. and Machiels, J.P. (2001) Chemoprotection and selection by chemotherapy of multidrug resistance-associated protein-1 (MRP1) transduced cells. *Curr Gene Ther*, **1**, 359-366.

Danos, O. and Mulligan, R.C. (1988) Safe and efficient generation of recombinant retroviruses with amphotropic and ecotropic host ranges. *Proc Natl Acad Sci U S A*, **85**, 6460-6464.

Darley, R.L., Pearn, L., Omidvar, N., Sweeney, M., Fisher, J., Phillips, S., Hoy, T. and Burnett, A.K. (2002) Protein kinase C mediates mutant N-Ras-induced developmental abnormalities in normal human erythroid cells. *Blood*, **100**, 4185-4192.

Davis, C.L., Harrison, K.L., McVicar, J.P., Forg, P.J., Bronner, M.P. and Marsh, C.L. (1995) Antiviral prophylaxis and the Epstein Barr virus-related post-transplant lymphoproliferative disorder. *Clin Transplant*, **9**, 53-59.

Davis, C.L., Wood, B.L., Sabath, D.E., Joseph, J.S., Stehman-Breen, C. and Broudy, V.C. (1998) Interferon-alpha treatment of posttransplant lymphoproliferative disorder in recipients of solid organ transplants. *Transplantation*, **66**, 1770-1779.

Davis, M.M. and Bjorkman, P.J. (1988) T-cell antigen receptor genes and T-cell recognition. *Nature*, **334**, 395-402.

De Boer, M.L., Mordvinov, V.A., Thomas, M.A. and Sanderson, C.J. (1999) Role of nuclear factor of activated T cells (NFAT) in the expression of interleukin-5 and other cytokines involved in the regulation of hemopoetic cells. *Int J Biochem Cell Biol*, **31**, 1221-1236.

Del Prete, G.F., De Carli, M., Ricci, M. and Romagnani, S. (1991) Helper activity for immunoglobulin synthesis of T helper type 1 (Th1) and Th2 human T cell clones: the help of Th1 clones is limited by their cytolytic capacity. *J Exp Med*, **174**, 809-813.

Del Val, M., Schlicht, H.J., Ruppert, T., Reddehase, M.J. and Koszinowski, U.H. (1991) Efficient processing of an antigenic sequence for presentation by MHC class I molecules depends on its neighboring residues in the protein. *Cell*, **66**, 1145-1153.

Delmer, A., Ajchenbaum-Cymbalista, F., Tang, R., Ramond, S., Faussat, A.M., Marie, J.P. and Zittoun, R. (1995) Overexpression of cyclin D2 in chronic B-cell malignancies. *Blood*, **85**, 2870-2876.

Devereux, S., Corney, C., Macdonald, C., Watts, M., Sullivan, A., Goldstone, A.H., Ward, M., Bank, A. and Linch, D.C. (1998) Feasibility of multidrug resistance (MDR-1) gene transfer in patients undergoing high-dose therapy and peripheral blood stem cell transplantation for lymphoma. *Gene Ther*, **5**, 403-408.

Di Florio, S., Sebastiani, C., Fagioli, M., Di Ianni, M., Alfonsi, D., Venditti, G., Pelicci, P.G. and Tabilio, A. (2000) Retrovirus-mediated transfer of the herpes simplex virus thymidine kinase and enhanced green fluorescence protein genes in primary T lymphocytes. *Br J Haematol*, **110**, 903-906.

Downing, G.J., Kim, S., Nakanishi, S., Catt, K.J. and Balla, T. (1996) Characterization of a soluble adrenal phosphatidylinositol 4-kinase reveals wortmannin sensitivity of type III phosphatidylinositol kinases. *Biochemistry*, **35**, 3587-3594.

Dropulic, B. (2001) Lentivirus in the clinic. *Mol Ther*, **4**, 511-512.

Dumont, F.J., Staruch, M.J., Grammer, T., Blenis, J., Kastner, C.A. and Rupprecht, K.M. (1995) Dominant mutations confer resistance to the immunosuppressant, rapamycin, in variants of a T cell lymphoma. *Cell Immunol*, **163**, 70-79.

Duraiswamy, J., Sherritt, M., Thomson, S., Tellam, J., Cooper, L., Connolly, G., Bharadwaj, M. and Khanna, R. (2003) Therapeutic LMP1 polyepitope vaccine for EBV-associated Hodgkin disease and nasopharyngeal carcinoma. *Blood*, **101**, 3150-3156.

Durandy, A. (2001) Anti-B cell and anti-cytokine therapy for the treatment of post-transplant lymphoproliferative disorder: past, present, and future. *Transpl Infect Dis*, **3**, 104-107.

Epstein, M.A. and Achong, B.G. (1968) Specific immunofluorescence test for the herpes-type EB virus of Burkitt lymphoblasts, authenticated by electron microscopy. *J Natl Cancer Inst*, **40**, 593-607.

Faumont, N., Trempat, P., Brousset, P., Delsol, G. and Meggetto, F. (2004) In Hodgkin's disease Reed-Sternberg cells and normal B-lymphocytes are infected by related Epstein-Barr virus strains. *Virus Res*, **101**, 163-173.

Ferby, I.M., Waga, I., Hoshino, M., Kume, K. and Shimizu, T. (1996) Wortmannin inhibits mitogen-activated protein kinase activation by platelet-activating factor through a mechanism independent of p85/p110-type phosphatidylinositol 3-kinase. *J Biol Chem*, **271**, 11684-11688.

Ferrand, C., Robinet, E., Contassot, E., Certoux, J.M., Lim, A., Herve, P. and Tiberghien, P. (2000) Retrovirus-mediated gene transfer in primary T lymphocytes: influence of the transduction/selection process and of ex vivo expansion on the T cell receptor beta chain hypervariable region repertoire. *Hum Gene Ther*, **11**, 1151-1164.

Fingar, D.C. and Blenis, J. (2004) Target of rapamycin (TOR): an integrator of nutrient and growth factor signals and coordinator of cell growth and cell cycle progression. *Oncogene*, **23**, 3151-3171.

Fox, D.S., Cruz, M.C., Sia, R.A., Ke, H., Cox, G.M., Cardenas, M.E. and Heitman, J. (2001) Calcineurin regulatory subunit is essential for virulence and mediates interactions with FKBP12-FK506 in Cryptococcus neoformans. *Mol Microbiol*, **39**, 835-849.

Fraser, J.D., Irving, B.A., Crabtree, G.R. and Weiss, A. (1991) Regulation of interleukin-2 gene enhancer activity by the T cell accessory molecule CD28. *Science*, **251**, 313-316.

Fraser, P. and Grosveld, F. (1998) Locus control regions, chromatin activation and transcription. *Curr Opin Cell Biol*, **10**, 361-365.

Fruman, D.A. (2004) Towards an understanding of isoform specificity in phosphoinositide 3-kinase signalling in lymphocytes. *Biochem Soc Trans*, **32**, 315-319.

Fruman, D.A. and Cantley, L.C. (2002) Phosphoinositide 3-kinase in immunological systems. *Semin Immunol*, **14**, 7-18.

Fruman, D.A., Snapper, S.B., Yballe, C.M., Alt, F.W. and Cantley, L.C. (1999) Phosphoinositide 3-kinase knockout mice: role of p85alpha in B cell development and proliferation. *Biochem Soc Trans*, **27**, 624-629.

Fu, Z., Aronoff-Spencer, E., Backer, J.M. and Gerfen, G.J. (2003) The structure of the inter-SH2 domain of class IA phosphoinositide 3-kinase determined by site-directed spin labeling EPR and homology modeling. *Proc Natl Acad Sci U S A*, **100**, 3275-3280.

Fuentes, J.J., Genesca, L., Kingsbury, T.J., Cunningham, K.W., Perez-Riba, M., Estivill, X. and de la Luna, S. (2000) DSCR1, overexpressed in Down syndrome, is an inhibitor of calcineurin-mediated signaling pathways. *Hum Mol Genet*, **9**, 1681-1690.

Gao, G.F., Rao, Z. and Bell, J.I. (2002) Molecular coordination of alphabeta T-cell receptors and coreceptors CD8 and CD4 in their recognition of peptide-MHC ligands. *Trends Immunol*, **23**, 408-413.

Gaspar, H.B., Gilmour, K.C. and Jones, A.M. (2001) Severe combined immunodeficiency--molecular pathogenesis and diagnosis. *Arch Dis Child*, **84**, 169-173.

Geiger, T.L., Leitenberg, D. and Flavell, R.A. (1999) The TCR zeta-chain immunoreceptor tyrosine-based activation motifs are sufficient for the activation and differentiation of primary T lymphocytes. *J Immunol*, **162**, 5931-5939.

Gerard, G.F., Fox, D.K., Nathan, M. and D'Alessio, J.M. (1997) Reverse transcriptase. The use of cloned Moloney murine leukemia virus reverse transcriptase to synthesize DNA from RNA. *Mol Biotechnol*, **8**, 61-77.

Gerber, P., Lucas, S., Nonoyama, M., Perlin, E. and Goldstein, L.I. (1972) Oral excretion of Epstein-Barr virus by healthy subjects and patients with infectious mononucleosis. *Lancet*, **2**, 988-989.

Gilboa, E., Mitra, S.W., Goff, S. and Baltimore, D. (1979) A detailed model of reverse transcription and tests of crucial aspects. *Cell*, **18**, 93-100.

Goff, S.P. (2001) Retroviridae: The Retroviruses and Their Replication. In Knipe, D.M., Howley, P. M., Griffin, D. E., Lamb, R. A., Martin, A., Roizman, B. and Straus, S. E. (ed.), *Fields Virology*. Lippincott Williams and Wilkins, Philadelphia, Vol. 2, pp. 1871-1940.

Gonthier, D.M., Hartman, G. and Holley, J.L. (1992) Posttransplant lymphoproliferative disorder presenting as an isolated skin lesion. *Am J Kidney Dis*, **19**, 600-603.

Gottschalk, S., Ng, C.Y., Perez, M., Smith, C.A., Sample, C., Brenner, M.K., Heslop, H.E. and Rooney, C.M. (2001) An Epstein-Barr virus deletion mutant associated with fatal lymphoproliferative disease unresponsive to therapy with virus-specific CTLs. *Blood*, **97**, 835-843.

Green, J.M., Noel, P.J., Sperling, A.I., Walunas, T.L., Gray, G.S., Bluestone, J.A. and Thompson, C.B. (1994) Absence of B7-dependent responses in CD28-deficient mice. *Immunity*, **1**, 501-508.

Green, M., Reyes, J., Webber, S. and Rowe, D. (2001) The role of antiviral and immunoglobulin therapy in the prevention of Epstein-Barr virus infection and post-transplant lymphoproliferative disease following solid organ transplantation. *Transpl Infect Dis*, **3**, 97-103.

Grignani, F., Kinsella, T., Mencarelli, A., Valtieri, M., Riganelli, D., Lanfrancone, L., Peschle, C., Nolan, G.P. and Pelicci, P.G. (1998) High-efficiency gene transfer and selection of human hematopoietic progenitor cells with a hybrid EBV/retroviral vector expressing the green fluorescence protein. *Cancer Res*, **58**, 14-19.

Gross, T.G. and Loechelt, B.J. (2003) Epstein-Barr virus associated disease following blood or marrow transplant. *Pediatr Transplant*, **7 Suppl 3**, 44-50.

Gross, T.G., Steinbuch, M., DeFor, T., Shapiro, R.S., McGlave, P., Ramsay, N.K., Wagner, J.E. and Filipovich, A.H. (1999) B cell lymphoproliferative disorders following hematopoietic stem cell transplantation: risk factors, treatment and outcome. *Bone Marrow Transplant*, **23**, 251-258.

Haddad, E., Paczesny, S., Leblond, V., Seigneurin, J.M., Stern, M., Achkar, A., Bauwens, M., Delwail, V., Debray, D., Duvoux, C., Hubert, P., de Ligny, B.H., Wijdenes, J., Durandy, A. and Fischer, A. (2001) Treatment of B-lymphoproliferative disorder with a monoclonal anti-interleukin-6 antibody in 12 patients: a multicenter phase 1-2 clinical trial. *Blood*, **97**, 1590-1597.

Hanenberg, H., Hashino, K., Konishi, H., Hock, R.A., Kato, I. and Williams, D.A. (1997) Optimization of fibronectin-assisted retroviral gene transfer into human CD34+ hematopoietic cells. *Hum Gene Ther*, **8**, 2193-2206.

Hanenberg, H., Xiao, X.L., Dilloo, D., Hashino, K., Kato, I. and Williams, D.A. (1996) Colocalization of retrovirus and target cells on specific fibronectin fragments increases genetic transduction of mammalian cells. *Nat Med*, **2**, 876-882.

Haque, T., Wilkie, G.M., Taylor, C., Amlot, P.L., Murad, P., Iley, A., Dombagoda, D., Britton, K.M., Swerdlow, A.J. and Crawford, D.H. (2002) Treatment of Epstein-Barr-virus-positive post-transplantation lymphoproliferative disease with partly HLA-matched allogeneic cytotoxic T cells. *Lancet*, **360**, 436-442.

Hay, N. and Sonenberg, N. (2004) Upstream and downstream of mTOR. *Genes Dev*, **18**, 1926-1945.

Herbst, H., Dallenbach, F., Hummel, M., Niedobitek, G., Pileri, S., Muller-Lantzsch, N. and Stein, H. (1991) Epstein-Barr virus latent membrane protein expression in Hodgkin and Reed-Sternberg cells. *Proc Natl Acad Sci U S A*, **88**, 4766-4770.

Heslop, H.E., Ng, C.Y., Li, C., Smith, C.A., Loftin, S.K., Krance, R.A., Brenner, M.K. and Rooney, C.M. (1996a) Long-term restoration of immunity against Epstein-Barr virus infection by adoptive transfer of gene-modified virus-specific T lymphocytes. *Nat Med*, **2**, 551-555.

Heslop, H.E., Rooney, C.M. and Brenner, M.K. (1995) Gene-marking and haemopoietic stem-cell transplantation. *Blood Rev*, **9**, 220-225.

Heslop, H.E., Rooney, C.M., Rill, D.R., Krance, R.A. and Brenner, M.K. (1996b) Use of gene marking in bone marrow transplantation. *Cancer Detect Prev*, **20**, 108-113.

Heslop, H.E., Savoldo, B. and Rooney, C.M. (2004) Cellular therapy of Epstein-Barr-virus-associated post-transplant lymphoproliferative disease. *Best Pract Res Clin Haematol*, **17**, 401-413.

High, K.P., Joiner, K.A. and Handschumacher, R.E. (1994) Isolation, cDNA sequences, and biochemical characterization of the major cyclosporin-binding proteins of Toxoplasma gondii. *J Biol Chem*, **269**, 9105-9112.

Hochberg, D., Souza, T., Catalina, M., Sullivan, J.L., Luzuriaga, K. and Thorley-Lawson, D.A. (2004) Acute infection with Epstein-Barr virus targets and overwhelms the peripheral memory B-cell compartment with resting, latently infected cells. *J Virol*, **78**, 5194-5204.

Hodge, M.R., Rooney, J.W. and Glimcher, L.H. (1995) The proximal promoter of the IL-4 gene is composed of multiple essential regulatory sites that bind at least two distinct factors. *J Immunol*, **154**, 6397-6405.

Hoebe, K., Janssen, E. and Beutler, B. (2004) The interface between innate and adaptive immunity. *Nat Immunol*, **5**, 971-974.

Hori, T., Uchiyama, T., Tsudo, M., Umadome, H., Ohno, H., Fukuhara, S., Kita, K. and Uchino, H. (1987) Establishment of an interleukin 2-dependent human T

cell line from a patient with T cell chronic lymphocytic leukemia who is not infected with human T cell leukemia/lymphoma virus. *Blood*, **70**, 1069-1072.

Hwang, K.W., Sweatt, W.B., Brown, I.E., Blank, C., Gajewski, T.F., Bluestone, J.A. and Alegre, M.L. (2002) Cutting edge: targeted ligation of CTLA-4 in vivo by membrane-bound anti-CTLA-4 antibody prevents rejection of allogeneic cells. *J Immunol*, **169**, 633-637.

Introna, M., Barbui, A.M., Golay, J., Bambacioni, F., Schiro, R., Bernasconi, S., Breviario, F., Erba, E., Borleri, G., Barbui, T., Biondi, A. and Rambaldi, A. (1998) Rapid retroviral infection of human haemopoietic cells of different lineages: efficient transfer in fresh T cells. *Br J Haematol*, **103**, 449-461.

Inukai, K., Funaki, M., Anai, M., Ogihara, T., Katagiri, H., Fukushima, Y., Sakoda, H., Onishi, Y., Ono, H., Fujishiro, M., Abe, M., Oka, Y., Kikuchi, M. and Asano, T. (2001) Five isoforms of the phosphatidylinositol 3-kinase regulatory subunit exhibit different associations with receptor tyrosine kinases and their tyrosine phosphorylations. *FEBS Lett*, **490**, 32-38.

Jacinto, E. and Hall, M.N. (2003) Tor signalling in bugs, brain and brawn. *Nat Rev Mol Cell Biol*, **4**, 117-126.

jaHara, K., Maruki, Y., Long, X., Yoshino, K., Oshiro, N., Hidayat, S., Tokunaga, C., Avruch, J. and Yonezawa, K. (2002) Raptor, a binding partner of target of rapamycin (TOR), mediates TOR action. *Cell*, **110**, 177-189.

Jain, J., Burgeon, E., Badalian, T.M., Hogan, P.G. and Rao, A. (1995) A similar DNA-binding motif in NFAT family proteins and the Rel homology region. *J Biol Chem*, **270**, 4138-4145.

Jin, L. and Harrison, S.C. (2002) Crystal structure of human calcineurin complexed with cyclosporin A and human cyclophilin. *Proc Natl Acad Sci U S A*, **99**, 13522-13526.

Johnson, A.N. and Newfeld, S.J. (2002) The TGF-beta family: signaling pathways, developmental roles, and tumor suppressor activities. *ScientificWorldJournal*, **2**, 892-925.

Jolly, D. (1994) Viral vector systems for gene therapy. *Cancer Gene Ther*, **1**, 51-64.

Jones, C.J., Kipling, D., Morris, M., Hepburn, P., Skinner, J., Bounacer, A., Wyllie, F.S., Ivan, M., Bartek, J., Wynford-Thomas, D. and Bond, J.A. (2000) Evidence for a telomere-independent "clock" limiting RAS oncogene-driven proliferation of human thyroid epithelial cells. *Mol Cell Biol*, **20**, 5690-5699.

Jonuleit, H. and Schmitt, E. (2003) The regulatory T cell family: distinct subsets and their interrelations. *J Immunol*, **171**, 6323-6327.

Josephson, N.C., Trobridge, G. and Russell, D.W. (2004) Transduction of long-term and mobilized peripheral blood-derived NOD/SCID repopulating cells by foamy virus vectors. *Hum Gene Ther*, **15**, 87-92.

June, C.H., Bluestone, J.A., Nadler, L.M. and Thompson, C.B. (1994) The B7 and CD28 receptor families. *Immunol Today*, **15**, 321-331.

Kagi, D., Ledermann, B., Burki, K., Hengartner, H. and Zinkernagel, R.M. (1994) CD8+ T cell-mediated protection against an intracellular bacterium by perforin-dependent cytotoxicity. *Eur J Immunol*, **24**, 3068-3072.

Kahan, B.D. (2002) The limitations of calcineurin and mTOR inhibitors: new directions for immunosuppressive strategies. *Transplant Proc*, **34**, 130-133.

Kahan, B.D. (2003) Individuality: the barrier to optimal immunosuppression. *Nat Rev Immunol*, **3**, 831-838.

Kahan, B.D., Gibbons-Stubber, S., Tejpal, N. and Chou, T.C. (1992) Prospects for synergistic immunosuppressive drug therapy in the coming decade. *Transplant Proc*, **24**, 1263-1265.

Kalli, K., Huntoon, C., Bell, M. and McKean, D.J. (1998) Mechanism responsible for T-cell antigen receptor- and CD28- or interleukin 1 (IL-1) receptor-initiated regulation of IL-2 gene expression by NF-kappaB. *Mol Cell Biol*, **18**, 3140-3148.

Kanegane, H., Nomura, K., Miyawaki, T. and Tosato, G. (2002) Biological aspects of Epstein-Barr virus (EBV)-infected lymphocytes in chronic active EBV infection and associated malignancies. *Crit Rev Oncol Hematol*, **44**, 239-249.

Kavanaugh, M.P., Wang, H., Boyd, C.A., North, R.A. and Kabat, D. (1994) Cell surface receptor for ecotropic host-range mouse retroviruses: a cationic amino acid transporter. *Arch Virol Suppl*, **9**, 485-494.

Kavran, J.M., Klein, D.E., Lee, A., Falasca, M., Isakoff, S.J., Skolnik, E.Y. and Lemmon, M.A. (1998) Specificity and promiscuity in phosphoinositide binding by pleckstrin homology domains. *J Biol Chem*, **273**, 30497-30508.

Keating, S., Prince, S., Jones, M. and Rowe, M. (2002) The lytic cycle of Epstein-Barr virus is associated with decreased expression of cell surface major histocompatibility complex class I and class II molecules. *J Virol*, **76**, 8179-8188.

Kennedy, G., Komano, J. and Sugden, B. (2003) Epstein-Barr virus provides a survival factor to Burkitt's lymphomas. *Proc Natl Acad Sci U S A*, **100**, 14269-14274.

Khanna, R., Bell, S., Sherritt, M., Galbraith, A., Burrows, S.R., Rafter, L., Clarke, B., Slaughter, R., Falk, M.C., Douglass, J., Williams, T., Elliott, S.L. and Moss, D.J. (1999) Activation and adoptive transfer of Epstein-Barr virus-specific cytotoxic T cells in solid organ transplant patients with posttransplant lymphoproliferative disease. *Proc Natl Acad Sci U S A*, **96**, 10391-10396.

Khanna, R., Burrows, S.R., Kurilla, M.G., Jacob, C.A., Misko, I.S., Sculley, T.B., Kieff, E. and Moss, D.J. (1992) Localization of Epstein-Barr virus cytotoxic T cell epitopes using recombinant vaccinia: implications for vaccine development. *J Exp Med*, **176**, 169-176.

Kiani, A., Garcia-Cozar, F.J., Habermann, I., Laforsch, S., Aebischer, T., Ehninger, G. and Rao, A. (2001) Regulation of interferon-gamma gene expression by nuclear factor of activated T cells. *Blood*, **98**, 1480-1488.

Kiani, A., Rao, A. and Aramburu, J. (2000) Manipulating immune responses with immunosuppressive agents that target NFAT. *Immunity*, **12**, 359-372.

Kieff, E.a. and Rickinson, A.B. (2001) Epstein-Barr Virus and Its Replication. In Knipe, D.M., Howley, P. M., Griffin, D. E., Lamb, R. A., Martin, A., Roizman, B. and Straus, S. E. (ed.), *Fields Virology*. Lippincott Williams and Wilkins, Philadelphia, Vol. 2, pp. 2511-2574.

Kim, D.H., Sarbassov, D.D., Ali, S.M., King, J.E., Latek, R.R., Erdjument-Bromage, H., Tempst, P. and Sabatini, D.M. (2002) mTOR interacts with raptor to form a nutrient-sensitive complex that signals to the cell growth machinery. *Cell*, **110**, 163-175.

Kinsella, T.M. and Nolan, G.P. (1996) Episomal vectors rapidly and stably produce high-titer recombinant retrovirus. *Hum Gene Ther*, **7**, 1405-1413.

Kiziroglu, F. and Miller, R.G. (1990) Direct effect of cyclosporin A on CD8+ T lymphocytes in a primary mixed lymphocyte reaction. *Immunol Lett*, **24**, 77-86.

Koffman, B.H., Kennedy, A.S., Heyman, M., Colonna, J. and Howell, C. (2000) Use of radiation therapy in posttransplant lymphoproliferative disorder (PTLD) after liver transplantation. *Int J Cancer*, **90**, 104-109.

Kohn, D.B., Sadelain, M., Dunbar, C., Bodine, D., Kiem, H.P., Candotti, F., Tisdale, J., Riviere, I., Blau, C.A., Richard, R.E., Sorrentino, B., Nolta, J., Malech, H., Brenner, M., Cornetta, K., Cavagnaro, J., High, K. and Glorioso, J. (2003) American Society of Gene Therapy (ASGT) ad hoc subcommittee on retroviral-mediated gene transfer to hematopoietic stem cells. *Mol Ther*, **8**, 180-187.

Kotani, H., Newton, P.B., 3rd, Zhang, S., Chiang, Y.L., Otto, E., Weaver, L., Blaese, R.M., Anderson, W.F. and McGarrity, G.J. (1994) Improved methods of retroviral vector transduction and production for gene therapy. *Hum Gene Ther*, **5**, 19-28.

Koyasu, S. (2003) The role of PI3K in immune cells. *Nat Immunol*, **4**, 313-319.

Kuehnle, I., Huls, M.H., Liu, Z., Semmelmann, M., Krance, R.A., Brenner, M.K., Rooney, C.M. and Heslop, H.E. (2000) CD20 monoclonal antibody (rituximab) for therapy of Epstein-Barr virus lymphoma after hemopoietic stem-cell transplantation. *Blood*, **95**, 1502-1505.

Kurts, C., Kosaka, H., Carbone, F.R., Miller, J.F. and Heath, W.R. (1997) Class I-restricted cross-presentation of exogenous self-antigens leads to deletion of autoreactive CD8(+) T cells. *J Exp Med*, **186**, 239-245.

Kwong, Y.L., Chan, A.C. and Liang, R.H. (1997) Natural killer cell lymphoma/leukemia: pathology and treatment. *Hematol Oncol*, **15**, 71-79.

Lam, J.S., Reeves, M.E., Cowherd, R., Rosenberg, S.A. and Hwu, P. (1996) Improved gene transfer into human lymphocytes using retroviruses with the gibbon ape leukemia virus envelope. *Hum Gene Ther*, **7**, 1415-1422.

Laver, W.G. (1984) Antigenic variation and the structure of influenza virus glycoproteins. *Microbiol Sci*, **1**, 37-43.

Lever, A.M. (2000) Lentiviral vectors: progress and potential. *Curr Opin Mol Ther*, **2**, 488-496.

Li, Y., Corradetti, M.N., Inoki, K. and Guan, K.L. (2004a) TSC2: filling the GAP in the mTOR signaling pathway. *Trends Biochem Sci*, **29**, 32-38.

Li, Y., Inoki, K. and Guan, K.L. (2004b) Biochemical and functional characterizations of small GTPase Rheb and TSC2 GAP activity. *Mol Cell Biol*, **24**, 7965-7975.

Lin, X. and Barber, D.L. (1996) A calcineurin homologous protein inhibits GTPase-stimulated Na-H exchange. *Proc Natl Acad Sci U S A*, **93**, 12631-12636.

Liu, C.C., Persechini, P.M. and Young, J.D. (1995) Perforin and lymphocyte-mediated cytolysis. *Immunol Rev*, **146**, 145-175.

Liu, J., Farmer, J.D., Jr., Lane, W.S., Friedman, J., Weissman, I. and Schreiber, S.L. (1991) Calcineurin is a common target of cyclophilin-cyclosporin A and FKBP-FK506 complexes. *Cell*, **66**, 807-815.

Liu, K. and Rosenberg, S.A. (2001) Transduction of an IL-2 gene into human melanoma-reactive lymphocytes results in their continued growth in the

absence of exogenous IL-2 and maintenance of specific antitumor activity. *J Immunol*, **167**, 6356-6365.

LoGrasso, P.V., Hawkins, J., Frank, L.J., Wisniewski, D. and Marcy, A. (1996) Mechanism of activation for Zap-70 catalytic activity. *Proc Natl Acad Sci U S A*, **93**, 12165-12170.

Loren, A.W., Porter, D.L., Stadtmauer, E.A. and Tsai, D.E. (2003) Post-transplant lymphoproliferative disorder: a review. *Bone Marrow Transplant*, **31**, 145-155.

Lu, J., Giuntoli, R.L., 2nd, Omiya, R., Kobayashi, H., Kennedy, R. and Celis, E. (2002) Interleukin 15 promotes antigen-independent in vitro expansion and long-term survival of antitumor cytotoxic T lymphocytes. *Clin Cancer Res*, **8**, 3877-3884.

Lu, Y., Granelli-Piperno, A., Bjorndahl, J.M., Phillips, C.A. and Trevillyan, J.M. (1992) CD28-induced T cell activation. Evidence for a protein-tyrosine kinase signal transduction pathway. *J Immunol*, **149**, 24-29.

Lucan, M., Iacob, G., Lucan, C., Lapusan, C., Munteanu, A. and Sirbu, S. (2004) Ten years of cyclosporine use in renal transplantation: a single-center experience with 479 renal transplants. *Transplant Proc*, **36**, 177S-180S.

Lundorf, M.D., Pedersen, F.S., O'Hara, B. and Pedersen, L. (1999) Amphotropic murine leukemia virus entry is determined by specific combinations of residues from receptor loops 2 and 4. *J Virol*, **73**, 3169-3175.

Lundstrom, K. (2003) Latest development in viral vectors for gene therapy. *Trends Biotechnol*, **21**, 117-122.

Lynch, D.H. and Miller, R.E. (1994) Interleukin 7 promotes long-term in vitro growth of antitumor cytotoxic T lymphocytes with immunotherapeutic efficacy in vivo. *J Exp Med*, **179**, 31-42.

Mackinnon, S., Papadopoulos, E.B., Carabasi, M.H., Reich, L., Collins, N.H., Boulad, F., Castro-Malaspina, H., Childs, B.H., Gillio, A.P., Kernan, N.A. and et al. (1995) Adoptive immunotherapy evaluating escalating doses of donor leukocytes for relapse of chronic myeloid leukemia after bone marrow transplantation: separation of graft-versus-leukemia responses from graft-versus-host disease. *Blood*, **86**, 1261-1268.

Majewski, M., Korecka, M., Kossev, P., Li, S., Goldman, J., Moore, J., Silberstein, L.E., Nowell, P.C., Schuler, W., Shaw, L.M. and Wasik, M.A. (2000) The immunosuppressive macrolide RAD inhibits growth of human Epstein-Barr virus-transformed B lymphocytes in vitro and in vivo: A potential approach to prevention and treatment of posttransplant lymphoproliferative disorders. *Proc Natl Acad Sci U S A*, **97**, 4285-4290.

Malek, T.R. and Bayer, A.L. (2004) Tolerance, not immunity, crucially depends on IL-2. *Nat Rev Immunol*, **4**, 665-674.

Maloney, D.G. (2001) Mechanism of action of rituximab. *Anticancer Drugs*, **12 Suppl 2**, S1-4.

Mann, R., Mulligan, R.C. and Baltimore, D. (1983) Construction of a retrovirus packaging mutant and its use to produce helper-free defective retrovirus. *Cell*, **33**, 153-159.

Markowitz, D., Goff, S. and Bank, A. (1988) Construction and use of a safe and efficient amphotropic packaging cell line. *Virology*, **167**, 400-406.

Martinez-Martinez, S. and Redondo, J.M. (2004) Inhibitors of the calcineurin/NFAT pathway. *Curr Med Chem*, **11**, 997-1007.

Matloubian, M., Concepcion, R.J. and Ahmed, R. (1994) CD4+ T cells are required to sustain CD8+ cytotoxic T-cell responses during chronic viral infection. *J Virol*, **68**, 8056-8063.

Maus, M.V., Thomas, A.K., Leonard, D.G., Allman, D., Addya, K., Schlienger, K., Riley, J.L. and June, C.H. (2002) Ex vivo expansion of polyclonal and antigen-specific cytotoxic T lymphocytes by artificial APCs expressing ligands for the T-cell receptor, CD28 and 4-1BB. *Nat Biotechnol*, **20**, 143-148.

Mavilio, F., Ferrari, G., Rossini, S., Nobili, N., Bonini, C., Casorati, G., Traversari, C. and Bordignon, C. (1994) Peripheral blood lymphocytes as target cells of retroviral vector-mediated gene transfer. *Blood*, **83**, 1988-1997.

McCormack, M.P. and Rabbitts, T.H. (2004) Activation of the T-cell oncogene LMO2 after gene therapy for X-linked severe combined immunodeficiency. *N Engl J Med*, **350**, 913-922.

McMahon, L.P., Choi, K.M., Lin, T.A., Abraham, R.T. and Lawrence, J.C., Jr. (2002) The rapamycin-binding domain governs substrate selectivity by the mammalian target of rapamycin. *Mol Cell Biol*, **22**, 7428-7438.

Meyers, J.D., Flournoy, N. and Thomas, E.D. (1986) Risk factors for cytomegalovirus infection after human marrow transplantation. *J Infect Dis*, **153**, 478-488.

Miller, A.D. and Wolgamot, G. (1997) Murine retroviruses use at least six different receptors for entry into Mus dunni cells. *J Virol*, **71**, 4531-4535.

Miller, D.G., Adam, M.A. and Miller, A.D. (1990a) Gene transfer by retrovirus vectors occurs only in cells that are actively replicating at the time of infection. *Mol Cell Biol*, **10**, 4239-4242.

Miller, D.G., Edwards, R.H. and Miller, A.D. (1994) Cloning of the cellular receptor for amphotropic murine retroviruses reveals homology to that for gibbon ape leukemia virus. *Proc Natl Acad Sci U S A*, **91**, 78-82.

Miller, M., Kennewell, A., Takayama, Y., Bruskin, A., Bishop, J.M., Johnson, G. and Symonds, G. (1990b) Transformation of early erythroid precursor cells (BFU-E) by a recombinant murine retrovirus containing v-erb-B. *Oncogene*, **5**, 1125-1131.

Minami, Y., Kono, T., Miyazaki, T. and Taniguchi, T. (1993) The IL-2 receptor complex: its structure, function, and target genes. *Annu Rev Immunol*, **11**, 245-268.

Miyatake, S., Shlomai, J., Arai, K. and Arai, N. (1991) Characterization of the mouse granulocyte-macrophage colony-stimulating factor (GM-CSF) gene promoter: nuclear factors that interact with an element shared by three lymphokine genes--those for GM-CSF, interleukin-4 (IL-4), and IL-5. *Mol Cell Biol*, **11**, 5894-5901.

Moien-Afshari, F., McManus, B.M. and Laher, I. (2003) Immunosuppression and transplant vascular disease: benefits and adverse effects. *Pharmacol Ther*, **100**, 141-156.

Moon, J.J. and Nelson, B.H. (2001) Phosphatidylinositol 3-kinase potentiates, but does not trigger, T cell proliferation mediated by the IL-2 receptor. *J Immunol*, **167**, 2714-2723.

Morgenstern, J.P. and Land, H. (1990) Advanced mammalian gene transfer: high titre retroviral vectors with multiple drug selection markers and a complementary helper-free packaging cell line. *Nucleic Acids Res*, **18**, 3587-3596.

Mountain, A. (2000) Gene therapy: the first decade. *Trends Biotechnol*, **18**, 119-128.

Movassagh, M., Boyer, O., Burland, M.C., Leclercq, V., Klatzmann, D. and Lemoine, F.M. (2000) Retrovirus-mediated gene transfer into T cells: 95% transduction efficiency without further in vitro selection. *Hum Gene Ther*, **11**, 1189-1200.

Muallem, S. (1989) Calcium transport pathways of pancreatic acinar cells. *Annu Rev Physiol*, **51**, 83-105.

Muniappan, A., Banapour, B., Lebkowski, J. and Talib, S. (2000) Ligand-mediated cytolysis of tumor cells: use of heregulin-zeta chimeras to redirect cytotoxic T lymphocytes. *Cancer Gene Ther*, **7**, 128-134.

Muul, L.M., Tuschong, L.M., Soenen, S.L., Jagadeesh, G.J., Ramsey, W.J., Long, Z., Carter, C.S., Garabedian, E.K., Alleyne, M., Brown, M., Bernstein, W., Schurman, S.H., Fleisher, T.A., Leitman, S.F., Dunbar, C.E., Blaese, R.M. and Candotti, F. (2003) Persistence and expression of the adenosine deaminase gene for 12 years and immune reaction to gene transfer components: long-term results of the first clinical gene therapy trial. *Blood*, **101**, 2563-2569.

Nagel, W., Zeitlmann, L., Schilcher, P., Geiger, C., Kolanus, J. and Kolanus, W. (1998) Phosphoinositide 3-OH kinase activates the beta2 integrin adhesion pathway and induces membrane recruitment of cytohesin-1. *J Biol Chem*, **273**, 14853-14861.

Nakanishi, S., Catt, K.J. and Balla, T. (1995) A wortmannin-sensitive phosphatidylinositol 4-kinase that regulates hormone-sensitive pools of inositolphospholipids. *Proc Natl Acad Sci U S A*, **92**, 5317-5321.

Nalesnik, M.A., Jaffe, R., Starzl, T.E., Demetris, A.J., Porter, K., Burnham, J.A., Makowka, L., Ho, M. and Locker, J. (1988) The pathology of posttransplant lymphoproliferative disorders occurring in the setting of cyclosporine A-prednisone immunosuppression. *Am J Pathol*, **133**, 173-192.

Nelson, B.H. and Willerford, D.M. (1998) Biology of the interleukin-2 receptor. *Adv Immunol*, **70**, 1-81.

Nemerow, G.R. and Cooper, N.R. (1984) Early events in the infection of human B lymphocytes by Epstein-Barr virus: the internalization process. *Virology*, **132**, 186-198.

nmVerzeletti, S., Bonini, C., Marktel, S., Nobili, N., Ciceri, F., Traversari, C. and Bordignon, C. (1998) Herpes simplex virus thymidine kinase gene transfer for controlled graft-versus-host disease and graft-versus-leukemia: clinical follow-up and improved new vectors. *Hum Gene Ther*, **9**, 2243-2251.

Nossal, G.J. (1994) Negative selection of lymphocytes. *Cell*, **76**, 229-239.

Nunes, J., Klasen, S., Ragueneau, M., Pavon, C., Couez, D., Mawas, C., Bagnasco, M. and Olive, D. (1993) CD28 mAbs with distinct binding properties differ in their ability to induce T cell activation: analysis of early and late activation events. *Int Immunol*, **5**, 311-315.

Nunes, J.A., Collette, Y., Truneh, A., Olive, D. and Cantrell, D.A. (1994) The role of p21ras in CD28 signal transduction: triggering of CD28 with antibodies, but not the ligand B7-1, activates p21ras. *J Exp Med*, **180**, 1067-1076.

Oehen, S. and Brduscha-Riem, K. (1999) Naive cytotoxic T lymphocytes spontaneously acquire effector function in lymphocytopenic recipients: A pitfall for T cell memory studies? *Eur J Immunol*, **29**, 608-614.

Ohno, H., Aguilar, R.C., Fournier, M.C., Hennecke, S., Cosson, P. and Bonifacino, J.S. (1997) Interaction of endocytic signals from the HIV-1 envelope glycoprotein complex with members of the adaptor medium chain family. *Virology*, **238**, 305-315.

Okkenhaug, K., Bilancio, A., Farjot, G., Priddle, H., Sancho, S., Peskett, E., Pearce, W., Meek, S.E., Salpekar, A., Waterfield, M.D., Smith, A.J. and Vanhaesebroeck, B. (2002) Impaired B and T cell antigen receptor signaling in p110delta PI 3-kinase mutant mice. *Science*, **297**, 1031-1034.

Okkenhaug, K. and Vanhaesebroeck, B. (2003a) PI3K in lymphocyte development, differentiation and activation. *Nat Rev Immunol*, **3**, 317-330.

Okkenhaug, K. and Vanhaesebroeck, B. (2003b) PI3K-signalling in B- and T-cells: insights from gene-targeted mice. *Biochem Soc Trans*, **31**, 270-274.

Okkenhaug, K., Wu, L., Garza, K.M., La Rose, J., Khoo, W., Odermatt, B., Mak, T.W., Ohashi, P.S. and Rottapel, R. (2001) A point mutation in CD28 distinguishes proliferative signals from survival signals. *Nat Immunol*, **2**, 325-332.

Oshiro, N., Yoshino, K., Hidayat, S., Tokunaga, C., Hara, K., Eguchi, S., Avruch, J. and Yonezawa, K. (2004) Dissociation of raptor from mTOR is a mechanism of rapamycin-induced inhibition of mTOR function. *Genes Cells*, **9**, 359-366.

Papadopoulos, E.B., Ladanyi, M., Emanuel, D., Mackinnon, S., Boulad, F., Carabasi, M.H., Castro-Malaspina, H., Childs, B.H., Gillio, A.P., Small, T.N. and et al. (1994) Infusions of donor leukocytes to treat Epstein-Barr virus-associated lymphoproliferative disorders after allogeneic bone marrow transplantation. *N Engl J Med*, **330**, 1185-1191.

Paul, R.W., Morris, D., Hess, B.W., Dunn, J. and Overell, R.W. (1993) Increased viral titer through concentration of viral harvests from retroviral packaging lines. *Hum Gene Ther*, **4**, 609-615.

Paya, C.V., Fung, J.J., Nalesnik, M.A., Kieff, E., Green, M., Gores, G., Habermann, T.M., Wiesner, P.H., Swinnen, J.L., Woodle, E.S. and Bromberg, J.S. (1999) Epstein-Barr virus-induced posttransplant lymphoproliferative disorders. ASTS/ASTP EBV-PTLD Task Force and The Mayo Clinic Organized International Consensus Development Meeting. *Transplantation*, **68**, 1517-1525.

Peterson, R.T., Beal, P.A., Comb, M.J. and Schreiber, S.L. (2000) FKBP12-rapamycin-associated protein (FRAP) autophosphorylates at serine 2481 under translationally repressive conditions. *J Biol Chem*, **275**, 7416-7423.

Pflugl, G., Kallen, J., Schirmer, T., Jansonius, J.N., Zurini, M.G. and Walkinshaw, M.D. (1993) X-ray structure of a decameric cyclophilin-cyclosporin crystal complex. *Nature*, **361**, 91-94.

Piccirillo, C.A., Letterio, J.J., Thornton, A.M., McHugh, R.S., Mamura, M., Mizuhara, H. and Shevach, E.M. (2002) CD4(+)CD25(+) regulatory T cells

can mediate suppressor function in the absence of transforming growth factor beta1 production and responsiveness. *J Exp Med*, **196**, 237-246.

Pollok, K.E., Hanenberg, H., Noblitt, T.W., Schroeder, W.L., Kato, I., Emanuel, D. and Williams, D.A. (1998) High-efficiency gene transfer into normal and adenosine deaminase-deficient T lymphocytes is mediated by transduction on recombinant fibronectin fragments. *J Virol*, **72**, 4882-4892.

Porter, C.M. and Clipstone, N.A. (2002) Sustained NFAT signaling promotes a Th1-like pattern of gene expression in primary murine CD4+ T cells. *J Immunol*, **168**, 4936-4945.

Porter, D.L., Orloff, G.J. and Antin, J.H. (1994) Donor mononuclear cell infusions as therapy for B-cell lymphoproliferative disorder following allogeneic bone marrow transplant. *Transplant Sci*, **4**, 12-14; discussion 14-16.

Powell, J.D., Ragheb, J.A., Kitagawa-Sakakida, S. and Schwartz, R.H. (1998) Molecular regulation of interleukin-2 expression by CD28 co-stimulation and anergy. *Immunol Rev*, **165**, 287-300.

Powers, T. and Walter, P. (1999) Regulation of ribosome biogenesis by the rapamycin-sensitive TOR-signaling pathway in Saccharomyces cerevisiae. *Mol Biol Cell*, **10**, 987-1000.

Prilliman, K.R., Lemmens, E.E., Palioungas, G., Wolfe, T.G., Allison, J.P., Sharpe, A.H. and Schoenberger, S.P. (2002) Cutting edge: a crucial role for B7-CD28 in transmitting T help from APC to CTL. *J Immunol*, **169**, 4094-4097.

Pringle, C.R. (1999) Virus taxonomy--1999. The universal system of virus taxonomy, updated to include the new proposals ratified by the International Committee on Taxonomy of Viruses during 1998. *Arch Virol*, **144**, 421-429.

Prota, A.E., Sage, D.R., Stehle, T. and Fingeroth, J.D. (2002) The crystal structure of human CD21: Implications for Epstein-Barr virus and C3d binding. *Proc Natl Acad Sci U S A*, **99**, 10641-10646.

Puppo, F., Contini, P., Ghio, M. and Indiveri, F. (2002) Soluble HLA class I molecules/CD8 ligation trigger apoptosis of CD8+ cells by Fas/Fas-ligand interaction. *ScientificWorldJournal*, **2**, 421-423.

Radvanyi, L.G., Shi, Y., Vaziri, H., Sharma, A., Dhala, R., Mills, G.B. and Miller, R.G. (1996) CD28 costimulation inhibits TCR-induced apoptosis during a primary T cell response. *J Immunol*, **156**, 1788-1798.

Rao, A., Luo, C. and Hogan, P.G. (1997) Transcription factors of the NFAT family: regulation and function. *Annu Rev Immunol*, **15**, 707-747.

Rickinson, A.B. and Moss, D.J. (1997) Human cytotoxic T lymphocyte responses to Epstein-Barr virus infection. *Annu Rev Immunol*, **15**, 405-431.

Rickinson, A.B.a. and Kieff, E. (2001) Epstein-Barr Virus. In Knipe, D.M., Howley, P. M., Griffin, D. E., Lamb, R. A., Martin, A., Roizman, B. and Straus, S. E. (ed.), *Fields Virology*. Lippincott Williams and Wilkins, Philadelphia, Vol. 2, pp. 2575-2628.

Riddell, S.R., Elliott, M., Lewinsohn, D.A., Gilbert, M.J., Wilson, L., Manley, S.A., Lupton, S.D., Overell, R.W., Reynolds, T.C., Corey, L. and Greenberg, P.D. (1996a) T-cell mediated rejection of gene-modified HIV-specific cytotoxic T lymphocytes in HIV-infected patients. *Nat Med*, **2**, 216-223.

Riddell, S.R., Elliott, M., Lewinsohn, D.A., Gilbert, M.J., Wilson, L., Manley, S.A., Lupton, S.D., Overell, R.W., Reynolds, T.C., Corey, L. and Greenberg, P.D.

(1996b) T-cell mediated rejection of gene-modified HIV-specific cytotoxic T lymphocytes in HIV-infected patients [see comments]. *Nat Med*, **2**, 216-223.

Riddell, S.R., Greenberg, P.D., Overell, R.W., Loughran, T.P., Gilbert, M.J., Lupton, S.D., Agosti, J., Scheeler, S., Coombs, R.W. and Corey, L. (1992a) Phase I study of cellular adoptive immunotherapy using genetically modified CD8+ HIV-specific T cells for HIV seropositive patients undergoing allogeneic bone marrow transplant. The Fred Hutchinson Cancer Research Center and the University of Washington School of Medicine, Department of Medicine, Division of Oncology. *Hum Gene Ther*, **3**, 319-338.

Riddell, S.R., Warren, E.H., Lewinsohn, D., Mutimer, H., Topp, M., Cooper, L., de Fries, R. and Greenberg, P.D. (2000) Application of T cell immunotherapy for human viral and malignant diseases. *Ernst Schering Res Found Workshop*, 53-73.

Riddell, S.R., Watanabe, K.S., Goodrich, J.M., Li, C.R., Agha, M.E. and Greenberg, P.D. (1992b) Restoration of viral immunity in immunodeficient humans by the adoptive transfer of T cell clones. *Science*, **257**, 238-241.

Riviere, I., Gallardo, H.F., Hagani, A.B. and Sadelain, M. (2000) Retroviral-mediated gene transfer in primary murine and human T-lymphocytes. *Mol Biotechnol*, **15**, 133-142.

Robbins, P.D. and Ghivizzani, S.C. (1998) Viral vectors for gene therapy. *Pharmacol Ther*, **80**, 35-47.

Rodrigues, P. and Heard, J.M. (1999) Modulation of phosphate uptake and amphotropic murine leukemia virus entry by posttranslational modifications of PIT-2. *J Virol*, **73**, 3789-3799.

Roe, T., Reynolds, T.C., Yu, G. and Brown, P.O. (1993) Integration of murine leukemia virus DNA depends on mitosis. *Embo J*, **12**, 2099-2108.

Romagnani, S. (1991) Type 1 T helper and type 2 T helper cells: functions, regulation and role in protection and disease. *Int J Clin Lab Res*, **21**, 152-158.

Rooney, C., Smith, C., Ng, C., Loftin, S., Sixbey, J., Gan, Y., Srivastava, D., Bowman, L., Krance, R., Brenner, M. and Heslop, H. (1998a) Infusion of cytotoxic T cells for the prevention and treatment of Epstein-Barr virus-induced lymphoma in allogeneic transplant recipients. *Blood*, **92**, 1549-1555.

Rooney, C.M., Roskrow, M.A., Suzuki, N., Ng, C.Y., Brenner, M.K. and Heslop, H. (1998b) Treatment of relapsed Hodgkin's disease using EBV-specific cytotoxic T cells. *Ann Oncol*, **9 Suppl 5**, S129-132.

Rooney, C.M., Smith, C.A., Ng, C.Y., Loftin, S., Li, C., Krance, R.A., Brenner, M.K. and Heslop, H.E. (1995a) Use of gene-modified virus-specific T lymphocytes to control Epstein-Barr-virus-related lymphoproliferation. *Lancet*, **345**, 9-13.

Rooney, C.M., Smith, C.A., Ng, C.Y., Loftin, S.K., Sixbey, J.W., Gan, Y., Srivastava, D.K., Bowman, L.C., Krance, R.A., Brenner, M.K. and Heslop, H.E. (1998c) Infusion of cytotoxic T cells for the prevention and treatment of Epstein-Barr virus-induced lymphoma in allogeneic transplant recipients. *Blood*, **92**, 1549-1555.

Rooney, J.W., Sun, Y.L., Glimcher, L.H. and Hoey, T. (1995b) Novel NFAT sites that mediate activation of the interleukin-2 promoter in response to T-cell receptor stimulation. *Mol Cell Biol*, **15**, 6299-6310.

Roskrow, M.A., Suzuki, N., Gan, Y., Sixbey, J.W., Ng, C.Y., Kimbrough, S., Hudson, M., Brenner, M.K., Heslop, H.E. and Rooney, C.M. (1998) Epstein-Barr virus (EBV)-specific cytotoxic T lymphocytes for the treatment of patients with EBV-positive relapsed Hodgkin's disease. *Blood*, **91**, 2925-2934.

Rowe, M., Lear, A.L., Croom-Carter, D., Davies, A.H. and Rickinson, A.B. (1992) Three pathways of Epstein-Barr virus gene activation from EBNA1-positive latency in B lymphocytes. *J Virol*, **66**, 122-131.

Rowe, M., Niedobitek, G. and Young, L.S. (1998) Epstein-Barr virus gene expression in post-transplant lymphoproliferative disorders. *Springer Semin Immunopathol*, **20**, 389-403.

Rowell, J.F., Stanhope, P.E. and Siliciano, R.F. (1995) Endocytosis of endogenously synthesized HIV-1 envelope protein. Mechanism and role in processing for association with class II MHC. *J Immunol*, **155**, 473-488.

Rusnak, F. and Mertz, P. (2000) Calcineurin: form and function. *Physiol Rev*, **80**, 1483-1521.

Sadhu, C., Dick, K., Tino, W.T. and Staunton, D.E. (2003a) Selective role of PI3K delta in neutrophil inflammatory responses. *Biochem Biophys Res Commun*, **308**, 764-769.

Sadhu, C., Masinovsky, B., Dick, K., Sowell, C.G. and Staunton, D.E. (2003b) Essential role of phosphoinositide 3-kinase delta in neutrophil directional movement. *J Immunol*, **170**, 2647-2654.

Sadlack, B., Merz, H., Schorle, H., Schimpl, A., Feller, A.C. and Horak, I. (1993) Ulcerative colitis-like disease in mice with a disrupted interleukin-2 gene. *Cell*, **75**, 253-261.

Saemann, M.D., Zeyda, M., Stulnig, T.M., Bohmig, G.A., Wekerle, T., Horl, W.H. and Zlabinger, G.J. (2004) Janus kinase-3 (JAK3) inhibition: a novel immunosuppressive option for allogeneic transplantation. *Transpl Int*, **17**, 481-489.

Sakaguchi, S., Toda, M., Asano, M., Itoh, M., Morse, S.S. and Sakaguchi, N. (1996) T cell-mediated maintenance of natural self-tolerance: its breakdown as a possible cause of various autoimmune diseases. *J Autoimmun*, **9**, 211-220.

Salaun, C., Rodrigues, P. and Heard, J.M. (2001) Transmembrane topology of PiT-2, a phosphate transporter-retrovirus receptor. *J Virol*, **75**, 5584-5592.

Saoulli, K., Lee, S.Y., Cannons, J.L., Yeh, W.C., Santana, A., Goldstein, M.D., Bangia, N., DeBenedette, M.A., Mak, T.W., Choi, Y. and Watts, T.H. (1998) CD28-independent, TRAF2-dependent costimulation of resting T cells by 4-1BB ligand. *J Exp Med*, **187**, 1849-1862.

Sauce, D., Bodinier, M., Garin, M., Petracca, B., Tonnelier, N., Duperrier, A., Melo, J.V., Apperley, J.F., Ferrand, C., Herve, P., Lang, F., Tiberghien, P. and Robinet, E. (2002) Retrovirus-mediated gene transfer in primary T lymphocytes impairs their anti-Epstein-Barr virus potential through both culture-dependent and selection process-dependent mechanisms. *Blood*, **99**, 1165-1173.

Savoldo, B., Goss, J., Liu, Z., Huls, M.H., Doster, S., Gee, A.P., Brenner, M.K., Heslop, H.E. and Rooney, C.M. (2001) Generation of autologous Epstein-Barr virus-specific cytotoxic T cells for adoptive immunotherapy in solid organ transplant recipients. *Transplantation*, **72**, 1078-1086.

Scheid, M.P. and Woodgett, J.R. (2001) PKB/AKT: functional insights from genetic models. *Nat Rev Mol Cell Biol*, **2**, 760-768.

Schmouder, R.L. (2000) Immunosuppressive therapies for the twenty-first century. *Transplant Proc*, **32**, 1463-1467.

Schreiber, S.L. and Crabtree, G.R. (1992) The mechanism of action of cyclosporin A and FK506. *Immunol Today*, **13**, 136-142.

Schwartz, R., Eisner, A. and Dameshek, W. (1959) The effect of 6-mercaptopurine on primary and secondary immune responses. *J Clin Invest*, **38**, 1394-1403.

Schweitzer, A.N., Borriello, F., Wong, R.C., Abbas, A.K. and Sharpe, A.H. (1997) Role of costimulators in T cell differentiation: studies using antigen-presenting cells lacking expression of CD80 or CD86. *J Immunol*, **158**, 2713-2722.

Sehgal, S.N., Baker, H. and Vezina, C. (1975) Rapamycin (AY-22,989), a new antifungal antibiotic. II. Fermentation, isolation and characterization. *J Antibiot (Tokyo)*, **28**, 727-732.

Sherr, C.J. (1996) Cancer cell cycles. *Science*, **274**, 1672-1677.

Siegel, M.D., Zhang, D.H., Ray, P. and Ray, A. (1995) Activation of the interleukin-5 promoter by cAMP in murine EL-4 cells requires the GATA-3 and CLE0 elements. *J Biol Chem*, **270**, 24548-24555.

Smith, C.A., Ng, C.Y., Heslop, H.E., Holladay, M.S., Richardson, S., Turner, E.V., Loftin, S.K., Li, C., Brenner, M.K. and Rooney, C.M. (1995) Production of genetically modified Epstein-Barr virus-specific cytotoxic T cells for adoptive transfer to patients at high risk of EBV-associated lymphoproliferative disease. *J Hematother*, **4**, 73-79.

Stan, R., McLaughlin, M.M., Cafferkey, R., Johnson, R.K., Rosenberg, M. and Livi, G.P. (1994) Interaction between FKBP12-rapamycin and TOR involves a conserved serine residue. *J Biol Chem*, **269**, 32027-32030.

Starzl, T.E., Fung, J., Jordan, M., Shapiro, R., Tzakis, A., McCauley, J., Johnston, J., Iwaki, Y., Jain, A., Alessiani, M. and et al. (1990) Kidney transplantation under FK 506. *Jama*, **264**, 63-67.

Starzl, T.E., Nalesnik, M.A., Porter, K.A., Ho, M., Iwatsuki, S., Griffith, B.P., Rosenthal, J.T., Hakala, T.R., Shaw, B.W., Jr. and Hardesty, R.L. (1984) Reversibility of lymphomas and lymphoproliferative lesions developing under cyclosporin-steroid therapy. *Lancet*, **1**, 583-587.

Stassen, M., Jonuleit, H., Muller, C., Klein, M., Richter, C., Bopp, T., Schmitt, S. and Schmitt, E. (2004) Differential regulatory capacity of CD25+ T regulatory cells and preactivated CD25+ T regulatory cells on development, functional activation, and proliferation of Th2 cells. *J Immunol*, **173**, 267-274.

Steinman, R.M., Hawiger, D., Liu, K., Bonifaz, L., Bonnyay, D., Mahnke, K., Iyoda, T., Ravetch, J., Dhodapkar, M., Inaba, K. and Nussenzweig, M. (2003) Dendritic cell function in vivo during the steady state: a role in peripheral tolerance. *Ann N Y Acad Sci*, **987**, 15-25.

Steven, N.M., Leese, A.M., Annels, N.E., Lee, S.P. and Rickinson, A.B. (1996) Epitope focusing in the primary cytotoxic T cell response to Epstein-Barr virus and its relationship to T cell memory. *J Exp Med*, **184**, 1801-1813.

Stocker, H., Andjelkovic, M., Oldham, S., Laffargue, M., Wymann, M.P., Hemmings, B.A. and Hafen, E. (2002) Living with lethal PIP3 levels:

viability of flies lacking PTEN restored by a PH domain mutation in Akt/PKB. *Science*, **295**, 2088-2091.

Stockschlader, M., Haiss, M., Exner, S., Schmah, O., Veelken, H., Follo, M., Ruger, R. and Finke, J. (1999) Expansion and fibronectin-enhanced retroviral transduction of primary human T lymphocytes for adoptive immunotherapy. *J Hematother Stem Cell Res*, **8**, 401-410.

Straathof, K.C., Bollard, C.M., Rooney, C.M. and Heslop, H.E. (2003) Immunotherapy for Epstein-Barr virus-associated cancers in children. *Oncologist*, **8**, 83-98.

Sugiura, R., Sio, S.O., Shuntoh, H. and Kuno, T. (2001) Molecular genetic analysis of the calcineurin signaling pathways. *Cell Mol Life Sci*, **58**, 278-288.

Sun, Q., Burton, R.L. and Lucas, K.G. (2002) Cytokine production and cytolytic mechanism of CD4(+) cytotoxic T lymphocytes in ex vivo expanded therapeutic Epstein-Barr virus-specific T-cell cultures. *Blood*, **99**, 3302-3309.

Suzuki, H., Terauchi, Y., Fujiwara, M., Aizawa, S., Yazaki, Y., Kadowaki, T. and Koyasu, S. (1999) Xid-like immunodeficiency in mice with disruption of the p85alpha subunit of phosphoinositide 3-kinase. *Science*, **283**, 390-392.

Tanner, J.E. and Alfieri, C. (1996) Interactions involving cyclosporine A, interleukin-6, and Epstein-Barr virus lead to the promotion of B-cell lymphoproliferative disease. *Leuk Lymphoma*, **21**, 379-390.

Taylor, G.M. and Sanders, D.A. (2003) Structural criteria for regulation of membrane fusion and virion incorporation by the murine leukemia virus TM cytoplasmic domain. *Virology*, **312**, 295-305.

Temin, H.M. (1985) Reverse transcription in the eukaryotic genome: retroviruses, pararetroviruses, retrotransposons, and retrotranscripts. *Mol Biol Evol*, **2**, 455-468.

Temin, H.M. and Mizutani, S. (1970) RNA-dependent DNA polymerase in virions of Rous sarcoma virus. *Nature*, **226**, 1211-1213.

Thomas-Vaslin, V., Damotte, D., Coltey, M., Le Douarin, N.M., Coutinho, A. and Salaun, J. (1997) Abnormal T cell selection on nod thymic epithelium is sufficient to induce autoimmune manifestations in C57BL/6 athymic nude mice. *Proc Natl Acad Sci U S A*, **94**, 4598-4603.

Thomis, D.C., Marktel, S., Bonini, C., Traversari, C., Gilman, M., Bordignon, C. and Clackson, T. (2001) A Fas-based suicide switch in human T cells for the treatment of graft-versus-host disease. *Blood*, **97**, 1249-1257.

Thompson, M.P. and Kurzrock, R. (2004) Epstein-Barr virus and cancer. *Clin Cancer Res*, **10**, 803-821.

Thomson, A.W. (1992) The effects of cyclosporin A on non-T cell components of the immune system. *J Autoimmun*, **5 Suppl A**, 167-176.

Thorley-Lawson, D.A. (2001) Epstein-Barr virus: exploiting the immune system. *Nat Rev Immunol*, **1**, 75-82.

Tiberghien, P., Ferrand, C., Lioure, B., Milpied, N., Angonin, R., Deconinck, E., Certoux, J.M., Robinet, E., Saas, P., Petracca, B., Juttner, C., Reynolds, C.W., Longo, D.L., Herve, P. and Cahn, J.Y. (2001) Administration of herpes simplex-thymidine kinase-expressing donor T cells with a T-cell-depleted allogeneic marrow graft. *Blood*, **97**, 63-72.

Tierney, R.J., Steven, N., Young, L.S. and Rickinson, A.B. (1994) Epstein-Barr virus latency in blood mononuclear cells: analysis of viral gene transcription during primary infection and in the carrier state. *J Virol*, **68**, 7374-7385.

Tonks, A., Pearn, L., Tonks, A.J., Pearce, L., Hoy, T., Phillips, S., Fisher, J., Downing, J.R., Burnett, A.K. and Darley, R.L. (2003) The AML1-ETO fusion gene promotes extensive self-renewal of human primary erythroid cells. *Blood*, **101**, 624-632.

Tonks, A., Tonks, A.J., Pearn, L., Mohamad, Z., Burnett, A.K. and Darley, R.L. (2004) An optimised retroviral transduction protocol which preserves the self-renewing subpopulation of human haematopoietic cells. *Submitted for publication.*

Tsai, M.K., Chu, S.H., Hu, R.H., Chiang, Y.J., Chueh, S.C., Lai, M.K. and Lee, P.H. (2001) Renal transplantation with Simulect (basiliximab) plus Sandimmune Neoral-based immunosuppression: a report of 41 cases in Taiwan. *Transplant Proc*, **33**, 3194.

Uckert, W., Willimsky, G., Pedersen, F.S., Blankenstein, T. and Pedersen, L. (1998) RNA levels of human retrovirus receptors Pit1 and Pit2 do not correlate with infectibility by three retroviral vector pseudotypes. *Hum Gene Ther*, **9**, 2619-2627.

Ui, M., Okada, T., Hazeki, K. and Hazeki, O. (1995) Wortmannin as a unique probe for an intracellular signalling protein, phosphoinositide 3-kinase. *Trends Biochem Sci*, **20**, 303-307.

van den Broek, M.E., Kagi, D., Ossendorp, F., Toes, R., Vamvakas, S., Lutz, W.K., Melief, C.J., Zinkernagel, R.M. and Hengartner, H. (1996) Decreased tumor surveillance in perforin-deficient mice. *J Exp Med*, **184**, 1781-1790.

van der Loo, J.C., Liu, B.L., Goldman, A.I., Buckley, S.M. and Chrudimsky, K.S. (2002) Optimization of gene transfer into primitive human hematopoietic cells of granulocyte-colony stimulating factor-mobilized peripheral blood using low-dose cytokines and comparison of a gibbon ape leukemia virus versus an RD114-pseudotyped retroviral vector. *Hum Gene Ther*, **13**, 1317-1330.

van Mourik, I.D. and Kelly, D.A. (2001) Immunosuppressive drugs in paediatric liver transplantation. *Paediatr Drugs*, **3**, 43-60.

Vandenberghe, P., Freeman, G.J., Nadler, L.M., Fletcher, M.C., Kamoun, M., Turka, L.A., Ledbetter, J.A., Thompson, C.B. and June, C.H. (1992) Antibody and B7/BB1-mediated ligation of the CD28 receptor induces tyrosine phosphorylation in human T cells. *J Exp Med*, **175**, 951-960.

Vanhaesebroeck, B., Leevers, S.J., Ahmadi, K., Timms, J., Katso, R., Driscoll, P.C., Woscholski, R., Parker, P.J. and Waterfield, M.D. (2001) Synthesis and function of 3-phosphorylated inositol lipids. *Annu Rev Biochem*, **70**, 535-602.

Vezina, C., Kudelski, A. and Sehgal, S.N. (1975) Rapamycin (AY-22,989), a new antifungal antibiotic. I. Taxonomy of the producing streptomycete and isolation of the active principle. *J Antibiot (Tokyo)*, **28**, 721-726.

Vickers, A.E. (1994) Use of human organ slices to evaluate the biotransformation and drug-induced side-effects of pharmaceuticals. *Cell Biol Toxicol*, **10**, 407-414.

Vincenti, F. (2003) New monoclonal antibodies in renal transplantation. *Minerva Urol Nefrol*, **55**, 57-66.

Vincenti, F., Kirkman, R., Light, S., Bumgardner, G., Pescovitz, M., Halloran, P., Neylan, J., Wilkinson, A., Ekberg, H., Gaston, R., Backman, L. and Burdick, J. (1998) Interleukin-2-receptor blockade with daclizumab to prevent acute rejection in renal transplantation. Daclizumab Triple Therapy Study Group. *N Engl J Med*, **338**, 161-165.

Vlahos, C.J., Matter, W.F., Hui, K.Y. and Brown, R.F. (1994) A specific inhibitor of phosphatidylinositol 3-kinase, 2-(4-morpholinyl)-8-phenyl-4H-1-benzopyran-4-one (LY294002). *J Biol Chem*, **269**, 5241-5248.

Waegell, W., Babineau, M., Hart, M., Dixon, K., McRae, B., Wallace, C., Leach, M., Ratnofsky, S., Belanger, A., Hirst, G., Rossini, A., Appel, M., Mordes, J., Greiner, D. and Banerjee, S. (2002) A420983, a novel, small molecule inhibitor of LCK prevents allograft rejection. *Transplant Proc*, **34**, 1411-1417.

Wagner, H.J., Cheng, Y.C., Huls, M.H., Gee, A.P., Kuehnle, I., Krance, R.A., Brenner, M.K., Rooney, C.M. and Heslop, H.E. (2004) Prompt versus preemptive intervention for EBV lymphoproliferative disease. *Blood*, **103**, 3979-3981.

Wake, C.T. and Flavell, R. A. (1985). Multiple mechanisms regulate the expression of murine immune response genes. Cell, **42**, 623-8.

Waldmann, T.A., Dubois, S. and Tagaya, Y. (2001) Contrasting roles of IL-2 and IL-15 in the life and death of lymphocytes: implications for immunotherapy. *Immunity*, **14**, 105-110.

Wallis, C.V., Sheerin, A.N., Green, M.H., Jones, C.J., Kipling, D. and Faragher, R.G. (2004) Fibroblast clones from patients with Hutchinson-Gilford progeria can senesce despite the presence of telomerase. *Exp Gerontol*, **39**, 461-467.

Wang, Y., Brooks, S.R., Li, X., Anzelon, A.N., Rickert, R.C. and Carter, R.H. (2002) The physiologic role of CD19 cytoplasmic tyrosines. *Immunity*, **17**, 501-514.

Ward, S.G. (1996) CD28: a signalling perspective. *Biochem J*, **318 (Pt 2)**, 361-377.

Ward, S.G. and Cantrell, D.A. (2001) Phosphoinositide 3-kinases in T lymphocyte activation. *Curr Opin Immunol*, **13**, 332-338.

Ward, S.G. and Finan, P. (2003) Isoform-specific phosphoinositide 3-kinase inhibitors as therapeutic agents. *Curr Opin Pharmacol*, **3**, 426-434.

Watson, C.J., Friend, P.J., Jamieson, N.V., Frick, T.W., Alexander, G., Gimson, A.E. and Calne, R. (1999) Sirolimus: a potent new immunosuppressant for liver transplantation. *Transplantation*, **67**, 505-509.

Wei, M.Q., Lejnieks, D.V., Ramesh, N., Lau, S., Seppen, J. and Osborne, W.R. (1999) Sustained gene expression in transplanted skin fibroblasts in rats. *Gene Ther*, **6**, 840-844.

Wei, S.Q., Mizuuchi, K. and Craigie, R. (1998) Footprints on the viral DNA ends in moloney murine leukemia virus preintegration complexes reflect a specific association with integrase. *Proc Natl Acad Sci U S A*, **95**, 10535-10540.

Weiss, A. (1993) T cell antigen receptor signal transduction: a tale of tails and cytoplasmic protein-tyrosine kinases. *Cell*, **73**, 209-212.

Weiss, A., Wiskocil, R.L. and Stobo, J.D. (1984) The role of T3 surface molecules in the activation of human T cells: a two-stimulus requirement for IL 2 production reflects events occurring at a pre-translational level. *J Immunol*, **133**, 123-128.

Weiss, J., Schwinzer, B., Kirchner, H., Gemsa, D. and Resch, K. (1986) Effects of cyclosporin A on functions of specific murine T cell clones: inhibition of proliferation, lymphokine secretion and cytotoxicity. *Immunobiology*, **171**, 234-251.

Weissenhorn, W., Eck, M.J., Harrison, S.C. and Wiley, D.C. (1996) Phosphorylated T cell receptor zeta-chain and ZAP70 tandem SH2 domains form a 1:3 complex in vitro. *Eur J Biochem*, **238**, 440-445.

Weissman, I.L. (1994) Developmental switches in the immune system. *Cell*, **76**, 207-218.

Wenger, R. (1986) Cyclosporine and analogues: structural requirements for immunosuppressive activity. *Transplant Proc*, **18**, 213-218.

Williams, B.L., Irvin, B.J., Sutor, S.L., Chini, C.C., Yacyshyn, E., Bubeck Wardenburg, J., Dalton, M., Chan, A.C. and Abraham, R.T. (1999) Phosphorylation of Tyr319 in ZAP-70 is required for T-cell antigen receptor-dependent phospholipase C-gamma1 and Ras activation. *Embo J*, **18**, 1832-1844.

Wills, M.R., Carmichael, A.J., Mynard, K., Jin, X., Weekes, M.P., Plachter, B. and Sissons, J.G. (1996) The human cytotoxic T-lymphocyte (CTL) response to cytomegalovirus is dominated by structural protein pp65: frequency, specificity, and T-cell receptor usage of pp65-specific CTL. *J Virol*, **70**, 7569-7579.

Wolff, J.A., Ludtke, J.J., Acsadi, G., Williams, P. and Jani, A. (1992) Long-term persistence of plasmid DNA and foreign gene expression in mouse muscle. *Hum Mol Genet*, **1**, 363-369.

Wolffe, A.P. and Matzke, M.A. (1999) Epigenetics: regulation through repression. *Science*, **286**, 481-486.

Woodruff, M.F. (1967) Antilymphocyte serum: summary and further observations. *Transplantation*, **5**, Suppl:1127-1133.

Woods, N.B., Muessig, A., Schmidt, M., Flygare, J., Olsson, K., Salmon, P., Trono, D., von Kalle, C. and Karlsson, S. (2003) Lentiviral vector transduction of NOD/SCID repopulating cells results in multiple vector integrations per transduced cell: risk of insertional mutagenesis. *Blood*, **101**, 1284-1289.

Xiang, B.Q., Jia, Z., Xiao, F.X., Zhou, K., Liu, P. and Wei, Q. (2003) The role of loop 7 in mediating calcineurin regulation. *Protein Eng*, **16**, 795-798.

Yan, L. and Wei, Q. (1999) High activity of the calcineurin A subunit with a V314 deletion. *Biol Chem*, **380**, 1281-1285.

Yang, S., Delgado, R., King, S.R., Woffendin, C., Barker, C.S., Yang, Z.Y., Xu, L., Nolan, G.P. and Nabel, G.J. (1999) Generation of retroviral vector for clinical studies using transient transfection. *Hum Gene Ther*, **10**, 123-132.

Young, L.S. and Murray, P.G. (2003) Epstein-Barr virus and oncogenesis: from latent genes to tumours. *Oncogene*, **22**, 5108-5121.

Young, L.S. and Rickinson, A.B. (2004) Epstein-Barr virus: 40 years on. *Nat Rev Cancer*, **4**, 757-768.

Yusuf, I. and Fruman, D.A. (2003) Regulation of quiescence in lymphocytes. *Trends Immunol*, **24**, 380-386.

Yusuf-Makagiansar, H., Anderson, M.E., Yakovleva, T.V., Murray, J.S. and Siahaan, T.J. (2002) Inhibition of LFA-1/ICAM-1 and VLA-4/VCAM-1 as a

therapeutic approach to inflammation and autoimmune diseases. *Med Res Rev*, **22**, 146-167.

Zhang, W., Sloan-Lancaster, J., Kitchen, J., Trible, R.P. and Samelson, L.E. (1998) LAT: the ZAP-70 tyrosine kinase substrate that links T cell receptor to cellular activation. *Cell*, **92**, 83-92.

Zheng, X.F., Florentino, D., Chen, J., Crabtree, G.R. and Schreiber, S.L. (1995) TOR kinase domains are required for two distinct functions, only one of which is inhibited by rapamycin. *Cell*, **82**, 121-130.

Zheng, X.F. and Schreiber, S.L. (1997) Target of rapamycin proteins and their kinase activities are required for meiosis. *Proc Natl Acad Sci U S A*, **94**, 3070-3075.

Zhou, X., Cui, Y., Huang, X., Yu, Z., Thomas, A.M., Ye, Z., Pardoll, D.M., Jaffee, E.M. and Cheng, L. (2003) Lentivirus-mediated gene transfer and expression in established human tumor antigen-specific cytotoxic T cells and primary unstimulated T cells. *Hum Gene Ther*, **14**, 1089-1105.

Zhu, D., Cardenas, M.E. and Heitman, J. (1996) Calcineurin mutants render T lymphocytes resistant to cyclosporin A. *Mol Pharmacol*, **50**, 506-511.

Appendix I

List of Bacterial Reagents

Table 2.1 Bacterial culture media and reagents used

Luria-Bertani (LB) broth	Prepared to a final concentration of 0.5% (w/v) yeast extract (Oxoid), 0.17M NaCl (Fisher) and 1% (w/v) tryptone (Oxoid) in distilled water and stored at 4°C. All LB broth was sterilised before use and if required antibiotics were added following sterilisation.
Luria-Bertani (LB) agar	Prepared by adding 15g of bactoagar (Oxoid) to 1 litre of LB broth, before sterilisation. To prepare antibiotic selective agar plates, the required antibiotics were added to the agar following sterilisation and sufficient cooling. The agar plates were then poured immediately. Both LB agar and agar plates were stored at 4°C.
Antibiotics (Ampicillin and Kanamycin; Sigma)	Used to isolate transformed bacteria were prepared as 50 mg/ml stock solutions in distilled water and subsequently sterilised by filtration through a 0.2μm sterile filter (Sartorius). Aliquots were stored at –20°C and used at a final concentration of 50 μg/ml.
0.5M EDTA, pH 8.0	Prepared by dissolving 186.1g of Ethylenediaminetetra acetic acid (EDTA; Sigma) in 800 ml of distilled water and adjusting to pH 8.0 with sodium hydroxide pellets (approximately 20g). The final volume was made up to 1 litre with distilled water and then sterilised by autoclaving.
Tris-EDTA (TE)	Contained 10mM Tris-HCl, pH 8.0 and 1mM EDTA, pH 8.0 and wassterilised by autoclaving before use.
Tris-acetic acid buffered EDTA (TAE)	Prepared as a 50X stock by adding 24.2g Tris-base (USB), 100 ml of 0.5M EDTA, pH 8.0 and 57.1 ml glacial acetic acid (Sigma) to a final volume of 1 litre in distilled water.

Table 2.1 Cont'd

Lysozyme solution	Prepared by dissolving 0.1g of lysozyme (Sigma) in 100 µl 1M Tris pH 8.0 and making up to 10 ml with H_20.
3M Sodium acetate, pH 5.2	Prepared by dissolving 204.1g of sodium acetate (Sigma) in 400 ml of distilled water, adjusting the pH to pH 5.2 with glacial acetic acid and making up to a final volume of 500 ml with further distilled water.
Cesium Chloride (CsCl)	Was supplied ready to use by Roche and was stored at 15-22°C.
Phenol (liquified and washed in Tris buffer)	Was supplied by Sigma and stored at 4°C.
Phenol:Chloroform:Isoamylalcohol (25:24:1)	Was supplied by Sigma and stored at 4°C.
Chloroform:Isoamylalcohol (24:1)	Was supplied by Sigma and stored at 4°C.
DNA loading buffer	Prepared as a 6X stock solution containing 0.25% (w/v) bromophenol blue, 0.25% (w/v) xylene cyanol blue, 30% (v/v) glycerol and 50mM EDTA and stored at 4°C.

Appendix II

Plasmid maps and Sequencing Data

(a)

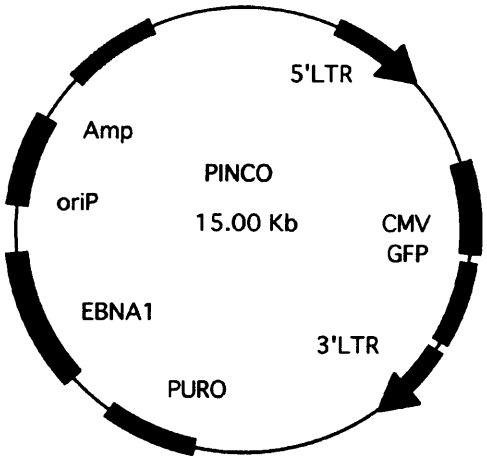

(b)

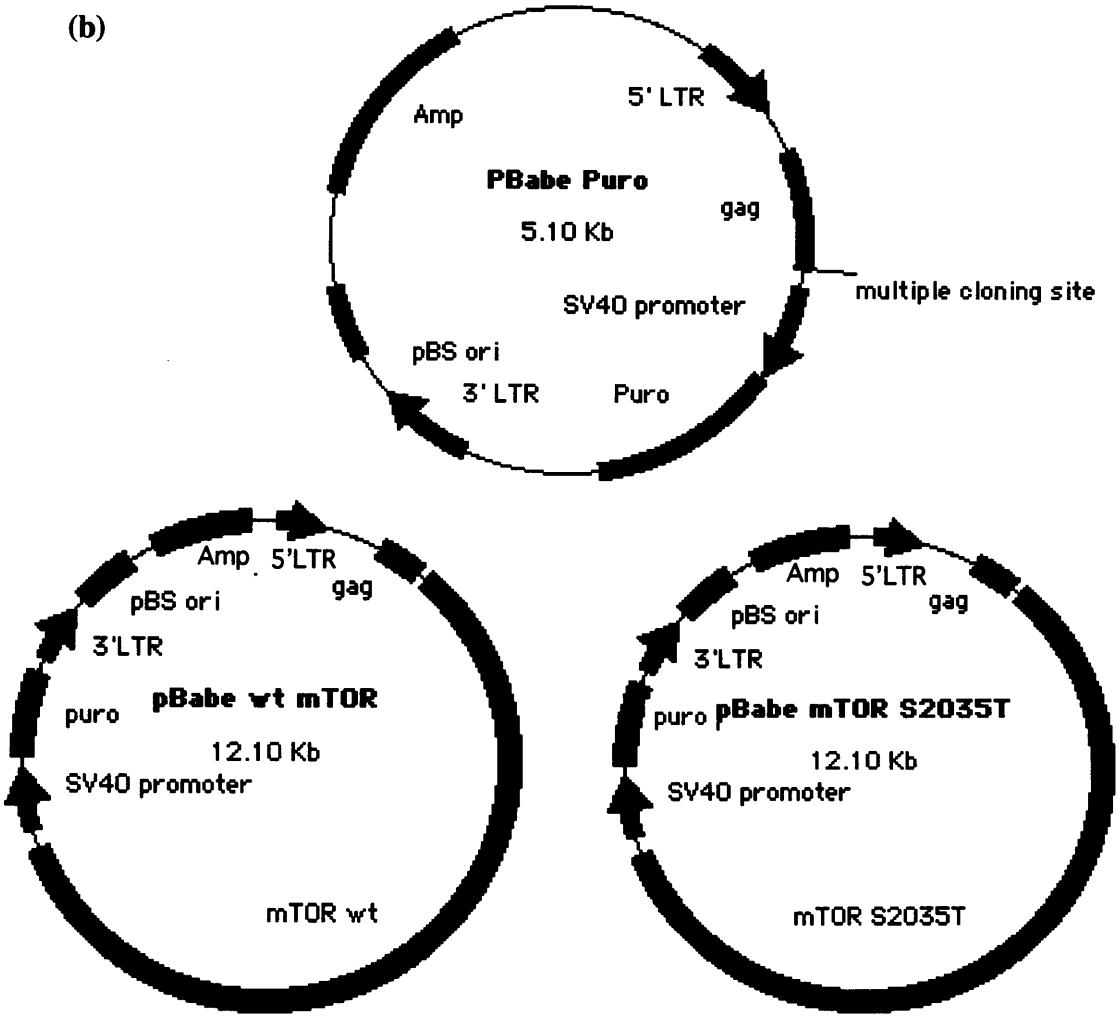

Retroviral vectors used in this study

The maps of the PINCO retroviral plasmid (a) and the pBabe puro, pBabe mTOR wt and pBabe mTOR S2035T plasmids (b) are shown.

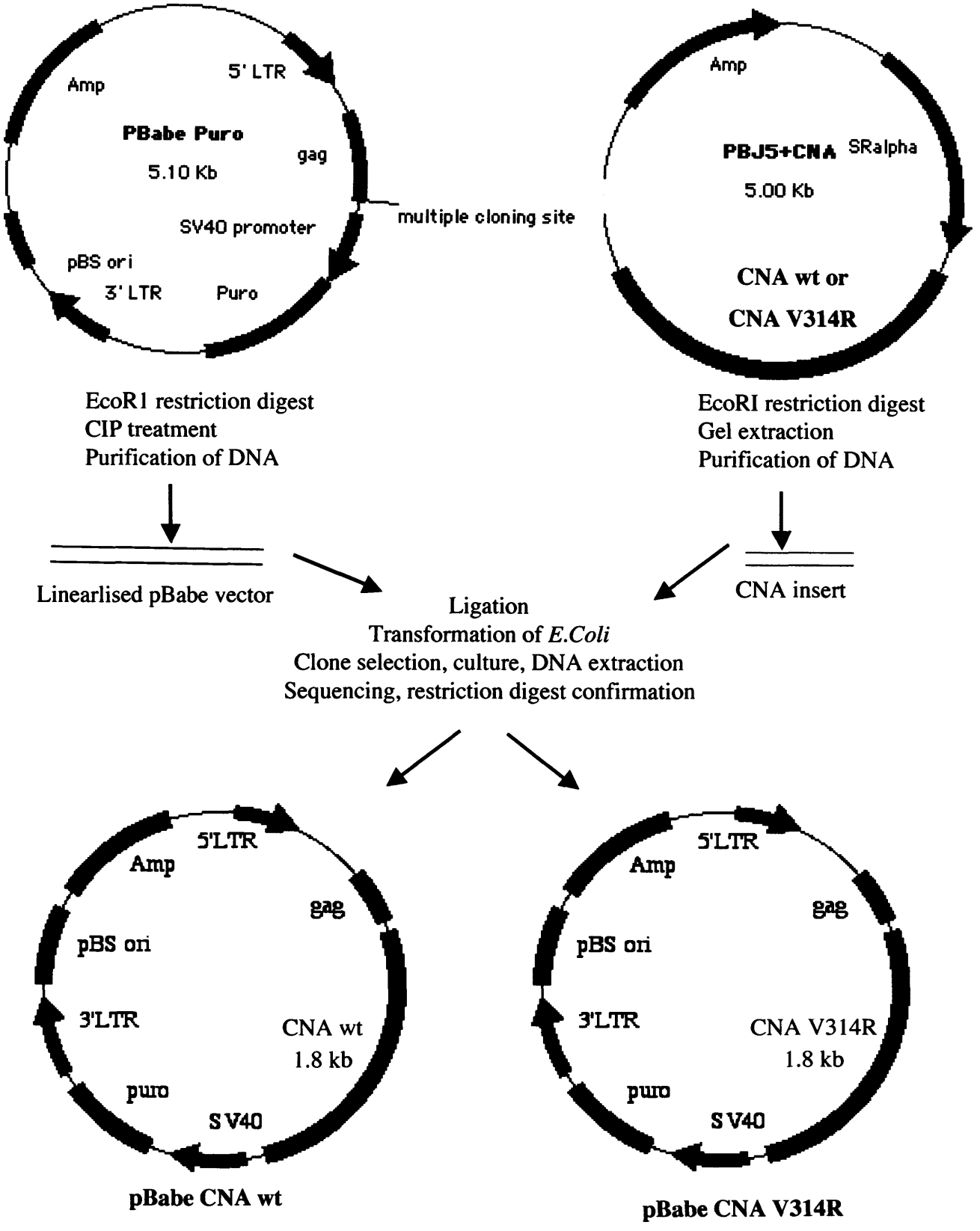

The construction of the pBabe CNA wt and pBabe CNA V314R retroviral plasmids

DNA base position

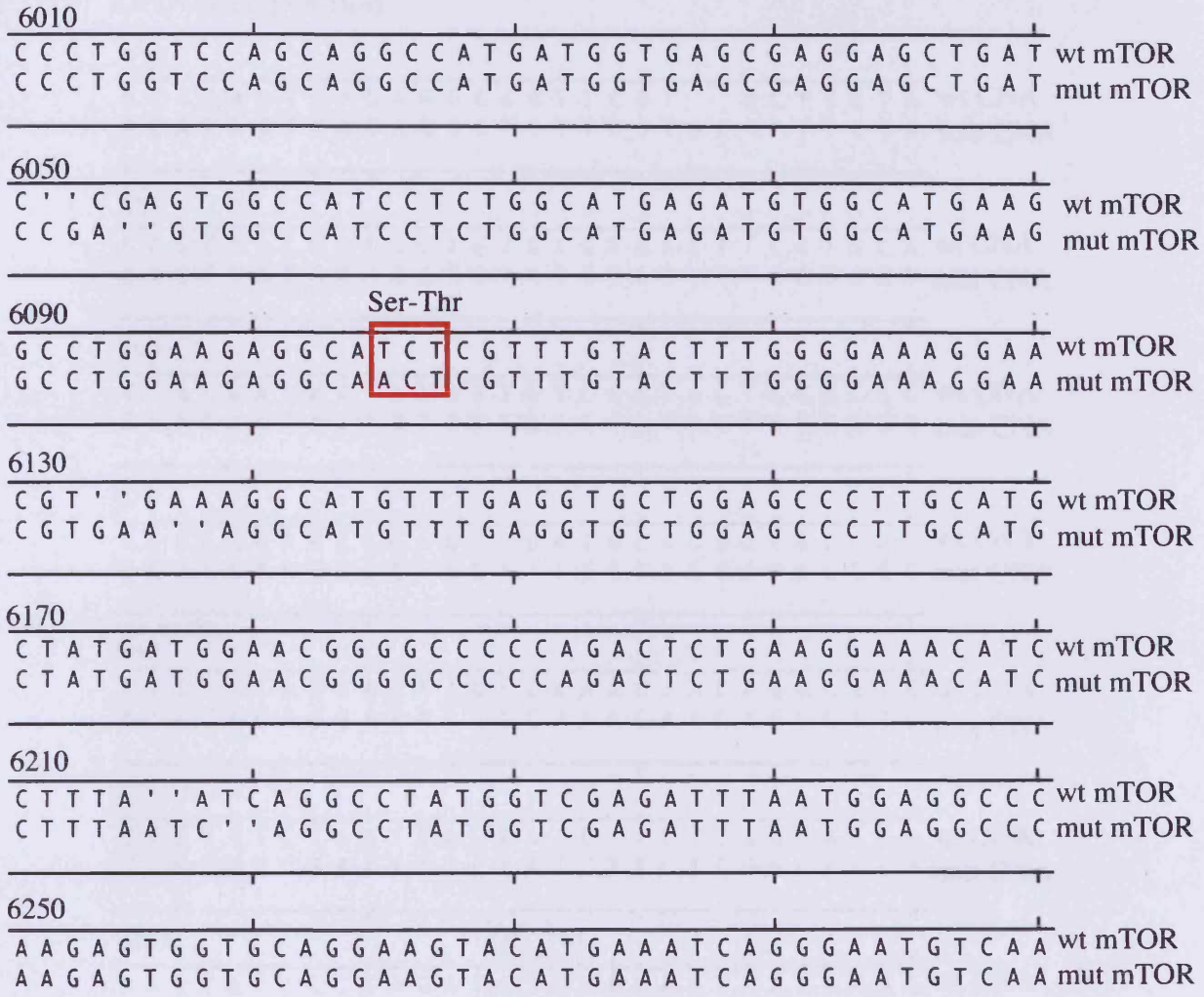

DNA sequencing data obtained from sequencing the wild type mTOR gene and mutant mTOR gene in pBabe wt mTOR and pBabe mTOR S2035T respectively. Only a fraction of the 7kB gene sequence is shown. The DNA sequence data for the mutant gene is aligned to the wild-type gene and the point mutation in the DNA sequence, leading to a serine to threonine change at amino acid position 2035 in the mTOR protein, is shown (S2035T).

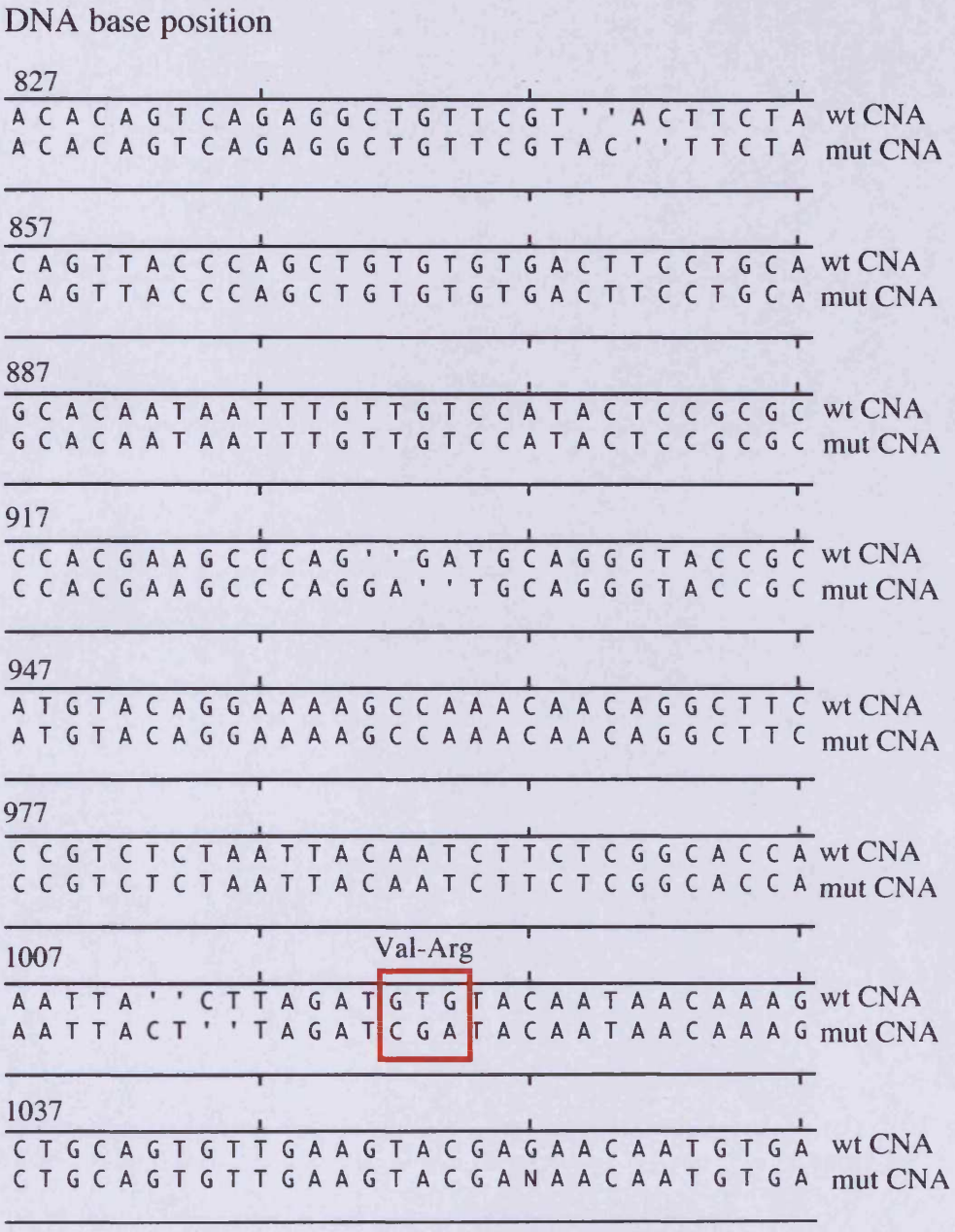

DNA sequencing data obtained from sequencing the wild type CNA gene and mutant CNA gene in pBabe wt CNA and pBabe CNA V314R respectively. Only a fraction of the 1.8 kB gene sequence is shown. The DNA sequence data for the mutant gene is aligned to the wild-type gene and the mutation which leads to a valine to arginine change at amino acid position 314 in the CNA protein, is shown (V314R).

LIST OF SUPPLIERS

Abcam	Abcam Ltd., Milton Rd., Cambridge, UK
Amersham Biosciences	Amersham Biosciences, Little Chalfont, Bucks, UK.
Beckman	Beckman Instruments Ltd., High Wycombe, Bucks, UK.
Becton Dickinson	Becton Dickinson UK Ltd., Cowley, Oxford, UK.
Bio101	Anachem, Luton, Bedfordshire, UK.
Biorad	Biorad, Hemel Hempstead, Watford, Herts, UK.
Biosource Europe	Watford, Hertfordshire, UK.
BioWhittaker	BioWhittaker Ltd., Verviers, Belgium
Boehringer Mannheim	Roche Diagnostics Ltd., Bell Lane, Lewes, UK.
Calbiochem	Merck Biosciences Ltd., Beeston, Nottingham, UK.
Chiron	Chiron UK, Birmingham, UK.
Clontech	BD Clontech UK, Basingstoke, Hampshire, UK.
Dako	Dako Ltd., Ely, Cambridge, UK.
DNA Star Inc.	West Ealing, London, UK.
Fisher Chemicals	Fisher Scientific Ltd., Loughborough, Leics, UK.
Flowgen	Ashby de la Zouch, Leicestershire, UK.
Fluka	Sigma Aldrich Company Ltd., Poole, Dorset, UK.
Gibco	Invitrogen Technologies, Paisley, UK.
Greiner	Greiner, Stonehouse, Gloucestershire, UK.
Hayman	Hayman, Essex, UK.
Heatsystems	Heatsystems-Ultrasonics Inc., New York, USA
Hendley	Essex C. A. Hendley (Essex) Ltd., Loughton, Essex, UK.
Hybaid	Hybaid Ltd., Ashford, Middlesex, UK.
ISL	Immune Systems Ltd., Paignton, TQ4 7XD UK.
Jencons	Jencons Scientific, Leighton Buzzard, Luton, UK
Kodak	Kodak (IBI Ltd.), Cambridge, UK.
Leica	Leica Microsystems Ltd., Milton Keynes, Bucks, UK.
Merck	Merck Ltd., Poole, Dorset, UK.

Miltenyi Biotec	GmBH Miltenyi Biotec UK Ltd., Bisley, Surrey, UK.
Molecular Probes Europe	PoortGebouw, Rijnsburgerweg, Leiden, The Netherlands
MWG Oligonucleotides	MWG Biotech, Ebersberg, Germany
New England Biolabs	New England Biolabs Ltd., Hitchin, Herts, UK.
Novartis	Novartis Pharmaceuticals, Horsham, UK
Oxoid	Oxoid Ltd., Basingstoke, Hampshire, UK.
PAA	PAA Laboratories, Linz, Austria.
Perkin Elmer	Perkin Elmer, Beakonsfield, Bucks, UK.
Promega	Promega, Southampton, UK.
Qiagen	Qiagen, Surrey, UK.
Roche	Roche Diagnostics Ltd., Lewes, East Sussex, UK
Sartorius	Sartorius, Gottingen, Germany.
Serotec	Serotec Ltd., Kidlington, Oxford, UK.
Sigma	Sigma, Poole, Dorset, UK.
Sorvall	Kendro Lab. Products Ltd., Bishops Stortford, Herts, UK.
Tomtec	Tomtec, Hamden, CT
Tropix	Cambridge Bioscience, Cambridge, UK.
Welsh Blood Service	Pontyclun, Talbot Green, Cardiff, Wales
Whatman	Whatman International Ltd., Maidstone, Kent, UK.

Appendix III

List of Suppliers

Appendix IV

Publication: Breslin *et al.*, 2005
British Journal of Pharmacology
Vol. 144, Pg. 791-800

British Journal of Pharmacology (2005) 144, 791–800
www.nature.com/bjp

LY294002 and rapamycin co-operate to inhibit T-cell proliferation

[1]Elaine M. Breslin, [1]Paul C. White, [1]Angharad M. Shore, [1]Mathew Clement & *,[1]Paul Brennan

[1]Infection and Immunity, Wales College of Medicine, Cardiff University, Henry Wellcome Research Building, Heath Park, Cardiff CF14 XX

1 T-cell proliferation is critical for mounting an effective adaptive immune response. It is regulated by signals through the T-cell receptor, through co-stimulation and through cytokines such as interleukin-2 (IL-2). Phosphatidylinositol 3-kinase (PI3K) lies downstream of each of these pathways and has been directly implicated in the regulation of lymphocyte proliferation.

2 In this study, we have shown that PI3K regulates cyclin D2 and cyclin D3, the first cell cycle proteins induced in T-cell proliferation, transcriptionally and post-transcriptionally. In T-lymphoblasts, LY294002, a PI3K inhibitor, prevents the induction of both D-type cyclin mRNA and protein, while rapamycin inhibits the induction of protein. Rapamycin inhibits mammalian target of rapamycin (mTOR), which lies downstream of PI3K.

3 Furthermore, our data show that the combination of LY294002 and rapamycin results in a co-operative inhibition of T-cell proliferation. This co-operation occurs in Kit225 cells stimulated with IL-2, and also in resting peripheral blood lymphocytes stimulated with antibodies to the T-cell receptor in the presence and absence of antibodies to CD28.

4 These data indicate that PI3K regulates T-cell proliferation in response to diverse stimuli, and suggest that combinations of inhibitors, perhaps isoform-selective, may be useful as alternative immunosuppressive therapies.
British Journal of Pharmacology (2005) **144,** 791–800. doi:10.1038/sj.bjp.0706061
Published online 13 December 2004

Keywords: LY294002; rapamycin; cyclin D2; phosphatidylinositol-3 kinase (PI3K); immunosuppression; T-cell proliferation; interleukin-2 (IL-2)

Abbreviations: CFSE, carboxyfluorescein diacetate succinimidyl ester; IL-2, interleukin-2; mTOR, mammalian target of rapamycin; PBLs, peripheral blood lymphocytes; PHA, phytohaemagglutinin; PI3K, phosphatidylinositol-3 kinase; pRb, retinoblastoma protein; STAT, signal transducer and activator of transcription

Introduction

T-cell proliferation is critical for mounting an effective adaptive immune response. Therapeutic strategies aimed at suppressing the immune system, in order to allow transplantation, target T-cells and prevent their proliferation (Kahan, 2003). T-cell proliferation is regulated by three types of cell surface molecules (Yusuf & Fruman, 2003). The key step is the recognition of peptide by the T-cell receptor. Co-stimulation, for example, through CD28, and cytokine stimulation are also required for maximal proliferation. The cytokine interleukin-2 (IL-2) can provide the signals necessary for T-cell cycle progression and differentiation. The IL-2 receptor can be targeted by blocking antibodies in order to aid in transplantation and prevent rejection of the allograft. Mutation of the common gamma chain utilized by IL-2 and other cytokines leads to immunodeficiency (Leonard, 2001). Thus, IL-2 signalling through the IL-2 receptor is an important step in mounting an effective T-cell proliferative response.

IL-2 signals through at least three cellular pathways (Nelson & Willerford, 1998). These include signals to signal transducer and activator of transcription-5 (STAT5) and STAT3, the Ras-MAP kinase pathway and the phosphatidylinositol 3-kinase (PI3K) pathway. We have previously shown that PI3K is important for IL-2-induced cell proliferation (Brennan *et al.*, 1997; 1999). Work using pharmacological inhibitors and analysis from mice deficient in subunits of the kinase (Brennan *et al.*, 1997; 1999; Okkenhaug *et al.*, 2002) has contributed to the substantial body of evidence demonstrating the importance of PI-3 kinase to the regulation of T-cell proliferation. PI3K also lies downstream of the T-cell receptor and the co-stimulatory molecule CD28 (Ward & Cantrell, 2001). Thus, links between PI3K and the cell cycle are likely to be critical for T-cell proliferation.

IL-2 induces the progression of T-cells through G1 to S phase of the cell cycle (Nelson & Willerford, 1998). This cell cycle progression is mediated through an increase in D-type cyclins. The cyclins are a group of proteins made and destroyed in a cyclical manner in the cell. When present at sufficient levels, the D-type cyclins activate cyclin-dependent kinases (cdk) 4 and 6. Cdk4 and cdk6 activity is critical to G1- to S-phase progress. The key substrates of cdk4 and cdk6 are members of the pocket protein family, typified by the retinoblastoma susceptibility gene product, pRb. The phosphorylation of pRb results in an increase in E2F transcriptional activity, which is required for the induction of genes involved in DNA synthesis (Sherr, 1996). Cdk4 and cdk6 activity can also be modulated by the levels of the cyclin-dependent kinase inhibitors, particularly p27kip1. Both cyclin

*Author for correspondence; E-mail: brennanp@cardiff.ac.uk
Published online 13 December 2004

D3 and p27kip 1 have been shown to be regulated by PI3K in T-cells (Brennan *et al.*, 1997). There have been a range of studies focused on p27kip1, but there are little data about how PI3K regulates the D-type cyclins in T-cells.

Two pharmacological agents are available to study PI3K and downstream pathways. The first is a widely used inhibitor, LY294002. This is a competitive ATP inhibitor of PI3K that is stable in aqueous solution (Vlahos *et al.*, 1994). Rapamycin, an immunosuppressant, inhibits a subset of PI3K pathways by inhibiting the molecule mTOR (Abraham & Wiederrecht, 1996). This study was performed to investigate the pathway leading from PI3K to the D-type cyclins and utilized both of these pharmacological inhibitors. We have shown that LY294002 inhibits cyclin D2 and cyclin D3 transcriptionally and post-transcriptionally, while rapamycin regulates cyclins on a post-transcriptional level. The different effects of the inhibitors prompted us to investigate the effect of a combination of the agents. Combining LY294002 and rapamycin resulted in significantly more inhibition of T-cell proliferation at doses that had little effect alone. They inhibited T-cell proliferation in response to IL-2, in response to activation of CD3, a component of the T-cell receptor, and in response to activation of CD3 in the presence of an antibody to CD28. This work suggests that inhibition of T-cell proliferation using a combination of a PI3K inhibitor, perhaps an isoform-selective one, and rapamycin could be beneficial as an alternative immunosuppressive regime.

Methods

Cell culture

Kit225 cells are an IL-2-dependent T-cell line derived from a patient with T-cell chronic lymphocytic leukaemia (Hori *et al.*, 1987). The cell line was cultured in RPMI media supplemented with 20 ng ml^{-1} IL-2 (Chiron, U.K.), 10% foetal calf serum, 2 mM L-glutamine, antibiotics (200 U ml^{-1} penicillin and 200 μg ml^{-1} streptomycin), and was maintained at 37°C in a 5% CO_2-humidified incubator. In the absence of IL-2, these cells accumulate in G1 phase of the cell cycle. The cells were deprived of IL-2 for 72 h prior to use in experiments by washing the cells twice in RPMI 1640 media, before resuspending in RPMI 1640 without IL-2. IL-2 receptor-expressing human peripheral blood-derived T-lymphoblasts were generated and maintained as described previously (Beadling *et al.*, 1994). The cells were quiesced by washing three times in RPMI 1640, and replaced in RPMI 1640 with 10% serum in the absence of IL-2 for 48–72 h.

Total lysate preparation, Western blotting and antibody detection

Cell samples were lysed in 2 × gel sample buffer (0.1 M Tris buffer, pH 6.8, 0.2 M dithiothreitol, 4% sodium dodecyl sulphate (SDS), 20% glycerol, 0.1% bromophenol blue). DNA was sheared by sonication and the samples were boiled for 5 min. The solubilized proteins were separated by SDS–polyacrylamide gel electrophoresis (SDS–PAGE) and transferred to PVDF membranes for immunoblotting using an alkaline phosphatase chemiluminescent detection protocol (Mehl *et al.*, 2001). Typically, the lysates from 4×10^5 cells were applied to each track of the gel. The cyclin E antibody (Cat. no. 554182) was from BD Transduction Laboratories (San Diego, CA, U.S.A.). Antibodies to cyclin D2 (M-20) (Cat. no. sc-593), cyclin D3 (C-16) (Cat. no. sc-182) and p27 kip1(Cat. no. sc-1641) were from Santa Cruz Biotechnology (Santa Cruz, CA, U.S.A.) and were used at a concentration of 200 ng ml^{-1}. Antibodies to phospho S6 (Ser 235/236) (Cat no. 2211), pan S6 (Cat no. 9611), phospho pRb amino acids (Ser 795) (Cat no. 9301) were from Cell Signaling Technologies (Beverly, MA, U.S.A.) and were used at a 1/1000 dilution of the stock supplied. The antibody to pan pRb (Cat no. 554136) was from BD Transduction Laboratories and was used at a 1/1000 dilution. The antibody to actin (Cat. no. A-2066) was from Sigma (Poole, Dorset, U.K.) and was used at a 1/1000 dilution of the stock supplied.

Cell counting and viability analysis

Cells were seeded at concentrations of 2.5×10^5 cells ml^{-1} in a 24-well plate. Following a 30-min incubation with the pharmacological inhibitor, and stimulation with IL-2, cells were incubated at 37°C for the course of the experiment. Aliquots of 250 μl were removed for analysis at appropriate times. A volume of 10 μl propidium iodide solution (50 μg ml^{-1}) was added in order to determine the levels of cell death in the samples. Cells in the live gate only were counted for a defined time on the flow cytometer. The PI data to determine the percentage of cell death were analyzed in the FL-3 channel, acquiring data on all cells, not just those in the live gate.

RNA extraction and RNase protection

Total RNA was extracted from human T-cells using the lithium chloride method. The cells were washed in phosphate-buffered saline (PBS) and resuspended in urea/lithium chloride buffer (500 mM urea, 300 mM $LiCl_2$ with 100 U ml^{-1} of heparin and 10 U ml^{-1} of RNAsin). The cells were lysed by passing the solution through a 19 G needle 10 times. The cells were then placed on ice overnight. The solution was spun for 20 min at 4°C and the pellet was resuspended in 0.5 ml of 10 mM Tris, pH 7.5, 0.5% SDS. The protein was removed using phenol/chloroform. Sodium acetate was added to a final concentration of 300 mM and RNA was precipitated by the addition of 2.2 v of ethanol. The suspension was placed at −20°C for 2 h and centrifuged at 13,000 × *g* for 10 min at 4°C. The resulting pellet of total RNA was washed with 70% ethanol and dried. The quality of the RNA was checked visually on a gel and by optical density measurements at 260 and 280 nm. The RNase protection was performed using the Multi-Probe RNase protection assays system from Pharmingen. The human cell cycle regulator multiprobe template set (hCYC-1) and T7 RNA polymerase were used to synthesize ^{32}P-labelled antisense riboprobes, which were hybridized to the RNA sample in solution at 54°C for 16 h. After digestion of free probe and other single-stranded RNA with RNases A and T1, the labelled 'RNase-protected' fragments were phenol : chloroform : isoamyl alcohol-extracted and ethanol-precipitated. The fragments were then resolved on 6% denaturing polyacrylamide gels and detected by autoradiography. Approximately 5000 c.p.m. of 'unprotected' labelled probe served as a reference to identify the fragments.

Analysis of cell proliferation with carboxyfluorescein diacetate succinimidyl ester (CFSE)

Quiesced cells were washed twice in PBS and resuspended in 1 ml PBS for each 10^7 cells. CFSE (Kurts *et al.*, 1997; Oehen & Brduscha-riem, 1999) was added to give a final concentration of 2.5 μM. The cell suspension was mixed thoroughly and placed at 37°C for 5 min. The reaction was terminated by the addition of 50 ml of RPMI with 10% fetal calf serum. The cells were washed twice and resuspended in RPMI at 2×10^6 cells ml^{-1}, in six-well plates, prior to stimulation. The fluorescence of the cells was determined by flow cytometry, acquiring data in the FL-1 channel. Cells in the viable gate were analyzed. The cell proliferation was determined by a decrease in cell fluorescence from day 0 to the final time point of day 4 in the Kit225 experiments, and day 6 in the experiments analysing primary human T-cells. CFSE profiles were analyzed using the proliferation platform of the FlowJo software (Tree Star, Inc., CA, U.S.A.).

Analysis of cell proliferation by tritiated thymidine incorporation

Human lymphocytes were isolated from whole blood using a Ficoll gradient. The PBLs isolated were plated out (10^5 cells in 180 μl of complete medium) in triplicate, in a 96-well round-bottomed plate and pretreated with LY294002 and rapamycin at a range of doses alone or in combination for 30 min at 37°C. Cells were then stimulated with anti-CD3 antibody (OKT3 2.5 ng ml^{-1}, CRUK) or anti-CD3 and anti-CD28 antibody (5 μg ml^{-1}, BD Biosciences) for 4 days and pulsed with tritiated thymidine (0.5 μCi per well; Amersham Life Sciences, U.K.) for the last 16 h of the experiment; incorporation of ^{3}[H]thymidine was assessed by liquid scintillation counting.

Results

Kinetics of changes of D-type cyclins in response to IL-2 in human peripheral T-cells

As our first step, we characterized the induction of D-type cyclins in response to IL-2 in human peripheral T-cells in order to examine the kinetics of the changes in the cell-cycle proteins. Lymphocytes were isolated from whole blood using a Ficoll gradient and T-lymphoblasts were prepared by activating with phytohaemagglutinin (PHA) and IL-2 for 4 days and then stimulating in IL-2 for a further 2 days. These cells were then removed from IL-2 for 2 days prior to beginning the experiment to allow them to accumulate in G1 phase of the cell cycle. The cells were then stimulated by the addition of IL-2 to induce cell cycle entry. Protein extracts were generated at the defined intervals and run on a polyacrylamide gel. Changes in the levels of cell cycle proteins were investigated using specific antibodies. Figure 1 shows that both D-type cyclins are induced. Cyclin D2 is induced quickly with an increase in the corresponding protein band observed at 3 h. No change in the level of p27kip1, a cdk inhibitor, is obvious at this point, while the loss of p27kip1 parallels the induction of the D-type cyclins at later times. Cyclin E induction is a later event with the induction obvious at 6 h rather than 3. All these events happen prior to cell cycle entry, which occurs after approximately 12 h.

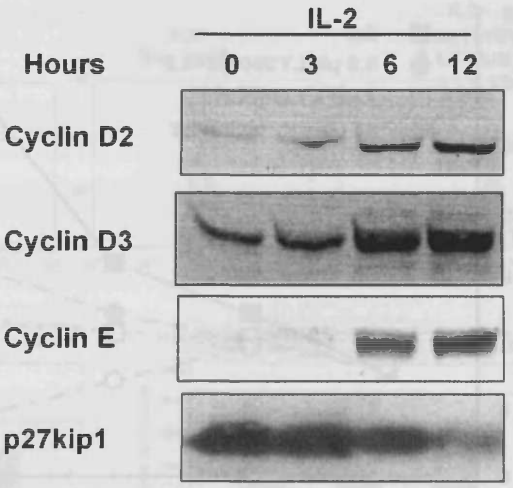

Figure 1 IL-2 induces D-type cyclins in primary human T-cells. Human T-cells were activated and grown in PHA (1 μg ml^{-1}) and IL-2 (20 ng ml^{-1}) for 1 week. They were removed from IL-2 (20 ng ml^{-1}) for 2 days and stimulated with IL-2 (20 ng ml^{-1}) for the times indicated. Cells were lysed and protein extracts generated. Protein extracts were resolved by SDS–PAGE and Western blotted. Cell cycle proteins were assayed by antibody detection. Each blot is representative of five or more experiments. A typical time course of cyclin induction is illustrated.

LY294002 and rapamycin inhibit proliferation and D-type cyclin induction in human T-cells

In order to explore the role of PI3K in IL-2-mediated T-cell proliferation, we used the inhibitor LY294002. Previously activated human T-lymphoblasts were incubated with three different doses of LY294002 in the presence of IL-2. Cell number and cell viability was assessed by flow cytometry. Figure 2a shows that LY294002 inhibits cell proliferation in a dose-dependent manner. Flow-cytometric analysis demonstrated that this was not due to an increase in cell death (data not shown).

To elucidate the role of PI3K on cell cycle events, we treated cells with LY294002 and rapamycin, which inhibits a subset of PI3K pathways. Human T-cells were prepared as before, and pretreated with LY294002 or rapamycin before stimulation with IL-2 for the times indicated. Protein extracts were generated at the defined intervals and run on a polyacrylamide gel. Changes in the levels of cell cycle proteins were investigated using specific antibodies. Figure 2b shows the effects of pretreatment of T-cells with either LY294002 or rapamycin. Both LY294002 and rapamycin inhibited the induction of cyclin D2 and D3.

Regulation of cyclin RNA by IL-2

Changes in protein levels observed in the cell can be a result of altering transcription or translation. In order to determine if LY294002 or rapamycin could alter cyclin RNA levels, we performed an RNase protection assay with probes for cyclin D2. Total RNA extracts were generated from human T-cells, treated as before. Figure 3 shows a graph of normalized data from three different experiments. The RNA levels were normalized to housekeeping genes GAPDH and L32. LY294002 (10 μM) caused a 50% decrease in cyclin D2

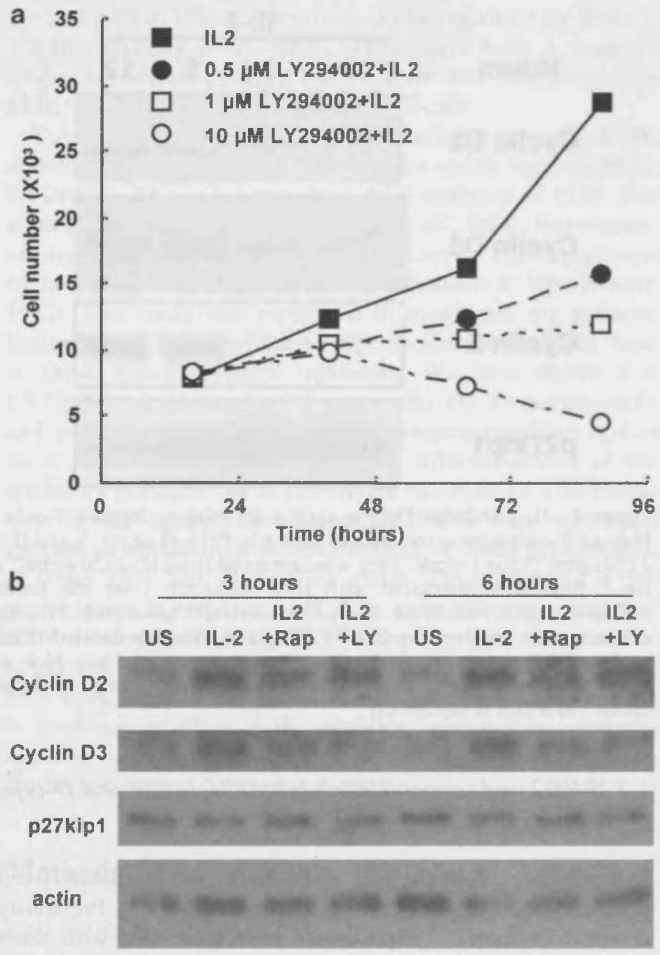

Figure 2 LY294002 inhibits IL-2-mediated T-cell proliferation and IL-2-induced cell cycle protein changes. (a) Human T-cells were generated as described for Figure 1. They were incubated with three concentrations of LY294002 for 30 min prior to stimulation with IL-2. The concentrations of LY294002 were 0 μM (solid squares), 0.5 μM (solid circles), 1 μM (open squares) and 10 μM (open circles). After the defined times (as indicated), cells were counted by flow cytometry. Only the live cells were counted. The graph is from a single experiment and is representative of observations from more than 10 experiments. (b) Human T-cells generated as for Figure 1 were preincubated with either rapamycin (20 nM) or LY294002 (10 μM), a PI3K inhibitor, for 30 min. They were then stimulated with IL-2 (20 ng ml^{-1}). Protein samples were taken at defined times, and the level of cell cycle proteins was determined following SDS–PAGE and Western blotting.

mRNA, while the effect of rapamycin was not significant. This study showed that that LY294002 inhibited the induction of cyclin D2 and D3 (not shown) mRNA by IL-2. Other studies from our laboratory indicate that PI3K can directly transactivate both D-type cyclin promoters (data not shown). Rapamycin did not substantially affect the levels of D-type cyclin mRNA. This indicates that LY294002 regulated cyclin D2 transcription but rapamycin only affected cyclin D2 post-transcriptionally.

Combinations of LY294002 and rapamycin inhibit proliferation of the Kit225 T-cell line

The effects of LY294002 and rapamycin on cyclin D2, coupled with the information regarding the regulation of p27kip1

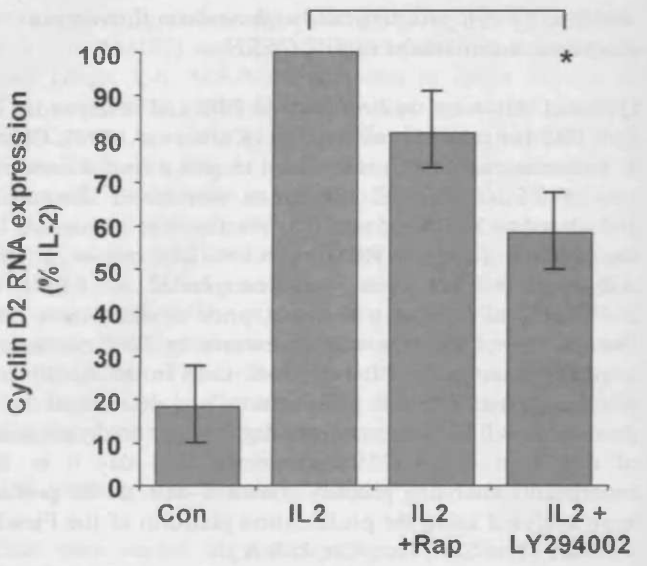

Figure 3 Regulation of cyclin RNA by IL-2. Human T-cell samples generated in parallel with those in Figure 1 were treated with LY294002 and rapamycin (20 nM) for 30 min and stimulated with IL-2 for 3 h. Total RNA was extracted from the cells and the presence of cyclin mRNA levels was determined by RNase protection. The levels were quantified and normalized to the housekeeping gene L32 and expressed as percentage signal seen in cells treated with IL-2 alone. This graph represents cyclin data accumulated from three experiments. Student's *t*-test was used to ascertain the statistical significance of the results. The effects of the LY294002 on cyclin D2 RNA expression were significant ($P<0.05$). The effects of rapamycin were not significant.

(Medema *et al.*, 2000; Kops *et al.*, 2002; Stahl *et al.*, 2002), prompted us to investigate the effect of combinations of the two agents on T-cell proliferation. We hypothesized that the effects of these two inhibitors may co-operate to cause enhanced inhibition of proliferation. This hypothesis was first investigated using quiesced Kit225 cells, an IL-2-dependent leukemic T-cell line (Brennan *et al.*, 1997; 1999). They accumulate in G1 phase of the cell cycle following the removal of IL-2. The Kit225 cells were stained with the protein dye CFSE, which allows the analysis of cell division by flow cytometry (Kurts *et al.*, 1997; Oehen & Brduscha-riem, 1999). Cell proliferation was determined within the live gate only, excluding an effect on cell survival. Figure 4a shows a typical flow cytometry profile from this experiment. The numbers on the histograms denote the proposed number of population divisions the cells have undergone. Stimulation of Kit225 cells with IL-2 caused proliferation and a decrease in fluorescence, illustrated by a shift to the left on the histogram.

The curves generated by the CFSE profile were analysed using the proliferation platform of the FlowJo software. This analysis allocates cells to populations that have divided, based on a best-fit root mean square function. FlowJo also returns various values that provide a measure of proliferation. Two of these measurements are Division Index and % Divided. Division Index is the average number of divisions that a cell (that was present in the starting population) has undergone. % Divided is the percentage of cells of the original sample, which divided (assuming that no cells died during the culture). The allocation of cells to populations also allows a calculation of

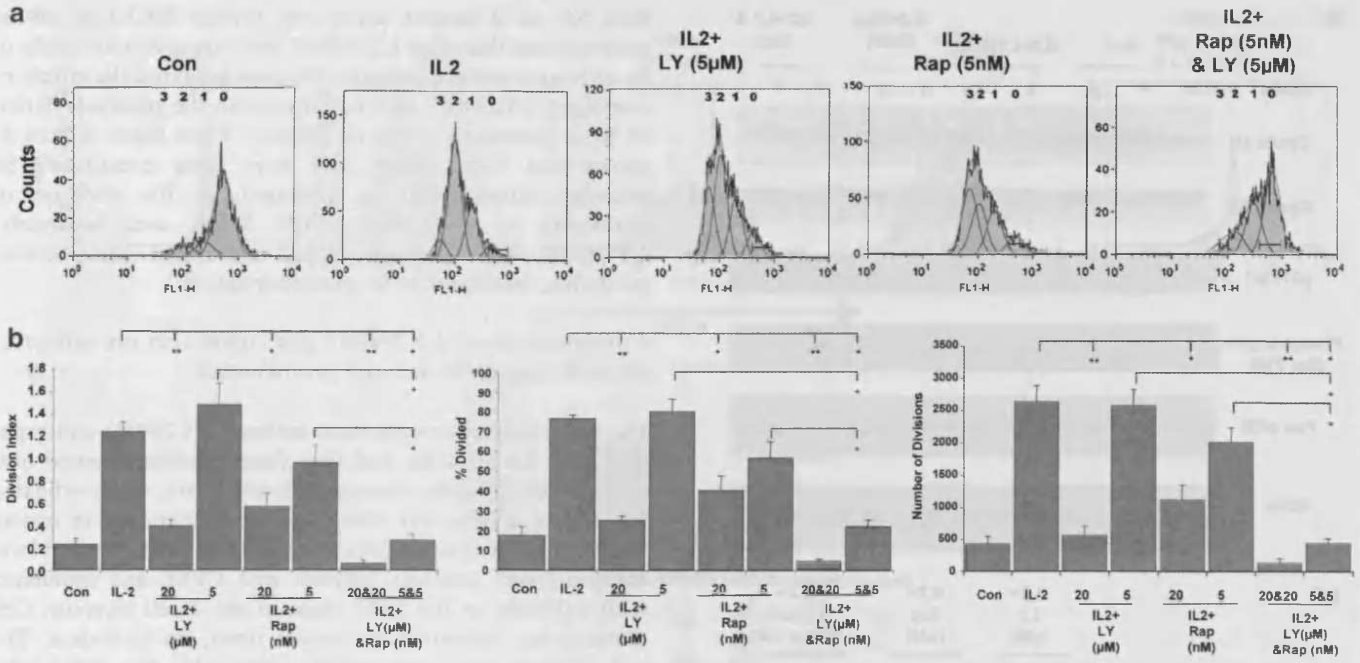

Figure 4 Combinations of LY294002 and rapamycin co-operate to inhibit IL-2-induced proliferation. Quiesced Kit225 cells were stained with a cell protein dye, CFSE. They were then treated with LY294002 or rapamycin at the concentrations shown and stimulated as indicated. (a) Representative flow cytometry histograms, measured after 4 days, are illustrated. The numbers on the histograms denote the proposed number of population divisions the cells have undergone. (b) The curves generated by the CFSE profile were analysed using the proliferation platform of the FlowJo software. The three measurements calculated (Division Index, % Divided and Number of Divisions) are indicated as histograms. The graphs were generated from three different experiments. The numbers under the axis represent inhibitor concentrations. The error bars represent the standard error from three experiments. Student's *t*-tests were used to ascertain if the results were significant, with * indicating a significance level of $P<0.05$ and ** indicating $P<0.01$.

the number of cell divisions. Each cell in population 1 has divided once, while each cell in population 2 has divided twice, and so on. We have calculated these three measurements for Kit225 cells treated with LY294002 and rapamycin to allow the best quantitation of the effects of these inhibitors on the CFSE profiles. Each of these is indicated as histograms (Figure 4b). All of the measurements show similar patterns. Paired *T*-tests were performed to determine if the samples are significantly different from those that have been treated with IL-2 alone, with $P<0.05$ indicated by * and $P<0.01$ indicated by **.

All the three histograms show that 20 μM LY294002 and 20 nM rapamycin significantly inhibit Kit225 cell proliferation. The lower doses, 5 μM LY294002 and 5 nM rapamycin, did not significantly affect cell division. However, the combination of 5 μM LY294002 and 5 nM rapamycin together caused a significant inhibition of cell division, as indicated by all three of the measurements generated from the CFSE profiles.

Combined LY294002 and rapamycin treatment alters cell cycle proteins through parallel pathways

Changes in the levels of cell cycle proteins were investigated using specific antibodies. Kit225 cells were quiesced. They were pretreated with LY294002 and rapamycin for 30 min as before and then treated with IL-2 for the times indicated. Total cell lysates were generated and analyzed for a range of cell cyclin proteins. Figure 5 shows that both cyclin D2 and D3 expression is inhibited by the combination of LY294002 and rapamycin. While 5 μM LY294002 and 5 nM rapamycin when used alone reduced the levels of cyclin D2, they did not affect cyclin D3. The levels of p27kip1 showed no consistent change across the experiment, probably because longer treatment with IL-2 is required to alter p27kip1. An increase in phospho pRb is observed in cells treated with IL-2 and is lost in cells treated with the combination of 5 μM LY294002 and 5 nM rapamycin. Total pRb levels also change during T-cell proliferation, as it is a cell cycle-regulated gene. The results for the actin blot suggest that changes observed in the protein extracts from cells treated with LY294002 and rapamycin could not be due to protein loading as the actin level is comparable to that seen in the control sample. These data indicate that the inhibition of proliferation is likely to be due to a loss of cdk activity, due in part to reduced D-type cyclin induction.

We analyzed the effects of combined LY294002 and rapamycin treatment on a pathway that lies downstream of the molecules affected by these inhibitors. Using SDS–PAGE, the phosphorylation status of S6 was monitored. S6 is the substrate of S6 kinase. S6 kinase activity is regulated by the PI3K pathway through PDK-1 and is also regulated by mTOR, placing it downstream of both inhibitors. Figure 5b shows that Kit225 cells have some constitutive S6 phosphorylation. This is increased by treatment with IL-2. LY294002 (20 μM) is sufficient to completely ablate this phosphorylation, while 5 μM LY294002 causes a reduction of S6 phosphorylation to control levels. Both concentrations of rapamycin, 20 and 5 nM, completely inhibited S6 phosphorylation and so S6 phosphorylation was also completely ablated in cells treated

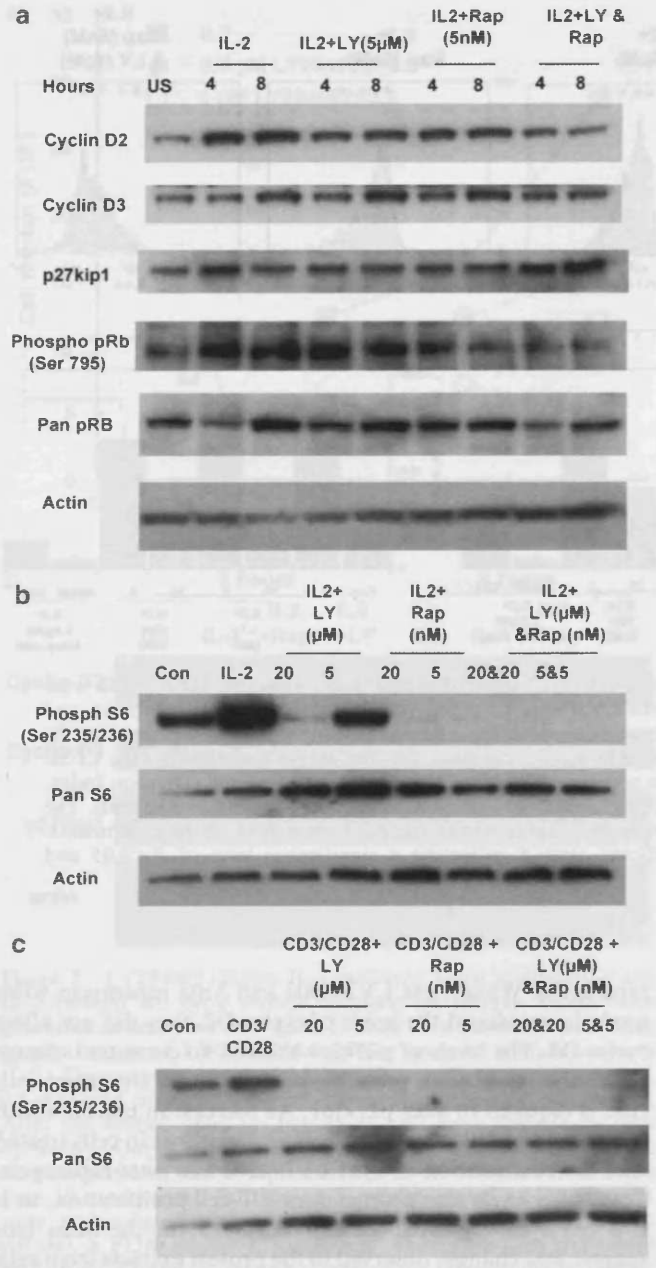

Figure 5 Combinations of LY294002 and Rapamycin co-operate to inhibit T-cell cycle proteins. (a) In experiments parallel to Figure 4, Kit225 total lysate protein samples were taken at defined times and the levels of cell cycle proteins were determined following SDS–PAGE and Western blotting. An antibody to the actin protein was used as a loading control. (b) Kit225 cells, washed out for 4 days, were pretreated with LY294002 and rapamycin alone and in combination for 30 min at the doses indicated, and then stimulated with IL-2 for 30 min. Cytosolic extracts were generated and the phosphorylation status of S6 was monitored following SDS–PAGE and Western blotting. (c) T-cell blasts were generated as described for Figure 1. They were pretreated with LY294002 and rapamycin alone, and in combination for 30 min at the doses indicated, and then stimulated with anti-CD3 (OKT3, 2.5 ng ml^{-1}, CRUK) and CD28 (5 μg ml^{-1}, BD Biosciences) for 30 min. Protein extracts were generated, and the phosphorylation status of S6 was monitored following SDS–PAGE and Western blotting.

with LY294002 and rapamycin. These results parallel the phosphorylation of S6kinase (data not shown). This suggests that LY294002 must be having an effect on pathways other than S6, as it cannot cause any further inhibition of the pathway and thus that LY294002 and rapamycin are likely to be altering parallel pathways. We also analyzed the effects of combined LY294002 and rapamycin on the phosphorylation of S6 in previously activated primary T-cell blasts. Figure 5c shows that T-cell blasts also have some constitutive S6 phosphorylation. This is increased by the addition of antibodies to CD3 and CD28. When used separately, LY294002 and rapamycin caused a dramatic, and indistinguishable, inhibition of S6 phosphorylation.

Combinations of LY294002 and rapamycin are effective at inhibiting CD3-induced proliferation

Having observed co-operation between LY294002 and rapamycin in Kit225 cells and that these inhibitions could also decrease S6 phosphorylation in T-cell blasts, we investigated the effects of the two inhibitors on proliferation in resting PBLs. Human lymphocytes were isolated from whole blood using a Ficoll gradient, labelled with CFSE and stimulated with antibody to the CD3 chain of the T-cell receptor. Cell division was measured at various times, up to 6 days. The cell division was determined within the live gate only, excluding an effect on cell survival. Figure 6a shows a typical flow cytometry profile from this experiment and illustrates the effects of 5 μM LY294002 and 5 nM rapamycin alone and when combined. The numbers on the histograms denote the proposed number of population divisions the cells have undergone. The combined treatment of both LY294002 and rapamycin more strongly inhibited resting PBL division when compared to treatment of cells with inhibitors independently.

Data from four separate experiments were analyzed using the FlowJo proliferation platform and the number of divisions undergone in each population of cells was calculated. These were combined to generate the mean and standard error of the mean as shown in Figure 6b. Paired Student *T*-tests were performed to test if the differences between the combined treatments of LY294002 and rapamycin were significant when compared to the effects of the inhibitors used alone. The asterisk in Figure 6b indicates a significance level of $P<0.05$. Both inhibitors alone at doses of 5 μM LY294002 and 5 nM rapamycin reduced CD3-induced cell division, although the changes were not significant ($P=0.16$, 0.13, respectively), but the combined treatment of 5 μM LY294002 and 5 nM rapamycin caused a significant reduction of CD3-induced cell division ($P<0.05$, column 5 compared to columns 3 or 4). The graph also shows that the effects of the combined treatment of 5 μM LY294002 and 5 nM rapamycin causes significantly more inhibition than 5 nM rapamycin used alone ($P<0.05$). This combination is comparable with treatment of the CD3-stimulated cells with Cyclosporin A (CsA) at the standard dose of 0.5 μg ml^{-1}.

Combinations of LY294002 and rapamycin inhibit tritiated thymidine incorporation

Tritiated thymidine is another method of measuring cell proliferation. It is also an indirect measure of cell survival, as dead cells cannot incorporate thymidine. We used four different combinations of LY294002 and two concentrations of rapamycin to further investigate the effects of

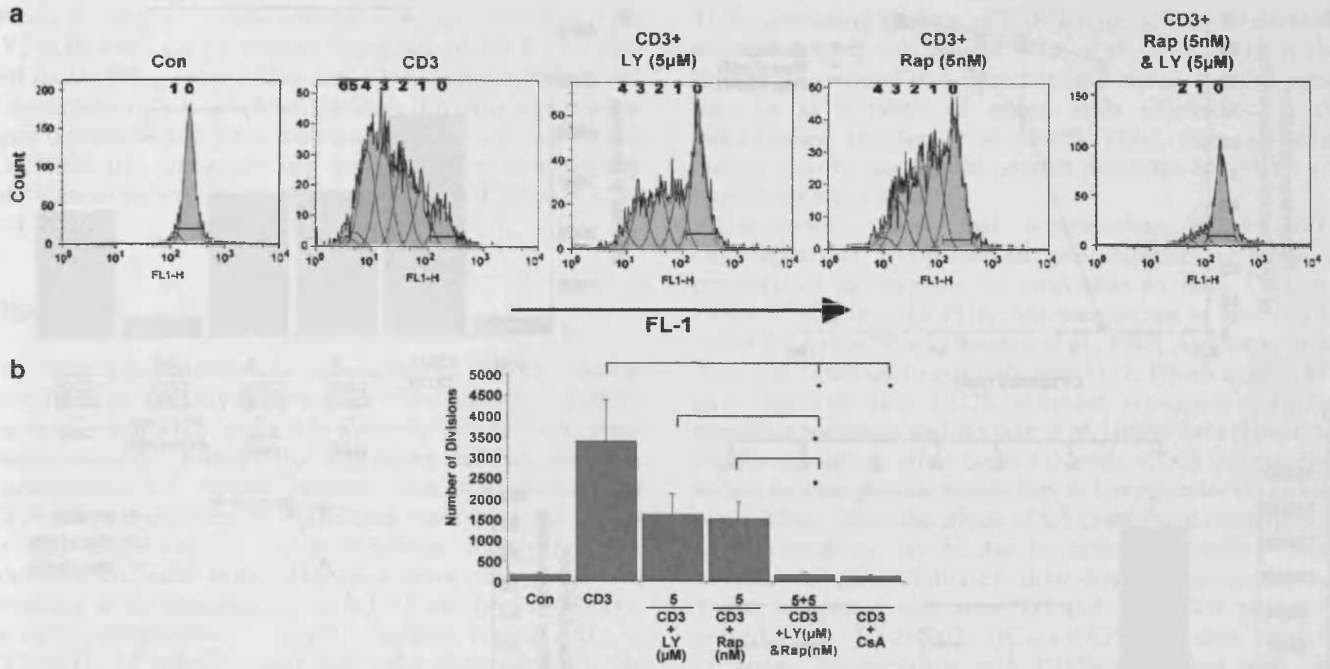

Figure 6 Combinations of LY294002 and rapamycin co-operate to inhibit cell division of primary human T-cells stimulated with anti-CD3. Primary human T-cells were stained with CFSE, pretreated with LY294002 or rapamycin, or a combination of the two inhibitors at the doses indicated for 30 min and stimulated with anti CD3 antibody (Okt3, 2.5 ng ml^{-1}). The cells were analysed by flow cytometry after 6 days. (a) Representative flow cytometry histograms for the 5 μM LY294002 and 5 nM rapamycin treatments, measured after 6 days, are illustrated. The numbers on the histograms denote the proposed number of population divisions the cells have undergone (b). The curves generated by the CFSE profile were analyzed using the proliferation platform of the FlowJo software as for the Kit225 experiments of Figure 4. (b) illustrates the graph generated using Number of Divisions as a measure of proliferation. The graph was generated from four different experiments. The numbers under the axis represent inhibitor concentrations. CsA at a standard dose of 0.5 μg ml^{-1} is used as a comparison. The error bars represent the standard error. Student's *t*-tests were used to ascertain the statistical significance of the results. (b) indicates a significance level of $P<0.05$ (*).

combining these inhibitors. Resting PBLs were isolated from blood and pretreated with various doses and combinations of LY294002 and rapamycin for 30 min prior to stimulation with an antibody to the CD3 chain of the T-cell receptor. Cells were left for 4 days and then 0.5 μCi of tritiated thymidine was added to each well of a 96-well plate. The plate was harvested after 16 h and incorporation was measured by liquid scintillation counting of tritium. Figure 7a illustrates the percentage inhibition following pretreatment with a range of doses of LY294002 in the absence and presence of rapamycin, from one experiment performed in triplicate. The same pattern of inhibition was seen in two further experiments. Both LY294002 and rapamycin, independently and combined, cause a reduction of incorporation of tritiated thymidine. Figure 7b illustrates the results as a histogram and allows the visualization of CD3 alone and CD3 in the presence of rapamycin. Student's *t*-tests were performed to determine if the effects of the combinations of LY294002 and rapamycin were significantly different from the inhibitors used alone. The combination of 2.5 μM LY294002 and 1 nM rapamycin causes significantly more inhibition of CD3-induced thymidine incorporation than either inhibitor alone. Furthermore, the combination of 5 μM LY294002 and 5 nM rapamycin also caused significantly more inhibition than the two inhibitors alone. Together, these data suggest that combinations of LY294002 and rapamycin are more powerful for inhibiting CD3-induced lymphocyte proliferation.

LY294002 and rapamycin co-operate to inhibit proliferation induced by antibodies to CD3 and CD28

CD28 is the primary T-cell co-stimulatory receptor. Binding of its specific ligands enhances T-cell proliferation and IL-2 synthesis. We examined the effects of combinations of LY294002 and rapamycin on resting PBLs stimulated with both an antibody to CD28 and antibody to CD3 using both CFSE analysis of cell division and tritiated thymidine incorporation. It has been reported that CD28 antibody clones vary in their ability to stimulated T-cells to produce IL-2 and increase intracellular calcium concentration. The CD28 antibody clone (CD28.2, BD Biosciences) used in these experiments is a strong co-stimulator for human T-lymphocytes. Similar to experiments described for CD3, resting PBLs were freshly isolated from human blood. For CFSE experiments, they were labelled for 5 min. The cells were pretreated with the inhibitors for 30 min. They were then stimulated with an antibody to CD3 and an antibody to CD28.

The CFSE analysis was performed after 6 days. Figure 8a shows the results from the CFSE analysis and incorporates data from four independent experiments. The addition of co-stimulation results in an increased number of cell divisions than observed in cells stimulated with anti-CD3 alone (Figure 6b). This is consistent with previous studies. LY294002 (5 μM) and 5 nM rapamycin have less effect alone than those observed in cells treated with anti-CD3 only (Figure 6b). However, the inhibitors combine to cause

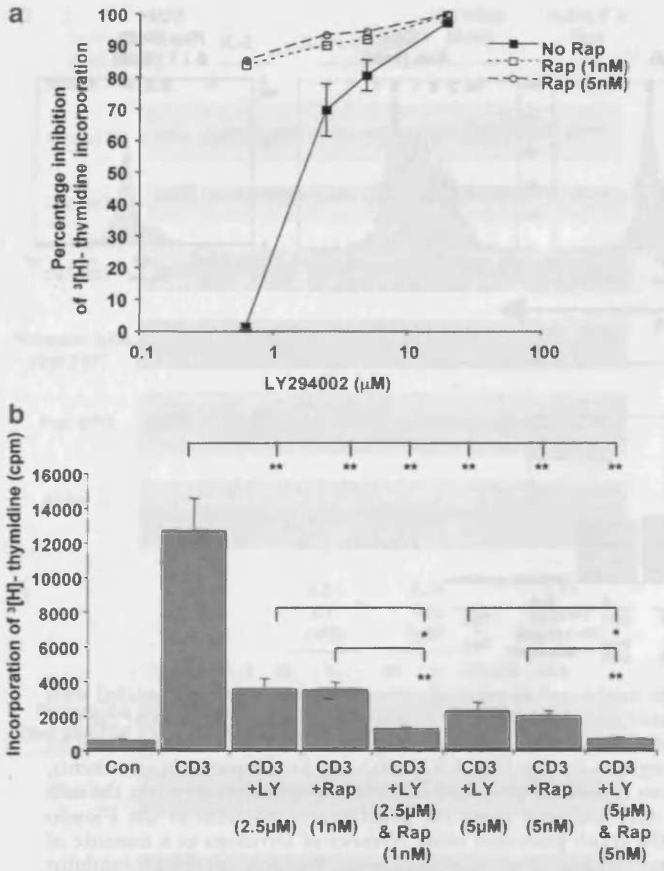

Figure 7 Combinations of LY294002 and rapamycin co-operate to inhibit thymidine incorporation into primary human T-cells stimulated with anti-CD3. Resting PBLs isolated from whole blood were pretreated with various doses and combinations of LY294002 and rapamycin for 30 min prior to stimulation with an antibody to the CD3 chain of the T-cell receptor for 4 days (OKT3, 2.5 ng ml^{-1}, CRUK). Cells were pulsed with 0.5 μCi of tritiated thymidine for the last 16 h of the experiment and the incorporation measured by liquid scintillation counting of tritium. (a) Illustrates the range of doses of LY294002 in the absence and presence of rapamycin. Both LY294002 and rapamycin, independently and combined, cause a reduction of incorporation of tritiated thymidine. (b) Illustrates the results as a histogram, indicating the percentage inhibition of ^{3}[H]thymidine incorporation, compared to anti-CD3-stimulated cells alone. A Student's *t*-test determined any significant levels of inhibition.

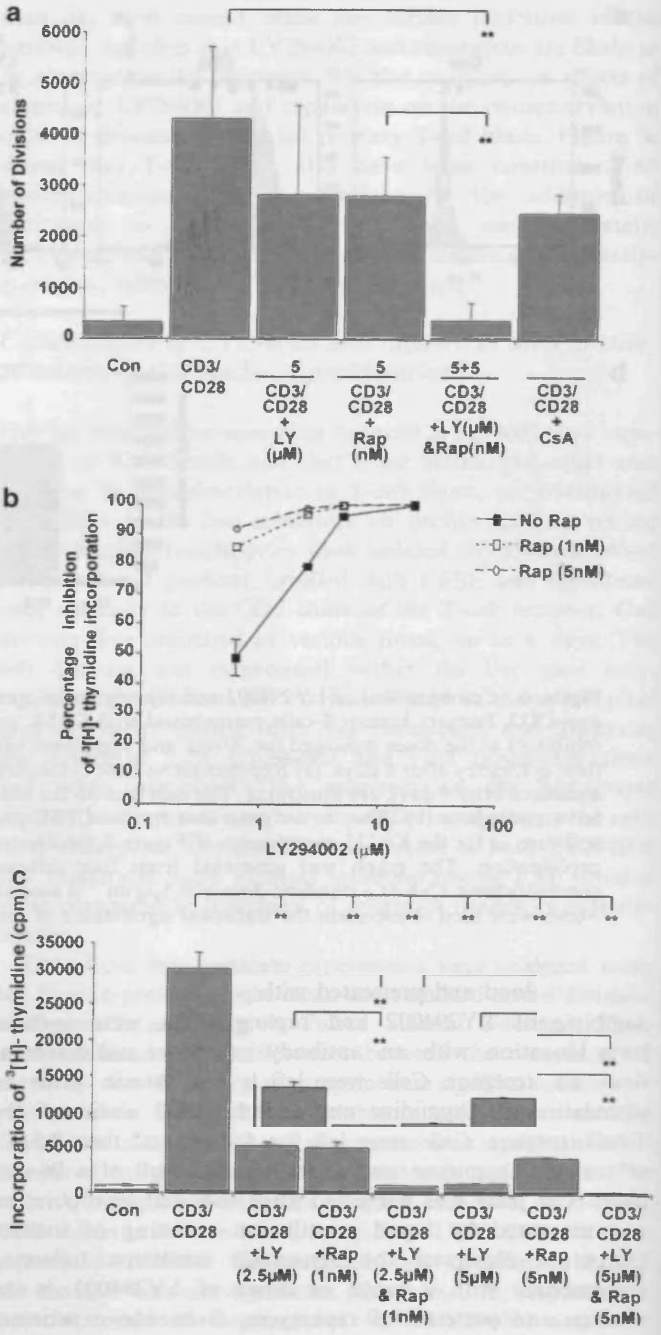

Figure 8 Combinations of LY294002 and rapamycin co-operate to inhibit proliferation in primary human T-cells stimulated with anti-CD3 and anti-CD28. We examined the effects of combinations of LY294002 and rapamycin on resting PBLs stimulated with both an antibody to CD28 (5 μg ml^{-1}, BD Biosciences) and antibody to CD3 (OKT3, 2.5 ng ml^{-1}, CRUK), using both CFSE analysis of cell division and tritiated thymidine incorporation similar to experiments described for CD3 in Figures 6 and 7. (a) Shows the results from CFSE analysis and incorporates data from four independent experiments. (b) Illustrates the range of doses of LY294002 in the absence and presence of rapamycin and indicates the percentage inhibition of ^{3}[H]thymidine incorporation, compared to anti-CD3/CD28 stimulated cells alone. Both LY294002 and rapamycin, independently and combined, cause a reduction of incorporation of tritiated thymidine. (c) Illustrates the results as a histogram. A Student's *t*-test determined any significant levels of inhibition.

a significant increase in the inhibition of cell division ($P<0.01$). The effect of the combined treatment of 5 μM LY294002 and 5 nM rapamycin is also significantly different from inhibition observed with rapamycin 5 nM used alone ($P<0.01$).

The effect of LY294002 and rapamycin was also investigated on tritiated thymidine incorporation stimulated by antibodies to CD3 and CD28. Figure 8b and c illustrate the data from one experiment performed in triplicate and the same pattern of inhibition was seen in two other experiments. The combination of CD3 and CD28 caused a higher incorporation of tritiated thymidine than CD3 alone (compare Figure 8c with Figure 7b). Both LY294002 and rapamycin alone caused a significant inhibition of tritiated thymidine incorporation. Interestingly, cells treated with antibodies to CD3 and CD28 were more sensitive to LY294002 ($IC_{50}=0.625\ \mu$M) than cells treated with anti-CD3 alone ($IC_{50}=2\ \mu$M). Similar to data observed in cells treated with anti-CD3 alone, the combination of 2.5 μM LY294002 and 1 nM rapamycin inhibited anti-CD3 and anti-CD28 treatment significantly more than either inhibitor alone

($P<0.01$). This is also the case for the combination of 5 μM LY294002 and 5 nM rapamycin. The doses used in Kit225 cells and resting PBLs treated with anti-CD3, 5 μM LY294002 and 5 nM rapamycin, also inhibited proliferation more significantly when combined than when used alone. Thus, combinations of LY294002 and rapamycin can combine to more effectively inhibit proliferation of lymphocytes stimulated through CD3 and CD28.

Discussion

This study was performed to investigate the pathway leading from PI3K to the D-type cyclins. We have shown that PI3K regulates cyclin D2 and D3 transcriptionally and post-transcriptionally, perhaps by regulating mRNA stability. Furthermore, our results indicate that combinations of LY294002, an inhibitor of PI3K, and rapamycin can give a stronger inhibition of cell proliferation than when the inhibitors are used alone. The data show that there is a difference in the susceptibility of Kit225 and primary T-cells, be they T-lymphoblasts or freshly isolated resting PBL, to LY294002. LY294002 (5 μM) had very little effect on the proliferation of Kit225 cells, while 1 μM LY294002 inhibits the proliferation of T-lymphoblasts (Figure 2) and 2.5 μM LY294002 inhibits the proliferation of resting PBL stimulated with anti-CD3 (Figure 7) or anti-CD3 with anti-CD28 (Figure 8). This is also the case for rapamycin, where resting PBLs are more sensitive than Kit225 cells. Our data also show that combinations of lower doses of both inhibitors are more effective in primary T-cells than Kit225 cells. These differences are likely to be due to the difference between primary cells and immortalized cell lines.

There are parallels in the effects of LY294002 and rapamycin on the p27kip1 pathway and the cyclin D pathway. LY294002 promotes p27kip1 transcription (Burgering & Kops, 2002) and rapamycin promotes the stability of the p27 protein (Nourse *et al.*, 1994). Thus, the PI3K pathway also regulates p27kip1 both transcriptionally and post-transcriptionally. The role for another target for rapamycin within the cell cycle is supported by the data showing that p27kip1-deficient mice are still susceptible to rapamycin (Luo *et al.*, 1996). It is likely that the inhibition of D-type cyclin expression by rapamycin can, in part, explain that data. Hashemolhosseini *et al.* (1998) showed that, in fibroblasts, both cyclin D1 mRNA and cyclin D1 protein levels are affected by rapamycin. T-cells do not express cyclin D1, but some conservation of mechanisms is likely.

Our data suggest that LY294002 and rapamycin are targeting both overlapping and parallel pathways. We have shown that S6 phosphorylation is altered by both LY294002 and rapamycin in Kit225 cells and T-cell blasts. In both cell types, LY294002 can co-operate with rapamycin at doses where rapamycin completely ablates S6 phosphorylation, suggesting that LY294002 is affecting other pathways. Rapamycin inhibits a subset of PI3K pathways, but TOR may be integrating other pathways too. There is evidence that TOR responds to nutrient levels in yeast (Barbet *et al.*, 1996). In mammalian cells, proliferation is stimulated by a combination of nutrients and growth factors. Accumulating evidence indicates that TOR might mediate signalling in response to both stimuli. In the presence of raptor, the newly identified TOR interacting protein, mTOR kinase activity is increased when stimulated with leucine (Kim *et al.*, 2002). TOR is also thought to respond to a mitochondrial signal, but this signal may be as a result of amino acids synthesized in the mitochondria (Crespo *et al.*, 2002). Thus, there are many distinct possibilities for the parallel pathways LY294002 and rapamycin are inhibiting.

Our results show that combinations of LY294002 and rapamycin co-operate to give effective inhibition of proliferation in response to antibodies to both CD3 and CD28. CD28, through PI3K, has been shown to directly alter cyclin D3 and p27kip1 (Boonen *et al.*, 1999; Appleman *et al.*, 2000; 2002) similar to our data with IL-2. Hsueh *et al.* (1997) have reported that CD28 activates rapamycin-insensitive signalling pathways and Boonen *et al.* (1999) have shown that rapamycin did not affect cyclin D3 levels. CD28 has also been shown to alter glucose metabolism in lymphocytes (Frauwirth *et al.*, 2002). Thus, the effects of LY294002 and rapamycin on CD28 signalling may be due to different signalling targets to that of IL-2. Tritiated thymidine incorporation into T-cells stimulated with anti-CD3 and anti-CD28 were more sensitive to LY294002 ($IC_{50}=0.625\,\mu$M) than tritiated thymidine incorporation into T-cells stimulated with anti-CD3 alone ($IC_{50}=2\,\mu$M). Results from similar systems have reported an IC_{50} for LY294002 inhibition of CD3-induced mouse T-cell proliferation as approximately 0.5 μM (Haeryfar & Hoskin, 2001) and for IL-7-induced human T-cell proliferation as less than 5 μM (Lali *et al.*, 2004). These different IC_{50} values reflect alternative cell types and stimuli, but may also reflect varied dependencies on PI3K for cell survival and proliferation.

This work suggests that inhibition of T-cell proliferation using a combination of a PI3K inhibitor and rapamycin could be beneficial as an alternative immunosuppressive regime. The therapeutic use of PI3K inhibitors is controversial. There are several different but closely related PI3Ks, which are known to have distinct biological roles. However, the first isoform-selective PI3K inhibitor, for p110δ, has been described by the ICOS corporation (Sadhu *et al.*, 2003a, b). Our data, which show that inhibition of PI3K and TOR can co-operate, suggest that these isoform-selective agents may be useful for combination therapies. Such combination therapies may allow lower doses to be administered and as such may avoid the serious side effects of immunosuppressive agents, such as nephrotoxicity, neurotoxicity and hyperlipidaemia. However, it must be stressed that, because of the potential toxicity of broad-spectrum PI3-kinase inhibitors such as LY294002, the use of PI3-kinase inhibitors in the clinic will not be feasible until these highly isoform-specific compounds are developed for clinical use. Recent data we have generated suggest that PI3K inhibitors may also be useful as combination therapies for lymphoma. Thus, our observations should inform the use of inhibitors of PI3K, possibly in conjunction with rapamycin, in the clinic.

E.M.B. is supported by a studentship from the Welsh Office for Research and Development. P.C.W. and P.B. are supported by the Leukaemia Research Fund (U.K.). A.M.S. and M.C. are supported by Tenovus, the Cancer Charity. We thank Professor Martin Rowe for advice and critical comments on the manuscript. We thank Dr Reginald James Matthews' group, especially Dr Jean Sathish for technical advice.

References

ABRAHAM, R.T. & WIEDERRECHT, G.J. (1996). Immunopharmacology of rapamycin. *Annu. Rev. Immunol.*, **14**, 483–510.

APPLEMAN, L.J., BEREZOVSKAYA, A., GRASS, I. & BOUSSIOTIS, V.A. (2000). CD28 costimulation mediates T cell expansion *via* IL-2-independent and IL-2-dependent regulation of cell cycle progression. *J. Immunol.*, **164**, 144–151.

APPLEMAN, L.J., VAN PUIJENBROEK, A.A., SHU, K.M., NADLER, L.M. & BOUSSIOTIS, V.A. (2002). CD28 costimulation mediates down-regulation of p27kip1 and cell cycle progression by activation of the PI3K/PKB signaling pathway in primary human T cells. *J. Immunol.*, **168**, 2729–2736.

BARBET, N.C., SCHNEIDER, U., HELLIWELL, S.B., STANSFIELD, I., TUITE, M.F. & HALL, M.N. (1996). TOR controls translation initiation and early G1 progression in yeast. *Mol. Biol. Cell*, **7**, 25–42.

BEADLING, C., GUSCHIN, D., WITTHUHN, B.A., ZIEMIECKI, A., IHLE, J.N., KERR, I.M. & CANTRELL, D.A. (1994). Activation of JAK kinases and STAT proteins by interleukin-2 and interferon alpha, but not the T cell antigen receptor, in human T lymphocytes. *EMBO J.*, **13**, 5605–5615.

BOONEN, G.J., VAN DIJK, A.M., VERDONCK, L.F., VAN LIER, R.A., RIJKSEN, G. & MEDEMA, R.H. (1999). CD28 induces cell cycle progression by IL-2-independent down-regulation of p27kip1 expression in human peripheral T lymphocytes. *Eur. J. Immunol.*, **29**, 789–798.

BRENNAN, P., BABBAGE, J.W., BURGERING, B.M., GRONER, B., REIF, K. & CANTRELL, D.A. (1997). Phosphatidylinositol 3-kinase couples the interleukin-2 receptor to the cell cycle regulator E2F. *Immunity*, **7**, 679–689.

BRENNAN, P., BABBAGE, J.W., THOMAS, G. & CANTRELL, D. (1999). p70(s6k) integrates phosphatidylinositol 3-kinase and rapamycin-regulated signals for E2F regulation in T lymphocytes. *Mol. Cell. Biol.*, **19**, 4729–4738.

BURGERING, B.M. & KOPS, G.J. (2002). Cell cycle and death control: long live Forkheads. *Trends Biochem. Sci.*, **27**, 352–360.

CRESPO, J.L., POWERS, T., FOWLER, B. & HALL, M.N. (2002). The TOR-controlled transcription activators GLN3, RTG1, and RTG3 are regulated in response to intracellular levels of glutamine. *Proc. Natl. Acad. Sci. U.S.A.*, **99**, 6784–6789.

FRAUWIRTH, K.A., RILEY, J.L., HARRIS, M.H., PARRY, R.V., RATHMELL, J.C., PLAS, D.R., ELSTROM, R.L., JUNE, C.H. & THOMPSON, C.B. (2002). The CD28 signaling pathway regulates glucose metabolism. *Immunity*, **16**, 769–777.

HAERYFAR, S.M. & HOSKIN, D.W. (2001). Selective pharmacological inhibitors reveal differences between Thy-1- and T cell receptor-mediated signal transduction in mouse T lymphocytes. *Int. Immunopharmacol.*, **1**, 689–698.

HASHEMOLHOSSEINI, S., NAGAMINE, Y., MORLEY, S.J., DESRIVIERES, S., MERCEP, L. & FERRARI, S. (1998). Rapamycin inhibition of the G1 to S transition is mediated by effects on cyclin D1 mRNA and protein stability. *J. Biol. Chem.*, **273**, 14424–14429.

HORI, T., UCHIYAMA, T., TSUDO, M., UMADOME, H., OHNO, H., FUKUHARA, S., KITA, K. & UCHINO, H. (1987). Establishment of an interleukin 2-dependent human T cell line from a patient with T cell chronic lymphocytic leukemia who is not infected with human T cell leukemia/lymphoma virus. *Blood*, **70**, 1069–1072.

HSUEH, Y.P., LIANG, H.E., NG, S.Y. & LAI, M.Z. (1997). CD28-costimulation activates cyclic AMP-responsive element-binding protein in T lymphocytes. *J. Immunol.*, **158**, 85–93.

KAHAN, B.D. (2003). Individuality: the barrier to optimal immunosuppression. *Nat. Rev. Immunol.*, **3**, 831–838.

KIM, D.H., SARBASSOV, D.D., ALI, S.M., KING, J.E., LATEK, R.R., ERDJUMENT-BROMAGE, H., TEMPST, P. & SABATINI, D.M. (2002). mTOR interacts with raptor to form a nutrient-sensitive complex that signals to the cell growth machinery. *Cell*, **110**, 163–175.

KOPS, G.J., MEDEMA, R.H., GLASSFORD, J., ESSERS, M.A., DIJKERS, P.F., COFFER, P.J., LAM, E.W. & BURGERING, B.M. (2002). Control of cell cycle exit and entry by protein kinase B-regulated forkhead transcription factors. *Mol. Cell. Biol.*, **22**, 2025–2036.

KURTS, C., KOSAKA, H., CARBONE, F.R., MILLER, J.F. & HEATH, W.R. (1997). Class I-restricted cross-presentation of exogenous self-antigens leads to deletion of autoreactive CD8(+) T cells. *J. Exp. Med.*, **186**, 239–245.

LALI, F.V., CRAWLEY, J., MCCULLOCH, D.A. & FOXWELL, B.M. (2004). A late, prolonged activation of the phosphatidylinositol 3-kinase pathway is required for T cell proliferation. *J. Immunol.*, **172**, 3527–3534.

LEONARD, W.J. (2001). Cytokines and immunodeficiency diseases. *Nat. Rev. Immunol.*, **1**, 200–208.

LUO, Y., MARX, S.O., KIYOKAWA, H., KOFF, A., MASSAGUE, J. & MARKS, A.R. (1996). Rapamycin resistance tied to defective regulation of p27Kip1. *Mol. Cell. Biol.*, **16**, 6744–6751.

MEDEMA, R.H., KOPS, G.J., BOS, J.L. & BURGERING, B.M. (2000). AFX-like Forkhead transcription factors mediate cell-cycle regulation by Ras and PKB through p27kip1. *Nature*, **404**, 782–787.

MEHL, A.M., FLOETTMANN, J.E., JONES, M., BRENNAN, P. & ROWE, M. (2001). Characterization of intercellular adhesion molecule-1 regulation by Epstein–Barr virus-encoded latent membrane protein-1 identifies pathways that cooperate with nuclear factor kappa B to activate transcription. *J. Biol. Chem.*, **276**, 984–992.

NELSON, B.H. & WILLERFORD, D.M. (1998). Biology of the interleukin-2 receptor. *Adv. Immunol.*, **70**, 1–81.

NOURSE, J., FIRPO, E., FLANAGAN, W.M., COATS, S., POLYAK, K., LEE, M.H., MASSAGUE, J., CRABTREE, G.R. & ROBERTS, J.M. (1994). Interleukin-2-mediated elimination of the p27Kip1 cyclin-dependent kinase inhibitor prevented by rapamycin. *Nature*, **372**, 570–573.

OEHEN, S. & BRDUSCHA-RIEM, K. (1999). Naive cytotoxic T lymphocytes spontaneously acquire effector function in lymphocytopenic recipients: a pitfall for T cell memory studies? *Eur. J. Immunol.*, **29**, 608–614.

OKKENHAUG, K., BILANCIO, A., FARJOT, G., PRIDDLE, H., SANCHO, S., PESKETT, E., PEARCE, W., MEEK, S.E., SALPEKAR, A., WATERFIELD, M.D., SMITH, A.J. & VANHAESEBROECK, B. (2002). Impaired B and T cell antigen receptor signaling in p110delta PI 3-kinase mutant mice. *Science*, **297**, 1031–1034.

SADHU, C., DICK, K., TINO, W.T. & STAUNTON, D.E. (2003a). Selective role of PI3K delta in neutrophil inflammatory responses. *Biochem. Biophys. Res. Commun.*, **308**, 764–769.

SADHU, C., MASINOVSKY, B., DICK, K., SOWELL, C.G. & STAUNTON, D.E. (2003b). Essential role of phosphoinositide 3-kinase delta in neutrophil directional movement. *J. Immunol.*, **170**, 2647–2654.

SHERR, C.J. (1996). Cancer cell cycles. *Science*, **274**, 1672–1677.

STAHL, M., DIJKERS, P.F., KOPS, G.J., LENS, S.M., COFFER, P.J., BURGERING, B.M. & MEDEMA, R.H. (2002). The forkhead transcription factor FoxO regulates transcription of p27Kip1 and Bim in response to IL-2. *J. Immunol.*, **168**, 5024–5031.

VLAHOS, C.J., MATTER, W.F., HUI, K.Y. & BROWN, R.F. (1994). A specific inhibitor of phosphatidylinositol 3-kinase, 2-(4-morpholinyl)-8-phenyl-4H-1-benzopyran-4-one (LY294002). *J. Biol. Chem.*, **269**, 5241–5248.

WARD, S.G. & CANTRELL, D.A. (2001). Phosphoinositide 3-kinases in T lymphocyte activation. *Curr. Opin. Immunol.*, **13**, 332–338.

YUSUF, I. & FRUMAN, D.A. (2003). Regulation of quiescence in lymphocytes. *Trends Immunol.*, **24**, 380–386.

(Received August 11, 2004
Revised September 30, 2004
Accepted October 15, 2004)